Regulation of the TNFR1-signalling complex by LUBAC and associated deubiquitinases

A DISSERTATION

SUBMITTED TO THE DEPARTMENT OF

MEDICINE OF

UNIVERSITY COLLEGE LONDON (UCL)

IN FULFILMENT OF THE REQUIREMENTS

FOR THE DEGREE OF

DOCTOR OF PHILOSOPHY

Sebastian Kupka

05/04/2017

I. Declaration

I, Sebastian Kupka confirm that the work presented in this thesis is my own. Information derived from the published and unpublished work of others has been acknowledged in the text and a list of references is given in the bibliography.

London, 05/04/2017

Sebastian Kupka

II. Abstract

TNF is an inflammatory cytokine, vital for innate immune responses but also involved in pathological conditions including rheumatoid arthritis, psoriasis and inflammatory bowel disease. Assembly of the TNFR1-signalling complex (SC) is regulated and post-translational modifications play a crucial part in executing this regulation.

The aim of this study was to characterise how LUBAC contributes to TNFR1-SC assembly, NF-κB and MAPK pathway activation and prevention of cell death by influencing complex composition and ubiquitination. Using mass spectrometry OTULIN, CYLD and SPATA2 were identified as constitutive interaction partners of LUBAC. Interaction studies revealed that despite constitutive binding of OTULIN, SPATA2 and CYLD with the LUBAC component HOIP, only SPATA2 and CYLD are recruited to SCs. Strikingly, CYLD requires HOIP and SPATA2 for its recruitment to SCs, where CYLD counteracts LUBAC by cleaving ubiquitin chains. Consequently, CYLD enables TNF-induced cell death and supresses NF-κB and MAPK activation in NOD2 signalling. Using a newly developed methodology TNFR1 and TRADD were identified as LUBAC substrates and absence of CYLD leads to increased ubiquitination of these proteins. In line with pro-survival functions of linear ubiquitination, depletion of either CYLD or SPATA2 protects cells from TNF-induced necroptosis.

OTULIN, on the other hand, antagonises linear ubiquitination and regulates LUBAC in basal conditions by deubiquitinating its subunits and preventing aberrant linear ubiquitination.

The protein A20 was found to require linear ubiquitin chains for its recruitment to the TNFR1-SC. A20, although negatively regulating NF-κB signalling, is required to prevent TNF-induced cell death by stabilising linear ubiquitination of TNFR1-SC components.

In summary, this study identified LUBAC to be central for CYLD and A20 recruitment to SCs and provides an explanation for the opposing role of CYLD and A20 in regulating TNF-mediated cell death despite their overlapping function in suppression of gene activatory pathways.

III. Table of Figures

Figure 1.1: Creation of lysine- and M1-linked ubiquitin chains 2
Figure 1.2: Ubiquitin structure and position of Lysine residues 3
Figure 1.3: Schematic of the ubiquitination system 4
Figure 1.4: The linkage type of a ubiquitin chain defines its topology 7
Figure 1.5: Model of different ubiquitin chain architectures 13
Figure 1.6: Schematic representation of CYLD 18
Figure 1.7: Schematic representation of A20 20
Figure 1.8: Schematic representation of OTULIN 22
Figure 1.9: Schematic of LUBAC and the structure of its subunits 23
Figure 1.10: Comparison of canonical and non-canonical NF-κB activation 32
Figure 1.11: Activation of Caspase-8 by proteolytic cleavage 40
Figure 1.12: TNF-induced complex II triggers apoptotic and necroptotic death 44
Figure 1.13: TNFR1-SC formation and regulation by the ubiquitin system 48
Figure 1.14: Death-promoting and -inhibiting factors in TNF signalling 50
Figure 1.15: The NOD2 signalling pathway 53
Figure 3.1: SPATA2, CYLD and OTULIN are constitutively associated with HOIP 74
Figure 3.2: SPATA2, CYLD, but not OTULIN are recruited to the TNFR1-SC 75
Figure 3.3: SPATA2 and CYLD recruitment to the TNFR1-SC requires HOIP 76
Figure 3.4: CYLD and SPATA2 recruitment to the NOD2-SC is HOIP-dependent 77
Figure 3.5: SPATA2 is destabilised in absence of CYLD 78
Figure 3.6: Binding of CYLD to HOIP is mediated by SPATA2 79
Figure 3.7: SPATA2 is required for recruitment of CYLD to the TNFR1-SC 80
Figure 3.8: OTULIN, SPATA2 and CYLD bind to the PUB domain of HOIP 81
Figure 3.9: The USP domain of CYLD is sufficient for binding to HOIP 82
Figure 3.10: SPATA2 binds CYLD and HOIP with different domains 83
Figure 3.11: A PIM in SPATA2 directly binds to the PUB domain of HOIP 84
Figure 3.12: The PIM in SPATA2 is highly evolutionary conserved 85
Figure 3.13: Enzymatically inactive OTULIN stabilises linear ubiquitin chains 86
Figure 3.14: Absence of OTULIN leads to accumulation of M1 ubiquitin chains 87
Figure 3.15: OTULIN's absence from the TNFR1-SC is not due to its activity 88
Figure 3.16: Ubiquitin-AP allows for enrichment of specific ubiquitin chains 90
Figure 3.17: OTULIN inhibits auto-ubiquitination of LUBAC 91
Figure 3.18: OTULIN deficiency does not increase TNF-induced gene activation 92
Figure 3.19: TNFR1 and TRADD are associated with M1-linked ubiquitin chains 93
Figure 3.20: Methodology to identify M1-ubiquitin chain-modified proteins 95
Figure 3.21: TNFR1, TRADD and RIP1 are modified with M1 ubiquitin chains 96
Figure 3.22: M1-ubiquitinated proteins cannot be isolated from HOIP-KO cells 97
Figure 3.23: Reduced ubiquitination of TRADD and TNFR1 in absence of HOIP 98

Figure 3.24: Ubiquitinated proteins are found in TX-100 insoluble fractions 100
Figure 3.25: Denatured proteins are not more efficiently enriched by Ubi-AP 102
Figure 3.26: HOIP-deficiency sensitises cells to necroptosis and apoptosis 103
Figure 3.27: Necrosome formation is enhanced in HOIP-deficient cells 104
Figure 3.28: CYLD inhibits K63- and M1- ubiquitination of the TNFR1-SC 106
Figure 3.29: CYLD cleaves linear and other ubiquitin chains from LUBAC targets 107
Figure 3.30: Ubiquitination of NEMO is increased in HOIP-N102A cells 108
Figure 3.31: Lack of CYLD/SPATA2 hardly affects gene activation pathways 109
Figure 3.32: CYLD-deficiency in BMDMs leads to enhanced gene activation 110
Figure 3.33: SPATA2 or CYLD deficiency reduces TNF-induced necroptosis 111
Figure 3.34: Recruitment of A20 to the TNFR1-SC depends on HOIP 112
Figure 3.35: Absence of A20 leads to reduction of M1-ubiquitination 113
Figure 3.36: A20-deficiency reduces M1 ubiquitination of the NOD2-SC 114
Figure 3.37: A20 supresses NF-κB activation independently of its DUB activity 115
Figure 3.38: A20 mediates resistance to TNF-induced cell death via its ZF7 116
Figure 4.1: Updated scheme of TNFR1-SC assembly and regulation by DUBs 125

IV. List of Tables

Table 1.1: Relative abundance of ubiquitin linkages (Dammer et al. 2011) 6
Table 2.1: Unconjugated antibodies 57
Table 2.2: Horseradish-peroxidase (HRP)-conjugated antibodies..... 58
Table 2.3: 5' PCR master mix set-up 68
Table 2.4: 2X Kapa-HiFi master mix set-up 69

V. Acknowledgments

I want to thank my supervisor Prof. Henning Walczak for granting me the possibility to embark on this PhD project in his laboratory and for allowing me to expand my knowledge and abilities.

Thanks to all members of the UCL Cancer Institute, past and present, for their friendship, support and being part of this wonderful experience, which makes my time in London truly unforgettable!

Thanks to everybody who contributed to this work in one way or the other! Thank you, Aida Daboh, Alexandra Sevko, Amandeep Bhamra, Annalisa Conti, Antonella Montinaro, Chahrazade Kantari, Diego de Miguel, Elodie Lafont, Eva Rieser, Helena Draberova, Itziar Areso, Johannes Lemke, Julia Zinngrebe, Katarzyna Wojdyla, Katrin Rittinger, Lucia Taraborrelli, Luigi Martino, Matthias Reichert, Maureen Spit Maurice Darding, Nieves Peltzer, Silvia Surinova, Silvia von Karstedt, Torsten Hartwig and Yutaka Shimizu.

My thanks go to Peter Draber without whom this project would not have been the same. Thanks for the stimulating discussions, in and outside of the lab, and for your comradery.

Thanks to my Students Anne Stinn and Marcel Hahn for their contributions and help.

Thumbs up and thanks to my fitness crew, Lucia Taraborrelli, Maurice Darding, Francesca Vena, Itziar Areso for successfully spicing up the daily lab routine.

Ich danke meiner Mutter Valeria für ihre Unterstützung bei all meinen Entscheidungen und ihr Vertrauen in mich. Ich möchte meinem Vater Werner dafür danken, mir diesen Lebensweg ermöglicht zu haben. Danke an euch beide für eure Wertevermittlung, welche mich stets durch jeden Tag geleitet.

My thanks and gratitude go to Viktoria for enriching my life with love and happiness. Thank you for always standing by me, and for being my moral support and cheering me up in difficult times!

VI. Table of Contents

I. Declaration i
II. Abstract ii
III. Table of Figures iii
IV. List of Tables v
V. Acknowledgments vi
VI. Table of Contents vii
1 Introduction 1
1.1 Ubiquitination 1
1.1.1 E3-ligases 4
1.1.2 Ubiquitin linkage abundance 5
1.1.3 Ubiquitin chain topology 6
1.1.4 Ubiquitin binding proteins 7
1.1.5 Linear ubiquitin chain specific UBDs 9
1.1.6 Proteasomal degradation by K48-ubiquitination 10
1.1.7 Cell signalling and K63-ubiquitination 12
1.1.8 Branched ubiquitin chains 13
1.2 Deubiquitination 15
1.2.1 Regulation of DUBs 16
1.2.2 Mode of chain cleavage 17
1.2.3 CYLD 18
1.2.4 A20 20
1.2.5 OTULIN 21
1.3 Linear Ubiquitin Chain Assembly Complex (LUBAC) 22
1.3.1 HOIP 24
1.3.2 HOIL-1 26
1.3.3 Sharpin 27
1.4 NF-κB pathway 28
1.4.1 Canonical NF-κB signalling 29
1.4.2 Non-canonical NF-κB activation 33
1.5 MAPKs 34
1.5.1 ERK-signalling cascade 35
1.5.2 JNK-signalling cascade 36
1.5.3 p38-signalling cascade 37
1.6 Cell death 37
1.6.1 Apoptosis 38
1.6.2 Necroptosis 42
1.7 TNFR1 signalling and its regulation by ubiquitin 45

1.7.1 Impact of defective ubiquitination on TNFR1-signalling 48
1.7.2 Shutdown of TNFR1-signalling by DUBs 50
1.7.3 TNFR1-induced cell death 50
1.8 Pattern recognition receptors 51
1.8.1 NOD2-signalling 52
1.9 Aim of this project 54
2 Materials & Methods 55
2.1 Materials 55
2.1.1 Chemicals & reagents 55
2.1.2 Buffers & solutions 55
2.1.3 Antibodies 57
2.1.4 Kits and Ready-to-Use Solutions 59
2.1.5 Instruments 59
2.1.6 Consumables 60
2.1.7 Software 62
2.1.8 Cell lines 62
2.2 Methods 64
2.2.1 Culturing of eukaryotic cells 64
2.2.2 Freezing and thawing of eukaryotic cells 64
2.2.3 Isolation of Bone Marrow Derived Macrophages (BMDMs) 64
2.2.4 Transient transfection 64
2.2.5 siRNA-mediated knockdown 65
2.2.6 Retro- and lentivrial infection of eukaryotic cells 65
2.2.7 Generation of knockout cell lines using Lentiviral CRISPR-Cas9 66
2.2.8 Use of inhibitors in cellular systems 66
2.2.9 Quantification of cell death 66
2.3 Molecular Biology 66
2.3.1 DNA restriction digest 66
2.3.2 Purification of DNA 67
2.3.3 Agarose gel electrophoresis of DNA 67
2.3.4 Gel extraction of DNA fragments 67
2.3.5 Ligation of DNA fragments for cloning 67
2.3.6 Transformation of competent E.coli 68
2.3.7 Isolation of Plasmid DNA 68
2.3.8 Isolation of genomic DNA 68
2.3.9 Polymerase Chain Reaction (PCR) 68
2.3.10 Preparation of cDNA 69
2.4 Biochemistry 70

2.4.1 Relative measurement of protein concentration 70
2.4.2 Quantitative determination of protein and DNA concentration 70
2.4.3 SDS polyacrylamide gel electrophoresis (SDS-PAGE) 70
2.4.4 Coomassie staining of SDS-PAGE gels 70
2.4.5 Western blot 70
2.4.6 Production of recombinant TNF 71
2.4.7 Production and coupling of ubiquitin affinity proteins 71
2.4.8 Production of deubiquitinases (DUBs) 73
2.4.9 Immunoprecipitation of protein complexes 73
2.4.10 TNFR1-SC purification 73
3 Results 74
3.1 Analysis of the interaction of CYLD, OTULIN and SPATA2 with HOIP 74
3.1.1 CYLD and SPATA2, but not OTULIN, are recruited to the TNFR1-SC 75
3.1.2 CYLD and SPATA2 recruitment to the TNFR1-SC is HOIP dependent 76
3.1.3 CYLD and SPATA2 are also recruited to the NOD2-SC 77
3.1.4 Deficiency in CYLD leads to loss of SPATA2 stability 78
3.2 Characterisation of the SPATA2-CYLD-HOIP interaction 78
3.2.1 CYLD interacts indirectly with HOIP via SPATA2 78
3.2.2 SPATA2 is required for recruitment of CYLD to the TNFR1-SC 80
3.2.3 OTULIN and CYLD interact with the PUB domain of HOIP 80
3.2.4 The USP domain of CYLD is sufficient for interaction with HOIP 82
3.2.5 SPATA2 binds CYLD and HOIP with different domains 82
3.2.6 SPATA2 contains a PIM that directly interacts with the PUB of HOIP 83
3.2.7 The PIM of SPATA2 is evolutionary conserved 84
3.3 Functional relevance of OTULIN for LUBAC function 85
3.3.1 Inactive OUTLIN stabilises M1-ubiquitination 85
3.3.2 Aberrant M1-linked ubiquitin chains are conjugated to unknown targets 86
3.3.3 Absence of OTULIN from the TNFR1-SC is not due to its DUB activity 88
3.3.4 Ubiquitin binding domains can be used to enrich ubiquitinated proteins 88
3.3.5 OTULIN controls LUBAC function in the cytosol 90
3.3.6 Absence or knockdown of OTULIN does not affect TNF-signalling 91
3.4 Discovery of LUBAC substrates 92
3.4.1 Comparison of M1- and total ubiquitination affinity purification 93
3.4.2 TNFR1 and TRADD are modified with M1-linked ubiquitin chains 94
3.4.3 Verification of the linear ubiquitination of TNFR1, TRADD and RIP1 97
3.4.4 Total TRADD and TNFR1 ubiquitination is affected by LUBAC absence 98
3.5 Comparison of different lysis conditions to extract the TNFR1-SC 99
3.5.1 Ubiquitinated TNFR1-SC components become Triton X-100 insoluble 99

3.5.2 Ubiquitinated TNFR1-SC proteins can be extracted by lysis in SDS 101
3.6 LUBAC-deficiency sensitises cells to cell death 102
3.7 Functional analysis of CYLD-deficiency on TNFR1 signalling 105
3.7.1 Deficiency in CYLD leads to increased TNFR1-SC ubiquitination 105
3.7.2 CYLD can remove linear- and other ubiquitin linkages from proteins 106
3.7.3 NEMO ubiquitination is increased in HOIP-N102A expressing cells 108
3.7.4 Deficiency in SPATA2 or CYLD has similar effects on gene activation 108
3.7.5 CYLD and SPATA2 are required for TNF-induced necroptosis 110
3.8 A20 recruitment and its involvement in TNFR1-SC regulation 111
3.8.1 A20 is recruited to the TNFR1-SC in a HOIP dependent manner 112
3.8.2 Linear ubiquitin chains are reduced in A20-deficient cells 113
3.8.3 Absence of A20 also decreases linear ubiquitination in the NOD2-SC 114
3.8.4 Presence of A20 supresses gene activatory signalling 115
3.8.5 A20 recruitment to linear ubiquitin chains prevents cell death 115
4 Discussion 117
4.1 LUBAC constitutively associates with SPATA2/CYLD or OTULIN 117
4.2 Recruitment of CYLD to signalling complexes via LUBAC 119
4.3 TNFR1 and TRADD are LUBAC substrates 120
4.4 Regulation of TNFR1-SC ubiquitination by CYLD, OTULIN and A20 123
4.4.1 CYLD counteracts LUBAC function in signalling complexes 123
4.4.2 Regulation of TNF signalling by OTULIN 124
4.5 HOIP-dependent recruitment of A20 125
4.6 Regulation of TNF-induced cell death by LUBAC 127
4.7 Summary and future directions 129
5 Appendix 132
5.1 Abbreviations 132
5.2 List of publications 140
6 References 141

1 Introduction

1.1 Ubiquitination

Ubiquitin was discovered in 1975 as a ubiquitously expressed molecule (Ciehanover, Hod et al., 1978, Goldstein, Scheid et al., 1975, Hershko, Ciechanover et al., 1979). This 76 amino acid (aa) protein is conserved from yeast to human and involved in a vast amount of cellular functions (Hershko & Ciechanover, 1998, Komander & Rape, 2012). Ubiquitin is encoded by four different genes *RPS27A*, *UBA52*, *UBB* and *UBC*. *UBB* and *UBC* encode for ubiquitin repeats that form a linear ubiquitin chain (Wiborg, Pedersen et al., 1985). Ubiquitin expressed from *RPS27A* and *UBA52* is fused with the ribosomal protein S27a or L40, respectively, and is processed after translation (Baker & Board, 1991, Redman & Rechsteiner, 1989). These chains are readily disassembled by ubiquitin-specific proteases called deubiquitinases (DUBs) (Wilkinson, 1997). Ubiquitin is involved in regulation of cell signalling, protein degradation and recycling (Ciechanover, Finley et al., 1984, Glickman & Ciechanover, 2002, Hershko et al., 1979). As a posttranslational-modification, ubiquitin is conjugated to other molecules, a process known as ubiquitination. The conjugation of ubiquitin is usually made to a lysine residue (K) in the target molecule. In case of mono-ubiquitination, an isopeptide bond is formed between the N-terminus of the substrate's lysine and the C-terminus of the glycine (Gly) residue of the incoming ubiquitin (Figure 1.1). In a second step, ubiquitin itself can be targeted for ubiquitination by linking a distal ubiquitin to the target protein-bound proximal ubiquitin. This step again creates an isopeptide bond. Sequential addition of ubiquitin molecules, linked via the same lysine residue by an isopeptide bond, creates a ubiquitin chain. Alternatively, the distal ubiquitin can be conjugated to the amino-terminus of the proximal ubiquitin. This creates a peptide bond between the two ubiquitin moieties. This 'head-to-tail' linked chain is therefore referred to as a linear or M1 ubiquitin chain.

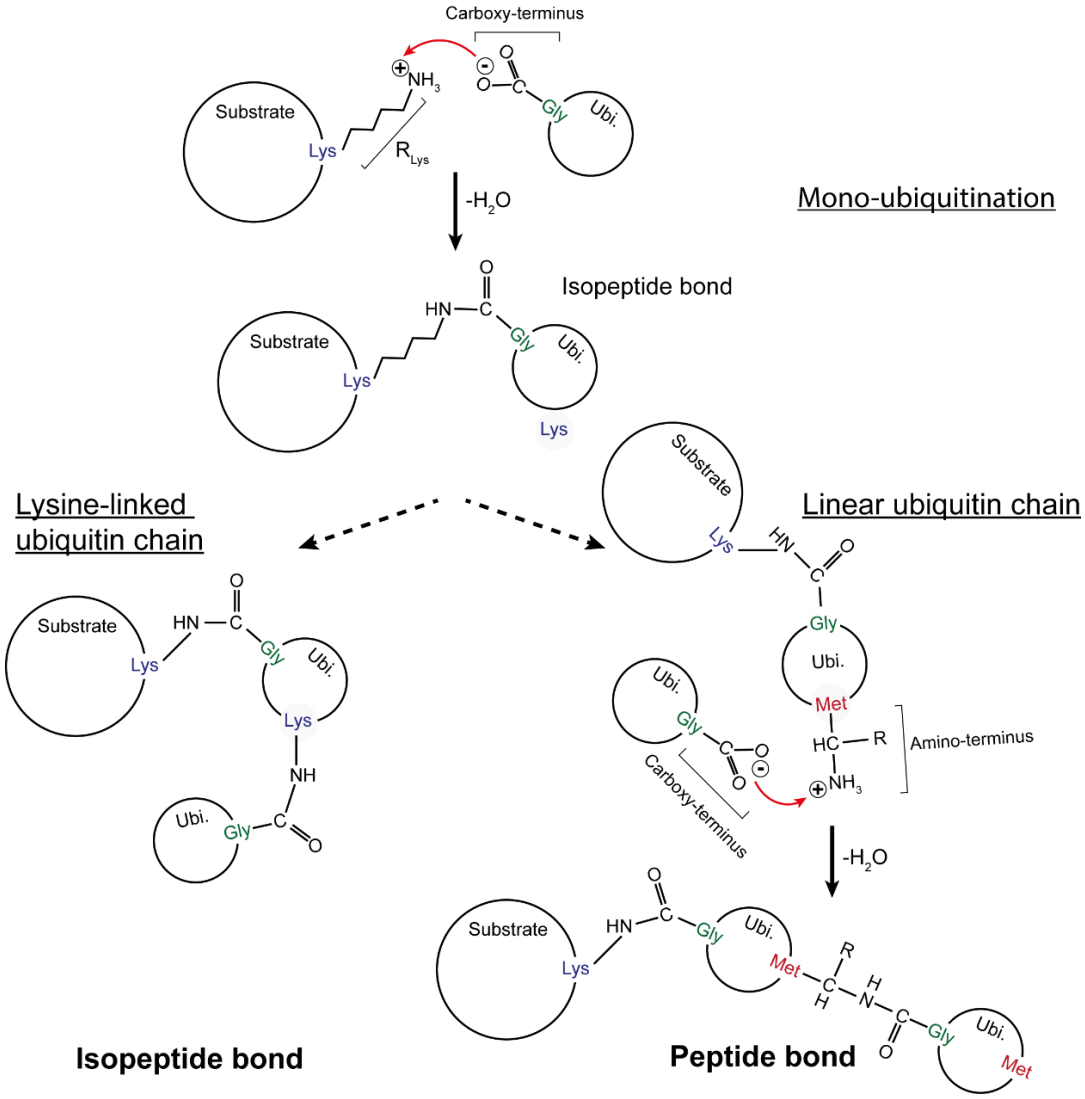

Figure 1.1: Creation of lysine- and M1-linked ubiquitin chains

The ubiquitin chain is structurally defined by one of seven lysines (K6, K11, K27, K29, K33, K48, K63) or the amino-terminal (N-terminal) methionine (M1), which is used to create the linkage (Figure 1.2) (Clague & Urbé, 2010, Komander & Rape, 2012).

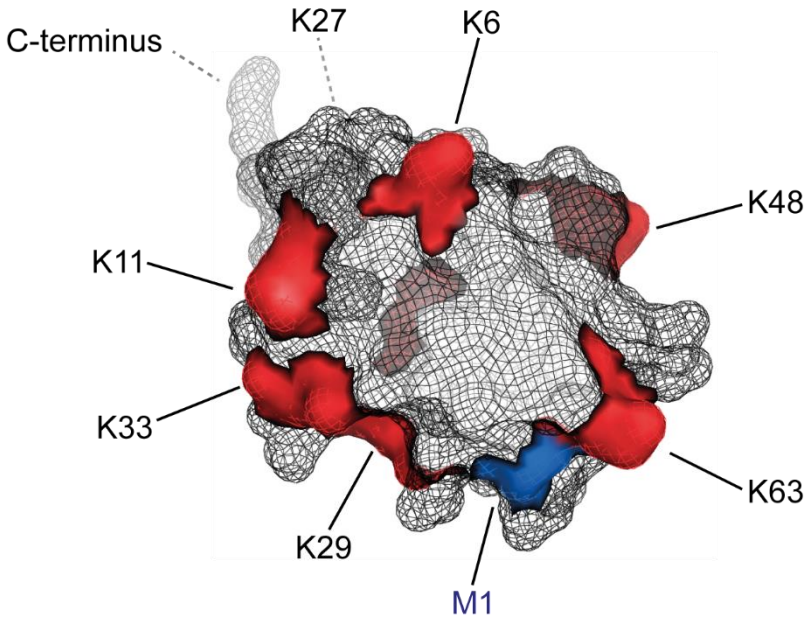

Figure 1.2: Ubiquitin structure and position of Lysine residues

The N-terminal methionine is depicted in blue, Lysine residues are marked red. PDB: 1UBQ.

The ubiquitination machinery is a hierarchy of ubiquitin-activating, -conjugating and -ligating enzymes (Figure 1.3). First, ubiquitin needs to be activated by an E1 ubiquitin-activating enzyme. In an adenosin triphosphat (ATP) dependent manner, the E1 forms a thioester bond between a cysteine sulfhydryl group and the C-terminal carboxyl group of ubiquitin. The human genome encodes only two E1s. The activated ubiquitin can then be transferred from the E1 to the active site of one of 35 different E2 ubiquitin-conjugating enzymes. The conjugation of ubiquitin to the target protein is finally catalysed by E3 ubiquitin ligases, which are able to bind to the substrate and the E2 at the same time (Scheffner, Nuber et al., 1995). More than 300 E3s are known, which mediate substrate recognition and often define the chain type which is created.

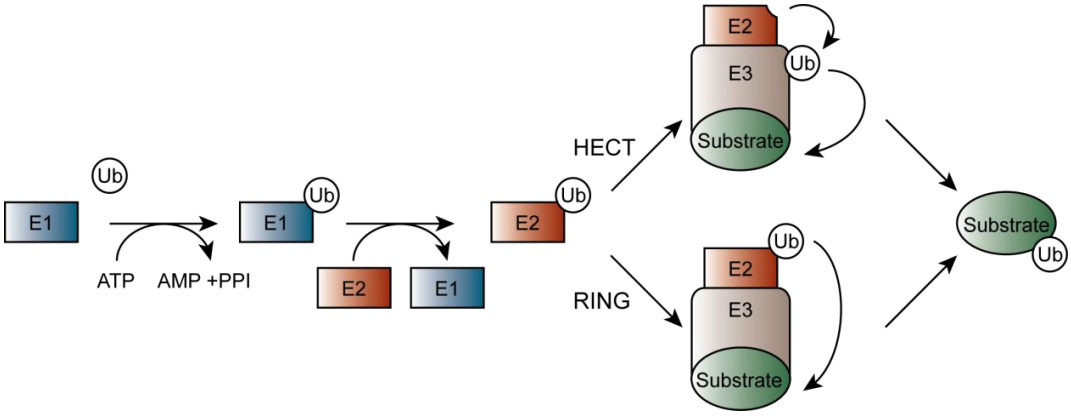

Figure 1.3: Schematic of the ubiquitination system

In an initial step, a thioester bond is formed between the cysteine sulfhydryl group of the E1 ubiquitin-activating enzyme and the C-terminal carboxyl group of ubiquitin. The activated ubiquitin is then transferred from the E1 to the active site of an E2 ubiquitin-conjugating enzyme. The last reaction is catalysed by an E3 ubiquitin ligase. HECT E3s form an E3-ubiquitin intermediate before transferring ubiquitin onto a substrate. RING E3s act as a scaffold by bringing E2 and substrate in close proximity, thus allowing a direct transfer of ubiquitin from the E2 to the substrate.

1.1.1 E3-ligases

Distinguished by their catalytic domain, there are two major classes of E3s. The homologous to the E6-AP carboxyl terminus (HECT) type E3s directly bind to ubiquitin in an intermediate reaction before transferring it onto the target protein (Figure 1.3) (Huang, Kinnucan et al., 1999, Verdecia, Joazeiro et al., 2003). Members of this family are characterised by their bilobal HECT-domain. Whilst the N-terminal lobe binds to the E2, the C-terminal lobe harbours the catalytic centre (Huibregtse, Scheffner et al., 1995). HECT E3s often contain additional protein interaction domains located at their N-terminus, whereas the HECT domain itself is usually located at the C-terminal end of the protein (Rotin & Kumar, 2009). HECT E3s mediate ubiquitination by forming a thioester-intermediate between ubiquitin and their catalytic cysteine. The loaded E3 then transfers ubiquitin to the amino-group of a target residue thus forming an isopeptide-bond (Figure 1.1) (Scheffner et al., 1995). Consequently, HECT E3s actively influence the linkage type of the resulting ubiquitin chain (Kim & Huibregtse, 2009).

In contrast to HECT E3s, really interesting new gene (RING) type E3s catalyse the direct transfer of ubiquitin from the E2 to the substrate without forming an E3-

ubiquitin-intermediate (Deshaies & Joazeiro, 2009). RING E3s function as ubiquitination adaptors by bringing E2 and substrate in close proximity (Zheng, Wang et al., 2000). This only allows for ubiquitination of certain residues which are in close proximity to the E2. Guiding substrates to the E2 may also involve domains other than the RING domain. Ubiquitin binding domains like zinc finger domains are often found in RING E3s (Li, Bengtson et al., 2008). Functionally, these domains may help to direct the E3 to signalling complexes and substrates.

A subclass of the RING-family is characterised by the presence of two RING domains separated by an in-between-RING (IBR) domain. These RING1-IBR-RING2 or RBR-domains are ~200aa long and characteristic for the RBR-family (Wenzel & Klevit, 2012). Interestingly, the RING2 of the RBR-family members ARIH1 and parkin mediate ubiquitination by formation of a ubiquitin thioester intermediate (Wenzel, Lissounov et al., 2011). Consequently, RBR-members are functioning as RING/HECT hybrids.

While many E3s readily ubiquitinate their substrates *in vitro*, their regulation *in vivo* is poorly understood. As constitutive ubiquitination of substrates is not always observed, ubiquitination in cells is likely regulated by signalling complex formation, which brings ligase and substrate in close proximity. Certain ubiquitin ligases also undergo auto-ubiquitination following their activation, which can either promote their activity or lead to their proteasomal degradation (de Bie & Ciechanover, 2011).

1.1.2 Ubiquitin linkage abundance

The diversity of E3s is not only required for their substrate specificity, but also relates to their capability to conjugate different ubiquitin-chain linkages (Yau & Rape, 2016). However, atypical ubiquitin linkages (non-K48- or K63-linked chains) represent only a fraction of the possible linkage types (Table 1.1) (Dammer, Na et al., 2011). This shows that K48- and K63-linkages are prevailing in cell signalling processes. Other linkage types seemingly fulfil more specialised tasks. Accordingly, these chain types may have been underestimated in this study, as they might only be generated following a certain stimulus. In many cases, the specific function of a given linkage type is not known, also because proteins are usually modified with several linkage types simultaneously (Yau & Rape, 2016). Moreover, their creation, removal and function may depend on each other, thus making it difficult to attribute a certain function to a specific chain. The complexity and functional aspects of ubiquitination and its role in cell signalling will be discussed in the following chapters.

Table 1.1: Relative abundance of ubiquitin linkages (Dammer et al. 2011)

Linkage type	Relative abundance [%]
K48	52
K63	38
K29	8
K11	2
K27, K33, K6, M1	<0.5

1.1.3 Ubiquitin chain topology

Formation of a ubiquitin chain, linked by one of the seven different lysine residues, results in a specific chain topology (Komander & Rape, 2012, Komander, Reyes-Turcu et al., 2009b). As shown in figure 1.4, depending on the lysine that is used to create the ubiquitin chain, a different molecular surface is created between the individual ubiquitin-moieties. Of significant importance are hydrophobic patches surrounding Ile36 and Ile44 as these areas are directly involved in binding of ubiquitin to other proteins. Importantly, the relative orientation of these patches within the ubiquitin chain is specific for each linkage type (Figure 1.4). Additionally, the linkage type defines the spatial conformation of the ubiquitin chain. K63-linked ubiquitin chains for instance adopt a straight and open conformation. K6-, K11- and K48-linked ubiquitin chains adopt a compact conformation. K48-linked tetra ubiquitin chains were also found to interact intramolecularly via their Ile44 patches, thus forming a tightly packed structure (Eddins, Varadan et al., 2007). The M1 linkage is a special case from a chemical point of view, as the peptide bond between the two linked ubiquitin moieties results in a rather rigid bond, where the only contact point between the two molecules is the linkage-point. The reduced flexibility of the linear linkage provides a structurally defined surface for ubiquitin-binding molecules. Lysine-linkages in contrast are very mobile and can adopt a range of conformations (Akutsu, Dikic et al., 2016, Komander et al., 2009b). Specifically, these chain types tolerate bending, which is required by certain ubiquitin binders, thus discerning it from the otherwise similar linear ubiquitin chain. Structural constrains can also have a negative effect on the ability of DUBs to cleave linear ubiquitin chains and several DUBs with otherwise broad specificity are ineffective in cleaving M1-linked chains (Ritorto, Ewan et al., 2014). Structural analysis of a DUB or ubiquitin binding domain (UBD) in a complex with the respective ubiquitin chain is usually the only way to uncover the underlying mechanism of chain recognition (Komander, Clague et al., 2009a). An interesting example is binding of Associated molecule with the SH3 domain of STAM (AMSH) to

K63-linked via two insertion Ins-1 and Ins-2 within its catalytic domain. Ins-1 specifically interacts with the distal ubiquitin while the proximal ubiquitin interacts with Ins-2 (Sato, Yoshikawa et al., 2008). Binding of AMSH stretches the K63-linkage which possibly facilitates cleavage of the chain (Lange, Lakomek et al., 2008). This mechanism of employing two distinct binding surfaces, combined with the flexibility of the K63-linkage, makes AMSH specific for these chains and unable to bind and cleave the structurally similar linear chain or any other linkage type (Ritorto et al., 2014, Sato et al., 2008).

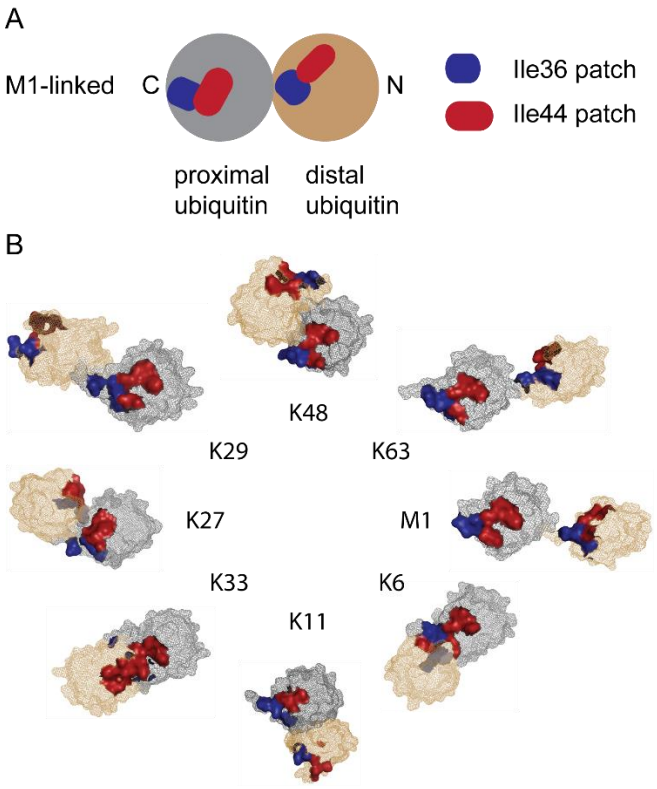

Figure 1.4: The linkage type of a ubiquitin chain defines its topology

(A) The C-terminus of the proximal ubiquitin can be attached to another protein. Conjugation of the C-terminus of a distal ubiquitin to one of the lysine residues or Met1 in the proximal ubiquitin creates a diubiquitin with a defined topology. The relative orientation of the hydrophobic patches surrounding Ile36 and Ile44 are unique between the linkage types.

(B) Overview of the different possible ubiquitin linkages and their topologies. Models were created with PyMol and published structural data. PDB accession files: M1 2W9N, K6 2XK5, K11 2XEW, K27 5GOD, K29 4S22, K33 4XYZ, K48 3AUL, K63 3H7P.

1.1.4 Ubiquitin binding proteins

Because of the distinct binding surface each ubiquitin linkage type creates, binding platforms are formed which recruit molecules with linkage-specific UBDs. 20 different

types of UBDs are known to have evolved to interact with the different ubiquitin linkage types. Most UBDs utilise the hydrophobic patch surrounding Ile44 of ubiquitin for binding (Dikic, Wakatsuki et al., 2009). The relative orientation of this patch depends on the linkage type of the chain and therefore determines whether this patch can create an interface with the ubiquitin binding domain. Several UBDs use an α–helix for binding to the Ile44 patch (Hicke, Schubert et al., 2005). This includes e.g. ubiquitin-interacting motif (UIM), ubiquitin-associated (UBA), GGA and TOM (GAT) and ubiquitin binding in ABIN and NEMO (UBAN) (Dikic et al., 2009, Hurley, Lee et al., 2006). Another group of UBDs bind ubiquitin via zinc fingers. These are for example Npl4 zinc finger (NZF), A20-type zinc finger (ZnF_A20) and ubiquitin-binding ZnF (UBZ) (Husnjak & Dikic, 2012). In addition to the Ile44 patch, several UBDs, including RAB5 guanine nucleotide exchange factor (RABEX5), bind to a polar surface in ubiquitin around Asp58 (Lee, Tsai et al., 2006). The affinity of a single UBD for polyubiquitin can be, with a K_D in the µM to mM range, rather low (Hjerpe, Aillet et al., 2009). However, some proteins harbour tandem UBDs or several UBDs across the protein. This increases the avidity of the protein to polyubiquitin. Although many UBDs are structurally similar and present across a variety of proteins, they are involved in very different cellular functions and often do not show the same linkage specificity (Dikic et al., 2009, Komander & Rape, 2012). Highly specialised UBDs exist which can only bind to one chain type. Linkage-specific binding of proteins can also be sometimes explained by the presence of tandem repeats of UBDs (Hirano, Kawasaki et al., 2006a). In this scenario, two consecutive UBDs are restricted in their conformation which, in turn, requires a surface across at least two ubiquitin-moieties which mediates specific binding to the UBDs in a linkage-specific manner. Such an example can be found in the DUB ataxin-3 which is involved in protein homeostasis by degradation of misfolded proteins. The tandem UIMs in ataxin-3 are separated by a short linker region that dictates specific binding to K48-linked chains. Interestingly, perturbation of this linker region can switch the linkage preference from K48- to K63-specific (Song, Zhou et al., 2010).

Nuclear magnetic resonance (NMR) studies of ubiquitin chains, complexed with different UBDs, revealed that the conformation each linkage-types adopts is variable and dependent on the UBD that it binds to (Komander & Rape, 2012, Komander et al., 2009b, Lange et al., 2008). Molecular discrimination of the different ubiquitin linkages is especially important for establishing a physiological function for each chain type. However, also monoubiquitination has specific functions. The endosomal-sorting complex required for transport (ESCRT) utilises UBD-containing proteins to

bind to ubiquitinated cargo which is then deposited in multivesicular bodies (MVBs) (Hirano et al., 2006a, Hirano, Suzuki et al., 2006b, Katzmann, Babst et al., 2001). In this context, mono-ubiquitination of cell surface receptors was identified to mediate their internalisation and lysosomal degradation (Haglund, Di Fiore et al., 2003). Mono-ubiquitination can also mediate proteasomal degradation. For example, the nuclear factor kappa B (NF-κB) precursor p105 undergoes partial proteasomal processing to form a p50 fragment. This process is triggered by mono-ubiquitination events, rather than conjugation of a polyubiquitin chain (Kravtsova-Ivantsiv, Cohen et al., 2009).

Ubiquitin binding domains can also be found in adaptor molecules or sometimes also in DUBs. The DUB A20, for instance, has seven zinc finger domains of which many were shown to bind to ubiquitin (Bosanac, Wertz et al., 2010, Evans, Ovaa et al., 2004, Tokunaga, Nishimasu et al., 2012). In other cases, kinases and other regulatory proteins require the interaction with a ubiquitin binding protein for their recruitment to signalling complexes. An example are the NZFs in TAK1-binding protein 2 and 3 (TAB2, TAB3) which preferentially bind to K63-linked ubiquitin chains (Kulathu, Akutsu et al., 2009, Ori, Kato et al., 2013). Their specificity is the result of simultaneous binding of the NZF to the hydrophobic Ile44 patch in the proximal and distal ubiquitin. TAB2/3 mediate the recruitment of TAK1 to signalling complexes (Kanayama, Seth et al., 2004, Ori et al., 2013). Another prominent example is radiation sensitivity abnormal 23 (Rad23) which has ~4-fold higher affinity for K48-ubiquitin linkages over K63-chains (Chen & Madura, 2002). Functionally, this is linked to proteasomal degradation as Rad23, while binding to ubiquitin with its UBA domain, can bind to the 26S proteasome with its ubiquitin like (UBL) domain (Schauber, Chen et al., 1998).

Overall, UBDs can specifically recognise binding platforms in signalling complexes which are created by various combinations of ubiquitin linkages. Hence, ubiquitin binders translate the ‘ubiquitin code’, which is generated by the different ubiquitin linkage types, and regulate signalling complex assembly and disassembly in a broad range of cell signalling pathways (Komander & Rape, 2012, Walczak, Iwai et al., 2012).

1.1.5 Linear ubiquitin chain specific UBDs

With the discovery of the linear ubiquitin chain assembly complex (LUBAC) and its ability to generate M1-linked ubiquitin chains, several linear ubiquitin specific UBDs were identified (Haas, Emmerich et al., 2009, Hadian, Griesbach et al., 2011, Rahighi & Dikic, 2012, Rahighi, Ikeda et al., 2009, Sato, Fujita et al., 2011, Tokunaga et al.,

2012, Walczak et al., 2012). Importantly, M1-linked chains are associated with NF-κB-activating pathways which usually employ proteins that can bind to ubiquitin. The rigid topology of the linear ubiquitin chain aligns the hydrophobic patches surrounding Ile44 in the proximal and Phe4 in the distal ubiquitin. This unique configuration is the basis for binding by several linear ubiquitin specific UBDs, as discussed below.

NF-kappa-B essential modulator (NEMO) and A20-binding inhibitor of NF-kappa-B activation (ABIN) were shown to specifically bind to M1-linkages via their UBAN domain (Rahighi et al., 2009, Verhelst, Carpentier et al., 2012, Wagner, Carpentier et al., 2008). The UBAN domain binds with high specificity to linear ubiquitin chains and likely helps to guide these molecules to signalling complexes in a spatiotemporal manner (Lo, Lin et al., 2009, Rahighi et al., 2009) The specificity is the result of a UBAN coiled-coil dimer, which creates a long interface involving the Ile44 in the distal and the Phe4 patch in the proximal ubiquitin. The NZF of the LUBAC subunit HOIL-1 also preferentially binds to linear ubiquitin chains (Sato et al., 2011). The specificity is achieved by simultaneous binding of the NZF to two distinct regions on the ubiquitin molecules. Similar to the UBAN dimer, the NZF core binds to the hydrophobic region surrounding Ile44 in the distal ubiquitin, while the α-helical tail of the NZF binds to the hydrophobic patch around Phe4 in the proximal ubiquitin (Sato et al., 2011). Another example is OTU Deubiquitinase With Linear Linkage Specificity (OTULIN), a DUB which specifically binds and cleaves linear ubiquitin chains with remarkable specificity. The interface on both ubiquitin molecules covers 1,925 $Å^2$ in total involving the Ile44- on the distal and the Phe4-patch on the proximal ubiquitin (Keusekotten, Elliott et al., 2013). Importantly, the binding orientates the linear ubiquitin linkage perfectly near the catalytic centre of OTULIN, thus excluding non-specific cleavage of other linkage types.

1.1.6 Proteasomal degradation by K48-ubiquitination

One of the best understood ubiquitin modification is the K48-linked chain (Ciehanover et al., 1978, Hershko & Ciechanover, 1998). It is an essential mechanism for targeting proteins for proteasomal degradation (Chau, Tobias et al., 1989). K48-chain-mediated degradation of proteins is involved in many cell functions including receptor signalling, cell cycle control and stress response (Glickman & Ciechanover, 2002). The topology of K48-linked chains differs from e.g. K63-linked chains by adopting a compact structure, which is markedly different regarding the position of exposed hydrophobic surfaces (Figure 1.4) (Varadan, Walker et al., 2002). It is not entirely

clear how K48-ubiquitination targets proteins to the proteasome. The 26S proteasome is composed of two large subunits; a regulatory and an active core unit (based on their sedimentation coefficient, also referred to as 19S and 20S, respectively), which are in turn composed of several functional modules (Finley, 2009). Although the proteasome contains UBDs itself, shuttling of ubiquitinated substrates to the proteasome also requires substrate adaptors. Members of the RAD and DSK family and DDI1, are examples of adaptors that possess UBA domain(s) and a UBL) domain (Hartmann-Petersen & Gordon, 2004, Schauber et al., 1998). Binding of these adaptors to K48-chains via their UBA allows subsequent shuttling of the bound protein to the proteasome. The adaptors are in turn recognised by the proteasome via their UBL domain. In the course of proteasomal degradation, the substrate is first bound by the 19S subunit and ubiquitin chains are hydrolysed by the deubiquitinating module Poh1 (Yao & Cohen, 2002). Removal of substrate-associated ubiquitin chains is vital for the process. The substrate protein is subsequently unfolded and guided to the entry of the catalytic core, where the protein is hydrolysed to short peptides (Finley, 2009). This process is also central for the generation of peptides that are loaded in the major histocompatibility complex (MHC). 8-10 amino acid long peptides are bound by the MHC class I before translocating to the cell membrane (Goldberg, Cascio et al., 2002, Kisselev, Akopian et al., 1999). The source can be endogenous but also viral, bacterial or any other pathogen-derived protein.

Perturbation of the proteasomal pathway has drastic effects on cell viability. Studies in yeast showed that the ability to create K48-chains is essential for survival as a Lys48 to Arg substitution mutant was not viable (Finley, Sadis et al., 1994, Spence, Sadis et al., 1995). However, ubiquitin that can only form K48-linked chains does not support viability in yeast, either (Xu, Duong et al., 2009b). Inhibition of the proteasome leads to a rapid accumulation of K48-ubiquitinated proteins (Kisselev & Goldberg, 2001, Xu et al., 2009b). In the context of cell death, it was shown that inhibition of the proteasome leads to an increase of otherwise degraded pro-apoptotic factors, like p53 (Lopes, Erhardt et al., 1997). In turn, because the proteasome is required for gene activation by e.g. turn-over of ubiquitinated IκBα, anti-apoptotic proteins are not upregulated in response to death receptor-induced gene activation (Li & Dou, 2000, Ling, Liebes et al., 2002). Perturbation of this vital pathway can therefore be harnessed to modulate the cell's response to different stimuli in cancer treatment as shown for the proteasomal inhibitor bortezomib (Velcade ®), which is approved for

treatment of multiple myeloma (Chauhan, Singh et al., 2008, Moreau, Richardson et al., 2012).

1.1.7 Cell signalling and K63-ubiquitination

In contrast to the strong association of K48-linked ubiquitin chains with proteasomal degradation, K63-linked chains are known to regulate non-degradative pathways (Chen & Sun, 2009). While mutation of K48 of ubiquitin is lethal in yeast, K63-dependent ubiquitination is not crucial for survival (Spence et al., 1995). However, cells carrying this mutation have defects in DNA repair and are sensitive to DNA-damaging agents (Spence et al., 1995). Indeed, an increased K63-ubiquitination of histones can be observed following DNA-damage (Al-Hakim, Escribano-Diaz et al., 2010, Huen, Grant et al., 2007, Kolas, Chapman et al., 2007). This localised increase in K63-linked chains functions as a recruiting platform for DNA-repair complexes (Al-Hakim et al., 2010). While some of the involved E3s, including RING finger protein 8 (RNF8) or Rnf168 harbour a ubiquitin binding domain, breast cancer 1 (BRCA1) requires an adaptor, Rap80, for its recruitment to the site of DNA damage (Al-Hakim et al., 2010, Kim, Chen et al., 2007a, Stewart, Panier et al., 2009). The specificity of Rap80 for K63-linkages is the result of simultaneous binding of two UIMs to the Ile44 patch (Sato, Yoshikawa et al., 2009). K48-chains cannot adopt the same orientation and are hence not recognised by Rap80 (Sato et al., 2009).

Following these early discoveries of atypical chain function, K63-linked ubiquitin chains were also found to be involved in the regulation of cell signalling pathways. A ubiquitin replacement strategy was used to evaluate the importance of K63-linked ubiquitin for TNF- and Interleukin-1 (IL-1)-signalling (Xu, Skaug et al., 2009a). In this approach, endogenous ubiquitin was knocked-down using short hairpin RNA (shRNA) and simultaneously replaced by expressing K63R ubiquitin. Surprisingly, TNF- and IL-1-signalling were differentially affected. Whilst TNF-induced NF-κB-signalling was largely normal in the cells expressing K63R ubiquitin, it was abrogated in IL-1 signalling (Xu et al., 2009a). This finding was supported by depletion of Ubc13, an E2 that is strongly associated with K63-ubiquitination (Wen, Wang et al., 2014), which abrogated IL-1β- but not TNF-mediated NF-κB activation (Xu et al., 2009a). This demonstrates that ubiquitin linkages can play redundant roles in certain signalling pathways, while their presence is required in others. In cytokine signalling, K63-linkages supposedly function as recruitment platforms for protein complexes required for gene activation (Ea, Deng et al., 2006, Kanayama et al., 2004, Tao,

Scacheri et al., 2009). This includes the TAB/ TGF-β-activated kinase 1 (TAB/TAK) complex and the NEMO/ inhibitor of κB kinase (NEMO/IKK) complex. Both complexes contain at least one factor that possesses ubiquitin binding capability (Ori et al., 2013, Rahighi et al., 2009). Seemingly, K63-linked chains make up most of the non-degradative ubiquitin chains in cells, suggesting that they represent a universal protein modification that can be utilised by many ubiquitin binding and modulating factors. Interestingly, K63-linked ubiquitin chains seem to be targeted for ubiquitination themselves. In this scenario, K63-linked chains may function as the "stem" for a branched ubiquitin chain (Figure 1.5). Additionally, the initial chain may also be extended with a different chain type to form a mixed chain (Figure 1.5). In many receptor signalling pathways, K63-linked chains are created by E3s of the TNF-receptor associated factor (TRAF)- family or cellular inhibitor of apoptosis protein 1/2 (cIAP1/2). Members of one or both classes are found in TNF, IL-1β and several innate immune receptors (Wajant, Henkler et al., 2001). In summary, K63-linked chains are debatably the most versatile non-degradative chain type that is associated with almost every signalling pathway involving polyubiquitination.

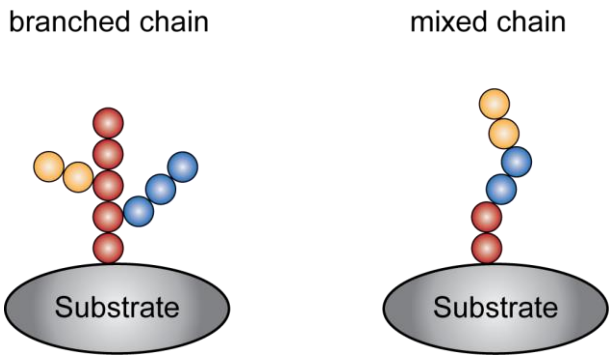

Figure 1.5: Model of different ubiquitin chain architectures

1.1.8 Branched ubiquitin chains

The existence of branched ubiquitin chains was previously suggested for Ring1B-mediated ubiquitination. Ring1B is a member of the polycomb group which was found to require K6-, K27-, and K48-linkages to be present on the same ubiquitin molecule (Ben-Saadon, Zaaroor et al., 2006). Later, CHIP, MuRF1 and Mdm2, in combination with the E2 UbcH5, were shown to generate forked ubiquitin chains composed of all possible lysine linkages, but mainly K11- ,K48- and K63-branched chains (Kim, Kim et al., 2007b). Similarly, in IL-1 and other innate immune signalling pathways,

treatment of ubiquitinated proteins with a K63-specific DUB, AMSH, does not only lead to the removal of K63-chains, but also releases linear ubiquitin chains which have been attached to these proteins. Because of the linkage-specificity of AMSH, it can be assumed that linear ubiquitin chains were attached on top of K63-linked chains (Emmerich, Bakshi et al., 2016, Emmerich, Ordureau et al., 2013). Whether the linear chains were part of a branched or mixed chain remains to be seen. Though the list of proteins containing branched or mixed ubiquitin chains has been increasing over the last decade, the function often remains elusive. One can envision a large diversity of chain configurations i.e. a mix of several linkage types branching off from another chain (Peng, Schwartz et al., 2003). These signalling platforms could potentially be removed completely from the target protein by a single DUB that can remove the most proximal chain, rather than removing the chains individually by different DUBs.

A functional relevance for branched ubiquitin chains was shown for the anaphase-promoting complex (APC/C), which conjugates ubiquitin chains which contain K11-linked branches. Notably, K11-branched chains were recognised better by the proteasome and substrates degraded more efficiently (Meyer & Rape, 2014). K11 chain synthesis can be mediated by the E2 UBE2S. Depletion of UBE2S led to reduced K11-ubiquitination of anaphase substrates resulting in their stabilisation despite abundant K48-ubiquitination (Min, Mevissen et al., 2015). In contrast to the theory that branched chains promote proteasomal degradation, Kim et al. found that, whilst troponin I ubiquitinated with either K48- or K63-chains was rapidly degraded by the 26S proteasome, degradation was drastically diminished when branched chains were conjugated (Kim et al., 2007b). This suggests that branching of ubiquitin chains can also protect proteins from proteasomal degradation.

Ultimately, the functional relevance of a ubiquitin chain depends on ubiquitin binders translating the signal context specifically, which results in different signalling outcomes. Branching of ubiquitin chains could allow for binding of two ubiquitin binding proteins with different linkage specificity, thus bringing them in close proximity. Also, mixed chains could increase the avidity of proteins that contain multiple UBDs with mixed specificity. On the other hand, a branched chain may obstruct potential binding sites for DUBs or UBDs. The complex nature of ubiquitin chain architecture, especially *in vivo*, makes it difficult to predict the biological function of a ubiquitin chain based on its mere presence on a protein.

1.2 Deubiquitination

Disassembly of ubiquitin chains and removal of ubiquitin which is conjugated to other proteins is mediated by DUBs. These proteases are specific in cleaving polyubiquitin linkages by hydrolysing the peptide and/or isopeptide bonds linking these chains (Nijman, Luna-Vargas et al., 2005). DUBs can be divided in two classes: cysteine- and metallo-proteases. Cysteine proteases comprise the large class of ubiquitin-specific proteases (USPs), ovarian tumour proteases (OTU), the Machado-Josephin disease proteases (MJDs) and the C-terminal hydrolases (UCHs). Metalloproteases are characterised by their JAB1/MPN/Mov34 metalloenzyme (JAMM) domain (Komander et al., 2009a). The human genome encodes more than 90 DUBs, suggesting a role in various signalling pathways. In addition to eukaryotic DUBs, some viruses and bacteria express DUBs that circumvent host defence mechanisms. As viruses and bacteria do not contain a ubiquitin system, these DUBs represent an adaptation to the host defence in order to increase their virulence (Edelmann & Kessler, 2008). For example, *Yersinia* species, a Gram-negative pathogen in the family of *Enterobacteriaceae*, express the deubiquitinase/deSUMOylase YopJ. This virulence factor was reported to inhibit NF-κB and MAPK signalling by removing K63-linked ubiquitin chains from TRAF2/3/6 and IκBα thereby promoting intracellular survival of *Yersinia* sp. (Orth, Xu et al., 2000, Sweet, Conlon et al., 2007, Zhou, Monack et al., 2005).

Many DUBs are general regulators of the ubiquitin system. This includes processing of newly translated linear ubiquitin chains by e.g. USP5 which specifically recognises the free C-terminus of the ubiquitin chain and cleaves it (Reyes-Turcu, Shanks et al., 2008). This is necessary to generate mono-ubiquitin which can then be used by the ubiquitination system to create different linkage types. The precise function of many DUBs is not clear. Generally, the function of DUBs is the termination of ubiquitin chain-dependent signalling events. However, this can also lead to activation of a certain response, as removal of degradative chains can stabilise a protein, thus allowing it to function. The transient interaction of DUBs with their substrates, as DUBs may not be part of the signalling complex directly, makes it difficult to study their function. The deubiquitinase DUBA is a negative regulator of IL-17A production in T cells. In resting cells, DUBA is ubiquitinated by the E3 UBR5, which leads to its proteasomal degradation (Rutz, Kayagaki et al., 2015). However, DUBA in turn can deubiquitinate UBR5 which protects it from proteasomal degradation. Activation by the T cell receptor causes DUBA to accumulate, possibly by inhibiting UBR5, which in turn leads to accumulation of UBR5. The vast increase of UBR5 allows it to inhibit

RORγt by targeting it for proteasomal degradation. This example shows that ubiquitination and deubiquitination are balanced by very dynamic processes, which can be shifted very quickly to either side in to evoke a signalling response. Because DUBs are not necessarily recruited to ubiquitin directly, many DUBs rely on additional protein interactions for their recruitment to signalling complexes. This also prevents random recruitment of DUBs to every ubiquitin-containing complex. DUBs are often functionally linked to an E3. The BRCC3 BRCA1/BRCA2 complex is an example of a close association of E3 and deubiquitinase. These E3s regulate DNA damage response, partially by utilising ubiquitination (Wu, Koike et al., 2008). *In vitro* analysis suggests that BRCA1 can create K48- and K63-linked ubiquitin chains (Christensen, Brzovic et al., 2007). K63-ubiquitin chains seem to function as a recruitment platform signal, whereas K48-linked chains are naturally associated with proteasomal degradation. The DUB BRCC3 has exclusive specificity for cleaving K63-linked ubiquitin chains. Therefore, as part of the BRCA1/BRCA2 complex, BRCC3 functions as a negative regulator of the DNA-repair complex by removing the recruitment platform.

It is noteworthy that most DUBs show no obvious specificity towards ubiquitin chain linkage types *in vitro* (Ritorto et al., 2014*)*. This brings up the question how non-specific deubiquitinases are targeted towards certain substrates but not others. One possibility of targeting DUBs to specific chains or substrates is achieved by locking the DUB in a specific place of the signalling complex. DUBs can be bound to other proteins which function as adaptors for their recruitment into signalling complexes. This restricts the ability of the DUB to engage targets which are too far away from their anchorage point. In addition, some DUBs have a restricted sub-cellular localisation. USP30, for example, is associated with the mitochondrial outer membrane and contributes to the maintenance of mitochondrial morphology (Nakamura & Hirose, 2008).

1.2.1 Regulation of DUBs

Subcellular localisation is however only one way of regulating DUB specificity. Ubiquitin chain topology itself can also directly affected ubiquitin binding and cleavage by the DUB. Structural analysis of DUBs upon their binding to ubiquitin revealed a conformational shift in the catalytic centre (Avvakumov, Walker et al., 2006, Johnston,

Riddle et al., 1999, Komander & Barford, 2008). This substrate-assisted catalysis prevents the DUB from arbitrarily cleaving Gly-Gly isopetide bonds in non-ubiquitin targets. Thus, only binding to the correct linkage type will activate the DUB and allow it to hydrolyse the chain. In addition, many DUBs are phosphorylated (http://www.phosphosite.org) on tyrosine, serine and threonine residues. These modifications likely regulate DUB function and activity, however, only few of these phosphorylation events are understood. It was, for instance, reported that Akt activates USP14 by phosphorylation (Xu, Shan et al., 2015). Since USP14 can cleave K48-linked ubiquitin chains, its phosphorylation could slow down protein degradation and may promote growth factor induced signalling.

1.2.2 Mode of chain cleavage

Hydrolysis of a ubiquitin chain can occur at internal linkage points (endo) or starting from the most distal ubiquitin (exo). Exo-DUBs, like the 26S proteasome-associated USP14, need access to the distal ubiquitin and start hydrolysing the chain sequentially towards the proximal ubiquitin that is conjugated to the protein (Hu, Li et al., 2005). In contrast, the endo-DUB AMSH-LP can initiate cleavage of the chain only at a linkage point between two ubiquitin molecules, which can, however, occur at any position of the chain (Sato et al., 2008). Another specialised DUB is USP5/IsoT which can only hydrolyse ubiquitin chains starting at the C-terminus. Because the C-terminus of polyubiquitin is used for the conjugation to other proteins, USP5/IsoT can only cleave unattached, free ubiquitin chains. These are important functional limitations, as they determine how each class of DUBs is affected by the chain topology and organisation. In the following section, three DUBs (i.e. CYLD, OTULIN and A20) involved in the regulation of TNFR1-signalling will be discussed in more detail.

1.2.3 CYLD

The tumour suppressor Familial Cylindromatosis Protein (CYLD) was first identified as the causative gene in patients suffering from familial cylindromatosis (Biggs, Wooster et al., 1995, Bignell, Warren et al., 2000). The disease is known for the large benign tumours that occur mainly around the head region but can manifest in any haired skin area. Patients usually carry a heterozygous germline mutation of the *CYLD* gene. Causative for the disease, however, is the deletion of the wild type (WT) allele in the tumours (Bignell et al., 2000). The name cylindromatosis originates from the characteristically cylindrical growth of the tumour tissue: the tumour centre contains large cells, while basaloid cells dominate towards the periphery and show a characteristic jigsaw-like pattern. Mutations of the *CYLD* gene in these patients reside mostly in the enzymatically active USP domain (Figure 1.6). Full deficiency in CYLD in mice does not lead to spontaneous development of tumours or any other overt phenotype. However, these mice are more susceptible to chemically and DSS-induced colitis-associated tumorigenesis (Massoumi, Chmielarska et al., 2006, Zhang, Stirling et al., 2006). In contrast, mice expressing exon 9 truncated CYLD, which truncates the USP domain and abolishes its enzymatic activity, die shortly after birth due to lung failure (Trompouki, Tsagaratou et al., 2009). Liver-specific deletion of CYLD exon 9 leads to fibrosis, apoptosis of hepatocytes and development of hepatocellular carcinoma, which is completely prevented by deletion of TNFR1 (Nikolaou, Tsagaratou et al., 2012). Lastly, intestinal epithelial cell (IEC)-specific deletion of Fas-associated protein with a death domain (FADD) that leads to colitis and epithelial cell necrosis is largely rescued by concomitant ablation of CYLD activity in IECs (Welz, Wullaert et al., 2011). Taken together, data obtained from *in vivo* experiments suggests that CYLD promotes e.g. TNF-induced cell death but is also required to maintain tissue homeostasis and to prevent tumour development.

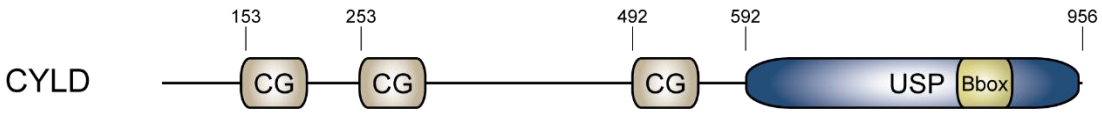

Figure 1.6: Schematic representation of CYLD

CG CAP-Gly, **USP** Ubiquitin specific protease domain, **Bbox** B-box-type zinc finger domain

Functionally, CYLD was identified as deubiquitinase of the USP-family. Initial studies found CYLD to be involved in the regulation of TNF-signalling (Brummelkamp, Nijman

et al., 2003, Kovalenko, Chable-Bessia et al., 2003). In addition to the C-terminal USP domain, CYLD has three cytoskeleton-associated protein-glycine conserved (CAP-Gly) domains that are involved in cytoskeleton-associated transport of vesicles and other cell organelles (Figure 1.6) (Li, Finley et al., 2002). These domains were also suggested to mediate the interaction with NEMO and TRAF2 (Kovalenko et al., 2003, Saito, Kigawa et al., 2004). Within the USP domain sits a B-box-type zinc finger domain (Bbox) with largely unknown function. The Bbox was shown to be dispensable for CYLD activity *in vitro* but was suggested to promote cytoplasmic localisation (Komander, Lord et al., 2008). As Bbox domains often mediate protein-protein interactions, it is likely that CYLD binds to other proteins via this domain. Despite reported protein interactions of CYLD, the mechanism by which CYLD is recruited to signalling complexes is unknown.

Like its recruitment, the physiological function of CYLD remains enigmatic. Early experiments utilised overexpression models of CYLD and concluded that CYLD functions as an inhibitor of gene-activation (Kovalenko et al., 2003, Trompouki, Hatzivassiliou et al., 2003). In contrast, others reported no or only mild effects of CYLD-deficiency on cytokine-induced gene activation (Moquin, McQuade et al., 2013, Reiley, Zhang et al., 2006, Zhang et al., 2006). Apart from gene activation, CYLD regulates induction of cell death, as CYLD overexpression sensitises cells to TNF-induced cell death and its depletion by RNA interference (RNAi), or gene knockout provides protection against the cytotoxic effect of TNF (Hitomi, Christofferson et al., 2008, Moquin et al., 2013, O'Donnell, Perez-Jimenez et al., 2011).

Once recruited to signalling complexes, CYLD is thought to remove ubiquitin chains from its target proteins including TRAF2, TRAF6, NEMO and Receptor-interacting serine/threonine-protein kinase 1 (RIP1) (Brummelkamp et al., 2003, Kovalenko et al., 2003, Moquin et al., 2013). Removal of polyubiquitin by CYLD could lead to the destabilisation of the protein complex, thus abrogating signalling. CYLD is also regulated by post-translational modifications. In NF-κB signalling, CYLD is rapidly phosphorylated. Contradicting reports regarding the inhibitory/activating role of this modification exist (Hutti, Shen et al., 2009, Reiley, Zhang et al., 2005). One study suggested phosphorylation of CYLD at S418 to be mediated by the IKK-complex and was reported to inhibit TRAF2 deubiquitination by CYLD (Reiley et al., 2005). In a screen for IKKε substrates, CYLD was identified as a target for phosphorylation and the authors concluded that S418 phosphorylation decreases CYLD activity (Hutti et

al., 2009). CYLD is also a substrate of Caspase-8 and cleavage at position D215 is thought to inactivate CYLD (O'Donnell, Perez-Jimenez et al., 2011). In accord with the cell death promoting function of CYLD, prevention of this cleavage by mutation (D215N) leads to increased susceptibility towards TNF-induced cell death (O'Donnell et al., 2011).

1.2.4 A20

TNF can induce the expression of the deubiquitinase TNF-induced protein 3 (*TNFAIP3*). This protein, also called A20, was proposed to have a dual role as a deubiquitinase and E3 ligase (Wertz, O'Rourke et al., 2004). The OTU domain of A20 was shown to cleave K48-ubiquitin chains *in vitro* (Ritorto et al., 2014). Interestingly, following phosphorylation at Ser381, presumably by IKKβ, A20 is also capable of cleaving K63-ubiquitin chains (Wertz, Newton et al., 2015). A20 is best known for its proposed function in shutting down TNF-induced gene activation, as part of a negative feedback loop (Boone, Turer et al., 2004, Wertz et al., 2004). In line with this hypothesis, A20 efficiently inhibits gene activation emanating from different receptors including TNFR1, Toll-like receptor 4 (TLR4), CD40 and NODs (Boone et al., 2004, Chu, Vahl et al., 2011, Hitotsumatsu, Ahmad et al., 2008, Tokunaga et al., 2012, Turer, Tavares et al., 2008, Wertz et al., 2004). Rising concentrations of A20 are supposedly responsible for the deubiquitination of RIP1, whilst simultaneously mediating K48-ubiquitination of RIP1 which, in turn, targets RIP1 for proteasomal degradation (Wertz et al., 2004). This could lead to disassembly of the signalling platform and shutdown of gene activation. A20's N-terminal OTU-domain is followed by seven zinc finger (ZF) motifs, some of which are able to bind ubiquitin chains (Figure 1.7) (Bosanac et al., 2010, Lu, Onizawa et al., 2013, Tokunaga et al., 2012).

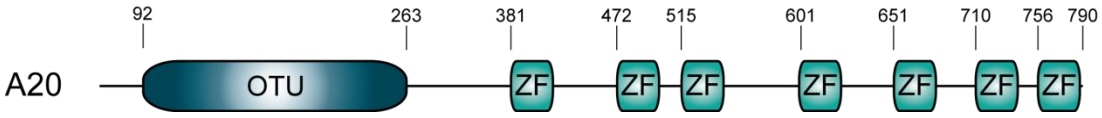

Figure 1.7: Schematic representation of A20

OTU Ovarian tumour domain, **ZF** Zinc finger

ZF4 was shown to bind to K63-linked ubiquitin chains and is required for efficient repression of NF-κB (Bosanac et al., 2010). Peculiarly, ZF4 was also suggested to

be responsible for the E3 ligase function (Wertz et al., 2004). This mode of action seems, however, unlikely as the *in vivo* importance in mice of both the OTU- and ZF4-domain is questionable. Indeed, complete deletion of A20 is causative for severe tissue inflammation, cachexia and perinatal death, which is MyD88-dependent (Lee, Boone et al., 2000, Turer et al., 2008). Co-deletion of TNFR1 does not ameliorate the phenotype (Boone et al., 2004). Reduced expression of A20 or defective function caused by polymorphisms in *TNFAIP3* found in humans leads to increased susceptibility to autoimmunity (Adrianto, Wen et al., 2011, Zhou, Wang et al., 2016, Zhu, Wang et al., 2015). Coming back to the importance of the OTU- and ZF4-domain, an inactivating point mutation of the catalytic cysteine within the OTU domain (C103A) or disruption of the ZF4 folding (C609A, C613A) in mice does not lead to a spontaneous inflammatory phenotype (Lu et al., 2013). However, these mice perform worse in models of acute and chronic inflammation but do not phenocopy full deficiency in A20 (Lu et al., 2013, Wertz et al., 2015). These findings raise the question which domain of A20 is responsible for protection from perinatal lethality. Domains other than the OTU and ZF4 are poorly characterised and no mice with different domain-specific alterations have been reported. However, ZF7 of A20 was found to suppress NF-κB activation (Tokunaga et al., 2012, Verhelst et al., 2012, Yamaguchi, 2015). This domain binds specifically to linear ubiquitin chains and is required for overexpression-mediated suppression of NF-κB (Tokunaga et al., 2012, Verhelst et al., 2012). This is an especially interesting observation as the ZFs are sufficient to prevent TNF-induced cell death but not a mutant carrying an inactivating point mutation of ZF7 (Yamaguchi, 2015). This points to a function of A20 which involves LUBAC and linear ubiquitin chains.

1.2.5 OTULIN

The unique function of LUBAC to create linear ubiquitin chains is counteracted by an equally specialised deubiquitinase called OTULIN (Keusekotten et al., 2013). OTULIN, also known as gumby, was identified in a mutagenesis screen as a gene that regulates the vascular development in mice (Rivkin, Almeida et al., 2013). Mice that have a point mutation in OTULIN, causing reduced deubiquitinase activity, die embryonically at day E12.5-E14 and are characterised by defective cranial vascularisation (Rivkin et al., 2013).

Figure 1.8: Schematic representation of OTULIN

PIM PUB-interacting motif, **OTU** Ovarian tumour domain

OTULIN has an exquisite specificity for linear ubiquitin chains and is unable to hydrolyse other linkage types. This preference is due to substrate-assisted catalysis: binding of OTULIN to linear ubiquitin leads to a conformational change in OTULIN that allows for repositioning of the catalytic triad into an active conformation (Keusekotten et al., 2013). OTULIN is constitutively associated with HOIP via a PUB-interacting motif (PIM) which interacts with the PNGase/ubiquitin-associated (PUB) domain of HOIP (Figure 1.8) (Rivkin et al., 2013). In TNF-signalling OTULIN was shown to negatively regulate induction of NF-κB as knockdown of OTULIN increased gene activation (Keusekotten et al., 2013). Interestingly, both reduction of OTULIN expression by RNAi and its overexpression sensitised HEK293 cells to TNF-induced cell death (Keusekotten et al., 2013), indicating that the level of linear ubiquitination must be tightly regulated to ensure homeostasis.

Recently, three individuals with homozygous hypomorphic mutation in OTULIN were reported to develop severe autoinflammatory syndrome (Damgaard, Walker et al., 2016). This condition termed OTULIN-related autoinflammatory syndrome (ORAS) is characterised by elevated cytokine production in myeloid cells caused by accumulation of linear ubiquitin chains resulting in autoactivation of these cells. Strikingly, the condition could be ameliorated in patients using antagonistic antibody therapy against TNF.

1.3 Linear Ubiquitin Chain Assembly Complex (LUBAC)

LUBAC is the only E3 ligase complex known to exclusively create M1-chains *de novo*. It consists of three subunits, Heme-oxidized IRP2 ubiquitin ligase 1 (HOIL-1, *RBCK1*), Shank-associated RH domain-interacting protein (Sharpin) and its main catalytic core unit HOIL-1 interacting protein (HOIP, *RNF31*) (Figure 1.9) (Gerlach, Cordier et al., 2011, Haas et al., 2009, Ikeda, Deribe et al., 2011, Kirisako, Kamei et al., 2006, Tokunaga, Nakagawa et al., 2011). Though the stoichiometry of this complex is not entirely clear, experimental data suggest that LUBAC primarily exists as a tripartite

complex where HOIP is simultaneously bound to Sharpin and HOIL-1. Together, they form a large complex ~600KDa in size (Tokunaga et al., 2011). In the context of LUBAC, Sharpin and HOIL-1 function as regulatory subunits that also confer complex stability. Indeed, absence of any of the LUBAC components leads to a marked reduction of the protein level of the other two components respectively (Gerlach et al., 2011, Haas et al., 2009, Ikeda et al., 2011, Tokunaga et al., 2011). The recruitment of LUBAC to signalling complexes is mediated by binding to other ubiquitin chains and all three LUBAC components contain UBDs, accordingly. Both HOIL-1 and the RBR of HOIP are able to assemble linear ubiquitin chains *in vitro (Stieglitz, Morris-Davies et al., 2012)*. However, the activity of HOIL-1 is comparably low and its function *in vivo* has not been fully addressed. The C-terminal active core of HOIP and HOIL-1 belongs to the RBR E3s (as described in 1.1.1 E3-ligases). Like other RBR-members, LUBAC conjugates ubiquitin chains in a HECT-like mechanism by loading the ubiquitin in its catalytic centre before directly conjugating it to its substrate (Stieglitz et al., 2012, Stieglitz, Rana et al., 2013).

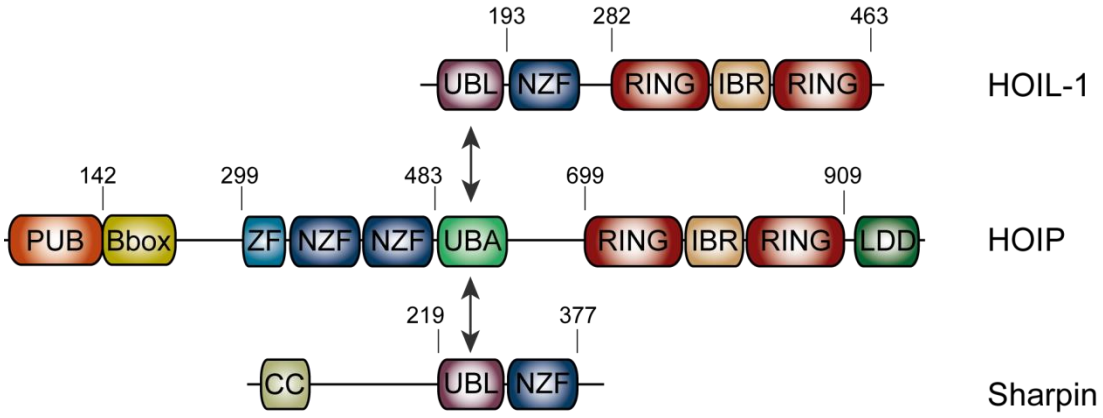

Figure 1.9: Schematic of LUBAC and the structure of its subunits

HOIL-1 and Sharpin utilise the UBL domain for the interaction with the UBA of HOIP. The RBR domain can be found in both HOIP and HOIL-1, while Sharpin is catalytically inactive. **CC** coiled coil, **IBR** in-between-RING, **RING** really interesting gene domain, **LDD** Linear ubiquitin chain determining domain

LUBAC has been suggested to regulate several different pathways including TNFR1-, NOD2, IL-1R, CD40 TLR3, WNT and Retinoic acid-inducible gene I (RIG-I) (Damgaard, Nachbur et al., 2012, Emmerich et al., 2016, Haas et al., 2009, Inn, Gack et al., 2011, Rivkin et al., 2013, Sasaki, Sano et al., 2013) Overexpression of HOIP, together with HOIL-1 or Sharpin, but not alone, triggers production of linear ubiquitin

chains (Gerlach et al., 2011, Kirisako et al., 2006). Interestingly, this suffices to activate NF-κB, indicating that linear chains can also function as a platform for gene activation, independently of any ligand (Gerlach et al., 2011).

Absence of LUBAC from SCs reduces gene activation triggered by e.g. TNF and IL-1β (Gerlach et al., 2011, Haas et al., 2009). It is therefore likely that linear ubiquitination promotes signalling complex formation which leads to enhanced activation of NF-κB and MAPKs (Peltzer, Rieser et al., 2014). However, in WNT signalling, LUBAC was proposed to function as a negative regulator, based on LUBAC overexpression in a WNT reporter assay (Rivkin et al., 2013). However, the mechanism that would allow LUBAC to modulate this pathway was not clarified, leaving the question whether this is indeed a direct effect of LUBAC. Retinoic acid-inducible gene 1 (RIG-I) signalling was also suggested to employ LUBAC as a negative regulator (Inn et al., 2011). LUBAC facilitates the ubiquitination of the ubiquitin ligase tripartite motif-containing protein 25 (TRIM25) and RIG-I, which leads to their subsequent proteasomal degradation (Inn et al., 2011). However, it is not clear whether TRIM25 or RIG-I are direct targets of LUBAC *in vivo*, or whether the ubiquitination of TRIM25 is secondary to the function of LUBAC in this pathway.

In addition to the role of LUBAC in gene activation, deficiency in any LUBAC-component sensitised various cell types to TNF-induced cell death (Gerlach et al., 2011, Haas et al., 2009, Ikeda et al., 2011). It is not clear what causes this sensitisation to cell death in absence of LUBAC. In this context, factors that depend on LUBAC and linear ubiquitin chains for their recruitment or activity have not been fully characterised. It is therefore required to identify these factors first, to explain the functional importance of linear ubiquitin chains.

1.3.1 HOIP

As mentioned in the previous section, the enzymatic activity of LUBAC resides in HOIP (Kirisako et al., 2006). It comprises several domains, in addition to its enzymatically active domain, which support LUBAC function, regulation and assembly (Figure 1.9). In the N-terminal region, HOIP comprises a PNGase/ubiquitin-associated (PUB) domain followed by a Bbox domain that shows sequence similarity to the Bbox present in CYLD (Komander et al., 2008). Additionally, HOIP has several ubiquitin binding domains (ZF, NZF1,2) which may contribute to efficient recruitment to signalling complexes. Mixed results exist regarding the domain that mediates the

interaction of HOIP with HOIL-1 and Sharpin. While it was reported that both HOIL-1 and Sharpin bind to the UBA domain of HOIP via their UBL domain (Tokunaga et al., 2011), others reported that the NZF2 of HOIP also mediates interaction with the UBL domain of Sharpin (Haas et al., 2009).

Interestingly, HOIP is in an autoinhibited state, which is released upon binding to HOIL-1 or Sharpin. Alternatively, deletion of the UBA domain in HOIP, which is responsible for the inhibition of the RBR domain, renders HOIP active independently of HOIL-1 or Sharpin interaction. The autoinhibition of HOIP was also suggested to function as a regulatory mechanism for LUBAC activity. In TLR4-signalling, LUBAC is required to efficiently activate NF-κB signalling (Bowman, Rodgers et al., 2015). Following LUBAC activation, HOIP is ubiquitinated at Lys1056 which leads to a conformational change in HOIP, blocking its enzymatic activity. Like the autoinhibition of HOIP, the ubiquitination-mediated inactivation utilises the N-terminus of HOIP to adopt the inhibitory conformation (Bowman et al., 2015).

Deficiency of HOIP results in embryonic lethality at day E10.5, due to vascular defects caused by aberrant cell death in endothelial cells (Peltzer et al., 2014). The lethality and vascular defects could be corrected by concomitant deletion of TNF or TNFR1. However, these mice still die at day E14.5 and E17.5, respectively. The discrepancy between TNF and TNFR1 deletion could possibly be explained by a role of lymphotoxin-α (LT-α), which can also bind to TNFR1 and induce cell death (Aggarwal, 2003). Interestingly, HOIP/TNFR1-deficient mice had intact vascularisation and showed little signs of cell death (Peltzer et al., 2014). Nevertheless, these mice showed signs of severe heart defects, suggesting that HOIP is also required for cardiovascular development at late-gestation.

HOIP-deficiency in humans was found to cause multiorgan autoinflammation, lymphangiectasia and combined immunodeficiency (Boisson, Laplantine et al., 2015). A hypomorphic Leu72 to Pro missense mutation in *RNF31* was causative for destabilisation of HOIP and, consequently, HOIL-1 and Sharpin protein levels. Fibroblasts, isolated from the patient, showed impaired IL-1β- and TNF-induced NF-κB activation (Boisson et al., 2015). In contrast, stimulation of monocytes with IL-1β led to an increased production of IL-6. Patient-derived B-cells were unresponsive to CD40L stimulation and plasmablast differentiation was markedly lower. This suggests that LUBAC function may be different between cell types.

1.3.2 HOIL-1

One of the regulatory cofactors of LUBAC is Haem-oxidized IRP2 ubiquitin ligase 1 (HOIL-1), also known as RANBP2-Type And C3HC4-Type Zinc Finger Containing 1 (RBCK1). HOIL-1 was first identified as an E3 that binds to oxidised Iron regulatory protein 2 (IRP2) (Yamanaka, Ishikawa et al., 2003). However, no additional studies have been conducted to date regarding a LUBAC-related function in that matter. Like HOIP, HOIL-1 contains a RBR domain at its C-terminus, a UBL domain and an NZF (Figure 1.9) (Haas et al., 2009, Tokunaga, Sakata et al., 2009). Its RBR, however, shows only weak activity in creating linear chains *in vitro* (Stieglitz et al., 2012). Overexpression of HOIP together with HOIL-1 can trigger activation of NF-κB (Tokunaga et al., 2009). However, expression of HOIL-1 that lacks its RBR together with HOIP shows no sign of diminished activity (Tokunaga et al., 2009). Interestingly, HOIL-1 that lacks the UBL domain is also not able to activate HOIP-mediated generation of linear ubiquitin (Tokunaga et al., 2009). These results show that HOIP requires the interaction with HOIL-1 for its activation likely due to the release of its auto-inhibition and that the N-terminus of HOIL-1 is sufficient to do so (Stieglitz et al., 2012).

Deficiency in HOIL-1 was reported in patients that presented with chronic autoinflammation (Boisson, Laplantine et al., 2012). As expected from earlier *in vitro* data, loss of HOIL-1 function or expression resulted in reduced LUBAC stability and activity in these patients. Consequently, NF-κB activation by IL-1 in patient-derived fibroblasts was reduced. Monocytes, however, were hyper-responsive to IL-1, showing that function and degree of LUBAC-mediated regulation of NF-κB is cell type-dependent. Surprisingly, Tokunaga et al. showed that HOIL-1 deficiency in mice does not cause any overt phenotype. However, this HOIL-1 deficient mouse strain was engineered by deletion of exon 7 and 8, leaving a large portion of the N-terminus intact. It is therefore possible that the remaining portion, which includes the UBL domain, is still able to e.g. release the auto-inhibition of HOIP. Like HOIP, HOIL-1 is also target for ubiquitination. Western blot analysis indicates that a significant amount of HOIL-1 is modified with a mono-ubiquitin (Haas et al., 2009). Interestingly, this modification is dependent on HOIP and Sharpin as ablation of either abrogates this modification (Gerlach et al., 2011, Ikeda et al., 2011, Peltzer et al., 2014, Tokunaga et al., 2011).

HOIL-1 was also described to regulate other pathways. In B- and T-cell receptor signalling, HOIL-1, but not HOIP or Sharpin, was shown to be a target of the

paracaspase MALT1 (Douanne, Gavard et al., 2016, Klein, Fung et al., 2015). Activation of the antigen receptors leads to activation of the canonical NF-κB pathway, which also employs LUBAC, by the CARD11/BCL10/MALT1 (CBM) complex. Cleavage of HOIL-1 reduces LUBAC stability and activity thus promoting abrogation of gene activation. The CBM complex is therefore part of a negative feedback loop that, in a first step, activates NF-κB triggered by the B- and T-cell receptors, but supports abrogation of the pathway by cleaving HOIL-1 (Elton, Carpentier et al., 2016).

1.3.3 Sharpin

Sharpin was initially reported to interact with members of the SH3 and multiple ankyrin repeat domains (SHANK) protein family (Lim, Sala et al., 2001). Sharpin shares some similarity with HOIL-1, as it also has a UBA domain followed by a NZF domain (Figure 1.9). The UBL domain mediates the interaction of Sharpin with the UBA of HOIP (Tokunaga et al., 2011). Like HOIL-1, presence of Sharpin stabilises LUBAC (Gerlach et al., 2011) and enables full activity of HOIP (Stieglitz et al., 2012). Deficiency in Sharpin is causative for chronic proliferative dermatitis (*cpdm*) in mice (HogenEsch, Gijbels et al., 1993). In this mouse model, a single base pair deletion causes a frame shift leading to a premature stop codon in exon 1. *Cpdm* mice are characterised by hyperkeratosis, parakeratosis and immune infiltrates in the skin, causing severe skin inflammation and hair loss starting as early as 6 weeks after birth. Additionally, these mice have signs of arthritis, enlarged lymph nodes, splenomegaly, and lack payer's patches in the ileum of the small intestine (Gijbels, Zurcher et al., 1996, HogenEsch, Janke et al., 1999). Consequently, these mice have abnormal B-cell development, overall lower serum and faecal IgG level and diminished immune response following antigenic challenge with Dinitrophenol- Keyhole limpet hemocyanin (DNP-KLH). The severity of the skin lesions is constantly progressing, which requires *cpdm* mice to be euthanised at the age of about 12 weeks. IL-4, IL-5, IL-13 and GM-CSF cytokines, indicative for a type 2 immune response, were found to be upregulated in these mice (HogenEsch, Torregrosa et al., 2001). This correlated with increased levels of eosinophil infiltrates in the skin. As IL-12 induces INF-γ production in T and NK cells, which supressed type 2 cytokine production, systemic treatment of Sharpin-deficient mice with recombinant IL-12 reduced clinical signs of dermatitis (HogenEsch et al., 2001). The inflammasome is responsible for activation of numerous inflammatory cytokines including IL-1β and IL-18 (Lamkanfi & Dixit, 2014). This multi-protein

complex, which also contains Caspase-1 and Caspase-11, is an important part of the innate immunity system. In the context of Sharpin-deficiency, deletion of caspase-1 and -11 in *cpdm* mice decreased levels of inflammatory cytokines and cell death leading to a substantial amelioration of the phenotype (Douglas, Champagne et al., 2015). However, TNF is causative for the onset of the symptoms, as its genetic ablation completely prevents the disease (Gerlach et al., 2011). Moreover, co-deletion of the crucial cell death components Caspase-8 and RIP3 delays the onset of *cpdm* (Rickard, Anderton et al., 2014a), a scenario in which gene activation is not affected. Similarly, skin-specific deletion of FADD and RIP3 prevents dermatitis in Sharpin-deficient mice (Kumari, Redouane et al., 2014). Thus, TNF-mediated cell death is responsible for the onset of the disease, rather than a dysfunction in TNF-dependent gene activation.

Conclusively, Sharpin, as component of LUBAC, forms part of the TNFR1-SC and absence of Sharpin leads to decreased TNF-induced gene activation and sensitises to TNF-induced cell death (Gerlach et al., 2011). Though Sharpin does not have any enzymatic activity on its own, MEFs derived from *cpdm* mice show reduced linear ubiquitination in response to TNF (Rickard et al., 2014a).

1.4 NF-κB pathway

Receptor-mediated cell signalling is one of the cell's most important ways to interact with their environment. In order to adapt and react to changes in the environment, cells are often required to produce additional proteins, which are induced by gene activation. Gene-activatory receptors function as detectors for various stimuli (e.g. cytokines, pathogens, or chemical substances) which subsequently relay the information through a signalling cascade to the respective effector molecules (Hayden & Ghosh, 2008). This usually leads to the activation of several transcription factors (Oeckinghaus, Hayden et al., 2011). Depending on the stimulus and the set of transcription factors which are triggered, the cell will start protein expression selectively (Zhou, Scoggin et al., 2003). One of these transcription factors is the nuclear factor kappa-light-chain-enhancer of activated B cells (NF-κB). After its discovery in B cells, NF-κB was identified as a member of a family of transcription factors which regulate gene activation in many cell types and in response to a large variety of stimuli (Sen & Baltimore, 1986a, Sen & Baltimore, 1986b). The NF-κB family can be divided in two classes. Class I consists of the precursors p100 and p105 which can be processed to p52 and p50, respectively (Fan & Maniatis, 1991, Xiao, Fong et

al., 2004). Class II comprises Rel-family members RelA (also known as p65), RelB and cRel (Chen & Greene, 2004). All five members have an N-terminal Rel homology domain (RHD). The RHD is composed of two immunoglobulin-like structures which mediate homo- and hetero-dimerisation between the family members and binding to cognate κB targets in the DNA (Chen & Greene, 2004). The function of the RHD is subject to posttranslational modifications including acetylation, phosphorylation and ubiquitination (Chen, Mu et al., 2002, Kiernan, Brès et al., 2003, Ryo, Suizu et al., 2003, Zhong, SuYang et al., 1997). These alterations have been reported to change dimerization preferences and DNA-binding activity of the subunit both in a positive or negative manner. All members contain also a transcriptional activator domain (TAD). As p50 and p52 lack this domain, they require dimerisation with members of the Rel-family to form a functional transcription factor (Hoffmann & Baltimore, 2006, Oeckinghaus et al., 2011). The complexity of NF-κB signalling becomes evident when considering the different possible combinations of homo- and heterodimers. In total, 12 combinations exist that can activate transcription. In addition, dimers which lack a TAD, but still bind to DNA, can potentially function as inhibitors, thus adding increased complexity to the system (Hoffmann & Baltimore, 2006).

Members of the NF-κB family are sequestered in the cytosol via binding of inhibitors of κB (IκBs) to the RHD. There are six known proteins in the IκB-family: three typical members IκBα, IκBβ, IκBε, and three atypical members IκBδ, IκBξ and Bcl-3 (Baeuerle & Baltimore, 1988, Baeuerle & Baltimore, 1989, Fujita, Nolan et al., 1993). All members have characteristic Ankyrin repeats which bind to the RHD of NF-κB members thus masking the nuclear localisation sequence (NLS) embedded in the RHD (Beg & Baldwin, 1993). An exception is Bcl-3, which superactivates p50 homo-dimers (Fujita et al., 1993). For class II NF-κB members to translocate to the nucleus, IκB must be removed. This form of NF-κB activation is termed canonical NF-κB signalling (Brown, Gerstberger et al., 1995). In contrast, p100 is activated through proteolytic cleavage, and is hence distinguished as non-canonical NF-κB signalling (Xiao, Harhaj et al., 2001).

1.4.1 Canonical NF-κB signalling

As described in the previous section, canonical activation of NF-κB signalling requires the translocation of NF-κB dimers to the nucleus, which is usually inhibited by IκBs. In case of e.g. TNF, IL-1β and several damage-associated molecular patterns

(DAMPs) and pathogen associated molecular patterns (PAMPs), activation of these pathways leads to phosphorylation of IκB kinases (IKKs) (Israël, 2010). These kinases, IKKα and IKKβ are complexed with the regulatory subunit IKKγ/NEMO (Chen, Parent et al., 1996, DiDonato, Hayakawa et al., 1997, Yamaoka, Courtois et al., 1998). The phosphorylation of IKKs marks the first step in the signalling cascade of NF-κB activation (Figure 1.10). The molecular basis for IKK activation is not fully understood, but strong evidence exists that TAK1 phosphorylates and activates IKKβ in a ubiquitin dependent manner (Wang, Deng et al., 2001). Alternatively, it was suggested that recruitment of NEMO to ubiquitinated proteins like RIP1 might lead to oligomerisation and therefore proximity-induced activation of IKK (Marienfeld, Palkowitsch et al., 2006, Zhou, Wertz et al., 2004). One of the hallmarks of NF-κB activation is the phosphorylation and degradation of IκBα (Baeuerle & Baltimore, 1988). Phosphorylation of IκBα on Ser32 and Ser36 by the IKKs triggers the ubiquitination of IκBα with K48-linked chains on lysine K21 and K22 by the β-TRCP F-box-containing component of a Skp1-Cullin-F-box (SCF)-type E3 ubiquitin ligase complex (SCFβ-TrCP) (Spencer, Jiang et al., 1999, Winston, Strack et al., 1999, Yaron, Hatzubai et al., 1998). Subsequently, IκBα is degraded by the 26S-proteasome, thus liberating the NF-κB dimer (Brown et al., 1995, Chen, Hagler et al., 1995). The degradation of IκB is substantial and can lead to the complete disappearance of IκBα from the cytosol. Degradation of IκBa unmasks the NLS in the NF-κB dimer, which allows it to enter the nucleus to bind to its cognate DNA binding sites (Chen et al., 1995, Ganchi, Sun et al., 1992). Other IκB members are degraded in a similar manner (Kanarek, London et al., 2010). Interestingly, the expression of several regulatory proteins is under the control of NF-κB promotors (Figure 1.10). This includes CYLD, A20 and IκBα (Oeckinghaus et al., 2011). The upregulation of these factors creates a negative feedback-loop which facilitates the shutdown of NF-κB signalling (Hoesel & Schmid, 2013). Indeed, DUBs like CYLD and A20 can remove ubiquitin from signalling complex components thus inhibiting continuous IKK activation (Trompouki et al., 2003, Zhang, Kovalenko et al., 2000). Most importantly, the reoccurrence of IκBα restores the inhibition of NF-κB by sequestering them in the cytosol. IκBα can also enter the nucleus, in order to displace NF-κB from the DNA (Arenzana-Seisdedos, Turpin et al., 1997, Sun, Ganchi et al., 1993). Regulation of canonical NF-κB activation and its termination is crucial to ensure correct gene transcription. This is because target genes can be roughly categorised based on the signal strength they require to be activated. This means that certain target genes will

be readily transcribed following a short impulse of NF-κB activation, while other genes may require a more continuous signal to achieve sufficient protein expression (Tian, Nowak et al., 2005). Apart from the signalling duration, also the strength of the impulse, i.e. the amount of simultaneously activated NF-κB, affects certain genes more than others (Nelson, Ihekwaba et al., 2004).

Contradicting reports exist concerning the importance of either IKK for the activation of TNF or IL-1. While Li et al. showed that IKKβ is essential and sufficient for activation for NF-κB activation by TNF and IL-1 (Li, Van Antwerp et al., 1999);, others showed that IL-1 can activate NF-κB also in the absence of IKKβ (Solt, Madge et al., 2007). The reason for this difference is not clear but it suggests that IKKα and IKKβ do not have redundant roles in every pathway. Regardless of the stimulus, IKKβ was shown to be more important for the canonical activation, while IKKα is essential for non-canonical activation of NF-κB.

Mice deficient in IKKβ die between days E12.5-13.5 due to severe liver apoptosis (Li et al., 1999). Interestingly, the embryonic lethality of IKKβ-deficient mice could be rescued by concomitant deletion of TNFR1 but these animals still died within the first month post-birth (Li et al., 1999). In line, NEMO-deficient mice, which are completely defective in canonical NF-κB activation induced by Lipopolysaccharide (LPS), TNF, IL-1 or Poly(I:C) also die between days E12.5-13.0 from severe liver damage due to apoptosis (Rudolph, Yeh et al., 2000). Death of these animals is likely the result of insufficient upregulation of anti-apoptotic factors in response to inflammatory and death-inducing ligands.

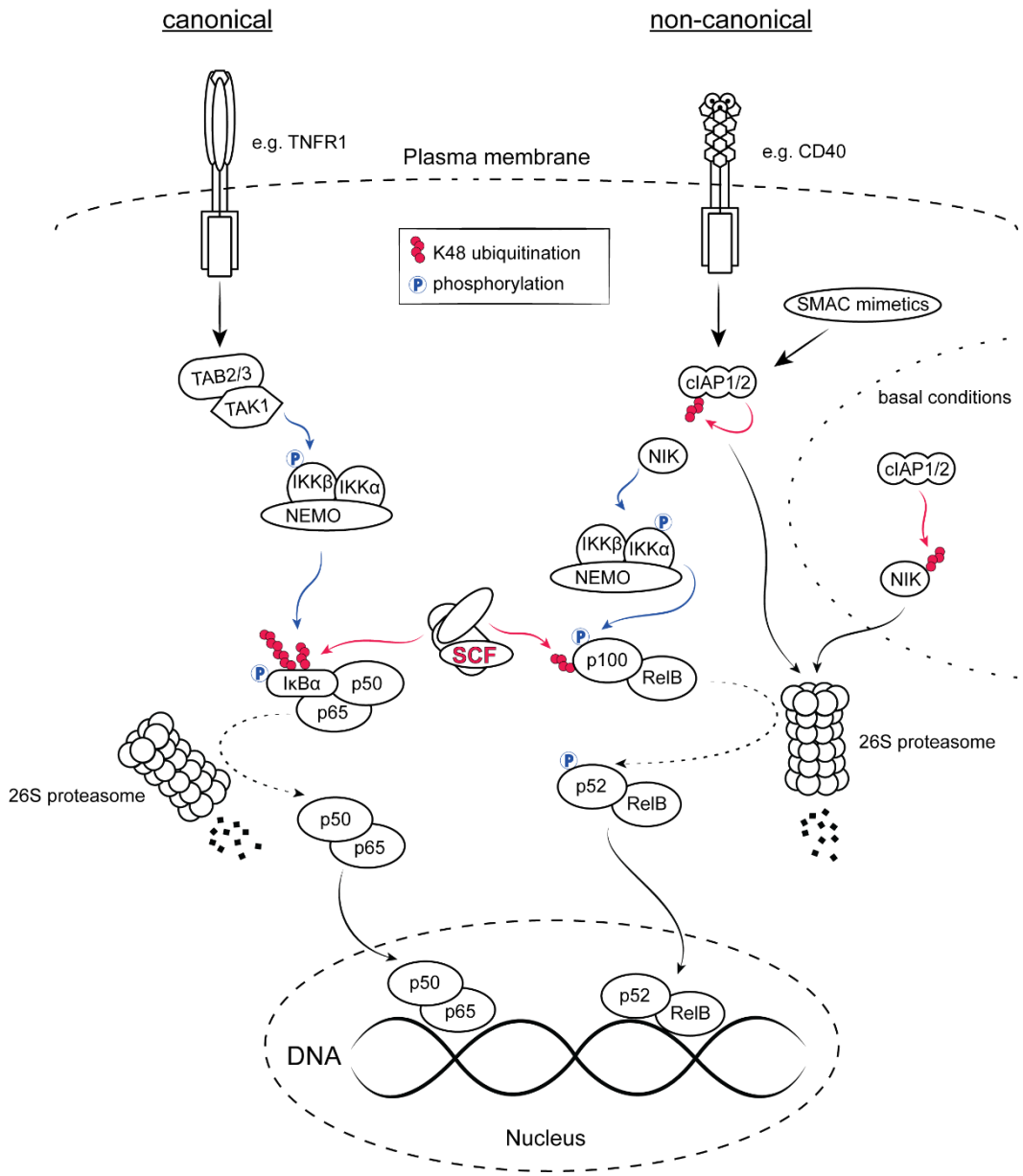

Figure 1.10: Comparison of canonical and non-canonical NF-κB activation

Canonical activation of NF-κB relies on activation of IKKβ by TAK1. Once activated, IKKβ phosphorylates IkBα which leads to its K48 ubiquitination and proteasomal degradation. Removal of IκBα unmasks the nuclear localisation sequence of the p65/p50 dimer which now can enter the nucleus and start transcription of its target genes.

Non-canonical NF-κB activation relies on activation of NIK. Under basal conditions, NIK is continuously ubiquitinated with K48 ubiquitin chains by cIAP1/2, leading to its proteasomal degradation. Certain signalling pathways like CD40 or TWEAK recruit and activate cIAP1/2, leading to their auto-ubiquitination and degradation. This can also be achieved by treatment with Smac mimetics. In absence of cIAPs, stabilised NIK phosphorylates IKKα, which in turn phosphorylates p100. Once activate, p100 is partially processed by the proteasome to give rise to a p52 fragment which, together with RelB, can enter the nucleus to drive gene transcription.

1.4.2 Non-canonical NF-κB activation

The signal for non-canonical NF-κB activation can emanate from members of the TNFR-superfamily, including CD40 (Coope, Atkinson et al., 2002), B cell-activating factor receptor (BAFFR) (Claudio, Brown et al., 2002), receptor activator of NF-κB (RANK) (Novack, Yin et al., 2003) and lymphotoxin β receptor (LTβR) (Dejardin, Droin et al., 2002). Non-canonical NF-κB signalling by p52/RelB was shown to be important for B cell survival and development of the lymphoid organs (Dejardin, 2006). Activation of this pathway involves cIAP1/2 and NF-κB inducing kinase (NIK) (Figure 1.10) (Xiao et al., 2001). In resting cells, NIK is subjected to continuous ubiquitination by an E3 complex consisting of TRAF2/3 and cIAP1/2 which leads its degradation (Vallabhapurapu, Matsuzawa et al., 2008, Zarnegar, Wang et al., 2008). Activation of any of the aforementioned receptors leads to the recruitment of TRAF family members and cIAP1/2 (Sun, 2011). Subsequently, cIAP1/2 ubiquitinate TRAF2/3 and, depending on the stimulus, themselves, which leads to their degradation. Consequently, NIK protein levels will accumulate, allowing it to phosphorylate IKKα. The non-canonical activation of NF-κB relies entirely on the activity of NIK, establishing it as the key activator of this pathway (Sun, 2011). Activated IKKα can then phosphorylate p100 at serine 866, 870, and possibly 872, which allows successive binding of the SCFβ−TrCP (Liang, Zhang et al., 2006). This region is named NIK-responsive element and resembles the phosphorylation site of IκBs. Mutation of SS866 and S870 in p100 completely abolishes its processing (Xiao et al., 2001). Phosphorylated p100 is ubiquitinated by SCFβ−TrCP at lysine K856 which is analogous to the for degradation responsible lysine in IκBα (Scherer, Brockman et al., 1995). Partial proteasomal processing of p100 generates a p52 fragment which, together with RelB, forms the active transcription factor (Figure 1.10). In contrast to canonical NF-κB activation, IKKβ and IKKγ (NEMO) are dispensable for this step, while IKKα is essential (Claudio et al., 2002, Dejardin et al., 2002). Seemingly, non-canonical NF-κB activation lacks the control of the IκB family. However, p100 was shown to act as an inhibitor of RelB translocation to the nucleus and processing of p100 to p52 alleviates this repression (Solan, Miyoshi et al., 2002). Additionally, p100 processing is strictly stimulation-dependent and even overexpression of p100 does not lead to significant generation of the p52 fragment (Xiao et al., 2001). This emphasises the importance of NIK/IKKα activation and consequently the regulation of NIK stability by ubiquitination via cIAP1/2. Alterations of cIAPs are consequently associated with a deregulation of non-canonical NF-κB signalling (Müller-Sienerth,

Dietz et al., 2011, Vince, Wong et al., 2007). SMAC-mimetics (SM)-induced depletion of cIAPs results in a stabilisation of NIK. Hence, while SMAC-mimetic treatment will block canonical NF-κB activation by e.g. TNF, non-canonical NF-κB activation will readily ensue. Since the non-canonical pathway requires degradation of TRAF and/or cIAPs first, and subsequent accumulation of NIK, gene activation occurs slower, but persists longer compared to canonical NF-κB activation (Saitoh, Nakayama et al., 2003). IKKα does not only phosphorylate p100 but also NIK, thus triggering its proteolysis (Razani, Zarnegar et al., 2010). Over time, decreasing NIK levels and re-emerging cIAP level will revert the non-canonical signalling to its basal condition.

1.5 MAPKs

Mitogen activated protein kinases (MAPKs) are among the most ancient kinase systems that function downstream of various extracellular signal receptors as hubs for signal transduction (Cargnello & Roux, 2011). The mechanisms and proteins involved are evolutionary well conserved in eukaryotic cells and involved in a variety of cellular processes like metabolism, cell division, motility, cell death, gene expression and survival. These kinases were first found to be activated by growth factors but later found to be activated by a large variety of cell signalling receptors (Widmann, Gibson et al., 1999). Members of this group can be divided in conventional and unconventional MAPKs. Conventional members are Extracellular signal regulated kinase 1/2/5 (ERK1/2/5), c-Jun N-terminal kinase 1/2 (JNK1/2) and p38 (α, β, γ, δ), which are characterised by their N-terminal Ser/Thr-kinase domain (Wada & Penninger, 2004). Unconventional MAPKs also have a Ser/Thr-kinase domain located at their N-terminus, but they have distinct additional features that do not comply with the composition of conventional MAPKs (Cargnello & Roux, 2011). Activation of conventional MAPKs is a hierarchical kinase cascade so that a MAPK is activated by a MAPK kinase (MAP2K or MKK), which, in turn, is activated by a MAPKK kinase (MAP3K) (Zhang & Liu, 2002). MAP3K are activated as a consequence of receptor stimulation and often involve interaction with members of the Ras/Rho pathway (Sahai, Olson et al., 2001). Examples of MAP3Ks are MAPK/ERK kinase kinase2/3 (MEKK2/3), rapidly accelerated fibrosarcoma 1 (Raf-1), tumor progression locus 2 (TPL-2) and TAK1. Activation of MAPKs by receptor members of the innate immune systems often involve TAK1 which phosphorylates MKK3, - 4, -6 and -7. Once activated, MKK3/6 activate p38 and MKK4/7 activate JNK

(Chang & Karin, 2001). Activation of TAK1 was shown to require ubiquitination mediated by e.g. TRAF2/6 (Wang et al., 2001).

MAP2Ks are a protein family with seven members called MAPK/ERK kinases (MEKs) (Akinleye, Furqan et al., 2013). Through the sequential activation of these kinases, MAPKs are phosphorylated in a conserved Thr-X-Tyr motif located in the kinase domain to lock it in an active conformation. MAPKs have a restricted set of substrates as they require Ser or Thr to be followed by a Pro residue (Biondi & Nebreda, 2003, Lu, 2004). However, as this amino acid sequence is not uncommon, MAPKs have evolved a second mechanism for substrate recognition. Located within their kinase domain, conventional MAPKs have a charged so called CD-region and a hydrophobic docking groove which mediates interaction with a consensus docking motif (D-motif) found in their substrates but also in MEKs (Enslen & Davis, 2001, Rubinfeld, Hanoch et al., 1999, Tanoue, Adachi et al., 2000, Tanoue & Nishida, 2003). These targets are usually kinases themselves called MAPK activated protein kinases (MAPKAPKs) and hence diversify the signal further. Members of this family are mitogen- and stress-activated kinases (MSKs), the p90 ribosomal S6 kinases (RSKs), MAPK-activated protein kinase 2/3 (MK2/3), and MK5 and MAPK-interacting kinases (MNKs) (Cargnello & Roux, 2011).

1.5.1 ERK-signalling cascade

The first members of the MAPKs discovered were found to be activated by receptors residing on the cell surface and hence named extracellular signal–regulated kinases (ERKs) (Boulton, Nye et al., 1991, Cooper, Bowen-Pope et al., 1982). ERK1 and ERK2 share more than 80% sequence identity and usually respond similarly to the same stimuli (Boulton et al., 1991, Roux & Blenis, 2004). The activation of ERKs is triggered by the MAP3Ks of the Raf-family and relayed through MEK1/2. However, other MAP3Ks, including tumour progression locus 2 (TPL-2), may also activate ERK in a cell type specific manner (Das, Cho et al., 2005, Shaul & Seger, 2007). ERK was found to be primarily activated by growth factors like epidermal growth factor (EGF) or other receptor tyrosine kinases ligands. However, other cytokines also activate ERK, though the activatory kinase is in many cases not clearly identified (Masuko-Hongo, Berenbaum et al., 2004). Within the cytoplasm, ERK has many direct substrates which regulate transcription, translation and chromatic remodelling (Kyriakis & Avruch, 2001) Following activation, ERK1/2 can also translocate from the

cytoplasm into the nucleus. There it can phosphorylate transcription activators like Elk-1, NF-AT and c-Fos (Yoon & Seger, 2006).

1.5.2 JNK-signalling cascade

Identified as an interaction partner of c-Jun, the c-Jun N-terminal kinases (JNKs) were found to be activated by many stress stimuli like UV-irradiation, heat and osmotic shock, oxidative stress but also several cytokines (Hibi, Lin et al., 1993, Kyriakis & Avruch, 1996). There are three genes encoding for JNK members which share more than 85% sequence identity, but show some functional differences (Gupta, Barrett et al., 1996, Kyriakis, Woodgett et al., 1995). While JNK1/2 are expressed in most cell types and thought to have overlapping function, JNK3 is predominantly expressed in the brain, heart and testis (Bode & Dong, 2007). Like the ERK-family, JNK proteins need to be activated by a dual-phosphorylation in a conserved Thr-Pro-Tyr (TPY) motif (Kyriakis & Avruch, 2001). The main MAP2Ks involved in this step are MEK4 and MEK7, which in turn can be activated by several MAP3Ks including ASK1/2, MEKK1-4, TAK1 and Tpl-2. Once activated, JNKs translocate to the nucleus, where they phosphorylate substrates including c-Jun, ELK-1 and ATF2.

JNK is also strongly associated with cell death progression (Liu & Lin, 2005). JNK1/2-deficient MEFs showed resistance to cell death caused by DNA damage- and UV-irradiation. Analysis of cell death pathways revealed an impaired cytochrome c release, pointing toward a role of JNK in the induction of apoptosis and the control of mitochondrial function (Tournier, Hess et al., 2000). JNK is also associated with amplification of ROS via a mitochondrial pathway in response to stress (Chambers & LoGrasso, 2011). Additionally, JNK activation might be inhibited by NF-κB signalling, as indicated by the prolonged JNK activation observed in IKK-deficient MEFs following TNF stimulation (Tang, Minemoto et al., 2001). TNF-signalling can induce cell death in absence of NF-κB activation. It is therefore possible that JNK indeed contributes to cell death induction. The cell death promoting properties of JNK correlate with the prolonged activation of JNK, while the first more transient wave of activation is indeed associated with the expression of pro-survival genes (Tang, Tang et al., 2002).

1.5.3 p38-signalling cascade

Like JNK activation, the MAPK p38 is a cell stress responsive pathway (Zarubin & Han, 2005). Four isoform constitute this family: p38 α, β, γ and δ. Structurally, p38α shares around 50% identity with ERK2 and is the most ubiquitously expressed form (Korb, Tohidast-Akrad et al., 2006). Activation of p38 by MEK3/6 requires dual phosphorylation at a conserved Thr-Gly-Tyr (TGY) motif in the activation loop of all p38 members. Several MAP3Ks are able to initiate p38 activation; Tpl-2, ASK1, MLK3, TAK1 and MEKK3/4 (Cuevas, Abell et al., 2007). p38 is part of the inflammatory response to various stimuli including LPS, TNF and IL-1β (Kang, Chen et al., 2008, Kim, Sano et al., 2008, Raingeaud, Gupta et al., 1995). As an upstream activator of gene transcription, several pro inflammatory cytokines including IL-6, IL-8 and CCL2 were shown to be regulated in a p38-dependent manner (Saccani, Pantano et al., 2002).

1.6 Cell death

The crudest way of cell death is caused by mechanical destruction of the cell and is usually associated with tissue trauma (e.g. injuries of the skin). Injury caused by chemicals, excessive heat or cold can also lead to cell death. Also infections that disturb normal cell function can lead to cell death (Ashida, Mimuro et al., 2011). In all these cases, the cell is destroyed by disruption of its cell membrane which is accompanied by loss of membrane potential that is required to generate energy and leakage of cytosolic contents into the surrounding (Zong & Thompson, 2006). Cellular demise, known as necrosis, is from an immunological point of view strongly associated with acute danger. Tissue damage can be the result of barrier loss i.e. the epithelium, normally protecting from the outside world, which potentially leads to intrusion of dangerous microorganisms. Naturally, as part of the immune response, the body will react to any kind of injury-related cell death even in absence of an infection (i.e. sterile inflammation) (Chen & Nuñez, 2010). Spillage of intracellular content includes the release of so called ‘alarmins’. These are cytokines and other substances that, outside of their intracellular compartment, provoke an immune reaction (Bianchi, 2007). For instance, the nuclear protein High-mobility group protein B1 (HMGB1) functions as a regulator of transcription but can trigger an inflammatory response when released into the extracellular space (Scaffidi, Misteli et al., 2002). Similarly, extracellular presence of Adenosine triphosphate (ATP), a coenzyme that is vital for the majority of cell processes involved in energy transfer, acts as a

chemoattractant and activator of cells of the innate immune system. (Trautmann, 2009). For example, differentiation of the T helper cell subset T_H17 in the lamina propria is triggered by ATP (Atarashi, Nishimura et al., 2008). Hence, uncontrolled breakdown of cells is intrinsically associated with activation of the immune system.

Cell death exists also as a controlled mechanism in multicellular organisms. Programmed cell death uses various pathways within the cell that can cause individual cells to die. It is part of the normal physiology and required to clear damaged, aged or mutated cells, tissue remodelling and to kill infected cells (Ellis, Yuan et al., 1991).

1.6.1 Apoptosis

Multicellular organisms developed a controlled way of cell death that does not necessarily set off an immune response. Compared to single cell organisms, multicellular organisms possess the luxury to sacrifice cells to maintain homeostasis and to consequently keep the whole organism alive. This process is known as apoptosis (Greek for "falling off"). Apoptotic cell death was first described based on particular morphological observations (Kerr, Wyllie et al., 1972). Later, studies of the nematode *Caenorhabditis elegans (C. elegans)* revealed programmed cell death during devolvement that caused 131 out of 1090 somatic cells inevitably to die as part of normal development (Sulston & Horvitz, 1977). The responsible factors required for this remarkable observation remained elusive for many years until a class of proteases were discovered to be responsible for the observed effects (Cerretti, Kozlosky et al., 1992, Yuan, Shaham et al., 1993). These proteases of the CED-family in *C. elegans* were found to be cysteine-aspartic proteases (caspases) which are conserved through evolution (Wang & Gu, 2001). Apoptotic cell death is therefore defined as caspase-mediated cell death (Figure 1.11). Cells that undergo apoptosis show a characteristic set of morphologies and biochemical markers (Elmore, 2007, Kerr et al., 1972). Apoptotic cells will release soluble chemoattractants like CX3C-chemokine ligand 1 (CX_3CL1) and express membrane markers including intercellular adhesion molecule 3 (ICAM3), to recruit specialised phagocytic cells (Moffatt, Devitt et al., 1999, Truman, Ford et al., 2008). Induction of apoptosis will also lead to extracellular exposure of phosphatidylserine (PtdSer), which is normally confined to the inner leaflet of the plasma membrane. PtdSer functions as an “eat-me” signal for professional phagocytes (Bratton, Fadok et al., 1997, Fadok, Voelker et al., 1992). This step is essential for inducing the engulfment of apoptotic cells by e.g.

macrophages (Ravichandran, 2011). Additionally, apoptotic cells undergo membrane fragmentation known as “blebbing” which leads to the formation of apoptotic bodies (Kerr et al., 1972). This process allows for a more efficient uptake of apoptotic bodies by phagocytic cells. Activation of caspases promotes this step by Caspase-3-mediated cleavage and activation of RHO-associated protein kinase 1 (ROCK1) which in turn phosphorylates the myosin light chain thus enhancing cellular contraction (Sebbagh, Renvoizé et al., 2001). During blebbing, the cellular content remains encapsulated and the process is therefore non-inflammatory (Poon, Lucas et al., 2014). However, the barrier function of the cell membrane becomes compromised over time and small molecules may diffuse through the membrane freely (Silva, 2010). This hallmark of cell death can be visualised with dyes which are sequestered from living cells but readily stain dead cells.

In the context of cell death induction, caspases can be classified as initiator and executioner caspases. The initiator caspases 2, 8, 9 and 10 activate the caspase-cascade leading to the activation of executioner caspases 3, 6 and 7 which then cleave non-caspase substrates (Kumar, 2007). Initiator caspases are composed of a pro-domain that contains protein interaction domains and a large and small catalytic subunit (Nicholson, 1999). Executioner caspases lack protein binding domains in their pro-domain. Caspases reside in cells as inactive pro-caspases (zymogens) that require activation by proteolytic cleavage. In cases of initiator caspases, induction of cell death causes oligomerization of pro-caspases which, most likely by proximity-induced proteolysis, results in cleavage and generation of a fragment comprising the pro-domain and the large subunit and a second fragment comprising the small subunit (Figure 1.11). In a second cleavage step, the pro-domain is removed from the large subunit which liberates the active subunits and allows for dimerization of an active complex. Executioner caspases cannot undergo auto-proteolytic activation but are activated by initiator caspases through cleavage between the large and small subunit. Subsequently, the pro-domain is removed in an autoproteolytic step, which generates the active subunit (Fuentes-Prior & Salvesen, 2004). Caspase have different preferences regarding their cleavage motif but overlap to a certain degree (McStay, Salvesen et al., 2008). Synthetic caspase inhibitors like zVAD-fmk or QVD-OPh inhibit every caspase to a certain extent.

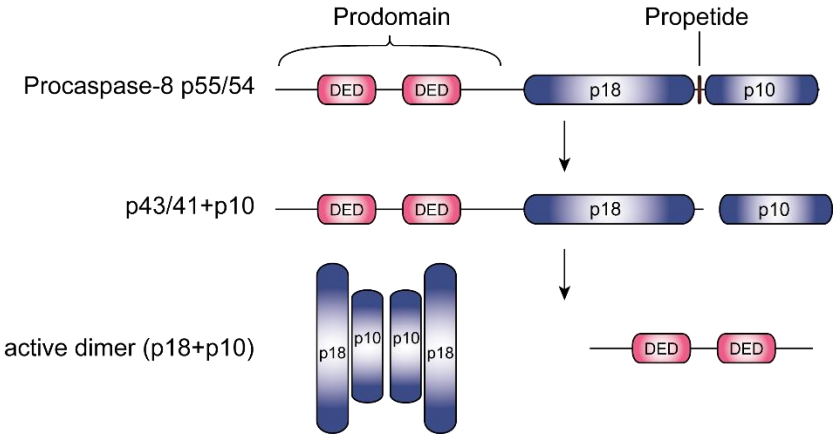

Figure 1.11: Activation of Caspase-8 by proteolytic cleavage

Procaspase-8 remains inactive in the cytosol under normal conditions. Oligomerisation upon recruitment to a signalling platform initiates a cascade of autoproteolytic cleavage steps. First, the pro-peptide between the large and small active subunit is cleaved. This generates a p43/41 fragment which comprises the prodomain and p18. Cleavage after the prodomain liberates p18 and allows for formation of the catalytic active p18 dimer composed of two p18/p10 dimers.

Executioner caspases can activate or inactivate non-caspase targets that promote apoptosis on several levels. The Poly (ADP-ribose) polymerase (PARP) and inhibitor of caspase-activated DNase (ICAD) are two examples of caspase regulated proteins. PARP is involved in DNA-damage repair and is cleaved in order to facilitate the degradation of chromosomes (Boulares, Yakovlev et al., 1999). Furthermore, cleavage of ICAD, the inhibitor of Caspase-Activated DNase (CAD), liberates CAD which degrades chromosomal DNA and facilitates chromosomal condensation during apoptosis (Enari, Sakahira et al., 1998). This process also leads to the characteristic ‘DNA-ladder’ that can be observed in gel-electrophoresis of DNA obtained from apoptotic cells, resulting from inter-nucleosomal DNA-cleavage (Williams, Little et al., 1974). Activation of caspases is also associated with the exposure of phosphatidylserine (PtdSer) as they cleave flippases and scramblases that normally maintain the membrane asymmetry by actively translocating PtdSer from the outer to the inner leaflet of the plasma membrane (Bratton et al., 1997, Fadok et al., 1992). During apoptosis, caspases cleave and inactivate the flippases ATP11A/ATP11C. Consequently, cells unable to cleave ATP11A do not expose PtdSer upon induction of apoptosis and are not engulfed by macrophages (Segawa, Kurata et al., 2016, Segawa, Kurata et al., 2014).

Mainly members of the TNF receptor superfamily, including CD95, TRAILR1/2, TNFR1 and DR3 can trigger apoptotic death following binding of their respective ligand. Engagement of CD95, for instance, leads to recruitment of FADD to the receptor via a homotypic death domain interaction (Scott, Stec et al., 2009). FADD, in turn, can recruit and activate Caspase-8, thus starting the apoptosis cascade. Receptor-mediated induction of apoptosis is referred to as the 'extrinsic pathway' (Elmore, 2007). In contrast, the intrinsic pathway is triggered, independently of death receptors, by e.g. radiation, hypoxia or reactive oxygen species (ROS).The hallmark of the intrinsic pathway is the permeabilization of the mitochondria, which is regulated by the B-cell lymphoma 2 (Bcl-2) family of proteins (Czabotar, Lessene et al., 2014). Mitochondrial outer membrane permeabilisation (MOMP) leads to release of cytochrome c (Eskes, Desagher et al., 2000, Li, Zhu et al., 1998). The release of cytochrome c triggers formation of the apoptosome which is comprised of cytochrome c, activating factor 1 (Apaf-1), and pro-caspase-9 (Li, Nijhawan et al., 1997, Srinivasula, Ahmad et al., 1998, Zou, Henzel et al., 1997). This complex supports the activation of effector caspases. In many cell types, the mitochondrial pathway is required to fully activate executioner caspases and trigger apoptosis downstream of death receptors activation (Fulda & Debatin, 2006). A link between the extrinsic and intrinsic pathway exists via Caspase-8-mediated cleavage of the cytosolic protein BH3-interacting domain death agonist (BID) to truncated BID (tBID). This allows for association and activation of Bcl2-associated X protein (BAX) and Bcl-2 homologous antagonist/killer (BAK), which translocate to the mitochondrial membrane and perforate it (Luo, Budihardjo et al., 1998).

Apoptosis is also part of immune cell development (Henson & Hume, 2006). During maturation, T- and B-cells can show reactivity to self-antigens due to the random nature of their receptor generation known as V(D)J-recombination (Hogquist, Baldwin et al., 2005, Jung & Alt, 2004). These auto-reactive T- and B-cells undergo a process termed negative selection. Binding to self-antigens in this stage of development will trigger apoptosis thus removing these cells from the organism (Kishimoto, Surh et al., 1998, Krammer, 2000). Additionally, peripheral tolerance of T-cells is maintained by activation-induced cell death (AICD), which is mediated by CD95/CD95L. Failure to undergo AICD is associated with autoimmunity and abnormal lymphoid development (Rieux-Laucat, Le Deist et al., 2003). autoimmune lymphoproliferative syndrome (ALPS) because of impaired clearance of B- and T-cells (Rao & Straus, 2006, Straus, Jaffe et al., 2001).

Deficiency in Caspase-8 results in embryonic lethality at around day E10.5 (Varfolomeev, Schuchmann et al., 1998). This observation was initially attributed to a vital role of cell death for embryonic development. These mice show hyperaemia, erythrocytosis in the liver, defective heart development and reduced numbers of hematopoietic precursor cells (Varfolomeev et al., 1998). However, it was found later, that Caspase-8 is required to inhibit another form of cell death called necroptosis (Kaiser, Upton et al., 2011).

1.6.2 Necroptosis

It was observed that TNF can induce caspase-independent cell death that resembles the morphology of necrosis (Holler, Zaru et al., 2000, Laster, Wood et al., 1988). Cells that undergo this form of cell death show signs of swelling, disruption of the cell membrane and lack of chromosomal fragmentation. Because of the inducible nature of cellular decay, this form of death is referred to as programmed necrosis or 'necroptosis' (Degterev, Huang et al., 2005). A common feature of this form of death is the lack or insufficient activation of caspases (Fulda, 2013). Necroptosis can be triggered by a variety of receptor signalling pathways including TNFR1, TNF-related apoptosis-inducing ligand 1/2 (TRAILR1/2), CD95, TLR3/4 (He, Liang et al., 2011, Holler et al., 2000). These receptor signalling complexes can induce cell death by triggering the formation of a complex consisting of FADD, Caspase-8, cellular FLICE-inhibitory protein (cFLIP), RIP1 and RIP3, also known as the necrosome (Figure 1.12). Within the necrosome, Caspase-8 has a regulatory role as it can cleave and inactivate RIP1 and RIP3 (Chan, Shisler et al., 2003, Feng, Yang et al., 2007, Lin, Devin et al., 1999). Caspase-8 function is regulated by cFLIP, which exists in two main isoforms. cFLIP shares similarity with Procaspase-8, as it contains an enzymatically inactive caspase-like domain and two death effector domains (DEDs). The long isoform, $cFLIP_L$, allows Caspase-8 activation, but leads to retention of the $cFLIP_L$/Caspase-8 heterodimer at the complex. The activity of Caspase-8 is therefore localised and directed towards other complex components (Micheau, Thome et al., 2002). In contrast, the short isoform $cFLIP_S$ is an inhibitor of Caspase-8 and therefore inhibits both apoptosis and necroptosis (Schilling, Geserick et al., 2014). Additionally, CYLD, which was also shown to promote necroptosis by facilitating the formation of the necrosome, is also cleaved and inactivated by Caspase-8 (O'Donnell et al., 2011). Failure to inhibit RIP1 activation by e.g. caspase-inhibition, results in activation of RIP1 by phosphorylation at S166 (Degterev, Hitomi et al., 2008, Hitomi et al., 2008). Phosphorylated RIP1 associates with RIP3 via a homotypic RIP homotypic interaction

motif (RHIM) interaction and phosphorylates it (Hitomi et al., 2008, Sun, Wang et al., 2012). The interaction of RIP1 and RIP3 is essential at this stage because RIP3 lacks a death domain and can therefore not be directly recruited to FADD (Moriwaki & Chan, 2013). Additionally, the association of RIP1 with RIP3 requires RIP1 kinase activity and can be inhibited by e.g. a class of inhibitors called necrostatins (Degterev et al., 2008, He, Wang et al., 2009). Phosphorylated RIP1 and RIP3 form fibre-like structures that are insoluble by most detergents (Li, McQuade et al., 2012). A kinase-dead form of RIP3 was shown to still interact with RIP1 but was not phosphorylated, indicating that RIP3 activation involves auto-phosphorylation (Cho, Challa et al., 2009). Following activation, RIP3 associates with and activates mixed lineage kinase like (MLKL) (Sun et al., 2012). MLKL was identified in a screen for chemical compounds which inhibit mediators of necroptosis. Activation of MLKL requires RIP3 and absence of RIP3 or its kinase inhibition blocks necroptotic cell death (Murphy, Czabotar et al., 2013, Sun et al., 2012, Wang, Sun et al., 2014).The necrosome is a supramolecular complex of ~2MDa in size that forms distinct foci upon formation that can be visualised by e.g. expressing fluorescently-tagged RIP1, RIP3 or MLKL (Feoktistova, Geserick et al., 2011, Li et al., 2012, Sun et al., 2012). The pseudokinase MLKL has no enzymatic activity. Phosphorylation by RIP3 leads to a conformational change in MLKL which opens its four-helix bundle motif located at the N-terminus (Hildebrand, Tanzer et al., 2014, Murphy et al., 2013). This allows MLKL to form oligomers which bind to phosphatidylinositol phosphates in membranes (Chen, Li et al., 2014, Dondelinger, Declercq et al., 2014). Upon translocation to the membrane, MLKL forms pores which leads to loss of membrane potential, cell swelling and break down of the cell. Unlike apoptosis, necroptotic death will not prevent the leakage of cytoplasmic content. DAMPs and alarmins will therefore be released into the surroundings similar to necrosis (Pasparakis & Vandenabeele, 2015).

RIP1 uses at least two domains, the DD and the RHIM for protein interactions which therefore support its scaffold function. The DD of RIP1 is required for TNFR1-SC recruitment but also mediates other DD-homotypic interactions with e.g. FADD (Park, Jeong et al., 2013). The RHIM mediates interaction with other RHIM-containing proteins including RIP3, TIR domain-containing adapter protein inducing IFN-beta (TRIF), and the putative nucleic acid sensor Z-DNA binding protein 1 (ZBP1, also known as DAI). ZBP1 was shown to induce inflammatory signalling and necroptosis upon viral infection (Upton, Kaiser et al., 2012). Interestingly, mutation of the RHIM in

RIP1 (RIP1^{mRHIM}) in mice leads to death around birth which is characterised by high levels of RIP3 phosphorylation (Lin, Kumari et al., 2016, Newton, Wickliffe et al., 2016). Blocking of the necroptotic pathway, e.g. by co-deletion of RIP3, prevented early lethality of RIP1^{mRHIM} mice (Newton et al., 2016). Most strikingly, also deletion of ZBP1 rescued perinatal lethality in RIP1^{mRHIM} mice (Lin et al., 2016, Newton et al., 2016). Because ZBP1 was found to interact with activated RIP3 in the absence of RIP1 interaction, it seems likely that the RHIM in RIP1 is required to prevent the association of ZBP1 with RIP3 and its subsequent activation. Intriguingly, there are two consecutive RHIMs present in ZBP1 and though the functional relevance is currently unknown, it may point towards an adaptor function of ZBP1 in this context.

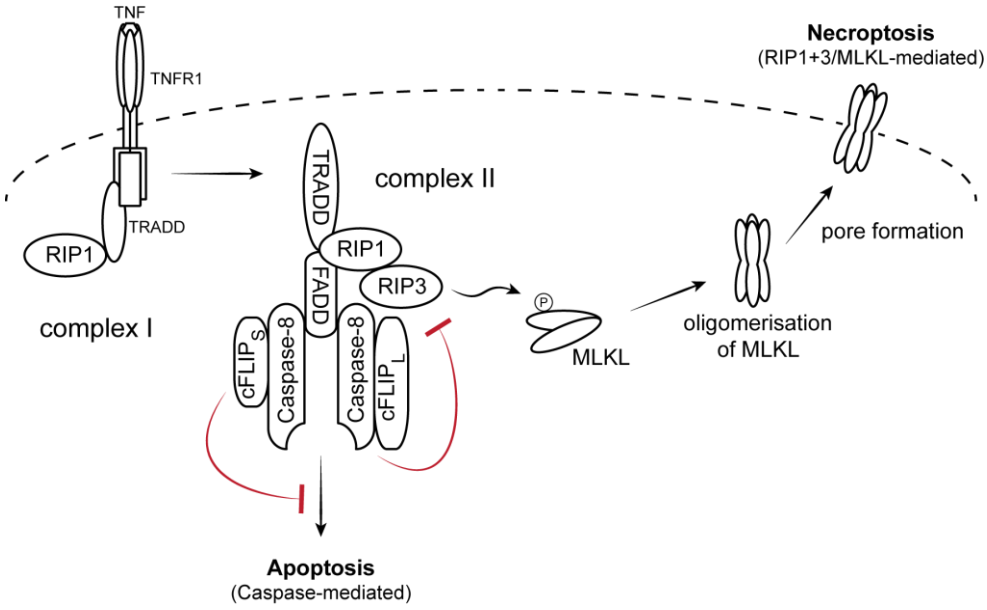

Figure 1.12: TNF-induced complex II triggers apoptotic and necroptotic death Following its activation, the TNFR1-SC can give rise to a secondary complex which is not bound to TNFR1. This so called complex II can associate, via RIP1, with FADD by homotypic death domain interaction. This allows recruitment of Caspase-8 to FADD. Proximity-induced activation of Caspase-8 triggers the signalling cascade leading to apoptosis. However, cFLIP$_S$ can form heterodimers with Caspase-8, thus inhibiting its activation and apoptosis. Association of Caspase-8 with cFLIP$_L$ on the other hand allows for localised Caspase-8 activity, which leads to cleavage of RIP1 and RIP3. In absence of Caspase-8 activity, the interaction of RIP1 and RIP3 via their RHIMs, leads to cross activation by phosphorylation. Activated RIP3 subsequently phosphorylates MLKL which leads to a conformational change in MLKL that enables its oligomerisation. Necroptotic cell death is executed by insertion of MLKL oligomers into phosphatidylinositol phosphate-containing membranes, which leads to pore formation and break down of the cell integrity.

What is the functional importance of necroptosis considering its seemingly destructive properties? Necroptosis has likely evolved as a backup mechanism to induce cell death in a scenario where caspases are inhibited (Kaiser, Upton et al., 2013). Viruses have evolved many ways to circumvent the anti-viral host-response. Infected cells can be recognised by the immune system and caspase-mediated cell death can be triggered to eliminate the infected cell. It is therefore not surprising that certain viruses have evolved mechanisms to inhibit caspase activation. Therefore, activation of the necroptosis machinery can surpass the viral-inhibition of caspases and still induce the death of an infected cell. Indeed, mice deficient in necroptosis show increased susceptibility to viral infections and fail to survive (Guo, Omoto et al., 2015, Kaiser, Sridharan et al., 2013). Necroptosis is also associated with pathological conditions including ischemia in the heart and kidney (Linkermann, Hackl et al., 2013). Inhibition of necroptotic cell death could therefore represent a potent treatment to prevent excessive tissue damage occurring during e.g. organ transplantation

1.7 TNFR1 signalling and its regulation by ubiquitin

Perhaps the most prominent member of the TNF-receptor superfamily is TNFR1. Its ligand TNF is a potent and multifunctional cytokine involved in inflammation and forms part of the innate immune response. Under normal conditions, TNF is not detectable in serum but it is produced in response to DAMPS, PAMPS and other inflammatory cytokines. TNF is involved in inflammatory pathophysiological conditions like inflammatory bowel disease, rheumatoid arthritis and psoriasis (Feldman, Combes et al., 2000, Peyrin-Biroulet, 2010). Because TNF itself induces the production of additional inflammatory cytokines in many cell types, anti-TNF therapy, i.e using TNF-antagonising antibodies or TNFR fusion proteins, proved to be effective for treatment of several inflammatory pathologies (Peyrin-Biroulet, 2010). Mice deficient for TNFR1 are resistant to LPS-induced shock (Pfeffer, Matsuyama et al., 1993, Rothe, Mackay et al., 1994, Simon, Park et al., 2010). Intriguingly, severe systemic inflammatory response syndrome (SIRS) was found to be prevented by administration of TNF-neutralising antibodies during lethal bacteraemia in baboons (Tracey, Fong et al., 1987).

TNF exists as a soluble and membrane-bound trimeric protein. The soluble form can, in addition to TNFR1, also bind to TNFR2. This related receptor can also signal gene activation but not cell death as it lacks the intracellular death domain (DD). The expression of TNFR2 is restricted to immune and endothelial cells. Membrane-bound

TNF is more efficient than soluble TNF in activating TNFR2 because of its higher affinity (Grell, Wajant et al., 1998). TNFR1, however, is readily activated by soluble and membrane-bound TNF.

The binding of TNF to TNFR1 leads to its trimerisation which creates an intracellular recruitment platform for the adaptor molecule TNFRSF1A Associated Via Death Domain (TRADD) (Hsu, Xiong et al., 1995). TRADD is supposedly the first protein in the signalling cascade (Figure 1.13). However, work on TRADD-deficient cells came to different conclusions regarding the necessity of TRADD for TNFR1-signalling. A study using TRADD-deficient MEFs showed absence of NF-κB and MAPKs signalling and resistance to TNF-induced cell death (Ermolaeva, Michallet et al., 2008, Pobezinskaya, Kim et al., 2008). In contrast, TRADD-deficient macrophages still weakly responded to TNF. Accordingly, whilst RIP1 recruitment to the TNFR1-SC is virtually absent in MEFs, it is only diminished in macrophages (Ermolaeva et al., 2008, Pobezinskaya et al., 2008). Like TNFR1-deficiency, resistance to a lethal dose of D-galactosamine N/Lipopolysaccharide (GalN/LPS) was also conferred by absence of TRADD (Pobezinskaya et al., 2008). Therefore, it seems that while TRADD is required for efficient formation and activation of the TNR1-SC, its significance in enabling gene activation may vary between cell types.

TRADD also acts as an adaptor for recruitment of TRAF2/6 and cIAP1/2 (Haas et al., 2009, Pobezinskaya et al., 2008, Vince, Pantaki et al., 2009). cIAP1/2 are E3 ligases which ubiquitinate many targets in the TNFR1-SC and absence of cIAP1/2 virtually abrogates ubiquitination of RIP1 (Haas et al., 2009). Although TRAFs are also E3s, their scaffolding function but not their enzymatic activity is essential for TNFR1-SC formation (Vince et al., 2009). K63- and K11-linked ubiquitination by cIAPs (Dynek, Goncharov et al., 2010, Varfolomeev, Goncharov et al., 2008) provides a binding platform for the recruitment of LUBAC which was shown to be required for full NF-κB and MAPK-signalling (Gerlach et al., 2011, Haas et al., 2009, Tokunaga et al., 2011). This ubiquitin network also enables binding of the TAB/TAK1- and NEMO/IKK-complex (Figure 1.13). All three LUBAC components HOIP, HOIL-1 and Sharpin contain ubiquitin binding domains which facilitate recruitment to signalling complexes or specific targets. RIP1 and NEMO have been identified as LUBAC substrates (Gerlach et al., 2011, Tokunaga et al., 2011). TAK1 and IKKα/β do not have a UBD and therefore depend on TAB2/3 and NEMO, respectively, for their recruitment. The NZF of TAB2 binds specifically to K63-ubiquitin chains, while NEMO was shown to preferentially bind to M1-polyubiquitin (Komander et al., 2009b, Kulathu et al., 2009,

Rahighi et al., 2009). Activation of IKKs and TAK1 mediates the NF-κB and MAPK signalling. Because activation of TAK1 and the IKKs relies on the ubiquitin system, lack or inhibition of cIAPs, LUBAC or the involved E2s leads to decreased NF-κB and MAPK signalling (Wertz, 2014).

RIP1 is amongst the most heavily ubiquitinated proteins within the TNFR1-SC (Gerlach et al., 2011). Therefore, RIP1 has a dual function as a kinase but also as a scaffold protein. This is also reflected in the phenotypes of RIP1-deficient and kinase-dead RIP1 (K45A) expressing mice. Complete deficiency of RIP1 leads to perinatal death of the mice, which is caused by multiorgan cell death and excessive inflammation. These mice are fully rescued by concomitant deletion of Caspase-8/RIP3 (Dillon, Weinlich et al., 2014) or RIP3/FADD (Rickard, O'Donnell et al., 2014b), demonstrating that uncontrolled cell death is causative for the phenotype of RIP1-deficient mice. Strikingly, RIP1 K45A knock-in mice are viable and show no signs of exacerbated cell death (Berger, Kasparcova et al., 2014). Additionally, RIP1 K45A mice are resistant to many TNF- and inflammation-related diseases. Notably, the perinatal lethality of full RIP1-deficiency cannot be rescued by ablation of *TNFR1*, indicating that RIP1 is also required to prevent cell death in other pathways (Rickard et al., 2014b).

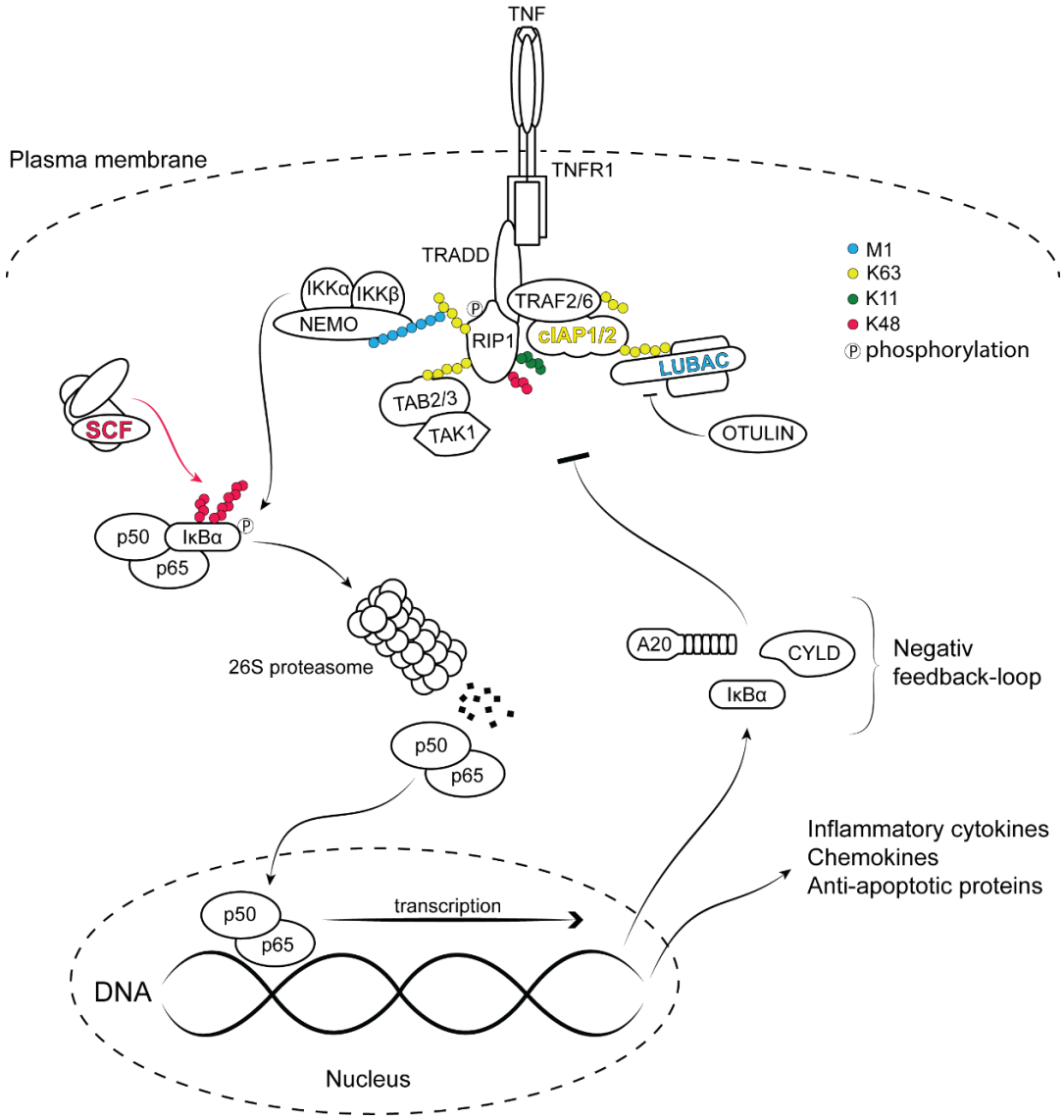

Figure 1.13: TNFR1-SC formation and regulation by the ubiquitin system

1.7.1 Impact of defective ubiquitination on TNFR1-signalling

Perturbation of the ubiquitin system can also drive the formation of a death-inducing complex (Figure1.14). Small-molecule SMAC mimetics bind to cIAPs and trigger their auto-ubiquitination, which leads to their degradation (Vince et al., 2007). Several tumour cell lines are in fact sensitised to death ligands when treated with SMAC mimetics (Fulda, 2014, Silke & Vucic, 2014, Varfolomeev et al., 2008). Mechanistically, the depletion of cIAPs by SMAC mimetics compromises the ubiquitination of TNFR1-SC components like RIP1, which normally prevents induction of cell death (Bertrand, Milutinovic et al., 2008, Haas et al., 2009, Li, Kobayashi et al., 2006). Additionally, IKK-mediated phosphorylation of RIP1 was shown to be required to prevent cell death (Dondelinger, Jouan-Lanhouet et al., 2015). Ubiquitination of

RIP1, TRAF2 and cIAP1/2 is also required for recruitment of LUBAC, NEMO/IKK and the TAB/TAK-complex. SMAC mimetics consequently block canonical NF-κB activation (Haas et al., 2009, Mahoney, Cheung et al., 2008). Similarly, a point mutation in RIP1 (K377R), which abolishes RIP1 ubiquitination completely, failed to restore IKK activation in RIP1-deficient Jurkat cells and sensitised them to TNF-induced cell death (Ea et al., 2006). Conclusively, it is thought that ubiquitination of the TNFR1-SC prevents formation of complex II, which can lead to cell death (Figure 1.14). However, RIP1 present in complex II is ubiquitinated even when cIAPs were depleted by SMAC-mimetics (de Almagro, Goncharov et al., 2015). Though it is not clear whether RIP1 becomes ubiquitinated in complex II again, it raises the question whether the overall ubiquitination of complex I, or whether specific ubiquitination events are required to prevent cell death.

Just like absence of cIAP1/2 from the TNFR1-SC, deficiency in any LUBAC component sensitises to TNF-induced cell death (Gerlach et al., 2011, Ikeda et al., 2011, Peltzer et al., 2014). The precise role of LUBAC in the prevention of cell death is still largely unknown. Absence of LUBAC was suggested to lead to reduced complex I formation i.e. the recruitment of signalling complex components. It is however unclear whether it is the impaired complex I formation that is responsible for emergence of a death inducing complex II. Additionally, lack of or increased DUB activity can lead to sensitisation to cell death. CYLD was found to be required for TNF-induced cell death in certain circumstances (Hitomi et al., 2008, Moquin et al., 2013). In contrast, knockdown but also overexpression of OTULIN sensitised cells to TNF-induced death (Keusekotten et al., 2013). This suggests that linear ubiquitination needs to be correctly balanced to ensure proper function.

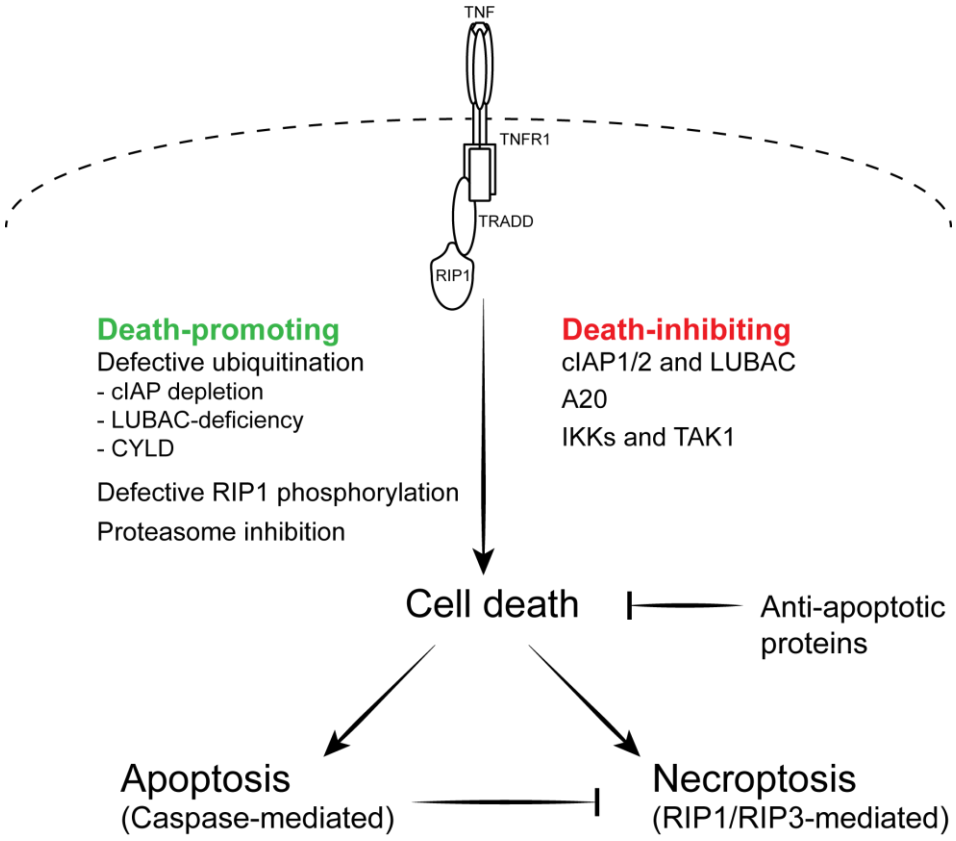

Figure 1.14: Death-promoting and -inhibiting factors in TNF signalling

1.7.2 Shutdown of TNFR1-signalling by DUBs

TNFR1-signalling employs a negative feedback-loop which facilitates the shutdown of gene activation. This also involves NF-κB-mediated expression of DUBs like A20, Cezanne and CYLD, (Enesa, Zakkar et al., 2008, Hoesel & Schmid, 2013, Oeckinghaus et al., 2011). Following gene activation, the increased expression of e.g. CYLD and A20 supports complex decomposition by removing different ubiquitin linkages (Jono, Lim et al., 2004, Lee et al., 2000). The upregulation of these DUBs is at least partially responsible for disassembly of the signalling complex, but other factors, including the upregulation of IκBα are also involved (Hoesel & Schmid, 2013).

1.7.3 TNFR1-induced cell death

Apart from the induction of inflammatory genes, the activation of TNFR1 can also trigger the formation of a cell death-inducing complex (Wajant, Pfizenmaier et al., 2003). The membrane-bound complex I mediates gene activation and remains attached to TNFR1. In a secondary event, dissociation of TRADD/RIP1 and potentially other molecules from TNFR1 leads to formation of a cytosolic complex II

which mediates cell death (Figure 1.12) (Micheau & Tschopp, 2003). It was reported that internalisation of the TNFR1-SC is required for the induction of death. Conclusively, TNFR1 lacking a putative internalisation motif can still induce gene activation but shows reduces induction of cell death (Schneider-Brachert et al., 2004).

In addition to perturbation of complex ubiquitination, inhibition of translation or the proteasome by e.g. cycloheximide and bortezomib respectively, leads to failure in upregulation of anti-apoptotic proteins including cFLIP, cIAPs or BCL-2 (Genestier, Bonnefoy-Berard et al., 1995, Micheau, Lens et al., 2001, Wang, Mayo et al., 1998). TAK1 is associated with the activation of NF-κB and MAPK but was also shown to have a direct effect on the ability of RIP1 to induce necroptosis. Inhibition of TAK1 or IKKs was shown to prevent an inhibitory phosphorylation of RIP1, which seems to inhibit cell death mediated by RIP1 kinase activity (Dondelinger et al., 2015). Moreover, inhibition of TAK1 or IKKs results in the formation of complex II and sensitises to TNF-induced cell death independently of NF-κB inhibition. Strikingly, RIP1 K45A kinase dead mice were impervious to treatment with a lethal dose of IKK-inhibitor TPCA-1 (Dondelinger et al., 2015). These examples show that TNF-signalling is controlled on several levels, which need to be correctly balanced to enable gene activation and prevent cell death.

1.8 Pattern recognition receptors

Pattern recognition receptors (PRRs) are a vital part of the innate immune system. PRRs are localised in the cell according to their function. On the cell membrane, PRRs are equipped to recognise extracellular pathogens, whilst endosome-located PRRs detect remnants of pathogens that infected host cells or were phagocytosed (Takeuchi & Akira, 2010). The detection relies on conserved motifs, pathogen-associated molecular patterns (PAMPs), which are common and essential to most pathogens. PRRs can be divided in four families: Toll-like receptors (TLR), NOD-like receptor (NLR), RIG-I-like receptors (RLR) and C-type lectin receptors (CLR) Primarily, PRRs detect molecules that are not present in the host. For example dsRNA, lipopolysaccharide (LPS) or flagellin is detected by TLR3, TLR4 and TLR5 respectively (Takeda & Akira, 2015). However, some of these molecules like dsRNA can also naturally be present in the host cell and function as a damage-associated molecular pattern (DAMP) molecule. However, because PRRs like TLR7 and TLR9 can also be activated by RNA- and DNA- associated autoantigens respectively, these

receptors can contribute to progression of diseases like systemic lupus erythematosus (Lau, Broughton et al., 2005).

1.8.1 NOD2-signalling

Nucleotide-binding oligomerization domain-containing protein 2 (NOD2) is a member of the NOD-like receptor (NLR) family and recognises peptidoglycan by binding to muramyl dipeptide (MDP) (Girardin, Boneca et al., 2003). As part of their cell wall, peptidoglycan is present in both gram-positive and gram-negative bacteria, though gram-positive bacteria contain about 10 times more peptidoglycan. NOD2 is therefore a very versatile receptor for detection of bacterial infections.

Individuals with homozygous mutation in NOD2 have a higher risk of developing Crohn's disease (Hugot, Chamaillard et al., 2001). This could be due to abnormal response to pathogens in these patients. Deficiency in NOD2 has also been shown to cause more severe graft versus host disease in a mouse model (Holler, Rogler et al., 2004). Lack of NOD2 in hematopoietic but not non-hematopoietic cells is involved in the perpetuation of the disease (Penack, Smith et al., 2009). Expression of NOD2 is mostly restricted to antigen presenting cells (APCs) but can also be induced by TNF or IFNγ.

MDP, present in the cytosol, will bind to the Leucine-rich repeat (LRR) of NOD2 which then induces its oligomerisation via its NACHT domain. Mutations in the NACHT domain are causative for the Blau syndrome (Miceli-Richard, Lesage et al., 2001) In its oligomerised state, NOD2 can recruit the kinase RIP2 via its Caspase activation and recruitment domain (CARD) (Figure 1.15). This creates a binding platform for several E3s; X-linked inhibitor of apoptosis (XIAP), cIAPs, Itchy E3 Ubiquitin Protein Ligase (ITCH) and Pellino3 (Bertrand, Doiron et al., 2009, Tao et al., 2009, Yang, Wang et al., 2013). Subsequently, these ubiquitin ligases conjugate K63- and possibly other linkage types to RIP2. Like in the TNFR1-SC, these ubiquitin linkages are recognised by the ubiquitin binders TAB2/3, NEMO, and LUBAC (Damgaard et al., 2012). In turn, LUBAC conjugates M1-linked chains to RIP2 (Fiil, Damgaard et al., 2013). Following their recruitment and activation, NEMO/IKK and TAB/TAK1 enable NF-κB and MAPK signalling which establishes an antimicrobial inflammatory response through gene activation.

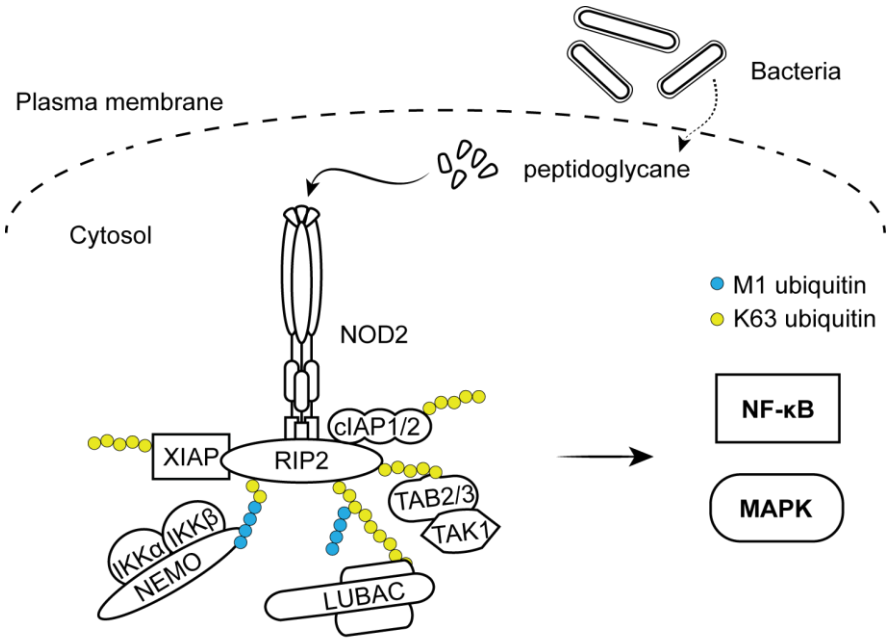

Figure 1.15: The NOD2 signalling pathway

The cytosolic NOD2 receptor can detect peptidoglycans derived from the bacterial cell wall. This leads to oligomerisation of NOD2 and subsequent recruitment of RIP2 via a homotypic CARD interaction. RIP2 functions as a scaffold protein for recruitment of the crucial E3s cIAP1/2 and XIAP which add K63-linked ubiquitin chains to RIP2. This allows for recruitment of LUBAC which in turn adds linear ubiquitin chains to RIP2 and possibly other components. Concerted action of K63- and M1-linked ubiquitin chains leads to recruitment of the NEMO/IKK and TAB/TAK complex, leading to activation of NF-kB and MAPK and gene activation.

1.9 Aim of this project

To find factors that might regulate LUBAC and therefore SCs to which LUBAC is recruited, a mass spectrometry (MS) analysis of HOIP was performed (Draber, Kupka et al., 2015, Kupka, De Miguel et al., 2016a). Analysis of the HOIP containing complex revealed constitutive association of HOIP with two DUBs, CYLD and OTULIN. An unknown factor, Spermatogenesis-associated protein 2 (SPATA2), was also among the high-scoring interacting proteins.

This study characterises the importance of the interaction of HOIP with OTULIN, SPATA2 and CYLD in the context of TNFR1- and NOD2-signalling. Additionally, A20, which was suggested to bind to linear ubiquitin chains (Tokunaga et al., 2012), was included in the analysis. To study the relevance of each factor for receptor signalling pathways, corresponding knockout cell lines were generated as a basis to answer the following questions:

I. How does the interaction of HOIP with OTULIN, SPATA2 and CYLD affect LUBAC function?

II. What is the function of the previously unrecognised TNFR1-SC component SPATA2?

III. Does LUBAC influence or mediate the recruitment of CYLD, OTULIN and SPATA2 to signalling complexes?

IV. Is ubiquitination of signalling complex components regulated by CYLD, SPATA2, OTULIN or A20?

V. What is the physiological relevance of this interaction network for gene activatory pathways and cell death?

2 Materials & Methods

2.1 Materials

2.1.1 Chemicals & reagents

Chemicals and other standard reagents were purchased from the following companies unless stated otherwise: Sigma Aldrich, Merck (Calbiochem), Invitrogen, Roche, Roth, Pierce.

2.1.2 Buffers & solutions

AP-lysis buffer	30 mM Tris-Base (pH7.4) 120 mM NaCl 2 mM EDTA 2 mM KCl 10% Glycerol (v/v/) 1% CHAPS (w/v) COMPLETE protease-inhibitor cocktail
Blocking buffer	5% (w/v) fat free milk powder 0.05% Tween-20 in PBS
Borax running buffer	10 mM sodium boric acid in H_2O
Cresol Red PCR dye	35% sucrose (w/v) in H2O 0.2 mM o-cresolsulfonephtalein
DUB buffer	150 mM NaCl 50 mM HEPES (pH 7.3) 2 mM Dithiothreitol (DTT)

Freezing medium (for eukaryotic cells)	90% FCS (v/v) 10% DMSO (v/v)
IP-lysis buffer	30 mM Tris-Base (pH7.4) 120 mM NaCl 2 mM EDTA 2 mM KCl 10% Glycerol (v/v/) 1% Triton X-100 (v/v) COMPLETE protease-inhibitor cocktail
MOPS Running Buffer (pH 7.7)	50 mM MOPS 50 mM Tris-Base 3.5 mM SDS 1.0 mM EDTA
Phosphate-buffered saline (PBS) (pH 7.4)	137 mM NaCl 8.1 mM Na_2HPO_4 2.7 mM KCl 1.5 mM KH_2PO_4
Propidium Iodide solution	1 µg/ml Propidium Iodide in PBS
Stripping buffer (pH 2.3)	50 mM Glycine in H_2O
Western blot wash buffer (PBS-T)	0.05% Tween-20 in PBS

Western blot Transfer Buffer (pH 8.3)	25 mM Tris 190 mM Glycine 20% Methanol (v/v)

2.1.3 Antibodies

Table 2.1: Unconjugated antibodies

IgG immunoglobulin, **IP** immunoprecipitation, **m** murine, **WB** western blot

Antibody	Isotype	Source	Application
A20 (sc-166692)	mIgG2a	Santa Cruz	WB
Actin (A5441)	mIgG1	Sigma	WB
cIAP1/2 (MAB3400)	mIgG2a	R&D Systems	WB
CYLD (sc-74435)	mIgG2a	Santa Cruz	WB
FLAG (D6W5B)	Rabbit	Cell Signaling	WB
FLAG (M2)	mIgG1	Sigma	WB
GAPDH (ab8245)	mIgG1	Abcam	WB
GFP (11814460001)	mIgG1	Roche	WB
GST (2622)	mIgG1	Cell Signaling	WB
HOIL-1	IgG2a	Haas et al., 2009	WB
HOIP (ARP43241_P050)	Rabbit	Aviva System Biology	WB
IκBα (9242)	Rabbit	Cell Signaling	WB
JNK (56G8)	Rabbit	Cell Signaling	WB
M1-ubiquitin (MABS199)	Rabbit (monoclonal)	Merck Millipore	WB
OTULIN (ab151117)	Rabbit	Abcam	WB
p38	Rabbit	Cell Signaling	WB
pERK (SC-7383)	Rabbit	Santa Cruz	WB
pIκBα (9246S)	mIgG1	Cell Signaling	WB
pJNK (98F2)	Rabbit	Cell Signaling	WB
pp38 (D3F9)	Rabbit	Cell Signaling	WB
pP65 (7F1)	Rabbit	Cell Signaling	WB
RIP1 (610459)	mIgG2a	BD	WB
RIP2 (SC-22763)	Rabbit	Santa Cruz	WB
RIP3 (IMG-5846A)	Rabbit	Imgenex	WB

Sharpin (14626-I-AP)	Rabbit	Proteintech	WB
SPATA2 (A302-494A)	Rabbit	Bethyl Laboratories	WB
SPATA2 (ab56565)	Rabbit	Abcam	WB
TNFR1 (8436)	mIgG2b	Santa Cruz	WB
TRADD (610572)	mIgG1	BD	WB
Ubiquitin (FK2)	mIgG1	Enzo	WB
V5 (sV5-10)	mIgG1	Sigma	WB

Table 2.2: Horseradish-peroxidase (HRP)-conjugated antibodies

Target antibody	**Origin**	**Source**
mIgG1	Goat	Southern Biotech
mIgG2a	Goat	Southern Biotech
mIgG2b	Goat	Southern Biotech
Rabbit-IgG	Goat	Southern Biotech

Cell culture media and additives

Ampicillin	Roth, Karlsruhe; Germany
Dulbecco"s Modified Eagle Medium	Invitrogen, California, USA
Dulbecco"s PBS	Invitrogen, California, USA
G418(Geneticin®)	Invitrogen, California, USA
Opti-MEM® Reduced Serum Medium	Invitrogen, California, USA
Penicillin/Streptomycin	Invitrogen, California, USA
RPMI 1640	Invitrogen, California, USA
Trypsin/EDTA solution	Invitrogen, California, USA

Beads and resins for protein purification

FLAG M2 affinity Gel	Sigma Aldrich, Missouri, USA
HALO-affinity resin	Promega, Wisconsin, USA

HisPur Ni-NTA Resin	Thermo Fisher Scientific, Massachusetts, USA
Protein A/G PLUS-Agarose	Santa Cruz, Dallas, USA

DNA isolation kits

DNA purification columns	Syd labs, Massachusetts, USA
QIAprep Maxi Kit	Qiagen, Hilden, Germany
QIAprep Spin Mini Kit	Qiagen, Hilden, Germany
QIAquick Gel Extraction Kit	Qiagen, Hilden, Germany
RevertAidTM H Minus strand cDNA synthesis kit	Fermentas, Massachusetts, USA

2.1.4 Kits and Ready-to-Use Solutions

InstantBlue	Expedeon Protein Solutions, San Diego, USA
Pierce ECL Plus	Thermo Fisher Scientific, Massachusetts, USA

2.1.5 Instruments

Äkta Prime	GE Healthcare, Little Chalfont, United Kingdom
Blotting equipment X cell IITM	Thermo Fisher Scientific, Massachusetts, USA
Dark Reader DR46B Transilluminator	Clare Chemical Research, Inc., Colorado, USA
Electronic Pipettor, ‘Matrix’	Thermo Fisher Scientific, Massachusetts, USA

Flow Cytometer FACSCalibur	Becton Dickinson, New Jersey, USA
Freezer -20° C	Liebherr, Biberach, Germany
Freezer -80° C, U570 premium	New Brunswick Scientific, New Jersey, United States
Light Microscope	Zeiss, Oberkochen, Germany
Millipore Super-Q water installation	Millipore, Billerica, United States
Multichannel pipette, ‘Xplorer’	Eppendorf, Hamburg; Germany
Multifuge 3S-R	Heraeus, Hanau, Germany
Multiskan Ascent	Thermo Labsystems, Vantaa; Finnland
NanoDrop Spectrophotometer ND-1000	NanoDrop Technologies, Wilmington, USA
pH Meter	Mettler Toledo, Greifensee, Switzerland
Photometer Ultrospec 3100 pro	GE Healthcare, Little Chalfont, United Kingdom
Pipettes (2 µl, 10 µl, 100 µl, 200 µl, 1 ml)	Gilson, Bad Camber, Germany
Scanner, CanoScan LiDE 110	Canon Inc., Tokyo, Japan
SRX-101A Tabletop Film Processor	Konica Minolta, Tokyo, Japan
Table Centrifuge Biofuge	Heraeus, Hanau, Germany
Thermomixer compact	Eppendorf, Hamburg, Germany
Vortex, Heidolph reax top	Heidolph, Schwabach, Germany

2.1.6 Consumables

50 ml Reagent Reservoir	Corning Inc., Corning, USA
Cell Culture Petri dishes	TPP, Trasadingen, Switzerland

Cell Culture Test Plates (6-, 12-, 24-well)	TPP, Trasadingen, Switzerland
Cell Sieve (40 µm pore size)	Becton Dickinson, New Jersey, USA
Cryogenic vials	Nunc, Wiesbaden; Germany
Falcons (15 ml and 50 ml)	TPP, Trasadingen, Switzerland
Hybond ECL Nitrocellulose Membrane	Amersham Bioscience, Buckinghamshire, UK
NuPAGE® 4-12% Bis-Tris Gels	Invitrogen, California, USA
PCR Tubes	StarLab, Ahrensburg, Germany
Pipette tips (0.1-10, 1-200, 101-1000 µl)	StarLab, Ahrensburg, Germany
Plastic pipettes (5 ml, 10 ml and 15 ml)	Becton Dickinson, Heidelberg; Germany
Polypropylene round bottom tube (5 ml)	Becton Dickinson, Heidelberg; Germany
Round and flat bottom 96-well test plates	TPP, Trasadingen, Switzerland
Safe-Lock Reaction Tubes (1,5ml, 2 ml)	Eppendorf, Hamburg, Germany
Single-Use Needles	Becton Dickinson, Heidelberg; Germany
Single-Use Syringe (1 ml, 2 ml	Becton Dickinson, Heidelberg, Germany
Single-Use Syringe (5 ml, 30 ml, 50 ml)	Terumo, Eschborn, Germany
Sterile filter (0.22 µm pore size)	Millipore, Billerica, United States
Tissue Culture flasks (25, 75, 150 cm2)	TPP, Trasadingen, Switzerland
Vivaspin Concentrator MWCO 10000	Sartorius, Goettingen, Germany
X-Ray film	Scientific Laboratory Supplies Ltd, Nottingham, UK

2.1.7 Software

ApE sequence analyser	M. Wayne Davis
Ascent Software Version 2.6	Thermo Labsystems, Vantaa, Finnland
Endnote	Thomson Reuters, New York, United States
Illustrator	Adobe, San Jose, United States
Microsoft® Excel 2003	Microsoft, Redmont; United States
Microsoft® Word 2003	Microsoft, Redmont; United States
Photoshop	Adobe, San Jose, United States
PyMol	Open Source (Schrödinger, New York, United States)
Vector NTI	Invitrogen, California, USA

2.1.8 Cell lines

A549

The adenocarcinoma cell line A549 was established from tissue obtained from a 58-year-old male patient (Giard, Aaronson et al., 1973).

HEK293T

Human embryonic kidney cells 293 (HEK293) were established by transformation of cells obtained from an aborted human foetus by adenoviral infection (Graham, Smiley et al., 1977). This resulted in an integration of the viral genome into chromosome 19. HEK293T cells are very suitable for DNA transfection and protein production.

HeLa

This cervix adenocarcinoma-derived cell line was established in 1951 by George Otto Gey from patient named Henrietta Lacks and is the first human epithelial cancer cell line successfully maintained for long-term cell culture (SCHERER, SYVERTON et al., 1953). HeLa cells have a hypertriploid chromosome number (3n+) leading to 76 to 80 total chromosomes (Bottomley, Trainer et al., 1969). Additionally, HeLa cells have multiple integrations of human papillomavirus 18 (Macville, Schröck et al., 1999).

K562

The first erythroleukaemia-type cell line which was immortalised for long-term culture was K562 (Lozzio & Lozzio, 1975). This line was derived from a 53-year-old female who presented with chronic myelogenous leukaemia.

Mouse Embryonic Fibroblasts (MEFs)

Fibroblast are involved in the maintenance of connective tissue by secreting components that reconstitute the extracellular matrix (Tracy, Minasian et al., 2016). Mouse Embryonic fibroblasts (MEFs) were isolated from day E13-15 old embryos by homogenising the embryos and resuspending the cell homogenate in 0.5% Trypsin in PBS. The enzymatic digest was incubated for 20 minutes at 37 ˚C. After addition of Fetal calf serum (FCS) containing DMEM, tissue was further homogenised by petting ~20 times. Released cells were washed by centrifugation and replacement with fresh medium, two times. Cells were then seeded in culture dishes and immortalised by transduction of SV40 large T antigen.

U937

The human lymphoma U937 was derived from a male patient who presented with histiocytic lymphoma in 1976 (Sundström & Nilsson, 1976). U937 cells can differentiate in response to several stimuli causing them to adopt macrophage-like morphology.

2.2 Methods

2.2.1 Culturing of eukaryotic cells

All cell lines were cultured in a humidified atmosphere adjusted to 5% CO_2 at 37 °C. HEK293T, HeLa and MEFs were maintained in Dulbecco's modified Eagle's medium (DMEM) with 5% foetal calf serum. To seed cells in different vessels or to prevent confluency, cells were detached by incubation in 1X Trypsin (Thermo Fisher Scientific) in PBS solution.

U937 and K562 and A549 cell lines were maintained at 37 °C in Roswell Park Memorial Institute medium (RPMI) supplemented with 10% FCS at 5% CO_2.

2.2.2 Freezing and thawing of eukaryotic cells

To preserve cell lines, 70% confluent cells were collected, washed once with normal medium and resuspended in freezing medium (FCS containing 10% Dimethyl sulfoxide(v/v).

2.2.3 Isolation of Bone Marrow Derived Macrophages (BMDMs)

BMDMs were obtained from 8-week-old mice. Hind legs were removed and tissue was separated from bones. Femur and tibia were opened on each site using scissors and bone marrow was flushed out using a 25-gauge needle and syringe. Cells were collected and resuspended in BMDM medium (RPMI medium containing 10%FCS, 1% penicillin/streptomycin (Invitrogen) and 10% of L929 cell-conditioned medium). After passing the cell suspension through a cell strainer, cells were plated in a 12-well plate. BMDM medium was replaced every two days and cells were incubated for a total of seven days before they were used in experiments.

2.2.4 Transient transfection

The day before transfection, cells were seeded and allowed to reach 50-70% confluency on the day of transfection. Per well of a 6-well plate, 1 µg DNA was diluted in 100 µl Opti-MEM. Likewise, TurboFect transfection reagent (Thermo Scientific) or Lipofectamine 2000 (Thermo Fisher) was diluted in in 100 µl Opti-MEM. The ratio of µg DNA/µl transfection reagent was maintained at a 1:3. The dilutions of DNA and

transfection reagent were mix and incubated for 30 minutes. Subsequently, the mixture was added dropwise to the cells. Cells were left to grow for another day before used in experiments.

2.2.5 siRNA-mediated knockdown

Transient knockdown of protein expression was achieved by reverse transfection of cells with siRNA using Lipofectamine 2000 (Invitrogen) following recommendations of the manufacturer. Lipofectamine 2000 was added to Opti-MEM medium and incubated for 5 minutes at room temperature. Next, siRNA (25 nM final concentration) was added and incubated for additional 20 minutes. The reaction mix was then added dropwise to the cells and the final volume was adjusted with antibiotic free medium. The ratio of Lipofectamine/siRNA was kept 3:1. All experiments were carried out 48-72 hours after transfection.

2.2.6 Retro- and lentivrial infection of eukaryotic cells

Genes of interest were cloned into the Murine Stem Cell Virus (MSCV) retroviral vector system (Clontech), which co-expresses green fluorescent protein (GFP) via an internal ribosomal entry site (IRES), and transfected in Phoenix-AMPHO cells (Nolan lab). This engineered HEK293 cell line constitutively expresses gag-pol and envelope protein for amphotropic viruses. Transfection was prepared by diluting DNA and Polyethylenimine (PEI) in Opti-MEM reduced serum medium (Thermo Fisher) The DNA/PEI ratio was kept at a 1:4. The transfection mixture was added dropwise to the cells. Next day, the medium was exchanged for antibiotic-free medium and cells were left an additional 24h in the incubator. After 48h and 72h, supernatants were collected and either directly used for cell infection or stored at -80 ˚C.

For cell infection, cells were seeded to reach 60% confluence on the day of infection. Viral supernatants were passed through a 0.45 µm filter diluted, 1:2 with antibiotics-free medium and Hexadimethrine bromide (polybrene) was added to a final concentration of 6 µg/ml before cells were subjected to spin-infection (2500 rpm, 45 min, 30 °C). After two days, GFP-positive cells were sorted by Fluorescence-activated cell sorting (FACS).

2.2.7 Generation of knockout cell lines using Lentiviral CRISPR-Cas9

Lentiviral particles for CRISPR-Cas9 mediated knockout (KO) were generated by transfection of Lenti-CRISPR v2 together with packaging vector psPAX2 and envelope coding vector pMD2G (Trono Lab) into HEK293T cells. Following guide RNAs were used: A20(KO) 5'-GGCGCTGTTCAGCACGCTCA; A20(ΔZnF2-5) 5'-GTGAACGTTGCCACAACGCC; A20(ΔZnF7) 5'-GTTGCAGTAGCCGTTGCACT; CYLD(KO) 5'-CACATCAATGATATCATCCC; OTULIN(KO) 5'-GAATTGCTTATACATGAAAG; HOIP(KO) 5'-TTGACACCACGCCAGTACCG. After collection of viral particle supernatants, transfection of cells was carried out identical to infection with retroviral particles. After 2 days, cells were subjected to puromycin (2 µg/ml) selection for one week or, in case of IRES-GFP expressing vectors, sorted for GFP positive cells. Selected populations were subcloned by serial dilution and single cell clones analysed for loss of protein expression by western blot and target gene sequencing.

2.2.8 Use of inhibitors in cellular systems

All chemical inhibitors of cellular functions were appropriately diluted in medium and then added to the cells 30 minutes prior to any stimulus or analysis.

2.2.9 Quantification of cell death

For analysis of cell death, suspension cells were collected centrifuged at 1500rpm for 5 minutes. In cases of adherent cells, supernatant containing floating dead cells was collected first, remaining adherent cells trypsinised and combined with the supernatant. After centrifugation, the cell pellet was resuspended in PBS containing 5 µg/ml propidium iodide (Sigma). Cells were analysed by FACS. Data is presented as mean ± standard error of the mean (SEM) (n = 3), statistics were performed using T-test.

2.3 Molecular Biology

2.3.1 DNA restriction digest

DNA restriction for analytic or preparative purpose was performed using FastDigest restriction enzymes) and buffers (Thermo Fisher Scientific). Per reaction, DNA was

diluted in water, mix with 10X buffer solution and 1µl of the appropriate enzyme(s) added. The total volume was kept at 30µl. Samples were incubated 30 minutes at 37 ˚C.

2.3.2 Purification of DNA

For purification of *in vitro* produced DNA, QIAquick PCR Purification Kit (Qiagen) was used according to the manufacture's recommendations. Alternatively, the buffer system was used in combination with third party DNA spin columns (Sydlabs). DNA was eluted in water.

2.3.3 Agarose gel electrophoresis of DNA

Separation of DNA for analytical or preparative purpose was achieved by agarose gel electrophoresis. Gels were prepared by melting 0.5-2% Agarose (w/v) in Borax buffer using a microwave oven. Gel solutions was then poured in gel casting trays (BioRad) and allowed to cool. Samples were applied in gel pockets and electrophoresis was carried out in Borax running buffer.

2.3.4 Gel extraction of DNA fragments

Recovery of DNA from agarose gels was achieved using QIAquick Gel Extraction Kit (Qiagen) according to the manufacturer's recommendations. DNA was visualised using a Dark Reader DR46B Transilluminator (Clare Chemical Research, Inc.) and excised using a scalpel. Gel pieces were weighed and three times the volume of gel extraction buffer (Qiagen) was added per 100mg of gel and dissolved at 55 ˚C. DNA was purified using provided spin columns (Syd labs) and eluted in water.

2.3.5 Ligation of DNA fragments for cloning

Compatible DNA overhangs or blunt ends were ligated using T4 DNA ligase (Thermo Fisher Scientific). For insertion of DNA fragments, originating from PCR reactions or DNA restriction, in vectors, the molar ratio of insert and vector was adjusted to 4:1. The provided 10X buffer solution was added before 1µl of T4 DNA ligase (5U/µl) was mix with the solution. Samples were left on room temperature for at least four hours to allow for ligation.

2.3.6 Transformation of competent *E.coli*

Chemically competent DG1 or BL21 (DE3) *E.coli* bacteria (Eurogentec) were mixed with approximately 10 ng Vector and left on ice for 15 minutes. Reaction tubes containing bacteria were then transferred to a water bath set at 42 ˚C for 35 seconds. Tubes were then allowed to cool on ice for 1 minute before addition of Super Optimal broth with Catabolite repression (SOC). Cells were allowed to grow for at least one hour before plating on agar plates containing the antibiotics to which the vector provides resistance. Following positive selection, individual clones were picked and verified by gene sequencing.

2.3.7 Isolation of Plasmid DNA

Propagation of plasmid DNA was carried out in DG1 *E.coli* bacteria (Eurogentec). Bacteria were allowed to grow in selection medium containing the appropriate antibiotics for 24 hours. Cells were collected and centrifuged at 13.000 rpm for 10 minutes. DNA was purified from the pellet using QIAprep Spin Mini Kit (Qiagen).

2.3.8 Isolation of genomic DNA

Genomic DNA from cultured cells was isolated using GenElute Mammalian Genomic DNA Miniprep Kit (Sigma), according to the manufacturer's recommendations.

2.3.9 Polymerase Chain Reaction (PCR)

Specific DNA fragments were amplified by PCR using a thermos cycler. For analytic purposes 5' DNA master mix was used and each reaction was set up as following:

Table 2.3: 5' PCR master mix set-up

Component	**Amount [µl]**
2.5X 5' Master mix	8
H_2O	8
Forward primer (10 µM)	1
Reverse primer (10 µM)	1
Cresol Red PCR dye	2

For preparative PCR amplification for e.g. cloning, KAPA HiFi HotStart ReadyMix PCR Kit (Kapa Biosystems) was used and prepared as following:

Table 2.4: 2X Kapa-HiFi master mix set-up

Component	**Amount [µl]**
2X Kapa-HiFi master mix	10
H_2O	6
Forward primer (10 µM)	1
Reverse primer (10 µM)	1
Cresol Red PCR dye	2

PCR-reaction tubes were placed in a Mastercycler pro PCR machine (Eppendorf). The standard temperature profile was set to:

Initial denaturation: 98 ˚C, 2min

Denaturation: 98 ˚C, 20s
Annealing: 50-68 ˚C, 15s
Elongation: 72 ˚C 1min/1kb
} 33x

Final elongation: 72 ˚C 30s

2.3.10 Preparation of cDNA

Complementary DNA (cDNA) was prepared by isolating mRNA from cultured cells using RNeasy Mini Kit (QIAGEN) according to the manufacturer's manual. Cells were collected and pelleted by centrifugation. Medium was aspirated and pellet resuspended in lysis buffer provided in the kit. RNA was purified by sequential binding and washing steps, using the provided RNA-binding spin columns. RNA was eluted in water. cDNA was generated using RevertAid First Strand cDNA Synthesis Kit (Thermo Fisher Scientific) according to the manufacturer's' manual. In brief, 1 µg RNA was mixed with 1 µl oligo(dt) in 12 µl H_2O total volume and incubated at 65 °C for 5 minutes. Subsequently, buffer, RNase Inhibitor, dNTP's and reverse transcriptase were and incubated at 42 °C for 60 minutes. Reverse transcriptase was heat-inactivated at 70 °C for 5 minutes.

2.4 Biochemistry

2.4.1 Relative measurement of protein concentration

Comparative analysis via western blot was supported by adjusting total cell lysates to equal amounts. Following lysis and centrifugation, 1-5 µl of the sample was used in the copper-based colorimetric Pierce Bicinchoninic acid (BCA) Protein Assay (Thermo Fisher Scientific). In brief, 50 parts component A was mixed with 1 part of component B. and distributed in a 96-well plate. Lysates were added to each well and proteins allowed to react until a violet colour was clearly visible in all samples. Absorbance at A562 nm was then measured using a Multiskan Ascent plate reader.

2.4.2 Quantitative determination of protein and DNA concentration

Concentration of DNA and proteins in aqueous solutions was determined with a NanoDrop Spectrophotometer.

2.4.3 SDS polyacrylamide gel electrophoresis (SDS-PAGE)

Samples were heated in 50 mM DTT-containing NuPAGE lithium dodecyl sulfate (LDS) Sample Buffer (Thermo Fisher Scientific) at 80 ˚C for 10 minutes. Separation of proteins according to their size was achieved by SDS-PAGE separation on 4-15% Mini-PROTEAN® TGX™ Precast Gels with TGX running buffer or NuPAGE Bis-Tris gels with MOPS running buffer.

2.4.4 Coomassie staining of SDS-PAGE gels

Proteins separated by SDS-PAGE were visualised by incubating the gel in InstantBlue (Expedion Protein Solutions).

2.4.5 Western blot

The transfer of proteins to a membrane allows their detection with specific antibodies. A pre-packed 0.2 µM nitrocellulose membrane assembly was used (BioRad, Trans-Blot® Turbo™ Mini Nitrocellulose Transfer Packs). The setup was composed of a layer of filter papers at the anode of the apparatus, on top a nitrocellulose membrane,

the gel and lastly another layer of filter papers. Protein transfer was carried out at a constant 20V output.

After the blotting procedure, the membrane was incubated for at least one hour in 5% milk powder in PBS-T to block unspecific protein bindings sites. The membrane was then washed three times for at least 10 minutes with PBS-T before adding a primary antibody. Primary antibodies were incubated for at least 1h at room temperature or overnight at 4 ˚C. The blot was washed three times with PBS-T and the corresponding secondary antibody was added and incubated for at least 1h at room temperature. Unless indicated otherwise, experiments were performed in biological triplicates and a representative result is shown.

2.4.6 Stripping of Western blot membranes

To re-probe a blot with another primary antibody, the blot was treated for 10min in stripping- buffer, to remove old primary/secondary antibodies. Stripping buffer was then removed and the blot was washed 3 times, followed by 10min incubation in 5% milk powder in TBST.

2.4.7 Production of recombinant TNF

A tandem affinity purification (TAP) tag, consisting of a His-tag followed by 3X Flag-tag, a PreScission cleavage site and 2X Strep-tag II was fused to the extracellular portion of TNF (aa78- 233). Alternatively, a poly-His-tag was added to TNF (aa78-233). Both fusion proteins were cloned into pQE30 vector (Draber et al., 2015). Proteins were expressed in BL21 (DE3) cells by induction with 1 mM Isopropyl-β-D-thio-galactoside (IPTG) and incubated overnight at 30 °C. Following lysis of bacteria, the soluble protein was purified by affinity chromatography on His GraviTrap TALON columns (GE Healthcare), eluted with 500 mM imidazole and dialyzed against storage buffer (50 mM Tris, pH 7.4, 100 mM NaCl, 0.02% Tween, 2 mM DTT, 0.5 M arginine). The final protein concentration was measured using a Nanodrop 2000 (Thermo Fisher Scientific) and samples were stored at -20 °C.

2.4.8 Production and coupling of ubiquitin affinity proteins

Coding sequence of OTULIN was cloned from cDNA isolated from K562 cells. The coding sequence of the K63-AP protein is based on the tUIM (Rx3(A7)) construct

described previously (Sims et al., 2012) and was synthesised by Life Technologies. The M1-AP protein (OTULIN aa58-352, C129A) was cloned by conventional PCR and ligated into pH6HTC His6HaloTag® T7 Vector (Promega) using XhoI and XbaI restriction sites. Total ubiquitin binding protein is derived from the Rabex5 UIM (aa147-198) and was synthesised (Life Technologies) as tandem repeat, separated by a TEV-linker, and integrated into pH6HTC His6HaloTag® T7 Vector (Promega) using XhoI and XbaI restriction sites. The sequence of the Rabex5 2XUIM-TEV is: MGIHVDQSDLLCKKGCGYYGNPAWQGFCSKCWREEYHKARQKQIQEDWELAER LQREEEEAFASSQGENLYFQSGGGIHVDQSDLLCKKGCGYYGNPAWQGFCSKC WREEYHKARQKQIQEDWELAERLQREEEEAFASSQ. The underlined sequence indicates the TEV-linker.

A second M1-AP tool based on tandem repeats of the NEMO UBAN domain (aa289-360), separated by a TEV-linker, and was synthesised (Life Technologies) and cloned into pH6HTN His6HaloTag® T7 Vector (Promega) using XbaI and NotI restriction sites. The sequence of the NEMO 2XUBAN-TEV is: MEQHKIVMETVPVLKAQADIYKADFQAERQAREKLAEKKELLQEQLEQLQREYSKL KASCQESARIEDMRKRHVLEPTTEDLYFQSDNDEQHKIVMETVPVLKAQADIYKAD FQAERQAREKLAEKKELLQEQLEQLQREYSKLKASCQESARIEDMRKRHV. The underlined sequence indicates the TEV-linker. Expression vectors were transformed into competent BL21 (DE3) bacteria. Halo-tagged proteins were expressed by auto induction using 2YT Broth medium (ForMedium) according to the manufacturer's recommendation. Proteins were extracted using bacteria lysis buffer (50 mM HEPES, pH 7.6, 150 mM NaCl, 100 µg/ml Lysozyme, 2 mM DTT) and lysate was sonicated for one minute. Lysates were cleared by centrifugation at 25,000 rpm for 45 minutes. Cleared lysates of HALO-OTULIN was aliquoted and frozen at -20 °C. Aliquots were then used to freshly couple HALO-tagged ubiquitin affinity proteins to HALO-beads (Promega) according to the manufacturer's recommendation prior to experiment. All other HALO-tagged proteins were purified from lysates using a HisTrap HP 5ml column (GE Healthcare) attached to an ÄKTA Prime (GE Healthcare). Following binding of the protein, the column was washed with 15 times the column volume with lysis buffer. Elution of HALO-tagged proteins was achieved by running an increasing gradient of Immidazole through the column and fractions of the eluent were collected and analysed by coomassie SDS-PAGE. 50% (v/v/) Glycerol was added to the protein solutions which were stored at -80 ˚C for long term, and -20 ˚C for short term (< 3 month) storage.

2.4.9 Production of deubiquitinases (DUBs)

Coding sequences for OTULIN and USP21 were cloned from cDNA. Coding sequence for vOTU was synthesised (Life technologies). Sequences were cloned into GEX6- P2 vector. Expression vectors and transformed into BL21 (DE3) bacteria. glutathione S-transferase (GST)-tagged proteins were expressed as described for ubiquitin affinity proteins. GST-tagged DUBs were purified using Glutathione agarose beads (Sigma) according to manufacturer's manual. Following binding, beads were washed three times with DUB-buffer (50 mM HEPES, pH 7.6, 150 mM NaCl, 5 mM DTT). PreScission protease (GE Healthcare) was added (160 U per 1ml of beads, 4 °C, overnight) in order to remove the GST-tag and to elute the proteins. Protein concentration was measured with a Nanodrop 2000 (Thermo Scientific) and glycerol was added to a final concentration of 20%. Samples were aliquoted and stored at -80 °C. Recombinant human CYLD (aa583-956) was produced essentially as described previously (Komander et al., 2008), and kindly provided by Katrin Rittinger.

2.4.10 Immunoprecipitation of protein complexes

Ectopically expressed proteins were purified via their respective tag. Following cell lysis in IP-lysis buffer, lysate was cleared by centrifugation. FLAG-tagged proteins were immunoprecipitated using anti-FLAG (M2) beads (Sigma Aldrich). Where other antibodies have been used, 1 µg of antibody was bound to Protein A/G beads (Santa Cruz Biotechnology) prior to the addition to the lysate. Immunoprecipitations were carried out at 4 °C with gentle rotation for 4-16 hours. Beads were then washed three times with lysis buffer and reduced using LDS sample buffer.

2.4.11 TNFR1-SC purification

Flag-tagged TNF (1 µg/ml) in medium (37 °C) was added to the cells for the indicated time. Stimulation medium was removed and cells were washed with cold PBS in order to slow down propagation of signalling. PBS was removed and cells were lysed in IP-lysis buffer. Cellular debris was cleared by centrifugation at 13.000 rpm for 20 minutes. 1/100 of the amount of FLAG-TNF used for the stimulation was added to lysates obtained from non-stimulated cells as a negative control. 10 µg M2 beads (Sigma) were then added to the lysate and incubated overnight at 4 °C. Next day, samples were washed three times with IP-buffer and then reduced in sample buffer.

3 Results

In order identify and analyse HOIP-associated proteins, K562-deficient cells were created by transfection of Zinc finger nucleases targeting the HOIP gene in exon XXX. Individual clones were obtained by serial dilution and disruption of the HOIP coding gene, *RNF31*, was validated by sequencing. Next, these cells were viraly reconstituted with vector control, HOIP-FLAG or enzymatic inactive HOIP-C885S-FLAG.

3.1 Analysis of the interaction of CYLD, OTULIN and SPATA2 with HOIP

To validate the constitutive interaction of CYLD, OTULIN and SPATA2 with HOIP, found by mass spectrometry (Draber et al., 2015), HOIP was immunoprecipitated from HOIP-deficient K562 cells reconstituted with either FLAG- tagged wild type or enzymatic inactive C885S HOIP and compared to empty vector control. Western blot analysis of these samples showed that Sharpin and HOIL-1 but also CYLD, OTULIN and SPATA2 interact with LUBAC, independently of its enzymatic activity (Figure 3.1). Hence, LUBAC is associated with two DUBs and SPATA2.

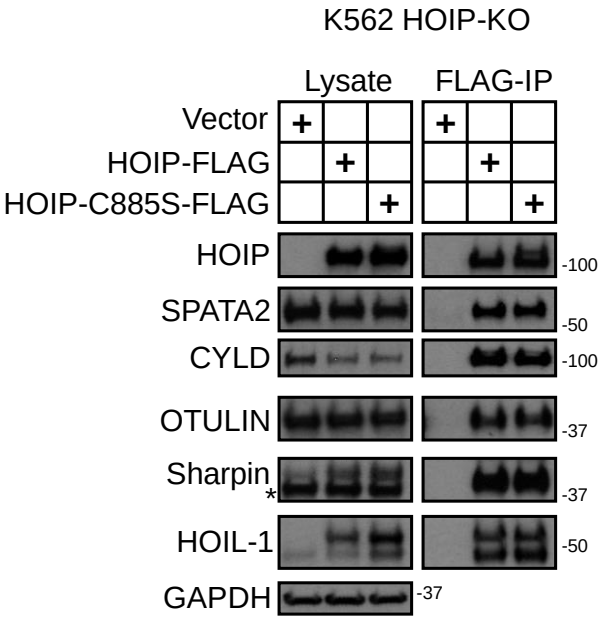

Figure 3.1: SPATA2, CYLD and OTULIN are constitutively associated with HOIP

HOIP-deficient K562 cells were virally reconstituted with either TAP-tagged (3XFLAG-2XStrep) HOIP WT or enzymatic inactive HOIP-C885S expression plasmids. empty TAP vector was transduced as a negative control. Cells were lysed and tagged HOIP was immunopurified using anti-FLAG M2 beads (Sigma). Next day, beads were washed to remove unbound proteins, samples were reduced in LDS-buffer and analysed by western blot for the association of SPATA2, CYLD and OTULIN with HOIP. * indicates non-specific detection.

3.1.1 CYLD and SPATA2, but not OTULIN, are recruited to the TNFR1-SC

The constitutive interaction of SPATA2, CYLD and OTULIN with HOIP suggested a simultaneous recruitment to signalling complexes. Indeed, immunoprecipitation of FLAG-TNF revealed recruitment of SPATA2, CYLD and HOIP to the native TNFR1-SC with similar kinetics (Figure 3.2). OTULIN, however, was not detected to form part of the TNFR1-SC, although every other LUBAC-associated protein and additional complex components were clearly detected (Figure 3.2). In summary, although SPATA2, CYLD and OTULIN constitutively interact with HOIP, only SPATA2 and CYLD are recruited to the TNFR1-SC with kinetics similar to HOIP, whilst OTULIN is not recruited at all.

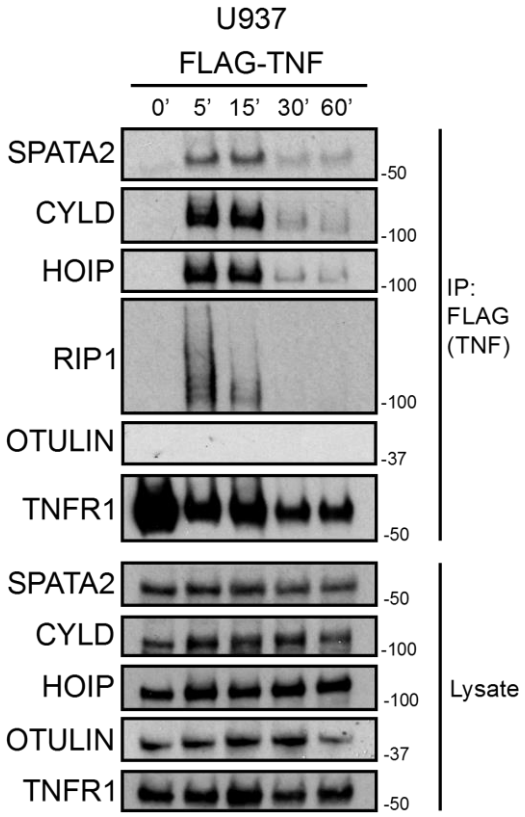

Figure 3.2: SPATA2, CYLD, but not OTULIN are recruited to the TNFR1-SC

(A) Immunoprecipitation of FLAG-TNF confirms recruitment of SPATA2 and CYLD but not OTULIN to the TNFR1-SC. U937 cells were stimulated with 1 µg/ml FLAG-TNF for the indicated time. As a control, FLAG-TNF was added after cell lysis and designated as time point 0'. Cells were lysed in IP-lysis buffer and the TNFR1-SC was isolated by anti-FLAG immunoprecipitation. Lysate and IP samples were separated on the same gel and analysed by western blot.

3.1.2 CYLD and SPATA2 recruitment to the TNFR1-SC is HOIP dependent

Because of the constitutive interaction of CYLD and SPATA2 with HOIP and their concomitant recruitment to the TNF-RSC, it is possible that these proteins are recruited in a HOIP-dependent manner. To address this, the TNFR1-SC was isolated from WT and HOIP-KO A549 cells. Strikingly, neither CYLD nor SPATA2 were recruited to the TNFR1-SC in the absence of HOIP (Figure 3.3, A). This same result was also obtained in HeLa cells (Draber et al., 2015). It was, however, unclear whether CYLD or SPATA2 require HOIP as an adaptor for their recruitment or whether linear ubiquitin chains created by LUBAC are responsible for the recruitment. HOIP-deficient A549 cells were therefore reconstituted with either HOIP (HOIP-WT) or enzymatically inactive HOIP (HOIP-CS). Analysis of the TNFR1-SC showed that SPATA2 and CYLD were recruited independently of the enzymatic activity of HOIP (Figure 3.3, B). Hence, SPATA2 and CYLD require HOIP as a scaffold protein for their recruitment to the TNFR1-SC.

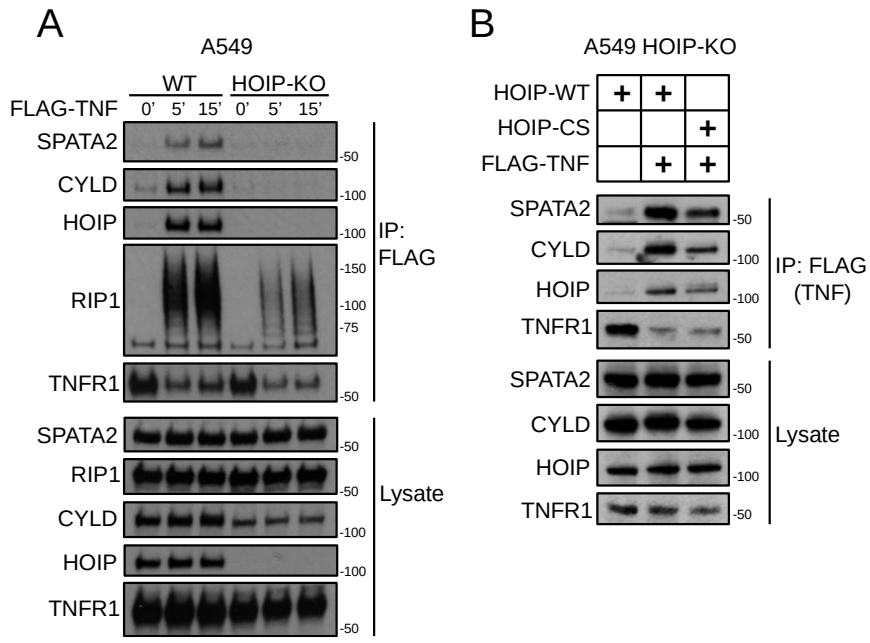

Figure 3.3: SPATA2 and CYLD recruitment to the TNFR1-SC requires HOIP

(A) Comparison of TNFR1-SC purifications derived from wild type and HOIP-deficient A549 cells shows that recruitment of CYLD and SPATA2 to the TNFR1-SC is dependent on HOIP. A549 cells, proficient or deficient for HOIP, were subjected to TNFR1-SC purification using 1 µg/ml FLAG-TNF for cell stimulation. FLAG-IP-purified complexes were analysed by western blot.

(B) The enzymatic activity of HOIP is not required for the recruitment of SPATA2 or CYLD to the TNFR1-SC. HOIP-deficient A549 cells were virally reconstituted with either wild type HOIP (HOIP-WT) or an enzymatically inactive HOIP-C885S (HOIP-CS). TNFR1-SC was purified using 1 µg/ml FLAG-TNF and analysed by western blot.

3.1.3 CYLD and SPATA2 are also recruited to the NOD2-SC

The analysis of the TNFR1-SC in absence of HOIP revealed a strong dependency of CYLD and SPATA2 on HOIP for their recruitment (Figure 3.4). It was therefore possible that HOIP is also required for the recruitment of these factors to other signalling complexes employing LUBAC, like the NOD2-signalling complex. A549 cells pro- or deficient for HOIP were therefore reconstituted with FLAG-tagged NOD2 as these cells do not naturally express this intracellular peptidoglycan receptor. The synthetic ligand L18-muramyl dipeptide (L18-MDP) was used to trigger signalling via NOD2 and the signalling complex was purified via FLAG-immunoprecipitation. Western blot analysis of these samples showed that SPATA2 and CYLD are indeed recruited to NOD2. Importantly, both proteins were absent from the NOD2-SC when HOIP was absent (Figure 3.4). Therefore, HOIP also acts as an adaptor for SPATA2 and CYLD recruitment to the NOD2-SC in addition to its linear ubiquitination activity.

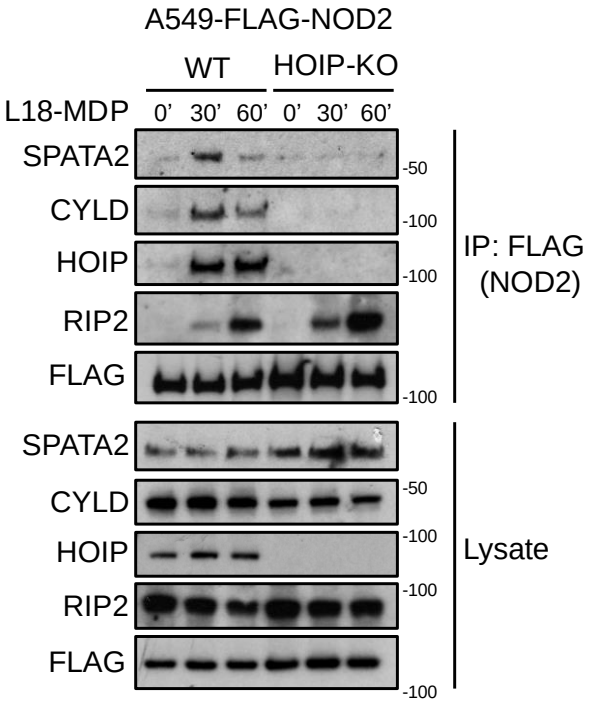

Figure 3.4: CYLD and SPATA2 recruitment to the NOD2-SC is HOIP-dependent

Wild type or HOIP-deficient A549 cells were reconstituted with FLAG-NOD2 to allow for purification of the NOD2-SC by anti-FLAG immunoprecipitation. After stimulation with 200ng/ml L18-MDP, the NOD2-SC was isolated via FLAG-immunoprecipitation and analysed by western blotting.

3.1.4 Deficiency in CYLD leads to loss of SPATA2 stability

Next, protein expression in HeLa cells lacking either HOIP, CYLD or OTULIN was analysed. As shown in Figure 3.5, the stability of SPATA2 was drastically decreased by absence of CYLD. SPATA2 protein levels remained unchanged in cell lines lacking either HOIP or OTULIN. This indicated that SPATA2 and CYLD might also be functionally associated.

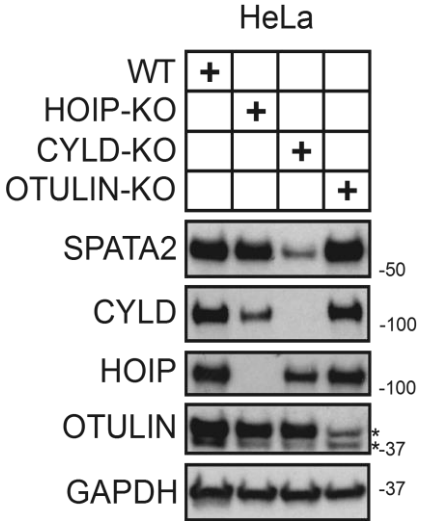

Figure 3.5: SPATA2 is destabilised in absence of CYLD

Protein expression level of SPATA2 is reduced in CYLD-, but not HOIP- or OTULIN-deficient HeLa cells. Cell lysates were generated from HeLa cells deficient for HOIP, CYLD or OTULIN and compared to control cells with regards to the protein level of SPATA2, CYLD HOIP and OTULIN using western blotting.

3.2 Characterisation of the SPATA2-CYLD-HOIP interaction

The interaction of OTULIN with HOIP was shown to be direct (Elliott, Nielsen et al., 2014, Schaeffer, Akutsu et al., 2014). However, a similar analysis using recombinant HOIP-PUB domain and the USP domain of CYLD did not suggest a direct interaction between these proteins (Kupka et al., 2016a). Because of the strong connection between CYLD, SPATA2 and HOIP, the interaction of these proteins was analysed more closely.

3.2.1 CYLD interacts indirectly with HOIP via SPATA2

CYLD, OTULIN and SPATA2 were overexpressed in different combinations to test their influence on each other with respect to binding to HOIP (Figure 3.6, A). Next, HOIP was purified and analysed for interacting proteins by western blot. In

accordance with the reported direct interaction, overexpression of OTULIN together with HOIP led to a drastic increase in the amount of OTULIN that is bound to HOIP, compared to endogenous levels (Figure 3.6, A). However, the over expression of CYLD led only to a marginal increase in HOIP-associated CYLD. This unproportioned increase suggested that the interaction of CYLD with HOIP is indirect and possibly requires an additional factor. Overexpression of SPATA2 alone did not significantly change the amount of endogenous CYLD that bound to the overexpressed HOIP. However, concomitant overexpression of SPATA2 with CYLD increased binding of CYLD to HOIP proportionally to the amount that was overexpressed (Figure 3.6, A). Importantly, SPATA2 was sufficient to fully restore CYLD binding, indicating that it is the only factor required and sufficient for binding of CYLD to HOIP. To validate this finding on an endogenous protein level background, knockdown of SPATA2 was performed using RNAi and the effect on association of CYLD and HOIP was analysed. Indeed, suppression of SPATA2 expression by RNAi drastically diminished the constitutive interaction of CYLD with HOIP (Figure 3.6, B). In summary, while the interaction of OTULIN and HOIP is direct, the binding of CYLD to HOIP is mediated by SPATA2.

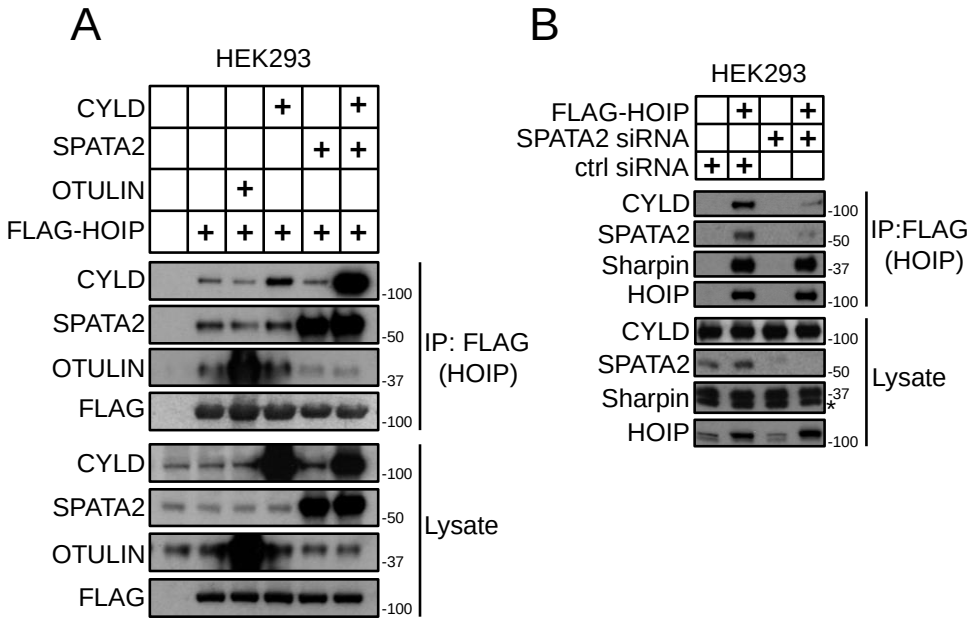

Figure 3.6: Binding of CYLD to HOIP is mediated by SPATA2

(A) SPATA2 is required and sufficient for binding of CYLD to HOIP. Combinations of SPATA2, CYLD, OTULIN and FLAG-HOIP were expressed in HEK293 cells. The resulting complexes were purified by FLAG-HOIP-immunoprecipitation and analysed by western blot.

(B) Binding of CYLD to HOIP is abrogated in absence of SPATA2. HEK293 cells were transfected with FLAG-HOIP and siRNA targeting SPATA2. HOIP was purified as in (A) and analysed for SPATA2 association via western blot. * indicates non-specific detection.

3.2.2 SPATA2 is required for recruitment of CYLD to the TNFR1-SC

Because the ablation of SPATA2 disrupted the constitutive interaction of CYLD with HOIP, the effect of SPATA2-loss on CYLD recruitment to the TNFR1-SC was also analysed. Purification of the TNFR1-SC revealed that CYLD was not recruited to the signalling complex following depletion of SPATA2 via RNAi in A549 cells (Figure 3.7). Importantly, presence of HOIP in the complex was unaffected, indicating that the recruitment of HOIP is an upstream event. Hence, loss of SPATA2 enables binding of CYLD to HOIP, which is required for the recruitment of CYLD to the TNFR1-SC.

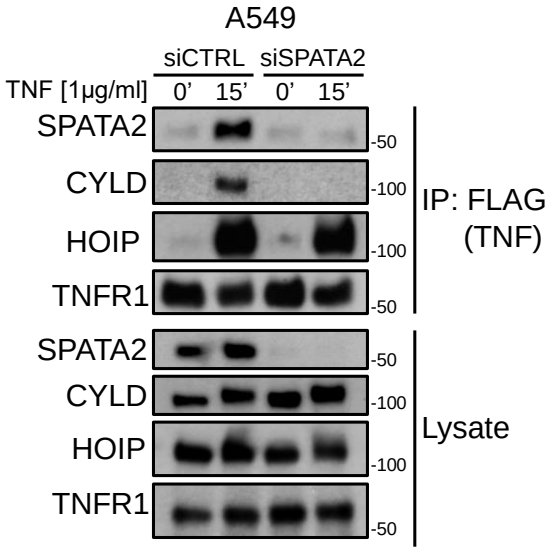

Figure 3.7: SPATA2 is required for recruitment of CYLD to the TNFR1-SC

Recruitment of CYLD to the TNFR1-SC is abrogated in absence of SPATA2. Control or SPATA2 siRNA was transfected in A549 cells. After 2 days, cells were stimulated with 1 µg/ml FLAG-TNF for the indicated time. The TNFR1-SC was isolated by anti-FLAG immunoprecipitation and analysed by western blot for the recruitment of SPATA2, CYLD and HOIP.

3.2.3 OTULIN and CYLD interact with the PUB domain of HOIP

To map the interaction of OTULIN, SPATA2 and CYLD with HOIP, different truncation mutants of TAP-tagged HOIP were expressed in HOIP-deficient K562 cells. Immunoprecipitation of HOIP revealed that constructs lacking the N-terminal PUB-domain did not interact with OTULIN, SPATA2 or CYLD anymore (Figure 3.8, A). However, the N-terminal deletion mutants still interacted with Sharpin and HOIL-1, indicating that HOIP, and not Sharpin or HOIL-1, interacts with OTULIN, SPATA2 and CYLD. The point mutation of asparagine (N) 102 to alanine (A) in the PUB domain of HOIP (HOIP-N102A) was shown to abolish the interaction of HOIP with OTULIN

(Elliott et al., 2014). HOIP-deficient A549 cells were therefore reconstituted with HOIP or HOIP-N102A to investigate the importance of this residue for binding of SPATA2/CYLD to HOIP. Analysis of the TNFR1-SC obtained from HOIP-N102A expressing cells showed that CYLD and SPATA2 were no longer recruited to the TNFR1-SC (Figure 3.8, B). Hence, the PUB domain is critical for mediating the interaction with both OTULIN and SPATA2/CYLD.

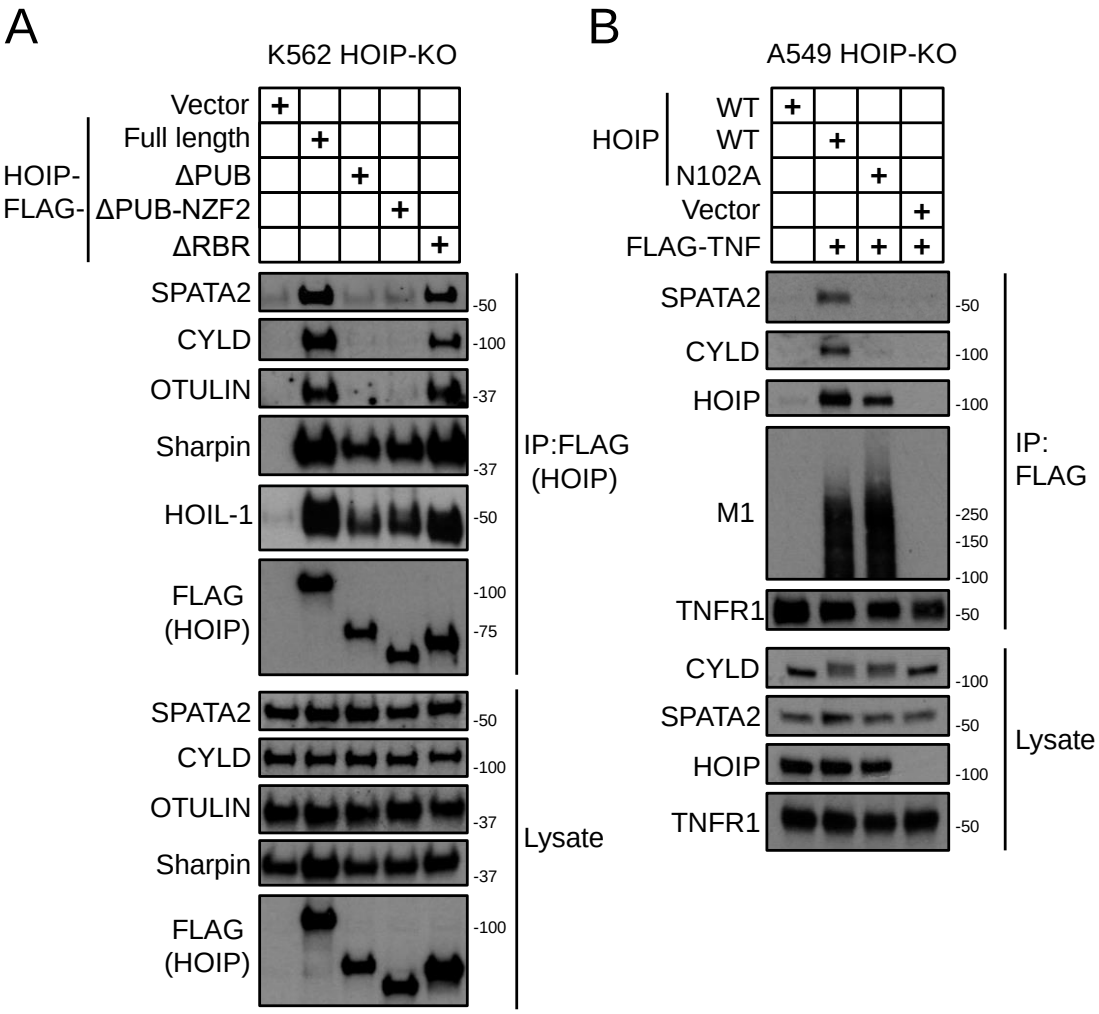

Figure 3.8: OTULIN, SPATA2 and CYLD bind to the PUB domain of HOIP

(A) Binding of SPATA2, CYLD and OTULIN to HOIP is lost in absence of HOIP's PUB domain. HOIP-deficient K562 cells were virally reconstituted with either vector, full length HOIP, ΔPUB-HOIP, or ΔPUB-NZF2-HOIP. FLAG-HOIP was purified using anti-FLAG M2 beads and samples were analysed for associated proteins using western blotting.

(B) Mutation of amino acid Asp102 to Ala in the PUB of HOIP abrogates recruitment of CYLD and SPATA2 to the TNFR1-SC. A549 cells deficient for HOIP were reconstituted with HOIP or HOIP-N102A. 1µg/ml FLAG-TNF was added to the cells for 15 minutes before washing and lysing the cells in IP-buffer. Subsequently, the TNFR1-SC was purified by anti-TNF immunoprecipitation and samples were analysed by western blot.

3.2.4 The USP domain of CYLD is sufficient for interaction with HOIP

The domain in CYLD, responsible for the interaction with HOIP, was determined by creating a truncated version of CYLD which only comprised the enzymatically active USP domain, but lacks the C-terminal CAP-Gly-domains (CYLD-USP). CYLD and CYLD-USP were expressed together with FLAG-HOIP and protein complexes were immunoprecipitated via the FLAG-tag. As seen in Figure 3.9, the USP domain of CYLD was sufficient for binding to HOIP. Moreover, the exogenously expressed USP domain competed with endogenous CYLD for binding to HOIP (Figure 3.9, lane 4).

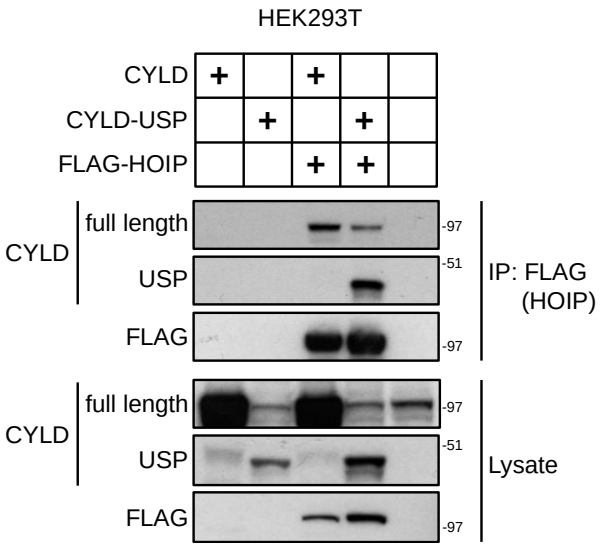

Figure 3.9: The USP domain of CYLD is sufficient for binding to HOIP

Immunoprecipitation of FLAG-HOIP co-purifies a C-terminal fragment of CYLD comprising the USP domain. Combinations of FLAG-HOIP, CYLD and the USP domain of CYLD were expressed in HEK293 cells. HOIP was immunoprecipitated by anti-FLAG IP and the complex was analysed using western blot.

3.2.5 SPATA2 binds CYLD and HOIP with different domains

SPATA2 acts as an adaptor between CYLD and HOIP, thus bridging the interaction of the two. To map the responsible domain in SPATA2, which mediates the interaction with HOIP and CYLD respectively, different truncation mutants were created. These GFP-tagged SPATA2 versions were expressed and analysed for binding to HOIP and CYLD. Analysis of these samples revealed that only truncations of the N-terminal region, comprising a part of SPATA2's PUB domain, still interacted with CYLD (Figure 3.10). The interaction with HOIP on the other hand was mediated by a domain located between aa167–417 in SPATA2 (Figure 3.10).

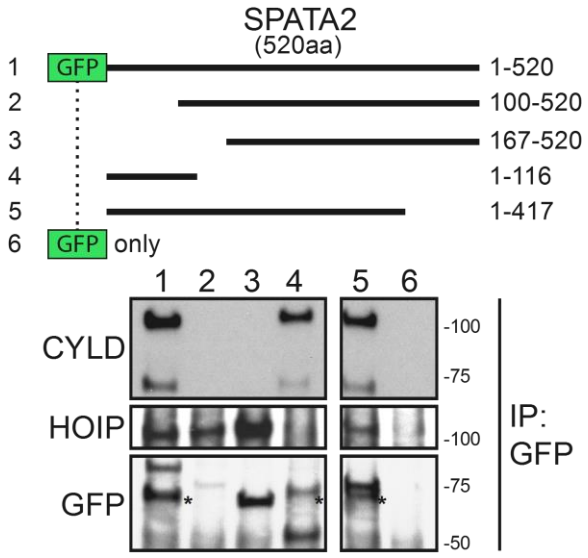

Figure 3.10: SPATA2 binds CYLD and HOIP with different domains

HOIP binds a motif in SPATA2 which is located between aa116-417, whereas CYLD bind to the N-terminus (aa1-116) of SPATA2. GFP-tagged full-length SPATA2 or truncations were expressed in HEK293 cells. Protein complexes were immunoprecipitated using anti-GFP and samples were analysed for associated HOIP and CYLD by western blotting. The experiment was performed two times * indicates non-specific detection.

3.2.6 SPATA2 contains a PIM that directly interacts with the PUB of HOIP

Because the interaction of SPATA2 was disrupted by the N102A mutation located in the PUB domain of HOIP, it is likely that SPATA2, like OTULIN, contains a PIM which directly binds to the PIM-pocket in the PUB domain. Therefore, peptide arrays spanning amino acid 201-520 of SPATA2 were spotted on a nitrocellulose membrane. These 20-mer peptides overlap by one aa and each spot is shifted by one aa towards the C-terminus. Hence, a potential binding motif shorter than 20 aa will be present in several neighbouring spots. The membrane was subsequently incubated with recombinant GST or GST-tagged PUB domain of HOIP (GST-PUB). After washing the unbound proteins away, specifically bound proteins were detected using standard western blot detection via antibodies. The result of membranes incubated with either GST (coloured in black) or GST-PUB (coloured in red) were graphically superimposed. The PIM of OUTLIN served as a positive control and readily bound to GST-PUB (Figure 3.11). Importantly, a sequence spanning aa 319-347 in SPATA2 specifically interacted with the PUB domain of HOIP. The corresponding sequence RGTYFSTQDDVDLYTDSEPR can be regarded as the PIM of SPATA2. Hence, SPATA2 directly binds to HOIP via a PUB-PIM interaction.

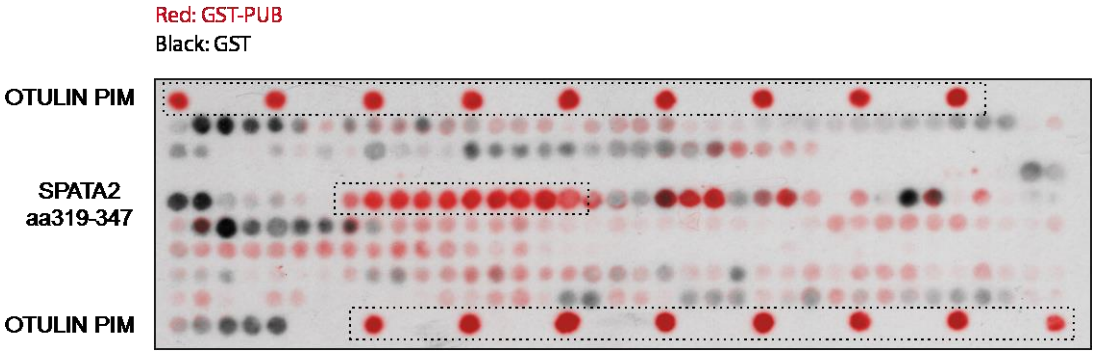

Figure 3.11: A PIM in SPATA2 directly binds to the PUB domain of HOIP

The PUB domain of HOIP binds to a motif located between aa319-347 of SPATA2. Arrays consisting of 20-mer overlapping peptides, corresponding to aa201–520 of SPATA2, were blotted on nitrocellulose membranes. The OTULIN PIM peptide served as a positive control. One membrane was incubated with recombinant GST-only (GST) the other one with GST-tagged PUB-domain of HOIP (GST-PUB). GST was subsequently detected by HRP immunofluorescence. The resulting image of GST-PUB detection was pseudo-coloured in red and overlaid with the GST-only image.

3.2.7 The PIM of SPATA2 is evolutionary conserved

Because the PIM of SPATA2 is required for binding to HOIP thus enabling recruitment of CYLD to signalling complexes, the importance of this domain is likely reflected by its evolutionary conservation. The PIM identified in human SPATA2 was therefore aligned to the corresponding sequence found in SPATA2 in other species (Figure 3.12, A). The sequence alignment shows a high degree of evolutionary conservation providing further evidence for the importance of this interaction for the function of SPATA2. OTULIN and SPATA2 contain an Asp and Tyr in the same position of the PIM, and both residues were shown to be critical for OTULIN binding to the PUB domain of HOIP (Elliott et al., 2014).

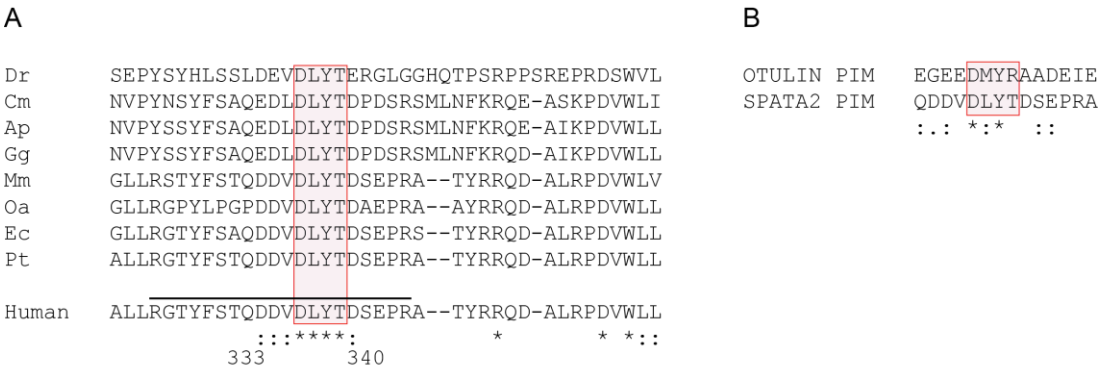

Figure 3.12: The PIM in SPATA2 is highly evolutionary conserved

(A) Sequence alignment of the SPATA2 PIM region found in different species indicates a high degree of evolutionary conservation especially between aa333-340 of human SPATA2. Dr, Danio rerio; Cm, Chelonia mydas; Ap, Anas platyrhynchos; Gg, Gallus gallus; Mm, Mus musculus; Oa, Ovis aries; Ec, Equus caballus; Pt, Pan troglodytes. Underlined sequence represents the PIM as determined by peptide arrays (Figure 3.11).

(B) D336 and Y338 of the human SPATA2 PIM are also found in human OTULIN.

***** indicates identity, **:** indicates similarity.

3.3 Functional relevance of OTULIN for LUBAC function

Having established the molecular basis for the interaction of CYLD, SPATA2 and OTULIN with HOIP, the functional consequence of this interaction was analysed. First, the effect of OTULIN on LUBAC's role in TNFR1-signalling was analysed. As OTULIN was absent from the TNFR1-signalling complex, a regulation of LUBAC prior to its recruitment to the TNFR1-SC was likely.

3.3.1 Inactive OUTLIN stabilises M1-ubiquitination

LUBAC was shown to generate linear ubiquitin chains upon overexpression of HOIP together with either Sharpin or HOIL-1 (Gerlach et al., 2011). Because of the constitutive interaction of OTULIN with HOIP, OTULIN likely functions as an inhibitor of LUBAC's function. OTULIN, or the enzymatically inactive OTULIN C126A, were therefore expressed together with LUBAC in order to assess the effect on LUBAC's function (Figure 3.13). Overexpression of LUBAC only slightly increased the amount of M1-linked ubiquitin chains detected in the lysate, however, this increase was reverted when OTULIN was co-overexpressed (Figure 3.13, lane 3). Strikingly, overexpression of OTULIN C126A together with LUBAC not only failed to revert increased linear ubiquitination but instead led to a drastic accumulation of M1-linked

chains. This indicates that enzymatically inactive OTULIN acts as a dominant negative inhibitor of endogenous OTULIN and M1-chain hydrolysis.

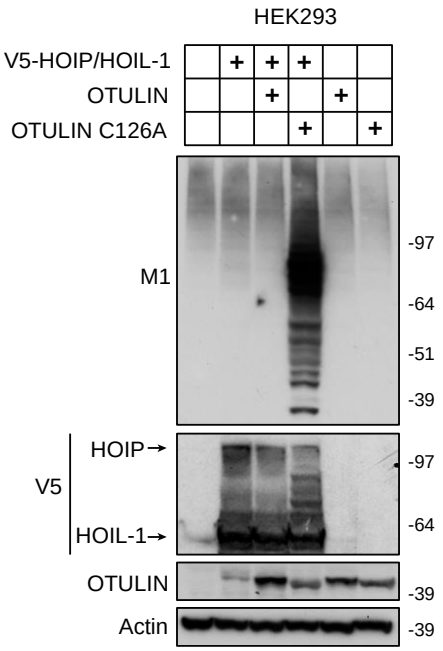

Figure 3.13: Enzymatically inactive OTULIN stabilises linear ubiquitin chains Deubiquitinase inactive OTULIN C126A acts in a dominant negative manner and stabilises linear ubiquitin chains generated by overexpressed LUBAC. V5-tagged LUBAC (V5-HOIP/HOIL-1) was overexpressed in HEK293 cells, together with OTULIN or enzymatically inactive OTULIN C126A. Two days after transfection, cells were lysed and analysed via western blotting.

3.3.2 Aberrant M1-linked ubiquitin chains are conjugated to unknown targets

OTULIN-deficient cells were described to accumulate linear ubiquitin chains (Rivkin et al., 2013). However, it was not clear whether these chains were attached to proteins or whether LUBAC generates free linear ubiquitin chains in absence of OTULIN. To address this question, lysates from OTULIN-deficient A549 cells were subjected to an *in vitro* deubiquitination assay. As shown in Figure 3.14, A, treatment with recombinant OTULIN or the non-specific DUB USP21 cleaved all linear ubiquitin chains. In contrast, treatment with IsoT (USP5), which requires a free C-terminus for hydrolysing ubiquitin chains, was unable to remove M1-ubiquitin chain conjugates (Figure 3.14, A). In a control, however, IsoT could cleave recombinant unanchored M1-linked ubiquitin chains (Figure 3.14, B). Interestingly, HOIL-1 showed increased ubiquitination, which was removed by treatment with OTULIN, suggesting that HOIL-

1 is modified by M1-linked ubiquitin in absence of OTULIN. In summary, the increase in linear ubiquitination in absence of OTULIN is not caused by accumulation of free linear ubiquitin chains. Instead, linear ubiquitin chains accumulate on unknown LUBAC substrates. Additionally, LUBAC components themselves might be linearly-ubiquitinated in absence of OTULIN, as seen on HOIL-1.

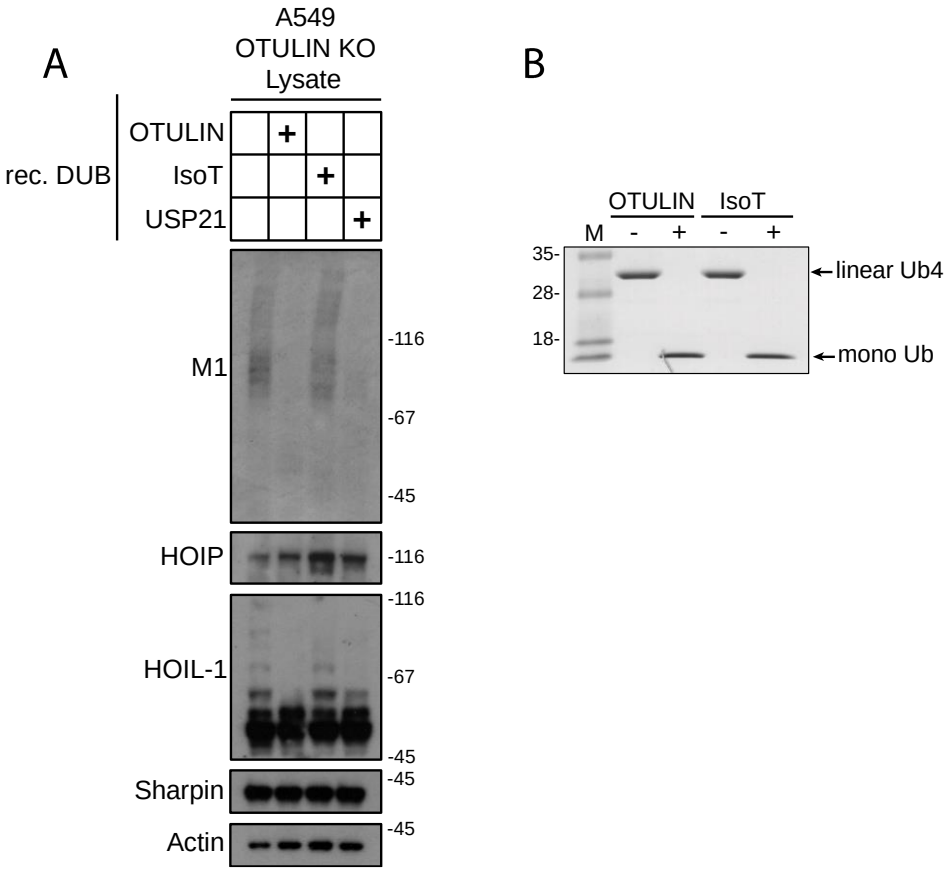

Figure 3.14: Absence of OTULIN leads to accumulation of M1 ubiquitin chains

(A) M1-linked ubiquitin chains that accumulated in absence of OTULIN are conjugated to proteins and are not free. OTULIN-deficient A549 cells were lysed in absence of protease inhibitors and resulting lysates were subjected to *in vitro* deubiquitination by adding 1µM recombinant OTULIN (specific for linear ubiquitin chains), IsoT (unable to cleave conjugated ubiquitin chains) or USP21 (able to cleave all all ubiquitin chain types). Samples were incubated for 1 hour at 37˚C. Samples were analysed by western blotting.

(B) The activity of OTULIN and IsoT used in (A) was verified using recombinant linear tetra-ubiquitin, demonstrating that IsoT can indeed cleave free linear ubiquitin chains. Samples were separated by SDS-PAGE and visualised using Coomassie Blue. The experiment was repeated two times.

3.3.3 Absence of OTULIN from the TNFR1-SC is not due to its DUB activity

The lack of OTULIN recruitment to the TNF-RSC was surprising, as another group reported that overexpressed OTULIN can be recruited to the TNFR1-SC upon stimulation (Schaeffer et al., 2014). To further investigate this discrepancy, OTULIN or enzymatically inactive OTULIN-C129A was overexpressed in OTULIN-deficient A549 cells and the TNFR1-SC was isolated using immunoprecipitation of FLAG-TNF. Analysis of the TNFR1-SC did not show any recruitment of active nor inactive OTULIN (Figure 3.15). Interestingly, despite of the absence of OTULIN from the SC, overexpression of active OTULIN, but not inactive OTULIN-C129A, drastically reduced the amount of linear ubiquitin chains present in the TNFR1-SC (Figure 3.15). However, it was not clear from which SC-components had reduced M1-ubiquitination in presence of OTULIN.

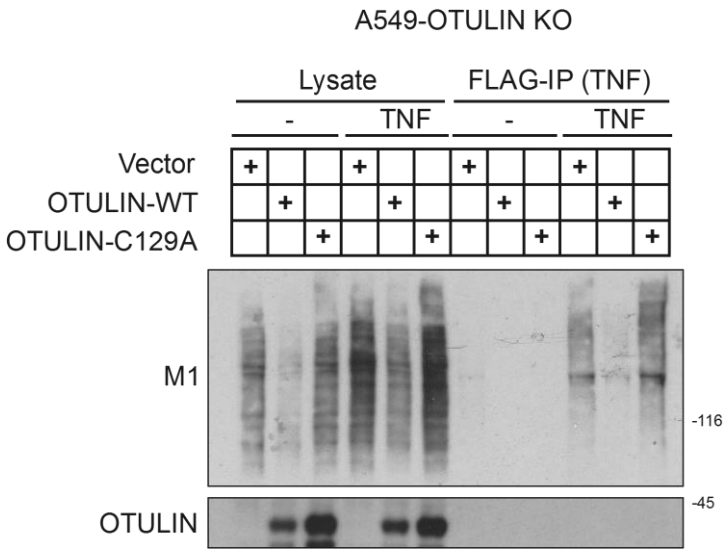

Figure 3.15: OTULIN's absence from the TNFR1-SC is not due to its activity

Both active and deubiquitinase-inactive OTULIN are absent from the TNFR1-SC. A549 OTULIN-KO cells were transfected with control empty vector, OTULIN (OTULIN-WT) or enzymatically inactive OTULIN-C129A. After two days, 1µg/ml FLAG-TNF was add to the cells for 15 minutes and the TNFR1-SC was isolated by immunoprecipitation of FLAG-TNF. Amount of M1-linked ubiquitin chains and recruitment of OTULIN to the TNFR1-SC was analysed using western blotting.

3.3.4 Ubiquitin binding domains can be used to enrich ubiquitinated proteins

Naturally occurring UBDs have an affinity for ubiquitin chains in the K_D range of µM to mM. Several studies demonstrated that tandem repeats of ubiquitin binding domains

increase the binding affinity (Hjerpe et al., 2009). Accordingly, high affinity ubiquitin-binding entities can be used to purify or detect ubiquitinated proteins. Based on this idea, different ubiquitin binding molecules were created that are capable of binding to different chain types with varying affinities. These proteins were fused to a HALO-tag which allows covalent binding to HALO-affinity resin. Because the inactive OTULIN C126A was found to stabilise M1-linked ubiquitin chains (Figure 3.15), a HALO-tagged OTULIN C126A was created to allow for specific affinity purification (AP) of M1-ubiquitinated proteins (M1-AP). Additionally, an affinity protein based on the UIM of RAP80 has exquisite specificity for K63-linked ubiquitin chains over M1-linked chains (Sims, Scavone et al., 2012) was produced as a HALO-tagged affinity protein allowing for affinity purification of K63-ubiqutinated proteins (K63-AP). The recombinant proteins were coupled to HALO-resin, and added to the cell lysates. Both affinity proteins enriched linear ubiquitin chains that were formed upon TNF stimulation (Figure 3.16, A). Importantly, M1-linked chains were only found in HOIP-proficient cells (Figure 3.16, A, B). Furthermore, substantial amounts of other ubiquitin chain types were only detected in K63-AP, detected by a total ubiquitin antibody. This is in line with reports that K63-linked chains are abundant in non-stimulated cells (Dammer et al., 2011). The specificity of the M1-AP was further validated by using recombinant K63- or M1-linked ubiquitin chains, which showed that only M1-linked chains were enriched by this method (Figure 3.16, C) Hence, ubiquitin affinity purification resins can be used to enrich for specific ubiquitin chains.

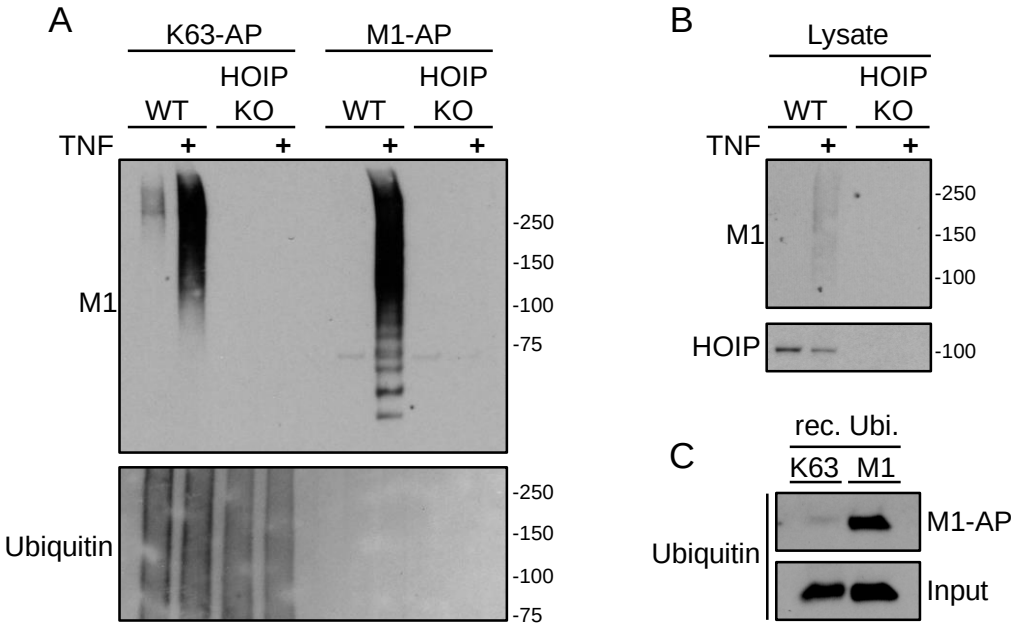

Figure 3.16: Ubiquitin-AP allows for enrichment of specific ubiquitin chains

(A) K63- or M1-linked ubiquitin chain-specific binding domains are specific for the respective chain type. M1-AP or K63-AP was performed by adding the corresponding bead-coupled proteins to lysates from non-stimulated or TNF-stimulated lysates obtained from either wild type or HOIP-KO A549 cells. Next day, beads were washed and bound linear or total ubiquitin chains were detected by western blotting.

(B) Western blot analysis of corresponding total lysates used for Ubi-AP in (A) .

(C) M1-AP shows weak association with K63-linked chains while efficiently binding to M1-linked ubiquitin chains. M1-AP was performed on recombinant penta-K63 or tetra-M1 ubiquitin chains. Samples were analysed via western blot. Experiment was performed two times.

3.3.5 OTULIN controls LUBAC function in the cytosol

To analyse the effect of OTULIN-deficiency on TNFR1-SC formation, an enrichment of linear ubiquitinated proteins via M1-AP was performed using wild type and OTULIN-deficient A549 cells. In this experiment, OTULIN-deficient cells show much higher levels of linear ubiquitin even in non-stimulated conditions (Figure 3.17, A). However, the ubiquitination of the TNFR1-SC component RIP1, was unchanged. The LUBAC components HOIL-1 and Sharpin, on the other hand, showed a marked increase in ubiquitination even prior to TNF stimulation in OTULIN-deficient cells (Figure 3.17, B). Hence, OTULIN functions as a steady-state inhibitor of aberrant ubiquitination of LUBAC, whilst ubiquitination of other LUBAC targets like RIP1 is not affected by OTULIN-deficiency.

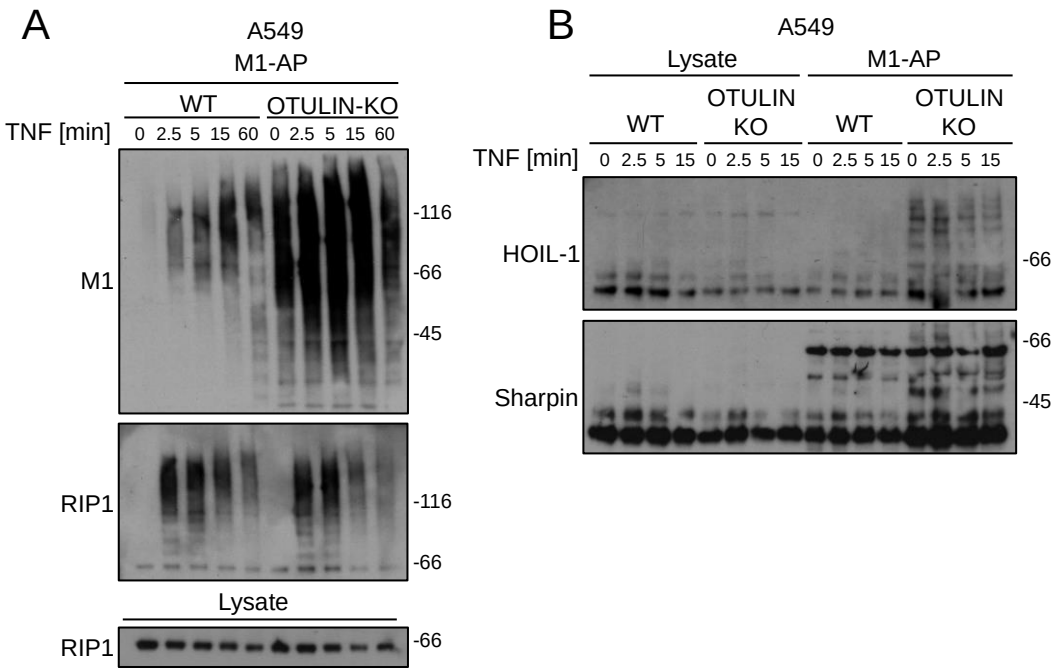

Figure 3.17: OTULIN inhibits auto-ubiquitination of LUBAC

(A) Absence of OTULIN leads to accumulation of M1-linked ubiquitin chains already in absence of exogenous stimuli. The ubiquitination of the LUBAC substrate RIP1 is, however, unaffected by absence of OTULIN. WT and OTULIN-deficient A549 cells were stimulated with 200ng/ml TNF for the indicated time and subjected to M1-AP and analysed by western blotting.

(B) The LUBAC components HOIL-1 and Sharpin are markedly ubiquitinated in absence of OTULIN, prior to stimulation with TNF. WT and OTULIN-deficient A549 cells were stimulated with 200ng/ml TNF for the indicated time and HOIL-1 and Sharpin was detected by western blotting.

3.3.6 Absence or knockdown of OTULIN does not affect TNF-signalling

Because OTULIN deficiency consistently led to a marked increase in linear ubiquitination of LUBAC and possibly other unknown proteins, the potential effect on TNF-induced gene activation was analysed. When comparing wild type and OTULIN-deficient A549 cells, no discernible difference in the activation of NF-κB but a slight reduction in JNK phosphorylation was detected, despite substantially increased M1-ubiquitination (Figure 3.18, A). Because knockout cells could have adapted to the condition of OTULIN-deficiency and aberrant linear ubiquitination, OTULIN expression was also transiently reduced by RNAi (Figure 3.18, B). However, also acute loss of OTULIN expression (2 days after siRNA transfection) did not lead to increased gene activation (Figure 3.18, B). It can therefore be concluded that an

increased linear ubiquitination caused by OTULIN deficiency does not lead to increased gene activation by TNF in the cells that were analysed.

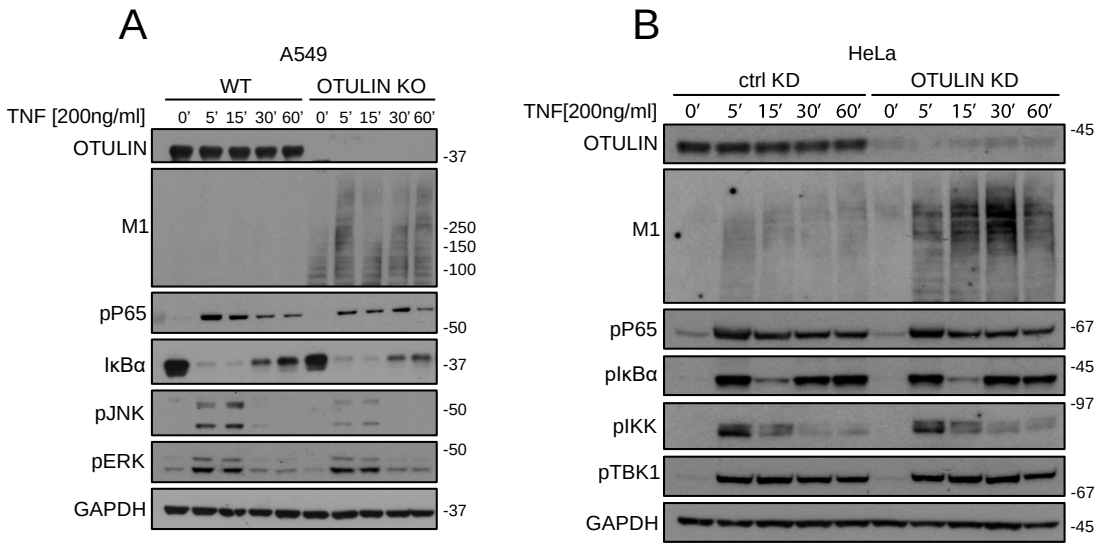

Figure 3.18: OTULIN-deficiency does not affect NF-κB signalling following stimulation with a non-physiological TNF-concentration

(A) Knockout of OTULIN does not lead to evident differences in the activation of gene inducing pathways. Wild type or OTULIN-deficient A549 cells were stimulated with 200ng/ml TNF for the indicated time, lysed and phosphorylation of P65, JNK, pERK and degradation of IκBα was detected by western blotting

(B) Like knockout, the knockdown of OTULIN does not lead to evident differences in the activation of gene inducing pathways. Two days after transfecting HeLa cells with control or OTULIN siRNA, cells were stimulated with 200ng/ml TNF for the indicated times and activation of NF-κB (i.e. phosphorylation of P65, IκBα, IKKα/β) and phosphorylation of TBK1 was compared to control transfected cells by western blotting.

3.4 Discovery of LUBAC substrates

Because of the limited knowledge about LUBAC substrates, it was required to establish novel tools and methods first, which could allow for the identification of such proteins. Ubiquitin affinity purification offers great versatility and further efforts were therefore undertaken to improve this method to identify ubiquitinated proteins but also the linkage types present on these proteins.

3.4.1 Comparison of M1- and total ubiquitination affinity purification

In addition to the M1- and K63-AP systems, a total ubiquitin binding protein was created to allow enrichment and analysis of the overall-ubiquitination of proteins (Ubi-AP). This HALO-tagged ubiquitin binding protein was designed based on the UIM of Rabex5, which was shown to have comparable affinity for the different linkage types (Shin, Lee et al., 2012). Ubi-AP allows for enrichment of all ubiquitinated proteins and those which are associated with ubiquitinated complexes. Comparison of M1- and Ubi-AP shows that both approaches enriched for M1-linked ubiquitin chains, but also the TNFR1-SC components TNFR1 and TRADD (Figure 3.19). TNFR1 and TRADD were heavily ubiquitinated following stimulation with TNF. In contrast, ubiquitinated pIκBα, which does not form part of the TNFR1-SC, was only enriched by Ubi-AP. However, based on this experiment it was not clear whether TNFR1 and TRADD are modified with linear ubiquitin chains or merely associated with other M1-modified proteins which form part of the same complex.

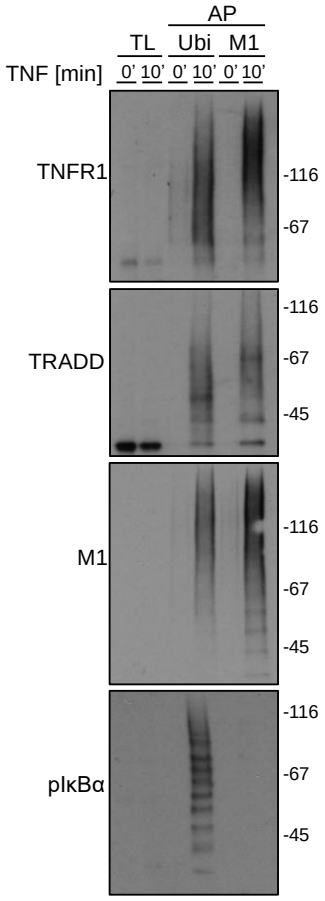

Figure 3.19: TNFR1 and TRADD are associated with M1-linked ubiquitin chains

M1-AP can capture ubiquitinated TNFR1, and TRADD from TNF-stimulated U937 cells. U937 cells were stimulated with TNF [200ng/ml] for 10 minutes, lysed and subjected to M1- or Ubi-AP. Samples were analysed by western blotting.

3.4.2 TNFR1 and TRADD are modified with M1-linked ubiquitin chains

Previously, the only substrates reported for LUBAC and M1-ubiquitination were RIP1 and NEMO (Gerlach et al., 2011). To identify previously unrecognised LUBAC targets, a methodology was established allowing for identification of proteins that are directly modified with linear ubiquitin chains (Figure 3.20). After stimulation of the cells, samples were first denatured in lysis buffer contain 1% Sodium dodecyl sulfate (SDS). This procedure disrupts any complex that has formed and dissociates all proteins. This step is important to prevent enrichment of proteins that merely bind to linear ubiquitin chains. Next, M1-affinity purification was performed to enrich linearly-ubiquitinated proteins. All non-bound proteins that were not M1-ubiquitinated were subsequently washed away. To evaluate the extent of linear ubiquitination of these proteins, recombinant OTULIN was added to these samples. This treatment removes all linear ubiquitin chains, while leaving all other chain types intact. Additionally, samples were treated with viral OTU (vOTU), a DUB that cleaves all chain types except M1-linked chains (Mevissen, Hospenthal et al., 2013). Following *in vitro* deubiquitination, samples were analysed by western blot.

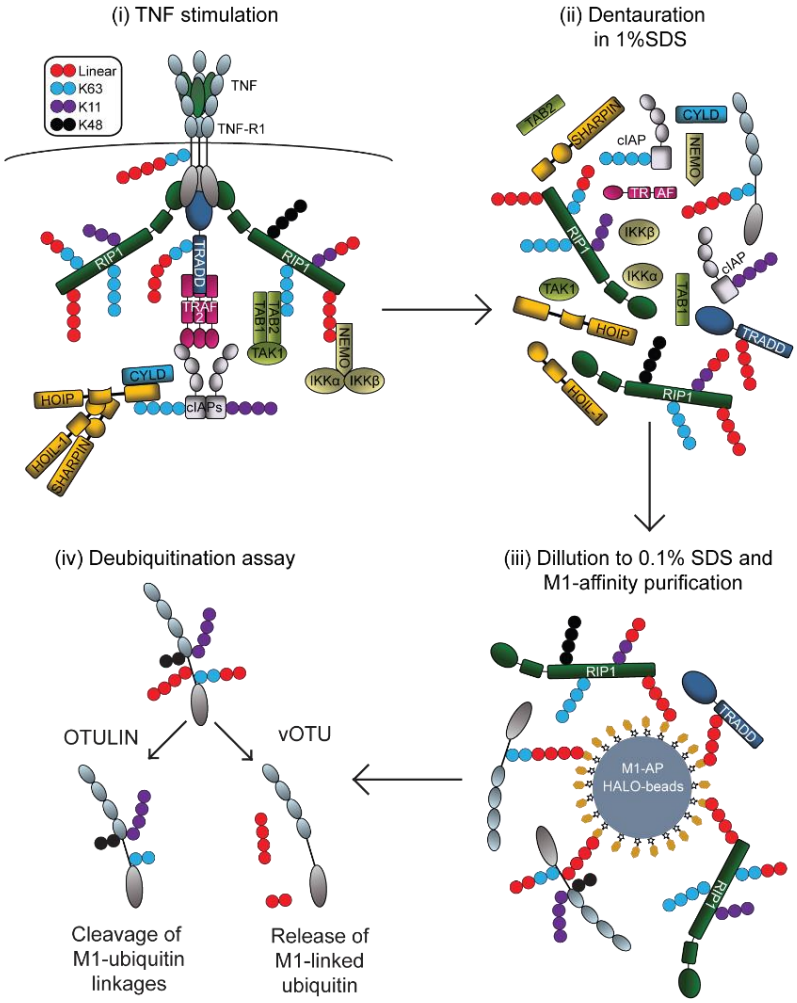

Figure 3.20: Methodology to identify M1-ubiquitin chain-modified proteins

(i) First, cells are stimulated with the respective ligand. (ii) Cells are lysed in lysis buffer containing 1% SDS to denature protein complexes and to dissociate non-ubiquitinated from ubiquitinated proteins. (iii) To enable affinity purification of ubiquitinated proteins, the SDS concentration in samples is diluted to 0.1% and affinity resin is added to the samples. (iv) Enriched ubiquitinated proteins are subjected to an *in vitro* deubiquitination assay. Addition of OTULIN will selectively remove linear ubiquitin chains, whilst vOTU will remove all other chain types but leave linear ubiquitin chains intact.

As shown in Figure 3.21, this method efficiently enriched M1-modified proteins from TNF-stimulated cells. Interestingly, a small amount of linear ubiquitin chains can also be enriched from non-stimulated cells, indicating that there may be tonic signalling, possibly coming from pathways other than TNF. Staining directly for TNFR1-SC components revealed that in addition to the reported LUBAC substrate RIP1 also TNFR1 and TRADD were enriched with this method (Figure 3.21). Treatment with OTULIN removed virtually all M1-linked ubiquitin chains and, importantly, led to a

decrease in the molecular weight of ubiquitinated TNFR1, TRADD and RIP1. This indicates that these proteins were indeed modified with linear ubiquitin chains. In contrast, treatment with vOTU led to the complete removal of ubiquitin chains from the proteins and occurrence of free linear ubiquitin chains. These free linear ubiquitin chains varied in length and some exceeded ~150 kDa. The majority, however, was between 4-9 ubiquitin molecules long. In summary, using this method, TNFR1 and TRADD were identified as previously unrecognised LUBAC substrates. Also, most linear ubiquitin chains in the TNFR1-SC are composed of 4-9 moieties.

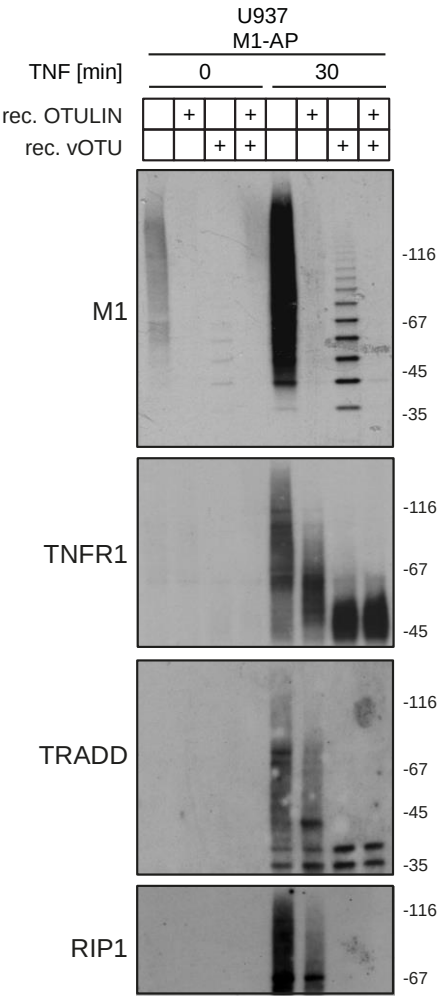

Figure 3.21: TNFR1, TRADD and RIP1 are modified with M1 ubiquitin chains

The linear ubiquitination of TNFR1, TRADD and RIP1 can be confirmed by *in vitro* deubiquitination with recombinant OTULIN, which leads to a decrease in their molecular weight. U937 cells were stimulated with 200ng/ml TNF or left untreated. M1-ubiquitinated proteins were subsequently isolated using HALO-OTULIN (M1-AP) and purified samples were subjected to *in vitro* deubiquitination using either OTULIN or vOTU (unable to cleave linear ubiquitin chains) and analysed by western blot.

3.4.3 Verification of the linear ubiquitination of TNFR1, TRADD and RIP1

To further validate the finding that TNFR1, TRADD and RIP1 are modified with linear ubiquitin chains, the M1-AP was also performed in A549 cells. HOIP-deficient A549 cells were included as a negative control. This experiment showed that also in A549 cells TNFR1, TRADD and RIP1 were efficiently bound by the M1-AP and a substantial portion of their ubiquitination could be removed by treatment with recombinant OTULIN (Figure 3.22). Importantly, M1-ubiquitinated TNFR1, TRADD or RIP1 was only retrieved from HOIP-proficient cells, which demonstrates the specificity of the M1-AP for linear ubiquitin chains.

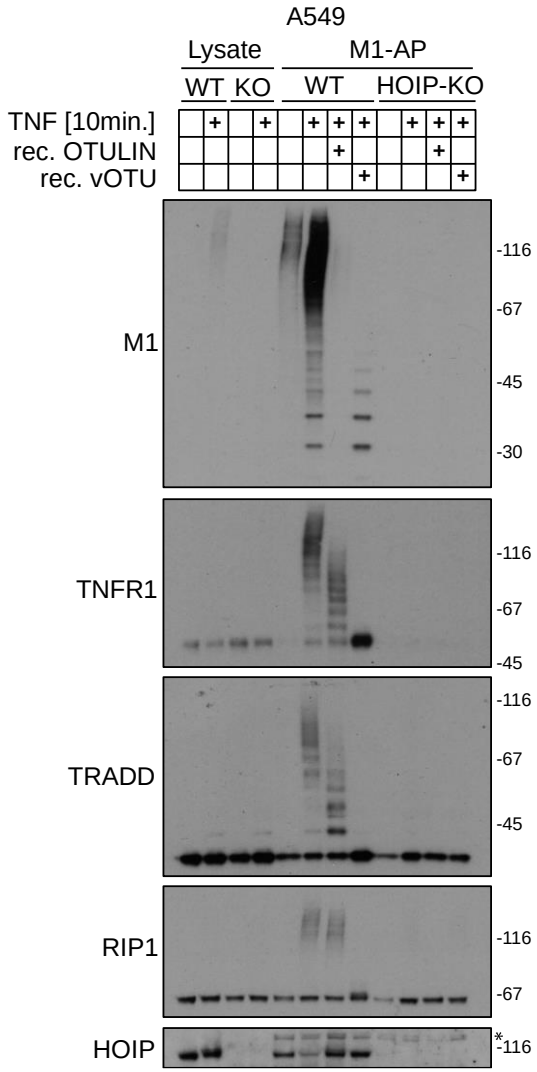

Figure 3.22: M1-ubiquitinated proteins cannot be isolated from HOIP-KO cells

M1-AP fails to isolate TNFR1, TRADD, RIP1 and M1-linked ubiquitin chains from HOIP-deficient cells. Wild type or HOIP-deficient A549 were stimulated with 200ng/ml TNF for 10 minutes and lysates were subjected to M1-AP. Samples were then subjected to an *in vitro* DUB-assay using OTULIN and/or vOTU before western blot analysis. * indicates non-specific detection.

3.4.4 Total TRADD and TNFR1 ubiquitination is affected by LUBAC absence

To test whether other chain types on these proteins are also affected by absence of LUBAC, HOIP-deficient (HOIP-KO) and -proficient cells were stimulated with TNF and subjected to total ubiquitin enrichment (Ubi-AP). Western blot analysis of these samples showed that in HOIP-deficient cells, the overall ubiquitination of TNFR1 and TRADD is reduced to an extent that exceeds the amount of M1-linked ubiquitin chains which were attached to these proteins (Figure 3.23). The ubiquitination of RIP1 and cIAP1/2 on the other hand was comparable between wild type and HOIP-KO cells. This indicates that in absence of LUBAC, TNFR1 and TRADD ubiquitination is primarily impaired.

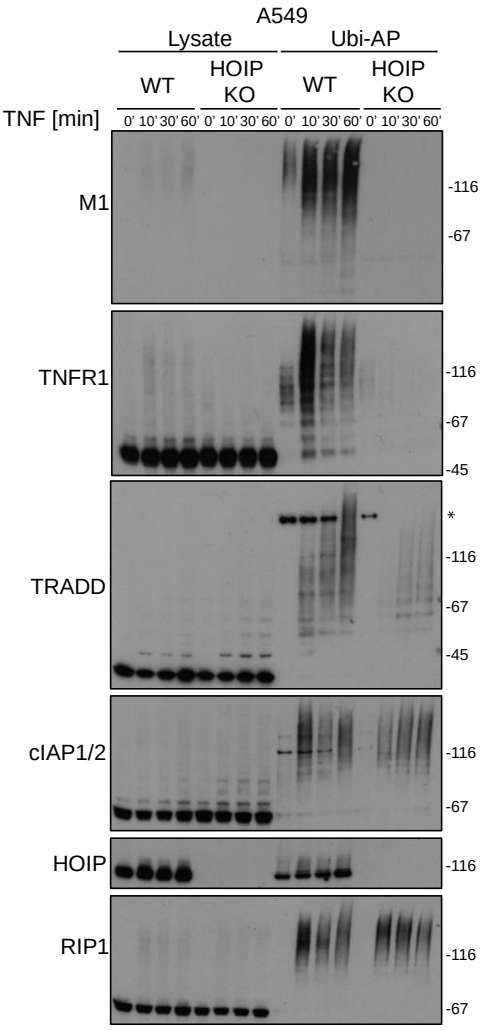

Figure 3.23: Reduced ubiquitination of TRADD and TNFR1 in absence of HOIP

WNon-sepcific isolation of ubiquitinated proteins from lysates obtained from HOIP-deficient cells demonstrates a defect in overall ubiquitination of TNFR1 and TRADD. Wild type and HOIP-deficient A549 were stimulated with 200ng/ml TNF for the indicated times. Ubiquitinated proteins were isolated from lysates using total Ubi-AP and samples were analysed by western blotting. * indicates non-specific detection.

3.5 Comparison of different lysis conditions to extract the TNFR1-SC

It was reported that the TNFR1-SC forms part of a Triton X-100-insolbule membrane fraction (Legler, Micheau et al., 2003). It is therefore likely that ubiquitinated proteins also form part of the Triton X100-insolbule fraction. Different lysis conditions were therefore compared to evaluate which lysis conditions are best to extract ubiquitinated proteins.

3.5.1 Ubiquitinated TNFR1-SC components become Triton X-100 insoluble

First, a sequential lysis was performed to separate fractions of different solubility i.e. membrane, cytosolic, etc. fractions. After stimulation of HeLa cells, samples were first lysed in 0.1% Saponin. This detergent was shown to form holes of around 100Å in plasma membranes, allowing leakage of small soluble proteins but retaining larger protein complexes and membrane bound proteins (Seeman, Cheng et al., 1973). After centrifugation, the soluble fraction was collected and the pellet resuspended in 1% Triton X-100 lysis buffer (TX-100), which efficiently solubilises most proteins including many membrane proteins, but leaves protein complexes intact. Lastly, the TX-100-insoluble pellet was lysed in the anionic detergent SDS. Used at 1%, it denatures protein structures and solubilises them effectively. Following 1% SDS lysis, samples were diluted to 0.1% SDS and all fractions were subjected to Ubi-AP. Lysis with Saponin did not liberate significant amounts of ubiquitinated proteins from cells, showing that these proteins and complexes are either membrane bound or too large to escape through the membrane holes (Figure 3.24, A). The fraction lysed with TX-100 contained some ubiquitinated RIP1 and TNFR1. Notably, large amounts of ubiquitinated TNFR1 were present in non-stimulated samples from both wild type and HOIP-KO cells. Interestingly, these conjugates were of similar size of around 100kDa but disappeared upon stimulation with TNF (Figure 3.24, A). Analysis of the TX-100 insoluble fraction by SDS lysis revealed a striking accumulation of ubiquitinated proteins. RIP1 and TNFR1 were heavily ubiquitinated and linear ubiquitin chains could be detected in the same fraction of wild type cells. In line with previous observations (Figure 3.23), the ubiquitination of TNFR1 was much lower in HOIP-deficient cells, whereas the ubiquitination of RIP1 was comparable to that of wild type cells.

To test whether the observations made in HeLa cells were also reproducible in a different cell line, a similar experiment was conducted in A549 cells. Surprisingly, ubiquitinated proteins were much less fractionated in these cells (Figure 3.24 B). A

significant portion of ubiquitinated RIP1, TNFR1 and M1-linked ubiquitin chains was detected in the TX-100 fraction but also in the TX-100 insoluble fraction. Interestingly, proteins isolated from the SDS fraction showed a different ubiquitination pattern which was generally shifted towards a higher molecular weight. Furthermore, M1-linked chains accumulated over time in the SDS fraction, whilst they decreased in the TX-100 fraction. In summary, ubiquitinated proteins accumulate in a Triton X-100-insoluble fraction which can be retrieved by lysis in SDS.

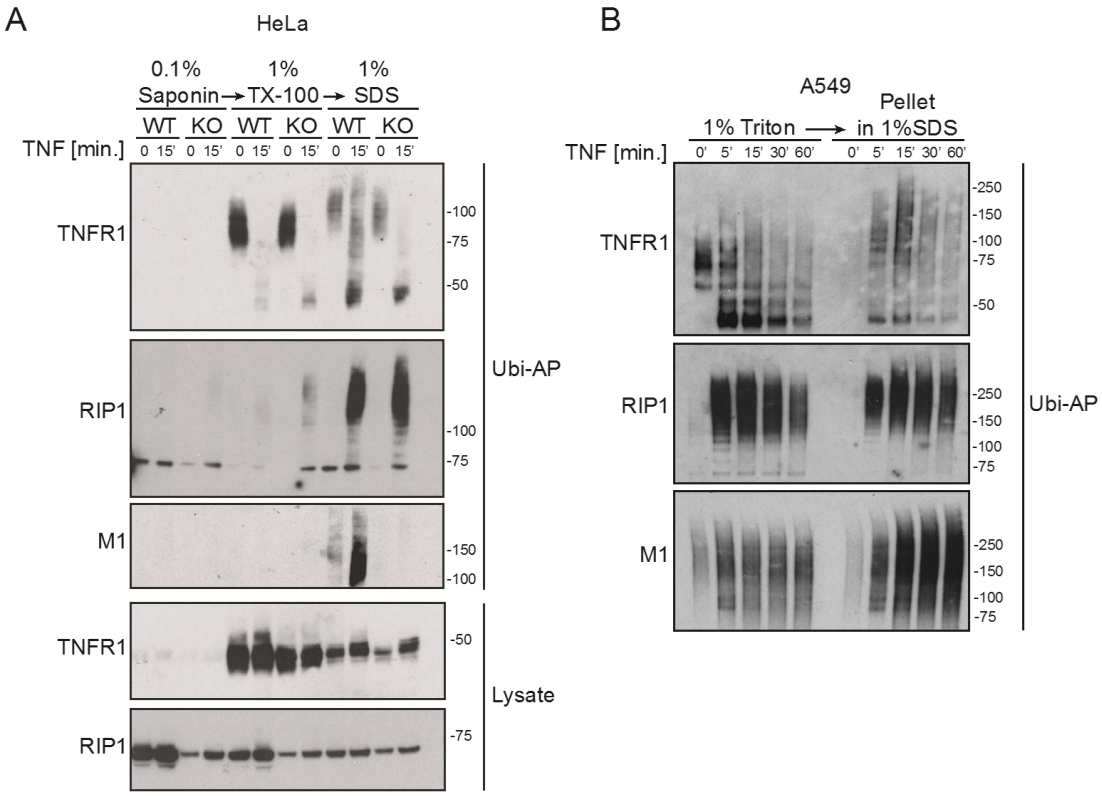

Figure 3.24: Ubiquitinated proteins are found in TX-100 insoluble fractions

(A) TNFR1-SC components are not fully soluble in a 1% Triton X-100-based buffer but can be extracted by lysing in 1%SDS. HeLa cells were stimulated with 200ng/ml TNF for the indicated time. First, cells were lysed in lysis buffer containing 0.1% Saponin. After centrifugation, the lysate was collected and the pellet was resuspended in 1% Triton X-100 lysis buffer and insoluble proteins were pelleted by centrifugation. After removal of the supernatant, the remaining pellet was lysed in 1% SDS and sonicated. Samples were then adjusted to 0.1% SDS concentration and cleared by centrifugation. Supernatants were then subjected to Ubi-AP and analysed by western blot. (B) A549 were stimulated with 200ng/ml TNF for the indicated time, lysed in 1% Triton X-100 lysis buffer and insoluble proteins were pelleted by centrifugation. After removal of the supernatant, the remaining pellet was lysed in 1% SDS and sonicated. Samples were then adjusted to 0.1% SDS concentration and cleared by centrifugation. Supernatants were then subjected to Ubi-AP and analysed by western blotting.

3.5.2 Ubiquitinated TNFR1-SC proteins can be extracted by lysis in SDS

Since SDS denatures protein structures, it was possible that lysis in 1%SDS simply enables better binding of the ubiquitin-binding protein used in the Ubi-AP by making the ubiquitin chains more accessible. To test for this possibility, U937 cells were stimulated with TNF and lysed in TX-100 buffer. The lysate was collected, split in two tubes, and the insoluble fraction removed by centrifugation. One sample was denatured with 1% SDS before diluting it down to 0.1% final concentration of SDS (TX-100→SDS). The second sample was just topped up to the same volume with lysis buffer (TX-100). The cell pellet containing the TX-100-insoluble fraction, which was left from the initial lysis, was resuspended in 1% SDS buffer, sonicated and diluted to 0.1% SDS before centrifugation. All samples were then subjected to Ubi-AP. Analysis of these samples by western blotting showed no difference between TX-100 lysis and samples that were additionally denatured in 1% SDS prior to Ubi-AP (Figure 3.25) However, as seen in HeLa cells (Figure 3.24, A), SDS-lysis of the TX-100 insoluble fraction retrieved ubiquitinated TNFR1, RIP1 and M1-linked ubiquitin chains (Figure 3.25). This shows that the observed enrichment of ubiquitinated proteins in a TX-100 insoluble fraction is not due to improved Ubi-AP from denatured samples.

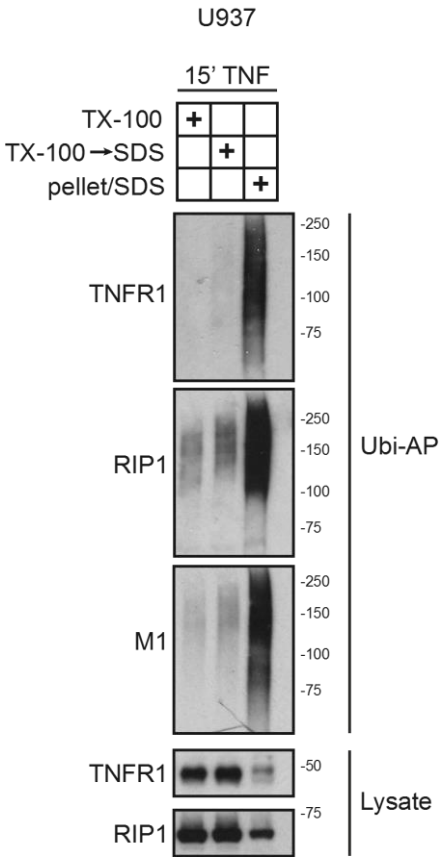

Figure 3.25: Denatured proteins are not more efficiently enriched by Ubi-AP

Superior enrichment of ubiquitinated proteins, following TNF stimulation, extracted by SDS lysis is not due to better binding of denatured proteins to ubiquitin binding domains. U937 cells were stimulated with 200ng/ml TNF for 15 minutes. Cells were lysed and cleared by centrifugation and split in two tubes. Subsequently, one sample was denatured with SDS. The remaining cell pellet was directly resuspended in SDS buffer. Samples were adjusted to the same volume so that the SDS concentration is 0.1% in all samples. Ubi-AP was performed and analysed by western blotting.

3.6 LUBAC-deficiency sensitises cells to cell death

The molecular basis for the sensitisation of LUBAC-deficient cells to TNF-induced cell death is poorly understood. In case of TNF-induced cell death, destabilisation of complex I, due to insufficient complex I modification in absence of HOIP, was suggested to facilitate the formation of complex II. To study TNF-induced cell death in HOIP-deficient cells in more detail, HeLa WT and HOIP-KO cells expressing RIP3 were generated. HeLa cells do not express RIP3 and are therefore resistant to necroptosis-inducing stimuli (Li et al., 2012). HeLa-RIP3 cells were stimulated with different combinations of TNF (T), zVAD (Z), SM-83 (S) or Nec1-S (Nec). SM-83 is a SMAC mimetic which efficiently leads to depletion of cIAPs by triggering their auto-

ubiquitination with K48-linked chains, leading to their proteasomal degradation (Lecis, De Cesare et al., 2013). Cell death, represented by uptake of propidium iodide, was measured by flow cytometry. As expected, HeLa cells were resistant to TNF but also to necroptosis induction by T+Z+S (Figure 3.26). However, expression of RIP3 strongly sensitised HeLa cells to T+Z+S but also to the apoptotic stimuli T+S. In contrast, HOIP-deficient HeLa cells already showed mild sensitivity to TNF-induced cell death and showed increased sensitisation to T+S-induced cell death compared to HeLa wild type. Strikingly, expression of RIP3 in HOIP-deficient cells lead to a dramatically increased sensitisation to TNF alone (Figure 3.26). Interestingly, these cells also succumbed to T+Z treatment without the need for cIAP-depletion by SM-83. Cell death induced by T+Z+S was blocked by Nec1-S, indicating that necroptosis was responsible for the cell death. This result shows that HOIP-deficiency leads to sensitisation to both apoptosis and necroptosis and mimics cIAP1/2-deficiency.

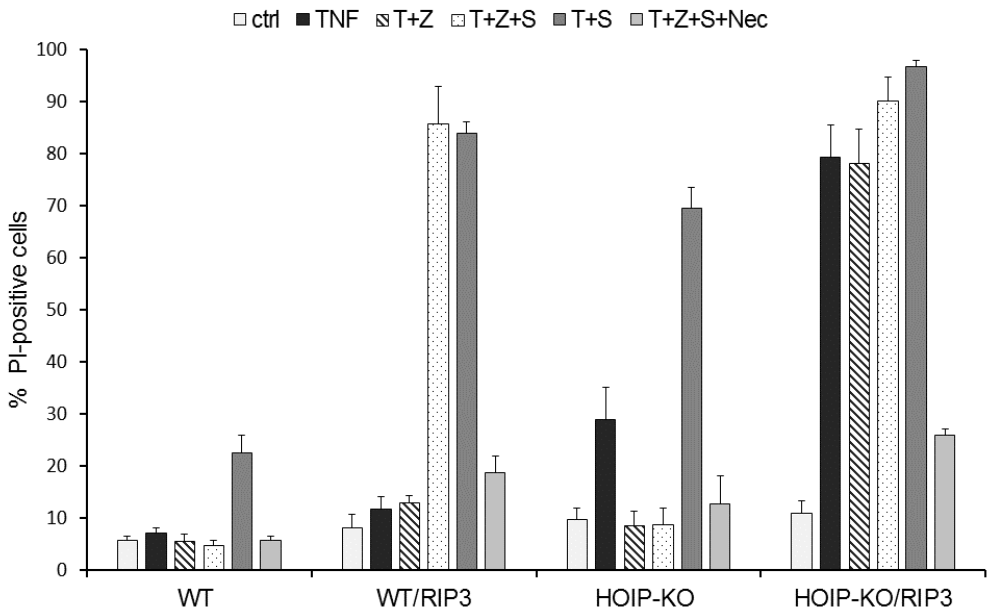

Figure 3.26: HOIP-deficiency sensitises cells to necroptosis and apoptosis

HOIP-deficiency mimics cIAP-deficiency and sensitises HeLa cells to TNF-induced apoptosis and, when RIP3 is present, to necroptosis. HeLa wild type (WT) or HOIP-KO cells were stably transfected with vector control or RIP3. Cells were stimulated with 200ng/ml TNF with the indicated inhibitors. After 24 hours, cell death was determined as % PI-positive cells by flow cytometry. Data from three biological replicates are presented as mean ± SEM.

At this stage, it was not clear whether the necrosome formation or activity is increased in HOIP-deficient HeLa-RIP3. The necrosome was therefore isolated from WT and HOIP-deficient cells by strep-affinity purification of tagged RIP3 and tested for

associate factors by western blotting (Figure 3.27). Because the necrosome is largely insoluble in conventional Triton-X100 lysis buffer, proteins in the pellet resulting from the first lysis step were further solubilised in 0.1% SDS and sonicated. RIP3 was immunopurified from both separate fractions. Analysis of the samples revealed a substantial increase in necrosome formation in HOIP-deficient cells (Figure 3.27). Moreover, association of RIP1, TRADD and FADD with RIP3 was readily observed in the Triton-X100-insoluble fraction of HOIP-deficient cells but not in wild type cells. Hence, HOIP is required to prevent cell death upstream of necrosome formation.

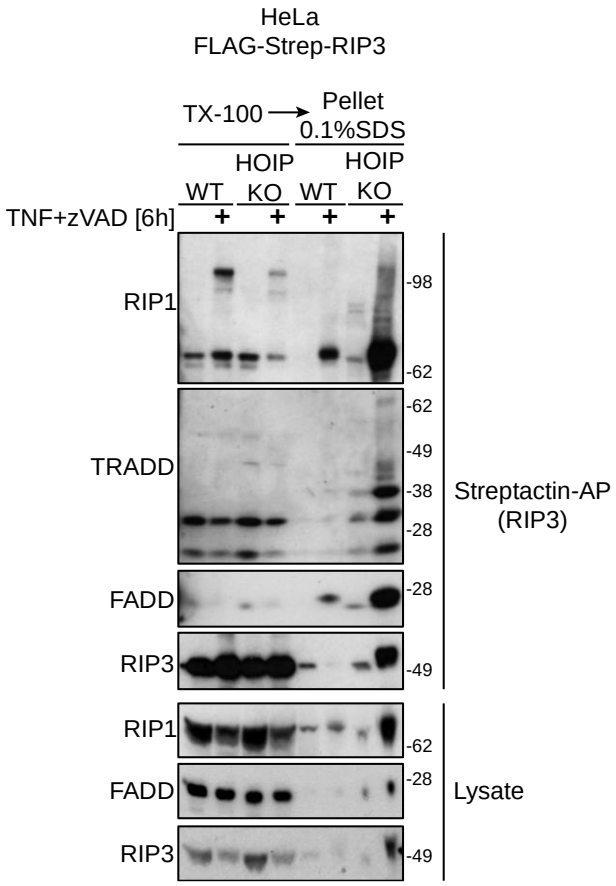

Figure 3.27: Necrosome formation is enhanced in HOIP-deficient cells

In absence of HOIP, the formation of the necrosome, consisting at least of TRADD, FADD, RIP3 and RIP1, is increased. Control and HOIP-deficient HeLa cells, stably expressing FLAG-Strep-tagged (TAP-tag) RIP3, were incubated with a combination of 200ng/ml TNF and 20μM zVAD for 6 hours. Subsequently, cells were lysed in IP-buffer containing 1% Triton-X100 and lysates were cleared by centrifugation. The supernatant was collected and the pellet resuspended in IP-buffer supplemented with 0.1% SDS, sonicated and cleared by centrifugation. Both fractions were subjected to affinity purification of TAP-tagged RIP3 using StrepTactin beads. Samples were analysed by western blotting.

3.7 Functional analysis of CYLD-deficiency on TNFR1 signalling

CYLD was suggested to negatively regulate K63-ubiquitination of various TNFR1-SC components (Kovalenko et al., 2003, Moquin et al., 2013). The constitutive interaction of CYLD with HOIP suggests that CYLD could also negatively regulate M1-ubiquitin chains.

3.7.1 Deficiency in CYLD leads to increased TNFR1-SC ubiquitination

To test the effect of CYLD on M1-and K63-ubiquitinated proteins, ubiquitin-AP was used to isolate these proteins from TNF-stimulated wild type or CYLD deficient A549 cells. Analysis of these samples showed that in absence of CYLD the ubiquitination of the LUBAC targets RIP1, TRADD and TNFR1 are markedly increased (Figure 3.28). Although the ubiquitination of cIAP1/2 also drastically increased in CYLD-deficient cells, the ubiquitination was already elevated prior to stimulation with TNF. Importantly, the total amount of M1-ubiquitination was also increased in CYLD deficient cells (Figure 3.28). This indicates that CYLD indeed counteracts M1-ubiquitination of TNFR1-SC components, in addition to the previously reported K63-ubiquitination.

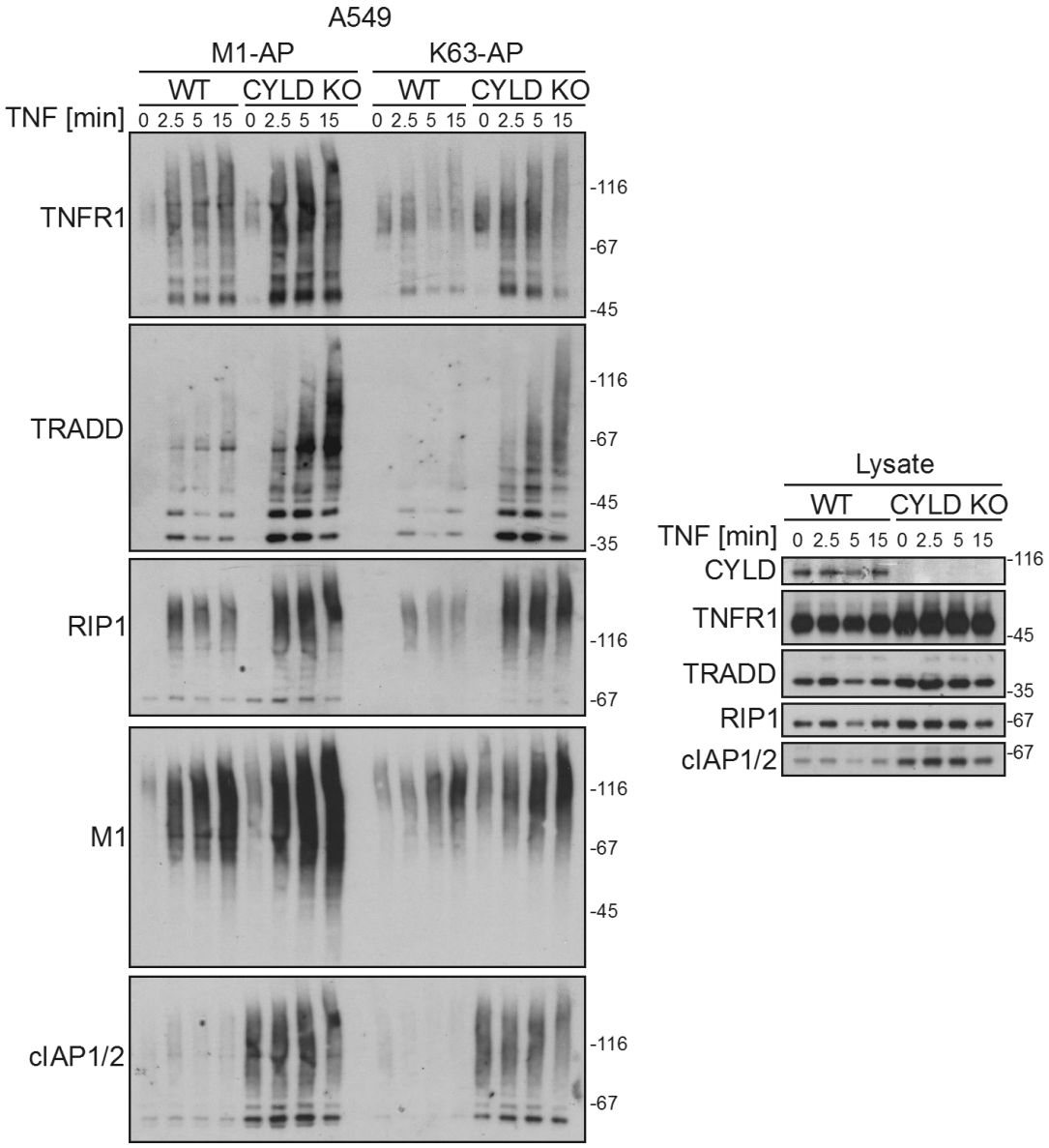

Figure 3.28: CYLD inhibits K63- and M1- ubiquitination of the TNFR1-SC

The comparison of M1- and K63-AP from wild type or CYLD-deficient A549 cell lysates demonstrates are marked increase in ubiquitinated TNFR1, TRADD, RIP1, cIAP1/2 and overall M1-ubiquitination in CYLD-deficient cells. Wild type and CYLD-deficient A549 cells were stimulated with 200ng/ml TNF for the indicated time. Cells were lysed and subjected to M1- and K63-AP and analysed by western blot.

3.7.2 CYLD can remove linear- and other ubiquitin linkages from proteins

Having identified a group of proteins which are modified with linear ubiquitin chains, the question was whether CYLD could indeed be responsible for removal of these modifications. Purified linearly-ubiquitinated proteins were therefore incubated with recombinant CYLD-USP, the active domain of CYLD. Western blot analysis of these samples showed a decrease in the molecular weight of TNFR1, TRADD and RIP1

(Figure 3.29). This was accompanied by complete removal of M1-linked ubiquitin chains. This shows that CYLD can remove and degrade linear ubiquitin chains from endogenously modified proteins.

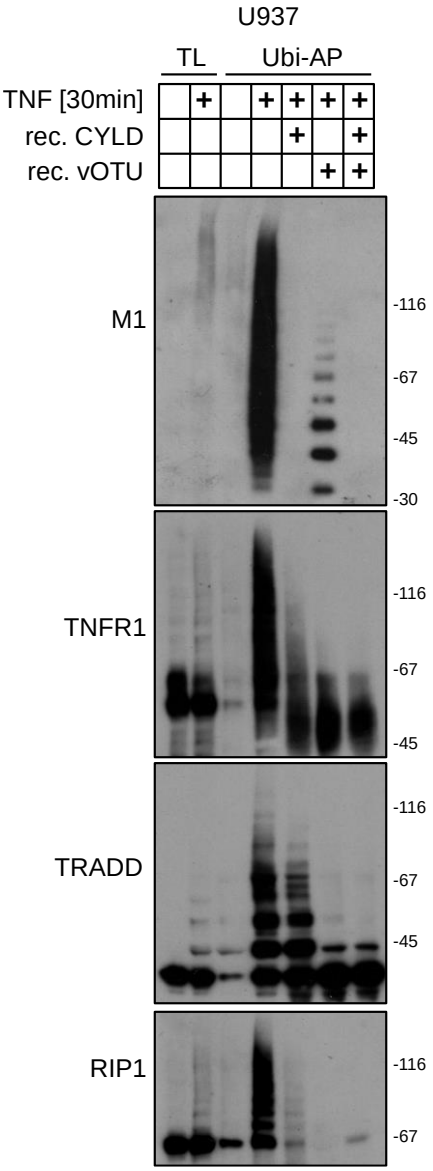

Figure 3.29: CYLD cleaves linear and other ubiquitin chains from LUBAC targets

Recombinant CYLD USP domain can effectively remove ubiquitination and linear ubiquitination from TNFR1, TRADD and RIP1 in an *in vitro* assay. U937 cells were stimulated with 200ng/ml TNF for 30 minutes or left untreated. M1-AP was performed and subjected to *in vitro* deubiquitination by addition of 1µM recombinant CYLD USP and/or vOTU and incubation for one hour. Samples were analysed by western blotting.

3.7.3 NEMO ubiquitination is increased in HOIP-N102A expressing cells

NEMO is crucial for the activation of the canonical NF-κB pathway (Rudolph et al., 2000). The activation of NEMO is accompanied by its ubiquitination, which also involves linear ubiquitination (Tokunaga et al., 2009). CYLD influences M1- and K63-ubiquitination of TNFR1-SC components (Figure 3.29), but it was unclear whether the interaction of HOIP with CYLD or OTULIN was required to regulate NEMO ubiquitination. To analyse this question, HOIP-deficient HeLa cells were reconstituted with HOIP that is either wild type (WT), enzymatically inactive (CS), or unable to bind to SPATA2/CYLD and OTULIN (NA). Following TNF stimulation and immunoprecipitation of NEMO, an increased amount of ubiquitinated NEMO could be observed comparing HOIP-WT to HOIP-NA expressing cells (Figure 3.30). In accord, NEMO, derived from cells which are devoid of HOIP or express inactive HOIP-CS, lacks this ubiquitination.

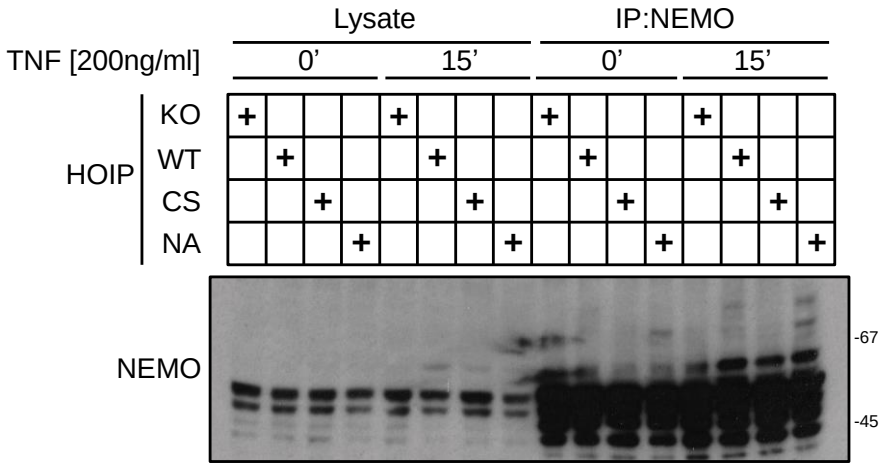

Figure 3.30: Ubiquitination of NEMO is increased in HOIP-N102A cells

By abrogating the interaction of OTULIN and SPATA2/CYLD with HOIP, through mutation of HOIP N102 to Ala, the ubiquitination NEMO is increased. HOIP-KO HeLa cells were virally reconstituted with either wild type, enzymatically inactive (CS) or N102A (NA) HOIP. Cells were stimulated with 200ng/ml TNF and subjected to immunoprecipitation of NEMO. Resulting samples were probed for NEMO by western blotting.

3.7.4 Deficiency in SPATA2 or CYLD has similar effects on gene activation

CYLD was suggested to negatively regulate TNF-induced gene activatory pathways (Kovalenko et al., 2003). However, other studies reported only minor effects on NF-κB induction and a slight increase in MAPK activation (Moquin et al., 2013, Reiley et

al., 2006, Zhang et al., 2006). Based on the inhibitory effects on ubiquitination in previous experiments (Figures 3.28-30), it was likely that CYLD deficiency enhances TNF-induced gene activation. Surprisingly, however, TNF stimulation of CYLD-deficient HeLa cells showed only minor differences in activation of NF-κB compared to control cells (Figure 3.31). In contrast, the activation of JNK was slightly enhanced. In accordance, loss of SPATA2 had no significant effect on the activation of NF-κB but slightly enhanced the activation of JNK. Taken together, absence of CYLD, or lack of CYLD recruitment by deletion of SPATA2, results in a slight enhancement of MAPK activation whilst the effect on NF-κB activation is limited.

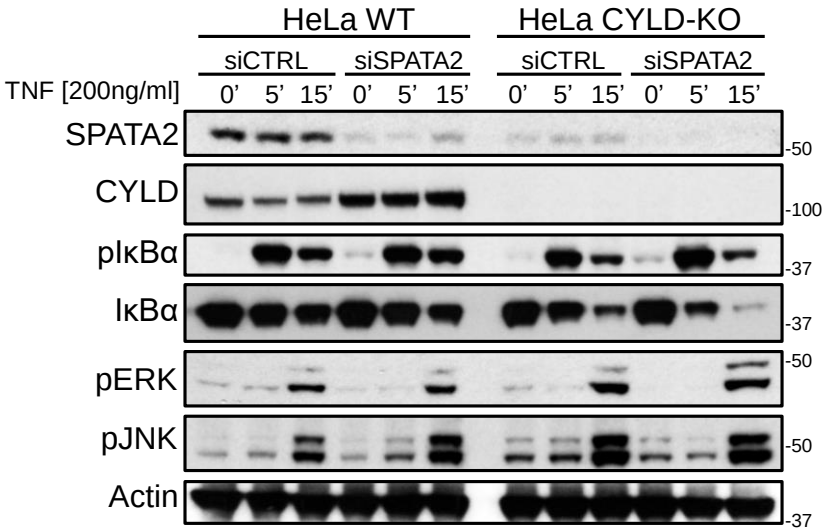

Figure 3.31: Lack of CYLD/SPATA2 only mildly affects gene activatory pathways

HNeither absence of SPATA2 or CYLD has a profound effect on the phosphorylation or degradation of IκBα, whereas the phosphorylation of JNK is slightly increased. HeLa cells, pro- or deficient in CYLD, were transfected with control or SPATA2-targeting siRNA. The cells were stimulated with 200ng/ml TNF for the indicated times, lysed and analysed by western blot.

Because cell lines, which were generated by clonal expansion, were used for the experiments shown in Figure 3.31, it could be that the observed effects are specific for the individual clone. For this reason, primary bone marrow derived macrophages were isolated from CYLD deficient mice and control litter mates. Stimulation of these cells with TNF showed again no appreciable difference in the activation of NF-κB but a slight enhancement of the MAPK pathway (Figure 3.32, A). Activation of NOD2 signalling by L18-MDP on the other hand revealed an increase NF-κB activation in

CYLD-deficient cells and again increased MAPK signalling (Figure 3.32, B). This shows that in TNF-signalling, deficiency in CYLD has minor effects on NF-κB but increases JNK activation. In NOD2 signalling, however, deficiency in CYLD indeed increases NF-κB activation, but also MAPK signalling. The potential of CYLD to modulate gene activation might therefore be pathway-dependent.

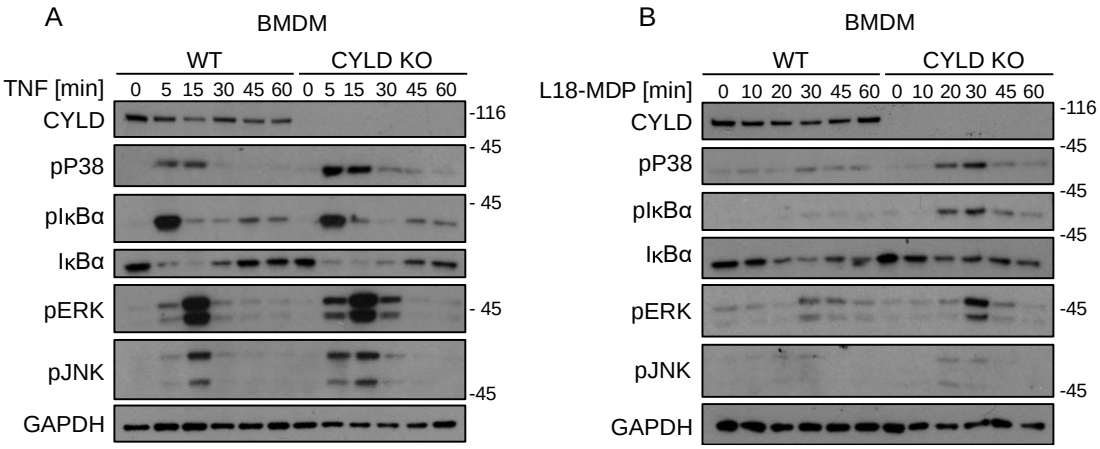

Figure 3.32: CYLD supresses gene activatory pathways in BMDMs

(A) CYLD-deficient BMDMs show normal IκBα phosphorylation and degradation but have slightly enhance phosphorylation of p38 and JNK in response to TNF. Bone marrow-derived macrophages were isolated from wild type or CYLD-deficient litter mates. Cells were stimulated with 200ng/ml TNF for the indicated time. Lysates were analysed by western blot. (B) CYLD-deficient Cells show increased NF-κB and MAPK signalling in response L18-MDP. BMDMs were prepared as in (A), stimulated with 200ng/ml L18-MDP and analysed by western blot.

3.7.5 CYLD and SPATA2 are required for TNF-induced necroptosis

In addition to the involvment of CYLD in the regulation of gene activation, CYLD was also shown to regulate cell death by promoting the formation of the death-inducing complex II, emenating from the TNFR1-SC (Hitomi et al., 2008, Moquin et al., 2013, O'Donnell et al., 2011). The murine cell line L929 readily undergoes necroptosis upon stimulation with a combination of zVAD and TNF (Vanlangenakker, Bertrand et al., 2011). Expression of SPATA2 or CYLD was therefore reduced in L929 cells by RNAi. As shown in figure 3.33, the combination of TNF and the caspase inhibitor zVAD induced necroptotic death which was blockable by the RIP1 kinase inhibitor Nec-1S. Importantly, knockdown of either CYLD or SPATA2 reduced the induction of necroptotis (Figure 3.33, A). The effect of CYLD knockdown was seemingly stronger, however, as seen in CYLD deficient HeLa cells, it also reduced expression levels of

SPATA2, thus functionally increasing the inhibitory effect on the induction of cell death (Figure 3.33, B). Hence, SPATA2 is required for CYLD to elicit its death-promoting function in TNF-induced necroptosis.

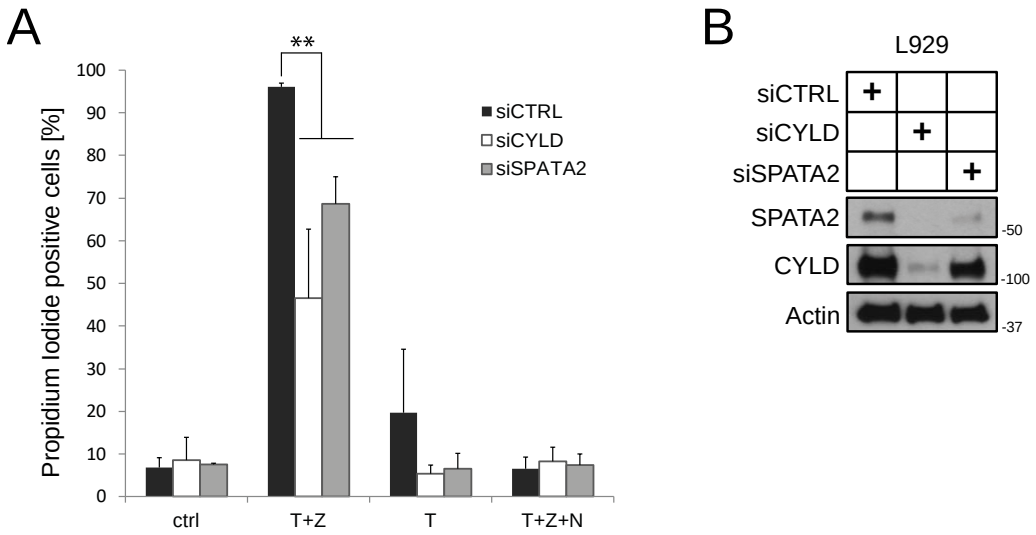

Figure 3.33: SPATA2 or CYLD deficiency reduces TNF-induced necroptosis

(A) Both the knockdown of CYLD or SPATA2 supress necroptosis induced by treatment with TNF+zVAD in L929 cells. Expression of SPATA2 or CYLD was reduced by transfection of siRNA. Two days after transfection, cells were treated with 200ng/ml TNF, TNF+zVAD [30µM] or TNF+zVAD and the necroptosis inhibitor NEC-1S [10µM] for 16h. Cell death was quantified by uptake of propidium iodide and measured by FACS analysis. Data from biological replicates are presented as mean ± SEM [n = 3], ** $p < 0.01$, statistics were performed using t test).

(B) As seen in CYLD-KO cells, also the knockdown of CYLD reduces SPATA2 protein level. Representative western blot result of the knockdown efficiency of CYLD and SPATA2 in L929 cells used in (A).

3.8 A20 recruitment and its involvement in TNFR1-SC regulation

A20 was implicated to function as a negative regulator of TNF-signalling due to its deubiquitinase activity (Wertz et al., 2004). However, the inhibitory effect of A20 also requires zinc finger 7 (ZF7), which specifically binds to linear ubiquitin chains (Tokunaga et al., 2012, Verhelst et al., 2012, Yamaguchi, 2015). This links A20 to LUBAC and it was likely that their function is in part dependent on each other.

3.8.1 A20 is recruited to the TNFR1-SC in a HOIP dependent manner

The mechanism for A20 recruitment to the TNFR1-SC was not clear but A20's ZF7, which can bind to M1-linked ubiquitin chains, is involved in this process (Tokunaga et al., 2012). Hence, it is possible that LUBAC is required for the recruitment of A20 to the TNFR1-SC. To test this possibility, the TNFR1-SC was isolated from wild type and HOIP-deficient A549 cells and A20 recruitment was analysed (Figure 3.34). Because A20 protein levels are low in basal condition, a three-hour time point was included to allow for TNF-induced upregulation of A20 expression. Strikingly, A20 was not recruited to the TNFR1-SC in absence of HOIP (Figure 3.34). Importantly, both early and late recruitment of A20 was fully dependent on LUBAC. Furthermore, the recruitment of A20 correlates with increasing amounts of linear ubiquitination. This demonstrates that LUBAC is required for the recruitment of A20 to the TNFR1-SC.

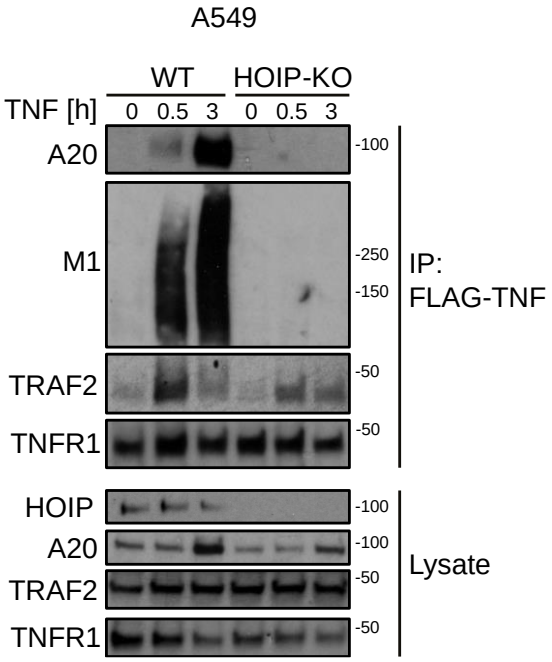

Figure 3.34: Recruitment of A20 to the TNFR1-SC depends on HOIP

TNFR1-SC analysis of wild type and HOIP-KO A549 cells demonstrates that recruitment of the deubiquitinase A20 to the TNFR1-SC is dependent on HOIP. A549 cells pro- or deficient in HOIP were stimulated with 1 µg/ml FLAG-TNF for 0, 0.5 and 3 hours. Cells were washed with PBS, lysed in IP-buffer and the TNFR1-SC was purified using anti-FLAG M2 beads. Samples were then analysed for the recruitment of A20 and analysed by western blotting.

3.8.2 Linear ubiquitin chains are reduced in A20-deficient cells

Next, A20-deficient cells were generated to analyse the effect of A20-deficiency on the ubiquitination of signalling complex components. Because A20 was reported to be able to hydrolyse K63- and K48-linked ubiquitin chains, it was possible that the ubiquitination of A20 substrates is enhanced in absence of A20. However, M1- and K63-AP revealed a significant loss of TNFR1 ubiquitination, while the ubiquitination of RIP1 remained unchanged (Figure 3.35). The ubiquitination of TRADD was also slightly reduced as seen by the increase in smaller ubiquitinated forms of TRADD. In line with the reduced ubiquitination of TRADD and TNFR1, linear ubiquitination, which was stable in wild type and A20-ctrl A549 cells for 3h, was reduced in A20-deficient and A20-ΔZF2-7 cells. Conclusively, lack of A20 leads to a destabilisation of linear ubiquitination and strong reduction of TNFR1 ubiquitination.

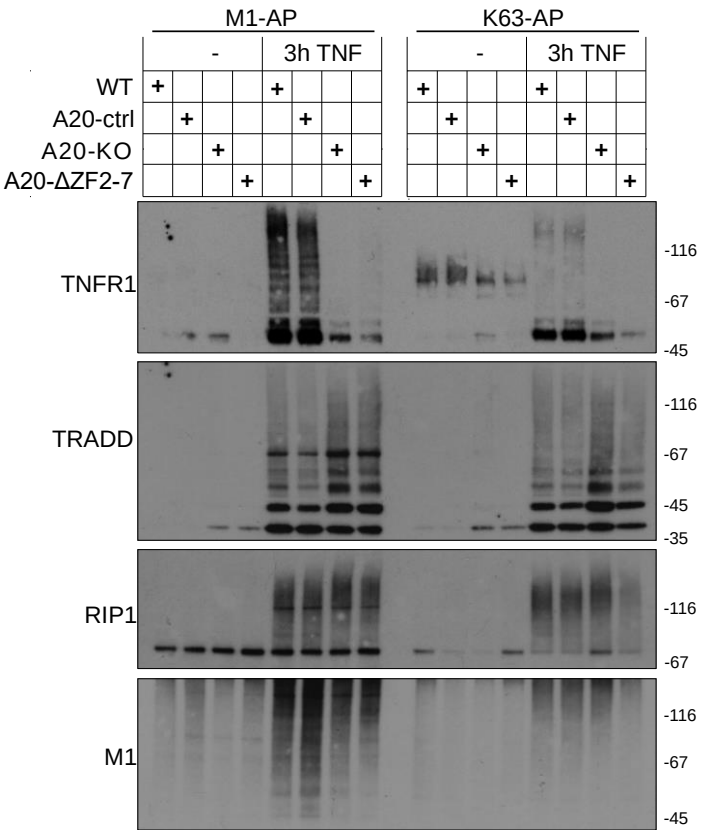

Figure 3.35: Absence of A20 leads to reduction of M1-ubiquitination

A549 cells in which A20 was targeted using CRISPR/Cas9 to either delete expression of ZF2-7 (A20-ΔZF2-7), or delete A20 expression by targeting exon 1 (A20-KO), show reduced M1-ubiquitination and reduced TNFR1 ubiquitination in response to TNF. Cells were stimulated with 200ng/ml TNF for 3h. Cells were then lysed and subjected to M1- and K63-AP and analysed via western blot.

3.8.3 Absence of A20 also decreases linear ubiquitination in the NOD2-SC

A20 was suggested to also regulate NOD2-signalling (Hitotsumatsu et al., 2008). Because absence of A20 had a marked effect on linear ubiquitination on the LUBAC substrate TNFR1 in TNF-signalling, ubiquitination of the NOD2-SC components RIP2 and XIAP were also analysed in absence of A20 (Figure 3.36). In line with the observations made for the TNFR1-SC, linear-ubiquitination of both LUBAC substrate was reduced in cells deficient for A20 or carrying a deletion of ZF2-7 (A20-ΔZF2-7) (Figure 3.36). This shows that also in NOD2-signalling A20 has a stabilising effect on linear ubiquitination.

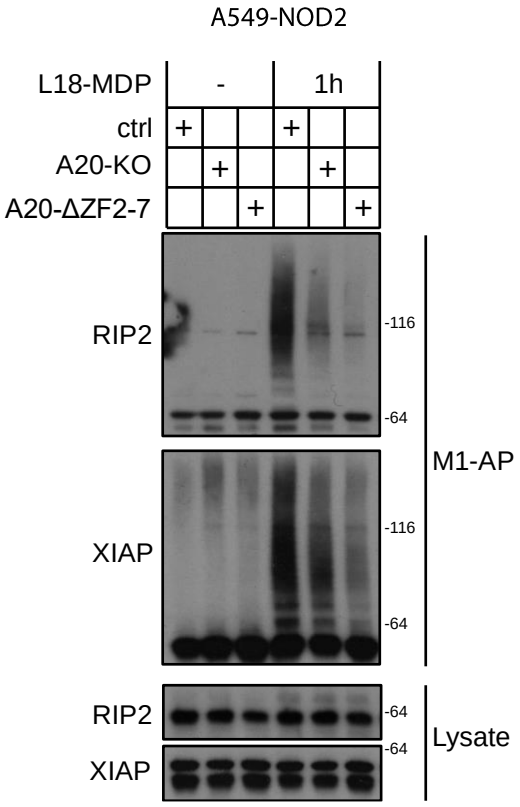

Figure 3.36: A20-deficiency reduces M1 ubiquitination of the NOD2-SC

A549 control cells, and cells in which A20 or A20's ZF2-7 were deleted using CRISPR/Cas9, were virally reconstituted with FLAG-NOD2 and show reduced ubiquitination of XIAP and the LUBAC substrate RIP2 in response to L18-MDP stimulation. Cells were stimulated with 200 ng/ml L18-MDP for 1 hour. M1-ubiquitinated proteins were affinity purified by M1-AP and analysed by western blot.

3.8.4 Presence of A20 supresses gene activatory signalling

Because A20 possesses DUB-activity, it was suggested that A20 supresses gene activation by deubiquitinating components of the TNFR1-SC (Wertz et al., 2004). However, based on the result presented in Figure 3.35, it is likely that A20's function is independent of its DUB-activity. A20-deficient MEFs were therefore reconstituted with A20 or A20-C103S, which lacks deubiquitinating activity. A20-deficient MEFs show rapid activation of NF-κB following TNF stimulation (Figure 3.37). Re-expression of A20 but also inactive A20-C103S reduced phosphorylation and degradation of IκBα. This indicates that the inhibitory effect of A20 on NF-κB signalling is independent of its deubiquitinating activity.

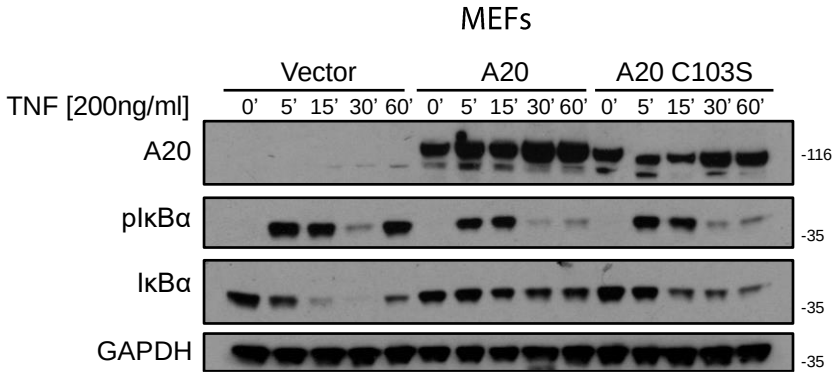

Figure 3.37: A20 supresses NF-κB activation independently of its DUB activity

A20-deficient MEFs were virally reconstituted with vector control, A20, or enzymatically inactive A20-C103S. Cells were stimulated with 200ng/ml TNF for the indicated time and phosphorylation and degradation of IκBα by western blotting.

3.8.5 A20 recruitment to linear ubiquitin chains prevents cell death

It was suggested that A20 prevents cell death by mediating the degradation and deubiquitination of RIP1 (Wertz et al., 2015, Wertz et al., 2004). Based on the results obtained in this study, this seems unlikely as the ubiquitination of RIP1 was unchanged in A20-deficient cells (Figure 3.35). A20-deficient MEFs were therefore reconstituted with either A20-WT and A20-C103S or A20 which harbours a point mutation in ZF7 (A20-ZF7$_{mut}$). Analysis of the TNFR1-SC isolated from these cells showed that linear ubiquitination was fully restored by expression of either A20-WT or A20-C103S (Figure 3.38, A). However, A20-ZF7$_{mut}$ was unable to restore linear ubiquitination (Figure 3.38, A). Next, these cells were analysed for their sensitivity to TNF-induced cell death. TNF+zVAD had a strong cytotoxic effect on A20-deficient

cells (Figure 3.38, B). This effect was rescued by re-expression of A20 but also inactive A20-C103S. Strikingly, A20-ZF7$_{mut}$, which is unable to bind to linear ubiquitin was unable to restore resistance (Figure 3.38, B). This shows that ZF7 of A20, and not its enzymatic activity, is required and sufficient to inhibit TNF-induced cell death.

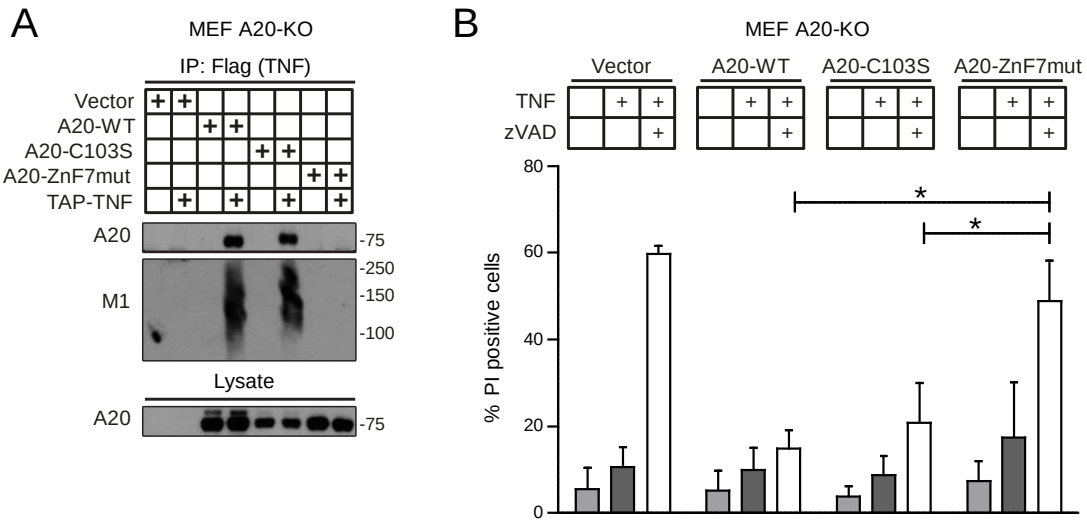

Figure 3.38: A20 mediates resistance to TNF-induced cell death via its ZF7

(A) Wild type and enzymatic inactive A20, but not A20-ZF7$_{mut}$, are recruited to the TNFR1-SC and normalise linear ubiquitin chain levels in the complex. MEFs deficient for A20 were reconstituted with either vector, A20, DUB-inactive A20 C103S (A20-CS) or A20-ZF7$_{mut}$. Cells were stimulated for 15 minutes with FLAG-TNF (500 ng/ml) and subjected to TNF-RSC purification. A20 recruitment and M1-ubiquitination was analysed by western blot

(B) TNF+zVAD-induced necroptosis observed in A20-deficient cells can be prevented by expression of either wild type A20 or enzymatic inactive A20-C103S, but not by expression of A20-A20-ZF7$_{mut}$. Cells, as described in (A), were stimulated with 200 ng/ml TNF and the indicated inhibitors and cell death was evaluated after 24h as percentage of propidium iodide positive cells (data are presented as mean ± SEM [n = 3], * $p < 0.05$, statistics were performed using t test).

4 Discussion

4.1 LUBAC constitutively associates with SPATA2/CYLD or OTULIN

The constitutive interaction of LUBAC with two DUBs was a surprising finding (Draber et al., 2015, Takiuchi, Nakagawa et al., 2014). The fact that OTULIN is remarkably efficient and specific in cleaving linear ubiquitin chains points towards a specialist function strongly linked to LUBAC. Other studies have reported a marked increase of linear ubiquitin chains in cell that are OTULIN-deficient (Keusekotten et al., 2013, Rivkin et al., 2013), which was also observed in this study. However, an increased M1-ubiquitination was already present prior to stimulation with TNF and ubiquitination of TNFR1-SC components did not change significantly or was reduced (Figure 3.17, A) (Draber et al., 2015). It is therefore not clear which proteins are modified with additional linear ubiquitin chains in absence of OTULIN, apart from LUBAC itself. It is likely that LUBAC substrates in other homeostatic pathways (e.g. DNA repair) exist, which accumulate linear ubiquitin chains because of OTULIN deficiency. In line with this theory, M1-AP can reveal basal levels of M1-ubiquitination (Figure 3.21) and overexpression of catalytic inactive OTULIN stabilised these linear ubiquitin modifications (Figure 3.13), suggesting that LUBAC is also active in other pathways yet to be discovered. An approach to identify these targets might therefore be to enrich for these M1-modified proteins from non-stimulated OTULIN-deficient cells, using M1-AP followed by mass spectrometry. Alternatively, linear ubiquitin could serve as bait for ubiquitin binding molecules which are involved in these unknown pathways. In both cases, these experiments are likely to identify novel factors associated with linear ubiquitination. One group of proteins affected by absence of OTULIN are LUBAC components themselves, which show a marked increase in ubiquitination (Figure 3.17, B). This suggests that OTULIN acts in particular on LUBAC, which possibly undergoes auto-ubiquitination as observed for other E3 ligases (de Bie & Ciechanover, 2011). Auto-ubiquitination of LUBAC might interfere with its function and OTULIN acts as a dedicated DUB to keep LUBAC functional, independently of signalling complexes. This idea is supported by the observation that OTULIN-deficient cells showed reduced ubiquitination of RIP1 in the TNFR1-SC and RIP2 in the NOD2-SC (Draber et al., 2015). It is intriguing to speculate that the auto-ubiquitination of LUBAC might represent a shut-off mechanism following its recruitment to signalling complexes, especially when considering that OTULIN does not form of signalling complexes and would therefore be unable to counteract this process. Interestingly, one study reported a dramatic increase in linear ubiquitination

of HOIP in absence of OTULIN but not in absence of CYLD (Hrdinka, Fiil et al., 2016). This further supports the theory that CYLD functions as a negative regulator of LUBAC in signalling complexes but not under basal conditions. OTULIN on the other hand is clearly required to prevent accumulation of linear ubiquitination of LUBAC substrates but also on LUBAC itself. Due to the efficiency of OTULIN in hydrolysing M1-linked ubiquitin chains, it may in fact be necessary to exclude OTULIN from SCs to allow for efficient linear ubiquitination in the first place.

The reason for absence of OTULIN from signalling complexes is still not fully understood. However, it was shown that at least two distinct pools of LUBAC exist; one is associated with OTULIN and another one with SPATA2/CYLD (Draber et al., 2015). As SPATA2 and OTULIN bind to the same motif in the PUB domain of HOIP, the binding of the two is mutually exclusive (Elliott, Leske et al., 2016, Kupka et al., 2016a). Phosphorylation of the PIM in OTULIN at Y56 was suggested as a possible mechanism to prevent its interaction with HOIP (Elliott et al., 2014, Schaeffer et al., 2014). One possible mechanism could therefore be that the PIM of OTULIN becomes phosphorylated following activation of TNF-signalling, whilst the PIM in SPATA2 is not. Indeed, a search on the phosphoproteomics database http://www.phosphosite.org/ revealed no record of SPATA2 PIM phosphorylation. Phosphorylated OTULIN PIM was found in basal conditions but evidence that OTULIN is phosphorylated following TNF stimulation is still missing. It will therefore be essential to identify the tyrosine kinase responsible for phosphorylation of OTULIN and how it is activated. This kinase could even be membrane associated and not form part of the TNFR1-SC directly. Thus, only recruited OTULIN would be phosphorylated, which might explain why only minute amounts of OTULIN were found to be phosphorylated. Alternatively, LUBAC's association with OTULIN might impose a form of steric hindrance, thus blocking LUBAC recruitment to the signalling complex. The DUB-activity of OTULIN, however, does not influence its recruitment (Figure 3.15) and inactive LUBAC also does not recruit OTULIN to SCs, thus excluding a regulation by linear ubiquitination. It is interesting to note that the CYLD/SPATA2 and HOIP interact in a 2:2 ratio because CYLD forms dimers via a homotypic Bbox interaction (Elliott et al., 2016). The dimer formation may increase LUBAC's avidity for binding to ubiquitinated TNFR1-SC components. A dimer formation involving OTULIN has not been reported so far and this could be the reason why LUBAC bound to OTULIN is not efficiently recruited to the TNFR1-SC. Once the underlying mechanism has been clarified, it may be possible to alter OTULIN regulation and allow its recruitment to SCs. One possibility could be to exchange the PIM in OTULIN

with the one found in SPATA2, to see whether PIM phosphorylation indeed is the reason for absence of OTULIN from SCs.

4.2 Recruitment of CYLD to signalling complexes via LUBAC

The recruitment mechanism of CYLD to signalling complexes remained elusive and several factors like NEMO, TRAF2 and Optineurin have been suggested to be involved in this process (Kovalenko et al., 2003, Nagabhushana, Bansal et al., 2011). Absence of these previously suggested factors did however not completely prevent CYLD recruitment to the TNFR1-SC. Strikingly, absence of HOIP completely abolished recruitment of CYLD to signalling complexes (Draber et al., 2015). Constitutive interaction of LUBAC with CYLD leads to a co-recruitment of CYLD to the signalling complexes that were analysed in this study. It therefore seems likely that HOIP-mediated CYLD recruitment to signalling platforms represents a general mechanism. Other pathways that are known to employ LUBAC (e.g. CD40, TLR3 or IL-1R) might therefore potentially be regulated by CYLD. *Vice versa*, it will be necessary to evaluate the involvement of LUBAC in pathways that were suggested to be regulated by CYLD (e.g. RANK signalling or Bcl3-dependent NF-κB activation (Jin, Chang et al., 2008, Massoumi et al., 2006).

In contrast to OTULIN, the interaction of CYLD with HOIP is indirect and mediated by SPATA2 (Elliott et al., 2016, Kupka et al., 2016a, Schlicher, Wissler et al., 2016, Wagner, Satpathy et al., 2016). Little is known about the function of SPATA2. Early studies identified SPATA2 to be potentially involved in spermatogenesis, due to its high expression in testis and strong upregulation during spermatogenesis (Onisto, Slongo et al., 2001). It is interesting to note that CYLD-deficient mice also have been reported to have defects in spermatogenesis (Wright, Reiley et al., 2007). Although CYLD-deficient mice show no overt phenotype, apoptotic cell death can be detected in germ cells. The authors attributed this to increased gene activation, leading to an upregulation of anti-apoptotic proteins which prevents the early wave of germ cell apoptosis (Wright et al., 2007). Early wave germ cell apoptosis is a necessary event to maintain tissue homeostasis. Defective early apoptosis therefore leads to increased apoptosis in a later stage during spermatogenesis. The function of SPATA2 during spermatogenesis has not been analysed but, considering the results obtained in this study, it is likely that loss of SPATA2 results in a functional deficiency of CYLD. It will also be interesting to analyse which pathway delivers the apoptotic stimulus. By crossing CYLD or SPATA2 deficient mice to e.g. TNF-deficient mice, the contribution

of death ligands could be analysed. The discovery of SPATA2 as a crucial molecule for CYLD recruitment to signalling complexes may also provide some new insight for studies of Brooke-Spiegler syndrome, familial cylindromatosis or multiple familial trichoepitheliomas. Patients which present with the respective phenotypes, but do not have a mutation in CYLD, should be analysed for mutations in the SPATA2 gene.

It was shown that SPATA2, in addition to enabling the binding of CYLD to HOIP, increases CYLD activity by binding to its USP domain (Elliott et al., 2016, Schlicher et al., 2016). It is not clear whether CYLD is recruited to or functions without SPATA2 in other signalling complexes but it must be assumed that without SPATA2, CYLD activity will be compromised. Alternatively, different adaptors might exist which fulfil a similar function as SPATA2. For instance, SPATA2-like (SPATA2L) was also identified as a constitutive interaction partner of CYLD (Sowa, Bennett et al., 2009). As SPATA2 is required and sufficient for recruitment of CYLD to the TNFR1- and NOD2-SC, SPATA2L is not involved in these complexes. However, analysis of signalling complexes which are regulated by CYLD should also be tested for the involvement of SPATA2, SPATA2L or other potential adaptors.

Absence of CYLD leads to a reduction in SPATA2 protein level (Figure 3.5). A similar observation was made in a different study (Elliott et al., 2016). At this stage, it is unclear whether this is the result of reduced translational level or whether SPATA2 protein stability is directly regulated by CYLD. Since CYLD is a deubiquitinase, it is tempting to speculate that SPATA2 is subject to ubiquitination which in turn might lead to its proteasomal degradation. Though no ubiquitinated SPATA2 was detected in this study, it may be required to inhibit the proteasomal pathway to stabilise any short-lived modification. An alternative explanation might be that CYLD stabilises the conformation of SPATA2. By creating SPATA2 point mutants unable to interact with HOIP and/or CYLD, the contribution of each protein to the observed effects could be analysed.

4.3 TNFR1 and TRADD are LUBAC substrates

Shortly after the identification of LUBAC as part of the TNFR1-SC, RIP1 and NEMO were identified as LUBAC substrates (Gerlach et al., 2011, Ikeda et al., 2011). However, these experiments were 2D-gel and mass spectrometry based and required large quantities of M1-modified protein for reliable detection. In this study, the M1-ubiquitin enrichment strategy in combination with ubiquitin linkage-specific DUBs led to the identification of TRADD and TNFR1 as previously unrecognised LUBAC

substrates (Figure 3.21). This method requires less cell material and allows for a sensitive analysis which can be adapted to various signalling pathways and proteins. However, it is noteworthy that NEMO could not be identified as a M1-modified protein with this assay (data not shown). The reason for this is not clear but the examination of the total ubiquitination of NEMO suggests that only a minute fraction of NEMO is modified with polyubiquitin chains, while a large portion is modified by mono-ubiquitination (Figure 3.30). A different study made a similar conclusion and demonstrated that NEMO is largely modified with K63-linked chains (Emmerich et al., 2013). Hence, detection of linear ubiquitin chains attached to NEMO may require several folds more sample for sufficient detection than e.g. RIP1. However, this finding also demonstrates that TNFR1 and TRADD are modified quantitatively more with M1-linked ubiquitin chains than NEMO and RIP1. By performing ubiquitin chain profiling, another study later described additional K63- and K11-ubiquitination of TNFR1 (Emmerich et al., 2016). The role of TNFR1 ubiquitination remains, however, elusive. Considering the longevity of linear ubiquitination, these chains could function as a regulatory signal coordinating recycling/degradation of activated SCs. Notably, it was suggested that K63-ubiquitination of TNFR1 enables receptor internalisation, which is required for induction of cell death (Fritsch, Stephan et al., 2014). However, this theory is not supported by the finding that lack of A20, which also leads to a selective loss of ubiquitination of TNFR1 (Figure 3.35), still sensitised to TNF-induced cell death (Figure 3.38). Considering that also LUBAC-deficiency leads to a dramatic reduction in TNFR1 ubiquitination (Figure 3.23), it seems more probable that ubiquitination of TNFR1 prevents cell death. This may involve the recruitment of additional, maybe unidentified factors, to ubiquitin chains. Analysis of TNFR1 ubiquitination revealed a strong ubiquitination in absence of any stimulus and was found in total- and K63-specific ubiquitin affinity purifications, but never in M1-APs (Figures 3.22, 3.23). Strikingly, the pre-stimulation ubiquitination pattern completely disappeared upon binding of TNF (Figure 3.24). Notably, ubiquitination of TNFR1 prior to stimulation was readily solubilised by TX-100 and absent from the TX-100-insoluble fraction. This contrasts with the activated form of TNFR1. TNFR1 was found to shuttle between cholesterol-rich membrane micro-domains and the trans-Golgi network (D'Alessio, Esposito et al., 2012, Jones, Ledgerwood et al., 1999). The pre-ubiquitinated TNFR1 may therefore be shuttling between the Golgi network and the membrane, but not membrane micro-domains, as they are characterised by TX-100 insolubility (Mazzone, Tietz et al., 2006). The pre-ubiquitination could represent an additional sorting signal or allow for rapid recruitment of UBDs or provide a first set of ubiquitin modifications as a basis for e.g. linear ubiquitination by LUBAC. The

identification of the residues carrying this modification and the E3 modifying them will be paramount for the analysis.

Western blot analysis showed that in HOIP-deficient cells, the overall ubiquitination of TNFR1 and TRADD is reduced to an extent that exceeds the amount of M1-linked ubiquitin chains that were attached to these proteins (compare Figure 3.21 to 3.23). This could potentially be explained by two different mechanisms: (i) linear ubiquitin chains, attached as branches on top of other chain types, may protect these chains from DUBs that are unable to cleave M1-linked ubiquitin chains. (ii) linear ubiquitin chains may function as additional binding platforms for other E3 ligases and LUBAC itself, which could further increase the ubiquitination of these proteins. Interestingly, the ubiquitination of RIP1 is seemingly unaffected by the absence of HOIP, which correlates with smaller amounts of M1-linked ubiquitin chains found on RIP1. To test the function of linear ubiquitination, proteins could be sequentially ubiquitinated with K63-linked chains and M1-linked chains, before subjecting them to an *in vitro* DUB assay. DUBs like A20 may be unable to cleave the K63-chain attached to the protein if these chains are additionally ubiquitinated with linear chains. First evidence to support this theory has recently been published (Wertz et al., 2015). Considering the drastic effect of HOIP deletion on the overall ubiquitination of TNFR1 and TRADD, it will be difficult to address whether linear ubiquitin chains act as specific binding platforms. Selective deletion of linear ubiquitin events would be necessary to preserve the general architecture of ubiquitin chains in the TNFR1-SC. Currently, no method has been found to reliably address this issue.

Little is reported concerning the ubiquitination of TRADD. One study suggested that ubiquitination-dependent degradation of TRADD as a consequence of obstructive renal injury (Misaki, Yamamoto et al., 2009). However, this study analysed ubiquitination of TRADD in an overexpression system and failed to provide sufficient evidence for direct ubiquitination of TRADD, as no immunoblot staining for TRADD directly was provided. Here, TRADD was found to be modified by linear ubiquitin and other chain types and to form part of the necrosome (Figure 3.27). The function of these modifications is currently unknown. Residue K292 in TRADD is one of four lysines which are conserved between mouse and human. Because it is located in the DD of TRADD, it is tempting to speculate that ubiquitination of TRADD at K229 might regulate its ability to mediate induction of cell death by TNF. Because the death domain of TRADD is also engaged in binding to TNFR1, K292 may, however, not be accessible for E3s or only following its release from TNFR1. The other three conserved lysine residues K25, K38, K63 could therefore be more likely targets for

ubiquitination. As TRADD serves as an adaptor protein, its ubiquitination likely provides additional binding platforms for the recruitment of e.g. the TAB/TAK and NEMO/IKK complex. Like for TNFR1, identification of the modified lysines will be required to address the function of these modifications.

4.4 Regulation of TNFR1-SC ubiquitination by CYLD, OTULIN and A20

4.4.1 CYLD counteracts LUBAC function in signalling complexes

The regulation of the TNFR1-SC by DUBs has been extensively studied in the past (Kupka, Reichert et al., 2016b). The identification of LUBAC as a main coordinator of DUB recruitment to SC changes the current view of signalling complex assembly and disassembly. However, many questions remain. The LUBAC-mediated recruitment of CYLD to signalling complexes seems counterintuitive. Why does LUBAC bring its own negative regulator into the complex? In theory, LUBAC and CYLD activity could reach equilibrium were ubiquitin chains are maintained at a certain level. However, because CYLD can also cleave K63-linked ubiquitin chains, and because K63-linked chains act as an anchor point for linear ubiquitin chains, CYLD-mediated deubiquitination should lead to termination of linear ubiquitination and disappearance of these chains. A time course analysis, however, revealed that the level of linear ubiquitination and protein ubiquitination in general, is quite stable even after three hours following TNF stimulation (Figure 3.34). A possible explanation could be the inactivation of CYLD after its recruitment. CYLD may therefore function as a gate-keeper for ubiquitin-dependent signalling complex formation. Based on this theory, the recruitment of CYLD could counteract the full activation of the signalling complex until a critical threshold is reached. Only sufficient signalling complex formation would lead to inactivation of CYLD by e.g. phosphorylation, which would prevent accidental or suboptimal activation of the TNFR1-SC. An inhibitory phosphorylation of CYLD, mediated by IKKε, was already described to promote cell transformation in breast cancer (Hutti et al., 2009). In accord, CYLD was found to exhibit a HOIP-dependent change in mobility in SDS-PAGE analysis following stimulation with TNF, which could be due to phosphorylation (Figure 3.8). A deeper analysis of the phosphorylation of CYLD will be required to characterise its role in TNFR1-SC ubiquitination and signalling.

4.4.2 Regulation of TNF signalling by OTULIN

Despite the lack of OTULIN in SCs, it is still possible that it influences linear ubiquitination without the permanent interaction with HOIP. In one possible scenario, OTULIN dissociates from HOIP after being recruited to the SC by e.g. phosphorylation of the OTULIN PIM domain (Elliott et al., 2014, Schaeffer et al., 2014). This would lead to an increased local concentration of OTULIN around the SC and allow OTULIN to freely move and trim linear ubiquitin chains. Mutation N102A in HOIP can be used to abrogate binding of OTULIN to LUBAC, but it also abolishes SPATA2 and, therefore, CYLD interaction. Hence, it is not possible to attribute the increase in linear ubiquitination to absence of either CYLD or OTULIN alone. A comparison of linear ubiquitination at the TNFR1-SC should be done by comparing SPATA2 PIM-mutant cells, which will lack HOIP/CYLD interaction, with OTULIN-Y56A, which is unable to bind HOIP. Ideally, the point mutation in OTULIN should be obtained by gene editing, as overexpression of OTULIN might lead to unphysiological protein level, leading to artificial deubiquitination events. Nevertheless, linear ubiquitination of the TNFR1-SC increases over time and can still be detected several hours following stimulation. It therefore seems that linear ubiquitin chains are largely impervious to cleavage by DUBs under normal conditions.

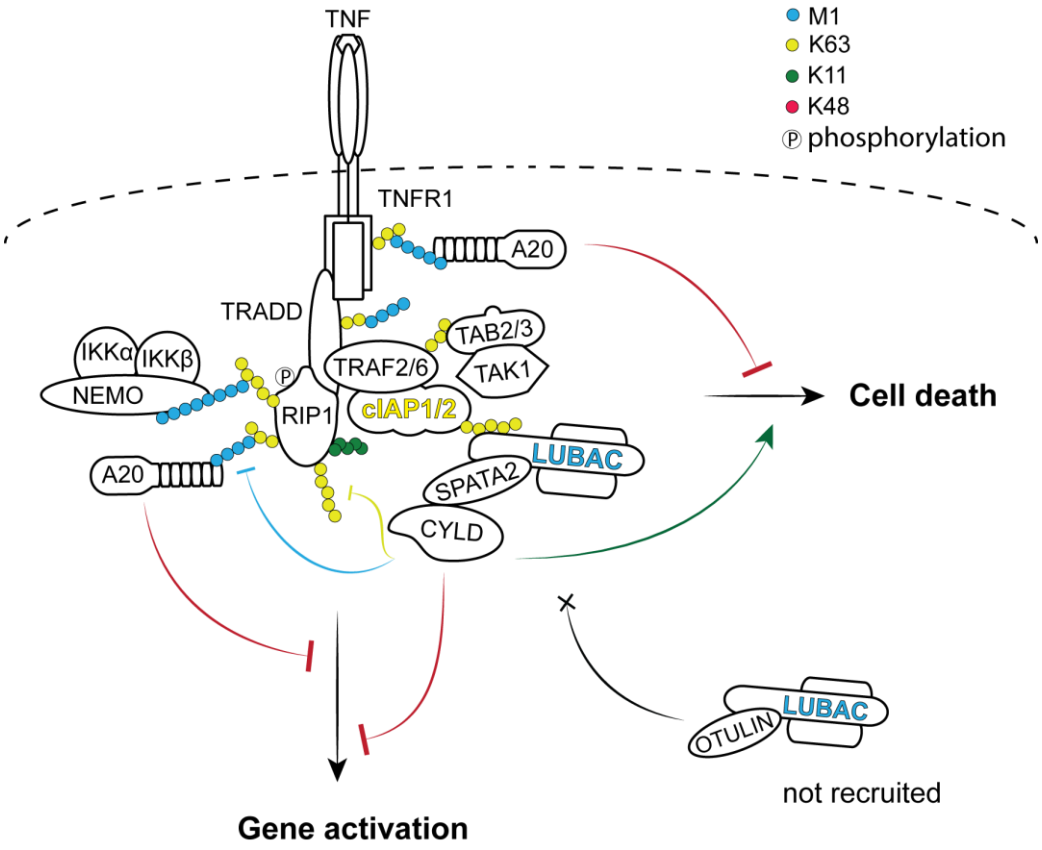

Figure 4.1: Updated scheme of TNFR1-SC assembly and regulation by DUBs

The interaction of CYLD, via SPATA2, with HOIP is required for its recruitment to the TNFR1-SC. Once recruited, CYLD can antagonise M1- and K63-linked ubiquitin chains. Despite its direct interaction with HOIP, OTULIN is not recruited to SCs. A20 is recruited to linear ubiquitination chains via its ZF7. A20 negatively regulates gene activation, possibly by competing with factors like NEMO for binding to linear ubiquitin chains. A20 also stabilises linear ubiquitin chains and can block TNF-induced cell death. In contrast, CYLD suppresses gene activation, likely due to removal of ubiquitin chains from the complex. This also facilitates complex II formation and promotes cell death.

4.5 HOIP-dependent recruitment of A20

Linear ubiquitination was found to be required for recruitment of A20 into SCs (Draber et al., 2015). Over time, increasing amounts of M1-linked ubiquitin chains and NF-κB-mediated A20 expression leads to recruitment of A20 via its ZF7 (Figure 3.38) (Draber et al., 2015). A20 was early on identified, both *in vitro* and *in vivo*, as a negative regulator of NF-κB signalling and inflammation (Evans et al., 2004, Lee et al., 2000). The precise role of A20 supressing gene activation is not fully understood. In addition to the OTU domain, which grants A20 its deubiquitinase activity, the seven zinc fingers were always of interest for subsequent studies. This is understandable as the OTU domain was shown to be dispensable for the survival function of A20 (Lu et al.,

2013). It is therefore plausible to assume that A20 exhibits its regulatory effect passively by binding to ubiquitin chains. The inhibitory effect on NF-κB could be the result of A20's competition with other factors like NEMO/IKK for binding to linear ubiquitin chains, thus preventing a reactivation of NF-κB signalling. Although mice lacking ZF4 were more susceptible to DSS induced colitis, like OTU-deficiency, the animals did not develop any phenotype in absence of a stimulus (Lu et al., 2013). Based on the results obtained in this thesis, one could speculate that it is ZF7 which mediates the survival function of A20. Firstly, A20-ZF7$_{mut}$ was unable to protect MEFs from TNF-induced cell death, while enzymatic inactive A20-C126S was fully preventing it (Figure 3.38, B). Secondly, cells lacking A20 or the zinc finger domains show diminished levels of linear ubiquitination and overall ubiquitination of TNFR1, which is consistent with increased susceptibility to TNF-induced cell death observed in HOIP-deficient cells. Because A20 requires linear ubiquitin chains for its recruitment (Figure 3.34) (Draber et al., 2015), but in turn also stabilises them, one can speculate that A20-binding to linear ubiquitin chains protects them from degradation. A recent report suggested, that M1-linked ubiquitin chains block A20-mediated removal of K63-linked ubiquitin chains (Wertz et al., 2015). However, because the deubiquitinase activity of A20 is dispensable for the effects observed in this study, it is unclear whether another DUB is responsible for the deubiquitination of TNFR1-SC components in absence of A20. Concomitant deletion of DUBs like CYLD, OTULIN or Cezanne in A20-deficient cells could identify the responsible DUB. Also, the experiments performed in this study do not exclude the possibility that TNFR1 is partially degraded following its internalisation. Based on this theory, A20 could in fact prevent the disintegration of TNFR1-trimer complexes thus stabilising the signalling complex and preventing formation of a cell death inducing complex. Surface receptors usually undergo degradation or recycling, once the signal has been transmitted (Maxfield & McGraw, 2004). Internalisation can be mediated by clathrin-coated-pit formation or be independent of it but both pathways lead to formation of sorting endosomes. These vesicles can fuse with lysosome, leading to the degradation of their content. However, certain receptors like transferrin were reported to exit the endosome and be externalised again by the *trans*-Golgi network (van Dam & Stoorvogel, 2002). Hence, it is possible that linear ubiquitin chains represent a sorting signal for the late TNFR1-SC. Intriguingly, A20 was shown to localise with lysosomes in a ZF7 dependent manner (Li, Hailey et al., 2008). Because A20 is recruited to linear ubiquitin chains, an involvement of LUBAC in targeting of the TNFR1-SC to

lysosomes is conceivable. These indications warrant a thorough analysis of the involvement of LUBAC in receptor trafficking and complex compartmentation.

4.6 Regulation of TNF-induced cell death by LUBAC

Deficiency in LUBAC sensitises cells to TNF-induced apoptosis and necroptosis (Figure 3.26). The reason for this sensitisation is not clear. Deficiency in LUBAC also reduces TNF-induced NF-κB activation. If insufficient gene activation were the cause for the embryonic lethality, one would expect a similar phenotype of HOIP- and e.g. NEMO-deficient mice. However, mice lacking HOIP die at E10.5 (Peltzer et al., 2014), whereas NEMO-deficient mice die at around E12.5 (Schmidt-Supprian, Bloch et al., 2000). This suggest that, while LUBAC-certainly impairs NF-κB activation, the cause for the earlier lethality goes beyond a defect in this pathway. It is important to mention that TNF-induced activation of ERK is also impaired in absence of LUBAC ((Peltzer et al., 2014)). The contribution of these pathways to the observed phenotype therefore still needs to be clarified. In any case, it is apparent that LUBAC-deficiency leads to increased sensitivity to cell death induced by TNF- TLR3 and potentially other ligands. The phenotype of LUBAC-deficient mice could therefore be explained by exacerbated cell death. Conclusively, cFLIP- or Caspase-8-deficiency leads to exacerbated cell death. Phenotypically, these mice die at day E10.5 and are characterised by cardiac, vascular and haematopoietic defects, similar to HOIP-deficient mice (Varfolomeev et al., 1998, Yeh, Itie et al., 2000). Deficiency in LUBAC is thought to destabilise complex I thus promoting the formation of a death inducing complex II (Haas et al., 2009). The pro-survival function of ubiquitination in TNFR1 signalling is mainly the result of the observation that depletion of cIAPs by e.g. SMAC-mimetics leads to a drastic reduction in ubiquitination of the TNFR1-SC which coincides with a sensitisation to TNF-induced cell death (Silke & Vucic, 2014). Despite the popularity of this theory, experimental data characterising the sequential events which lead to complex II formation is largely missing. Do complex II components originate from complex I or do they assemble from a different cytoplasmic pool which is merely activated by complex I components? Peculiarly, the formation of complex II is a rather late event following the engagement of TNFR1. Usually, evidence for complex II formation following TNF-treatment can be observed after 30 minutes. Considering that most gene activation has been triggered after 15 minutes suggests that the TNFR1-SC undergoes some major reorganisation, leading to formation of the death inducing complex. However, it was never clarified whether the presumed complex II formation

is indeed the result of a decomposing complex I. In fact, recent emerging evidence suggests that ubiquitination per se may not be as important for the formation of a death-inducing complex. Inhibition of TAK1 or IKKs was shown to induce cell death by perturbing RIP1 phosphorylation, even when ubiquitination was fully functioning and complex stability faultless (Dondelinger et al., 2015). Interestingly, treatment with SMAC mimetics has the same effect on the phosphorylation of RIP1. Hence, the sensitisation to TNF caused by depletion of cIAPs may in fact be the result of impaired RIP1 phosphorylation rather than decreased complex I stability. Importantly, also deficiency in Sharpin causes defective RIP1 phosphorylation (Dondelinger et al., 2015). The function of LUBAC in preventing cell death could therefore be explained by at least two mechanisms. (i) linear ubiquitination could indeed enable the recruitment of factors which directly or indirectly mediate the phosphorylation of RIP1. IKKs were proposed to mediate the death-inhibitory phosphorylation of RIP1 (Dondelinger et al., 2015). Because the NEMO/IKK complex utilises linear ubiquitin for its recruitment, the regulation of RIP1 phosphorylation has to be assumed as proposed by Dondelinger et al.. However, this does not answer the question how complex II is formed. (ii) On the other hand, linear ubiquitination may prevent formation of complex II by retaining e.g. RIP1 in complex I thus preventing formation of complex II. More experimental data is required to support this claim as studies addressing kinetics of complex I decomposition are missing. To understand this issue, the spatiotemporal complex composition of complex I vs II must be monitored by e.g. fluorescent microscopy. Electron microscopy showed that the TNFR1-SC is rapidly internalised leading to formation of vesicles which originate from the plasma membrane (Schneider-Brachert, Tchikov et al., 2004). Hence, compartmentation of the TNFR1-SC represents a regulatory mechanism. As LUBAC-deficiency sensitises cells to TNF-induced death, it is possible that LUBAC regulates the compartmentation of the SC. In a model of *Salmonella* infection, ubiquitin was found to target invading cytoplasmic bacteria for degradation by the autophagosome and lysosomal pathway (LaRock, Chaudhary et al., 2015). During this process, the pathogen becomes coated with ubiquitin chains by the host ubiquitin system. In this context, LUBAC was found to mediate the autophagy of *Salmonella* and infection-induced gene activation (Fiskin, Bionda et al., 2016, van Wijk, Fiskin et al., 2012). These studies also showed that ubiquitin is conjugated to endosomes containing invading bacteria. The autophagy machinery is specifically recruited by these ubiquitin modifications to the endosomes, thus allowing the degradation of the encapsulated bacteria (Fujita, Morita et al., 2013). Similarly, LUBAC and linear ubiquitination could promote the engulfment of the TNFR1-SC in a secondary vesicle. This might represent an efficient way to prevent

further signalling emanating from the engaged receptor signalling complex as the additional compartmentation does not allow interaction with cytosolic proteins. This could also explain why the death inducing complex was not found to be associated with the TNFR1-SC. Signalling events could only take place before the compartmentation of the TNFR1-SC is finished, hence failure to enclose the TNFR1-SC would allow further signalling like e.g. the formation of complex II. In this work, the TNFR1-SC was found to become Triton X-100-insoluble over time. It is not clear what causes the insolubility, but signalling complex formation is certainly part of the explanation, as TNFR1 is easily extractable via TX-100 prior to stimulation. It has been reported that high local concentration of the identical protein can trigger aggresome formation (Johnston, Ward et al., 1998). These vesicles, which are also called inclusion bodies are resistant to most detergents and were found to be associated with the microtubule-system (García-Mata, Bebök et al., 1999). It is possible that the cell disposes of the large TNFR1-SC in a similar way. Further microscopic analysis of the TNFR1-SC is necessary to characterise the fate of this signalling complex once it has been triggered. Monitoring membrane and marker proteins like the lysosome marker LAMP1 or the endosomal marker Rab7 will help to pin-point the location of the TNFR1-SC over time.

4.7 Summary and future directions

In this work, an intriguing network of LUBAC-regulated ubiquitination/ deubiquitination was unravelled. The recruitment principle of CYLD and A20 to signalling complexes has been enigmatic for several years. The discovery that LUBAC is essential for their recruitment raises exiting new questions. The phenotype of LUBAC deficiency was always attributed to the absence of linear ubiquitin chains from the complex, resulting in diminished gene activation and reduced complex stability. However, as also DUB recruitment is abolished in LUBAC-deficient cells, regulation of other ubiquitin chain types is likely to be altered. Hence, the phenotype of LUBAC deficiency might at least partially be caused by functional impairment of CYLD and A20 and possibly OTULIN. Future research therefore needs to separate the function of linear ubiquitin chains, DUB recruitment and individual linear ubiquitin binders. Complete deletion of LUBAC can therefore not be more than an initial test for the involvement of M1-chains in each pathway. Furthermore, specific alterations, like point mutations in linear ubiquitin binding domains, deletion of effectors downstream of LUBAC or mutation of lysine residues critical of linear ubiquitination will be essential. It will also be important to see which other pathways are effected by LUBAC absence. As basic levels of linear

ubiquitination can be observed, a role for LUBAC in cell homeostatic processes like DNA-repair, tonic receptor signalling or metabolism is possible. To unravel these novel aspects of LUBAC function, an unbiased approach should be taken. The newly devised strategy to enrich for proteins that are modified with M1-linkages used in this work might prove useful for such an undertaking. The advantage of this ligand- and cell-type independent approach is that in principle only proteins which are directly modified with linear ubiquitin chains are purified. In contrast to purification of whole signalling complex, this might improve the background of non-ubiquitinated proteins in a mass spectrometry-based analysis.

With the increasing evidence for a complex ubiquitin chain architecture (i.e. branched chains), novel strategies will be required to analyse the function of the individual linkage types. The use of chain type-specific DUBs for *in vitro* deubiquitination assays proved very insightful. However, their application becomes limited in the light of the existence of mixed chains, as cleavage of e.g. K63-linked chains might remove additional chain types which were attached to it. False negative results may also occur if a chain becomes DUB resistant due to branching. Ubiquitin chains should be regarded as functional units due to the many potential combinations of branching points. New methods should therefore focus on the analysis of a complete and unaltered ubiquitin chain ‘tree’, which would provide information on (i) the length of each chain type, (ii) the position of each branching point, (iii) the chain type itself, (iv) and ubiquitin binders which are associated with these chains.

In this work, two interesting previously unrecognised LUBAC substrates, TNFR1 and TRADD, were identified. The function of linear ubiquitin chains on these proteins remains however unanswered. Because HOIP deficiency not only leads to disappearance of M1-linked chains on TNFR1 and TRADD but also leads to reduction of their overall ubiquitination, a chain protective role of M1-chains can be assumed. Again, analysis of the intact chain architecture is likely to shed light on this hypothesis. Additionally, linear ubiquitin chains might have an active function by recruiting yet unidentified factors. Similar to other receptors like EGFR, the ubiquitination on TNFR1 might represent a sorting signalling targeting it to e.g. endosomes or lysosomes. It is also not clear, whether additional LUBAC targets exist in the TNFR1-SC. But one must keep in mind, that these factors could be recruited after the TNFR1-SC was partly disassembled and can no longer be retrieved by e.g. TNF-IP. The functional role of specific linear ubiquitination events is currently difficult to address. As an initial approach, the lysine residue which carries the linear ubiquitin chain can be mutated to abolish ubiquitination. However, it is likely that M1-linked ubiquitin chains are

conjugated on top of another chain type or *vice versa*. Hence, even if no linear ubiquitination can be detected on a protein after mutation of a lysine, the functional impact of mutating this residue could be due to disappearance of other chain types, too. A different way to study the function of linear ubiquitin chains might therefore be to inhibit the ubiquitin binders recognising these chains. The expression of either a dominant negative form or a decoy linear ubiquitin chains might help to understand the function of M1 ubiquitin chains more specifically. For that, a complete list of possible linear ubiquitin binders is still missing. By using linear ubiquitin as bait, it could be possible to enrich for these binders which could be identified by mass spectrometry.

Recent *in vivo* models addressing the function of LUBAC revealed a strong link between linear ubiquitination and the prevention of cell death (Peltzer et al., 2014, Rickard et al., 2014a, Zinngrebe, Montinaro et al., 2014). Though it is possible to detect increased complex II formation in LUBAC-deficient cells (Figure 3.27), the upstream events which lead to this increase are unknown. It is possible that linear ubiquitination acts as a stabiliser for complex I thus preventing association of RIP1 with FADD. However, sufficient experimental evidence for reduced complex I stability in absence of LUBAC is missing. Further experiments are therefore required to monitor the dissociation of receptor components from TNFR1. Of special interest is the fate of RIP1 as it is regarded as the main driver of TNF-induced cell death. Likewise, it is not clear how the transition of SC-components from complex I to complex II is regulated. What prevents RIP1 from engaging with FADD already at the TNFR1-SC? Is the dissociation of RIP1 from complex I altered in death-inducing conditions? Can RIP1 molecules which were not initially recruited to the TNFR1-SC engage in complex II formation? These seemingly basic questions are still waiting to be answered and it is very likely that LUBAC regulates at least some of these aspects.

5 Appendix

5.1 Abbreviations

A	Alanine
aa	Aminoacid
ABIN	A20 binding inhibitor of NF-κB
AP	Affinity purification
Apaf-1	Apoptotic protease-activating factor 1
APC	Antigen presenting cells
APC/C	Anaphase-promoting complex
ATG	Autophagy related gene
ATP	Adenosin triphosphate
BAX	Bcl2-associated X protein
BAX	Bcl2-associated X protein
Bbox	B-box-type zinc finger domain
BCA	Bicinchoninic acid
Bcl-2	B-cell lymphoma 2
BID	BH3-interacting domain death agonist
BIR	Baculoviral IAP repeat
bp	Base pair
BRCA	Breast cancer
C	Cysteine
CAD	Caspase-Activated DNase
CAP	Cytoskeleton-associated protein
CARD	Caspase activation and recruitment domains

CBM	CARD11-BCL10-MALT1
Cezanne	Cellular Zn finger anti-NF-κB
cFLIP	Cellular FLICE-inhibitory protein
CG	CAP-Gly
cIAP	Cellular inhibitor of apoptosis protein
CLR	C-type lectin receptors
Cpdm	Chronic proliferative dermatitis
C-terminus	Carboxy-terminus
CYLD	Familial Cylindromatosis Protein
Da	Dalton
DAMP	Damage-associated molecular pattern
DD	Death domain
DED	Death effector domain
DISC	Death inducing signalling complex
DMEM	Dulbecco's modified Eagle's medium
DNP-KLH	Dinitrophenol- Keyhole limpet hemocyanin
DTT	Dithiothreitol
DUB	Deubiquitinases
E	Glutamic acid
e.g.	For example, (lat: *exemplī grātiā*)
EGF	Epidermal growth factor
ERK	Extracellular signal regulated kinase
ESCRT	Endosomal-sorting complexes required for transport
FACS	Fluorescence-activated cell sorting

FADD	Fas-associated protein with a death domain
FCS	Fetal calf serum
G	Glycine
GalN	D-galactosamine N
GFP	Green fluorescent protein
Gly	Glycine
GST	Glutathione S-transferase
H	Histidine
HECT	Homologous with E6-`associated protein C-Terminus
HEK	Human embryonic kidney
HOIL-1	Heme-oxidized IRP2 ubiquitin ligase 1
HOIP	HOIL-1-interacting protein
HRP	Horseradish-peroxidase
i.e.	That is (lat:*id est*)
IBR	In-between-RING
ICAD	Inhibitor of caspase-activated DNase
IgG	Immunoglobulin G
IKK	Inhibitor of κB kinase
IL	Interleukin
INF	Interferon
IP	Immunoprecipitation
IPTG	Isopropyl-β-D-thio-galactoside
ITCH	Itchy E3 Ubiquitin Protein Ligase
IκB	Inhibitor of κB

JAMM	JAB1/MPN/Mov34 metalloenzyme
JNK	c-Jun N-terminal kinase
K	Lysine
K63-AP	K63-ubiquitin chain-affinity purification
kDa	Kilo Dalton
KO	Knockout
L	Leucine
LDD	Linear ubiquitin chain determining domain
LDS	lithium dodecyl sulfate
LPS	Lipopolysaccharide
LRR	Leucine-rich repeat
LT	Lymphotoxin
LUBAC	Linear ubiquitin chain assembly complex
M	Methionine
M1-AP	M1-ubiquitin chain-affinity purification
MAP2K	Mitogen-activated protein kinase kinase
MAP3K	Mitogen-activated protein kinase kinase kinase
MAPK	Mitogen-activated protein kinase
MAPKAPK	MAP Kinase Activated Protein Kinase
MDP	Muramyl dipeptide
MEFs	Mouse embryonic fibroblasts
MEKK	MAPK/ERK kinase kinase
MJD	Machado-Josephin disease proteases
MLKL	Mixed lineage kinase like

MNK	MAPK-interacting kinases
MOMP	Mitochondrial outer membrane permeabilisation
MS	Mass spectrometry
MVB	Multivesicular body
N	Asparagine
NEMO	NF-κB essential modulator
NF-κB	Nuclear factor-κB
NIK	NF-κB inducing kinase
NK-cell	Natural killer cell
NLR	NOD-like receptor
NLS	Nuclear localisation sequence
NMR	Nuclear magnetic resonance spectroscopy
NOD	Nucleotide-binding Oligomerisation Domain
N-terminus	Amino-terminus
NZF	Npl4-type zinc finger
OTU	Ovarian Tumour
OTULIN	OTU Deubiquitinase With Linear Linkage Specificity
PAMP	Pathogen associated molecular pattern
PARP	Poly (ADP-ribose) polymerase
PBS	Phosphate-buffered saline
PCR	Polymerase chain reaction
PEI	Polyethylenimine
PIM	PUB interacting motif
PtdSer	Phosphatidylserine

PUB	PNGase/ubiquitin-associated
R	Arginine
Raf-1	Rapidly accelerated fibrosarcoma 1
RANK	Receptor activator of NF-κB
RBCK1	RBCC protein interacting with PKC 1
RBR	RING-IBR-RING
RHD	Rel homology domain
RHIM	RIP homotypic interaction motif
RIG-I	Retinoic acid-inducible gene I
RING	Really Interesting New Gene
RIP1	Receptor interacting protein
RLR	RIG-I-like receptors
RNA	Ribonucleic acid
RNAi	Ribonucleic acid interference
RNF	RING finger protein
ROS	Reactive oxygen species
RPMI	Roswell Park Memorial Institute medium
S	Serine
SC	Signalling complex
SCF	Skp1/Cullin/F-box
SDS	Sodium dodecyl sulfate
SEM	Standard error of the mean
SHANK	SH3 and multiple ankyrin repeat domains protein
Sharpin	SHANK associated RH domain protein

shRNA	short hairpin RNA
siRNA	Small interfering RNA
SM	Smac mimetics
Smac	Second mitochondria-derived activator of caspase
SPATA2	Spermatogenesis-associated protein 2
SUMO	Small ubiquitin-related modifier
T	Threonine
TAB	TAK1 binding protein
TAD	Transcriptional activator domain
TAK1	TGF-β-activated kinase 1
TAP	Tandem affinity purification
TGFβ	Transforming growth factor β
TLR	Toll-like receptor
TNF	Tumour necrosis factor
TNFAIP3	TNF Alpha Induced Protein 3
TNFR1	TNF receptor 1
TNFR1-SC	TNFR1-signalling complex
TPL-2	Tumor progression locus 2
TRADD	TNFR1-associated death domain
TRAF	TNF-receptor associated factor
TRAIL	TNF-related apoptosis-inducing ligand
TRIF	TIR domain-containing adapter protein inducing IFN-beta
TRIM	Tripartite motif-containing protein
TX-100	Triton X-100

UBA	Ubiquitin-associated
UBAN	Ubiquitin-binding domains found in ABINs and NEMO
Ubc	Ubiquitin conjugating
UBD	Ubiquitin-binding domain
UBE	Ubiquitin-conjugating enzyme
Ubi-AP	Ubiquitin-affinity purification
UBL	Ubiquitin-like
UCH	Ubiquitin carboxyl-terminal hydrolase isozyme
UIM	Ubiquitin-interacting motif
USP	Ubiquitin-specific protease
v/v	Volume/volume
vOTU	Viral OTU
w/v	Weight/volume
WT	Wild-type
XIAP	X-linked inhibitor of apoptosis
ZBP1	Z-DNA-binding protein 1
ZF	Zinc finger

5.2 List of publications

Lafont E, Kantari-Mimoun C, Draber P, De Miguel D, Hartwig T, Reichert M, **Kupka S**, Shimizu Y, Taraborrelli L, Spit M, Sprick MR, Walczak H (2017) The linear ubiquitin chain assembly complex regulates TRAIL-induced gene activation and cell death. The EMBO journal

Kupka S, De Miguel D, Draber P, Martino L, Surinova S, Rittinger K, Walczak H (2016) SPATA2-Mediated Binding of CYLD to HOIP Enables CYLD Recruitment to Signaling Complexes. *Cell reports* **16:** 2271-2280

Kupka S, Reichert M, Draber P, Walczak H (2016) Formation and removal of poly-ubiquitin chains in the regulation of tumor necrosis factor-induced gene activation and cell death. *The FEBS journal* **283:** 2626-2639

Draber P, **Kupka S**, Reichert M, Draberova H, Lafont E, de Miguel D, Spilgies L, Surinova S, Taraborrelli L, Hartwig T, Rieser E, Martino L, Rittinger K, Walczak H (2015) LUBAC-Recruited CYLD and A20 Regulate Gene Activation and Cell Death by Exerting Opposing Effects on Linear Ubiquitin in Signaling Complexes. *Cell reports* **13**: 2258-2272

6 References

Adrianto I, Wen F, Templeton A, Wiley G, King JB, Lessard CJ, Bates JS, Hu Y, Kelly JA, Kaufman KM, Guthridge JM, Alarcón-Riquelme ME, Anaya JM, Bae SC, Bang SY, Boackle SA, Brown EE, Petri MA, Gallant C, Ramsey-Goldman R et al. (2011) Association of a functional variant downstream of TNFAIP3 with systemic lupus erythematosus. Nat Genet 43: 253-8

Aggarwal BB (2003) Signalling pathways of the TNF superfamily: a double-edged sword. Nat Rev Immunol 3: 745-56

Akinleye A, Furqan M, Mukhi N, Ravella P, Liu D (2013) MEK and the inhibitors: from bench to bedside. J Hematol Oncol 6: 27

Akutsu M, Dikic I, Bremm A (2016) Ubiquitin chain diversity at a glance. J Cell Sci 129: 875-80

Al-Hakim A, Escribano-Diaz C, Landry MC, O'Donnell L, Panier S, Szilard RK, Durocher D (2010) The ubiquitous role of ubiquitin in the DNA damage response. DNA Repair (Amst) 9: 1229-40

Arenzana-Seisdedos F, Turpin P, Rodriguez M, Thomas D, Hay RT, Virelizier JL, Dargemont C (1997) Nuclear localization of I kappa B alpha promotes active transport of NF-kappa B from the nucleus to the cytoplasm. J Cell Sci 110 (Pt 3): 369-78

Ashida H, Mimuro H, Ogawa M, Kobayashi T, Sanada T, Kim M, Sasakawa C (2011) Cell death and infection: a double-edged sword for host and pathogen survival. J Cell Biol 195: 931-42

Atarashi K, Nishimura J, Shima T, Umesaki Y, Yamamoto M, Onoue M, Yagita H, Ishii N, Evans R, Honda K, Takeda K (2008) ATP drives lamina propria T(H)17 cell differentiation. Nature 455: 808-12

Avvakumov GV, Walker JR, Xue S, Finerty PJ, Mackenzie F, Newman EM, Dhe-Paganon S (2006) Amino-terminal dimerization, NRDP1-rhodanese interaction, and inhibited catalytic domain conformation of the ubiquitin-specific protease 8 (USP8). J Biol Chem 281: 38061-70

Baeuerle PA, Baltimore D (1988) I kappa B: a specific inhibitor of the NF-kappa B transcription factor. Science 242: 540-6

Baeuerle PA, Baltimore D (1989) A 65-kappaD subunit of active NF-kappaB is required for inhibition of NF-kappaB by I kappaB. Genes Dev 3: 1689-98

Baker RT, Board PG (1991) The human ubiquitin-52 amino acid fusion protein gene shares several structural features with mammalian ribosomal protein genes. Nucleic Acids Res 19: 1035-40

Beg AA, Baldwin AS (1993) The I kappa B proteins: multifunctional regulators of Rel/NF-kappa B transcription factors. Genes Dev 7: 2064-70

Ben-Saadon R, Zaaroor D, Ziv T, Ciechanover A (2006) The polycomb protein Ring1B generates self atypical mixed ubiquitin chains required for its in vitro histone H2A ligase activity. Mol Cell 24: 701-11

Berger SB, Kasparcova V, Hoffman S, Swift B, Dare L, Schaeffer M, Capriotti C, Cook M, Finger J, Hughes-Earle A, Harris PA, Kaiser WJ, Mocarski ES, Bertin J, Gough PJ (2014) Cutting Edge: RIP1 kinase activity is dispensable for normal development but is a key regulator of inflammation in SHARPIN-deficient mice. J Immunol 192: 5476-80

Bertrand MJ, Doiron K, Labbé K, Korneluk RG, Barker PA, Saleh M (2009) Cellular inhibitors of apoptosis cIAP1 and cIAP2 are required for innate immunity signaling by the pattern recognition receptors NOD1 and NOD2. Immunity 30: 789-801

Bertrand MJ, Milutinovic S, Dickson KM, Ho WC, Boudreault A, Durkin J, Gillard JW, Jaquith JB, Morris SJ, Barker PA (2008) cIAP1 and cIAP2 facilitate cancer cell survival by functioning as E3 ligases that promote RIP1 ubiquitination. Mol Cell 30: 689-700

Bianchi ME (2007) DAMPs, PAMPs and alarmins: all we need to know about danger. J Leukoc Biol 81: 1-5

Biggs PJ, Wooster R, Ford D, Chapman P, Mangion J, Quirk Y, Easton DF, Burn J, Stratton MR (1995) Familial cylindromatosis (turban tumour syndrome) gene localised to chromosome 16q12-q13: evidence for its role as a tumour suppressor gene. Nat Genet 11: 441-443

Bignell GR, Warren W, Seal S, Takahashi M, Rapley E, Barfoot R, Green H, Brown C, Biggs PJ, Lakhani SR, Jones C, Hansen J, Blair E, Hofmann B, Siebert R, Turner G, Evans DG, Schrander-Stumpel C, Beemer FA, van Den Ouweland A et al. (2000) Identification of the familial cylindromatosis tumour-suppressor gene. Nat Genet 25: 160-5

Biondi RM, Nebreda AR (2003) Signalling specificity of Ser/Thr protein kinases through docking-site-mediated interactions. Biochem J 372: 1-13

Bode AM, Dong Z (2007) The functional contrariety of JNK. Mol Carcinog 46: 591-8

Boisson B, Laplantine E, Dobbs K, Cobat A, Tarantino N, Hazen M, Lidov HG, Hopkins G, Du L, Belkadi A, Chrabieh M, Itan Y, Picard C, Fournet JC, Eibel H, Tsitsikov E, Pai SY, Abel L, Al-Herz W, Casanova JL et al. (2015) Human HOIP and LUBAC deficiency underlies autoinflammation, immunodeficiency, amylopectinosis, and lymphangiectasia. The Journal of experimental medicine 212: 939-51

Boisson B, Laplantine E, Prando C, Giliani S, Israelsson E, Xu Z, Abhyankar A, Israël L, Trevejo-Nunez G, Bogunovic D, Cepika A-M, MacDuff D, Chrabieh M, Hubeau M, Bajolle F, Debré M, Mazzolari E, Vairo D, Agou F, Virgin HW et al. (2012) Immunodeficiency, autoinflammation and amylopectinosis in humans with inherited HOIL-1 and LUBAC deficiency. Nature immunology 13: 1178-1186

Boone DL, Turer EE, Lee EG, Ahmad RC, Wheeler MT, Tsui C, Hurley P, Chien M, Chai S, Hitotsumatsu O, McNally E, Pickart C, Ma A (2004) The ubiquitin-modifying enzyme A20 is required for termination of Toll-like receptor responses. Nature immunology 5: 1052-60

Bosanac I, Wertz IE, Pan B, Yu C, Kusam S, Lam C, Phu L, Phung Q, Maurer B, Arnott D, Kirkpatrick DS, Dixit VM, Hymowitz SG (2010) Ubiquitin binding to A20 ZnF4 is required for modulation of NF-kappaB signaling. Molecular cell 40: 548-57

Bottomley RH, Trainer AL, Griffin MJ (1969) Enzymatic and chromosomal characterization of HeLa variants. J Cell Biol 41: 806-15

Boulares AH, Yakovlev AG, Ivanova V, Stoica BA, Wang G, Iyer S, Smulson M (1999) Role of poly(ADP-ribose) polymerase (PARP) cleavage in apoptosis. Caspase 3-resistant PARP mutant increases rates of apoptosis in transfected cells. J Biol Chem 274: 22932-40

Boulton TG, Nye SH, Robbins DJ, Ip NY, Radziejewska E, Morgenbesser SD, DePinho RA, Panayotatos N, Cobb MH, Yancopoulos GD (1991) ERKs: a family of protein-serine/threonine kinases that are activated and tyrosine phosphorylated in response to insulin and NGF. Cell 65: 663-75

Bowman J, Rodgers MA, Shi M, Amatya R, Hostager B, Iwai K, Gao SJ, Jung JU (2015) Posttranslational Modification of HOIP Blocks Toll-Like Receptor 4-Mediated Linear-Ubiquitin-Chain Formation. mBio 6

Bratton DL, Fadok VA, Richter DA, Kailey JM, Guthrie LA, Henson PM (1997) Appearance of phosphatidylserine on apoptotic cells requires calcium-mediated nonspecific flip-flop and is enhanced by loss of the aminophospholipid translocase. J Biol Chem 272: 26159-65

Brown K, Gerstberger S, Carlson L, Franzoso G, Siebenlist U (1995) Control of I kappa B-alpha proteolysis by site-specific, signal-induced phosphorylation. Science 267: 1485-8

Brummelkamp TR, Nijman SM, Dirac AM, Bernards R (2003) Loss of the cylindromatosis tumour suppressor inhibits apoptosis by activating NF-kappaB. Nature 424: 797-801

Cargnello M, Roux PP (2011) Activation and function of the MAPKs and their substrates, the MAPK-activated protein kinases. Microbiol Mol Biol Rev 75: 50-83

Cerretti DP, Kozlosky CJ, Mosley B, Nelson N, Van Ness K, Greenstreet TA, March CJ, Kronheim SR, Druck T, Cannizzaro LA (1992) Molecular cloning of the interleukin-1 beta converting enzyme. Science 256: 97-100

Chambers JW, LoGrasso PV (2011) Mitochondrial c-Jun N-terminal kinase (JNK) signaling initiates physiological changes resulting in amplification of reactive oxygen species generation. J Biol Chem 286: 16052-62

Chan FK, Shisler J, Bixby JG, Felices M, Zheng L, Appel M, Orenstein J, Moss B, Lenardo MJ (2003) A role for tumor necrosis factor receptor-2 and receptor-interacting protein in programmed necrosis and antiviral responses. J Biol Chem 278: 51613-21

Chang L, Karin M (2001) Mammalian MAP kinase signalling cascades. Nature 410: 37-40

Chau V, Tobias JW, Bachmair A, Marriott D, Ecker DJ, Gonda DK, Varshavsky A (1989) A multiubiquitin chain is confined to specific lysine in a targeted short-lived protein. Science 243: 1576-83

Chauhan D, Singh A, Brahmandam M, Podar K, Hideshima T, Richardson P, Munshi N, Palladino MA, Anderson KC (2008) Combination of proteasome inhibitors

bortezomib and NPI-0052 trigger in vivo synergistic cytotoxicity in multiple myeloma. Blood 111: 1654-64

Chen GY, Nuñez G (2010) Sterile inflammation: sensing and reacting to damage. Nat Rev Immunol 10: 826-37

Chen L, Madura K (2002) Rad23 promotes the targeting of proteolytic substrates to the proteasome. Mol Cell Biol 22: 4902-13

Chen LF, Greene WC (2004) Shaping the nuclear action of NF-kappaB. Nat Rev Mol Cell Biol 5: 392-401

Chen LF, Mu Y, Greene WC (2002) Acetylation of RelA at discrete sites regulates distinct nuclear functions of NF-kappaB. EMBO J 21: 6539-48

Chen X, Li W, Ren J, Huang D, He WT, Song Y, Yang C, Zheng X, Chen P, Han J (2014) Translocation of mixed lineage kinase domain-like protein to plasma membrane leads to necrotic cell death. Cell Res 24: 105-21

Chen Z, Hagler J, Palombella VJ, Melandri F, Scherer D, Ballard D, Maniatis T (1995) Signal-induced site-specific phosphorylation targets I kappa B alpha to the ubiquitin-proteasome pathway. Genes Dev 9: 1586-97

Chen ZJ, Parent L, Maniatis T (1996) Site-specific phosphorylation of IkappaBalpha by a novel ubiquitination-dependent protein kinase activity. Cell 84: 853-62

Chen ZJ, Sun LJ (2009) Nonproteolytic functions of ubiquitin in cell signaling. Molecular cell 33: 275-86

Cho YS, Challa S, Moquin D, Genga R, Ray TD, Guildford M, Chan FK (2009) Phosphorylation-driven assembly of the RIP1-RIP3 complex regulates programmed necrosis and virus-induced inflammation. Cell 137: 1112-23

Christensen DE, Brzovic PS, Klevit RE (2007) E2-BRCA1 RING interactions dictate synthesis of mono- or specific polyubiquitin chain linkages. Nat Struct Mol Biol 14: 941-8

Chu Y, Vahl JC, Kumar D, Heger K, Bertossi A, Wojtowicz E, Soberon V, Schenten D, Mack B, Reutelshofer M, Beyaert R, Amann K, van Loo G, Schmidt-Supprian M (2011) B cells lacking the tumor suppressor TNFAIP3/A20 display impaired differentiation and hyperactivation and cause inflammation and autoimmunity in aged mice. Blood 117: 2227-36

Ciechanover A, Finley D, Varshavsky A (1984) Ubiquitin dependence of selective protein degradation demonstrated in the mammalian cell cycle mutant ts85. Cell 37: 57-66

Ciehanover A, Hod Y, Hershko A (1978) A heat-stable polypeptide component of an ATP-dependent proteolytic system from reticulocytes. Biochem Biophys Res Commun 81: 1100-5

Clague MJ, Urbé S (2010) Ubiquitin: same molecule, different degradation pathways. Cell 143: 682-5

Claudio E, Brown K, Park S, Wang H, Siebenlist U (2002) BAFF-induced NEMO-independent processing of NF-kappa B2 in maturing B cells. Nat Immunol 3: 958-65

Coope HJ, Atkinson PG, Huhse B, Belich M, Janzen J, Holman MJ, Klaus GG, Johnston LH, Ley SC (2002) CD40 regulates the processing of NF-kappaB2 p100 to p52. EMBO J 21: 5375-85

Cooper JA, Bowen-Pope DF, Raines E, Ross R, Hunter T (1982) Similar effects of platelet-derived growth factor and epidermal growth factor on the phosphorylation of tyrosine in cellular proteins. Cell 31: 263-73

Cuevas BD, Abell AN, Johnson GL (2007) Role of mitogen-activated protein kinase kinase kinases in signal integration. Oncogene 26: 3159-71

Czabotar PE, Lessene G, Strasser A, Adams JM (2014) Control of apoptosis by the BCL-2 protein family: implications for physiology and therapy. Nat Rev Mol Cell Biol 15: 49-63

D'Alessio A, Esposito B, Giampietri C, Ziparo E, Pober JS, Filippini A (2012) Plasma membrane microdomains regulate TACE-dependent TNFR1 shedding in human endothelial cells. J Cell Mol Med 16: 627-36

Damgaard RB, Nachbur U, Yabal M, Wong WW, Fiil BK, Kastirr M, Rieser E, Rickard JA, Bankovacki A, Peschel C, Ruland J, Bekker-Jensen S, Mailand N, Kaufmann T, Strasser A, Walczak H, Silke J, Jost PJ, Gyrd-Hansen M (2012) The ubiquitin ligase XIAP recruits LUBAC for NOD2 signaling in inflammation and innate immunity. Mol Cell 46: 746-58

Damgaard RB, Walker JA, Marco-Casanova P, Morgan NV, Titheradge HL, Elliott PR, McHale D, Maher ER, McKenzie AN, Komander D (2016) The Deubiquitinase OTULIN Is an Essential Negative Regulator of Inflammation and Autoimmunity. Cell 166: 1215-1230 e20

Dammer EB, Na CH, Xu P, Seyfried NT, Duong DM, Cheng D, Gearing M, Rees H, Lah JJ, Levey AI, Rush J, Peng J (2011) Polyubiquitin linkage profiles in three models of proteolytic stress suggest the etiology of Alzheimer disease. J Biol Chem 286: 10457-65

Das S, Cho J, Lambertz I, Kelliher MA, Eliopoulos AG, Du K, Tsichlis PN (2005) Tpl2/cot signals activate ERK, JNK, and NF-kappaB in a cell-type and stimulus-specific manner. J Biol Chem 280: 23748-57

de Almagro MC, Goncharov T, Newton K, Vucic D (2015) Cellular IAP proteins and LUBAC differentially regulate necrosome-associated RIP1 ubiquitination. Cell Death Dis 6: e1800

de Bie P, Ciechanover A (2011) Ubiquitination of E3 ligases: self-regulation of the ubiquitin system via proteolytic and non-proteolytic mechanisms. Cell Death Differ 18: 1393-402

Degterev A, Hitomi J, Germscheid M, Ch'en IL, Korkina O, Teng X, Abbott D, Cuny GD, Yuan C, Wagner G, Hedrick SM, Gerber SA, Lugovskoy A, Yuan J (2008) Identification of RIP1 kinase as a specific cellular target of necrostatins. Nat Chem Biol 4: 313-21

Degterev A, Huang Z, Boyce M, Li Y, Jagtap P, Mizushima N, Cuny GD, Mitchison TJ, Moskowitz MA, Yuan J (2005) Chemical inhibitor of nonapoptotic cell death with therapeutic potential for ischemic brain injury. Nat Chem Biol 1: 112-9

Dejardin E (2006) The alternative NF-kappaB pathway from biochemistry to biology: pitfalls and promises for future drug development. Biochem Pharmacol 72: 1161-79

Dejardin E, Droin NM, Delhase M, Haas E, Cao Y, Makris C, Li ZW, Karin M, Ware CF, Green DR (2002) The lymphotoxin-beta receptor induces different patterns of gene expression via two NF-kappaB pathways. Immunity 17: 525-35

Deshaies RJ, Joazeiro CA (2009) RING domain E3 ubiquitin ligases. Annu Rev Biochem 78: 399-434

DiDonato JA, Hayakawa M, Rothwarf DM, Zandi E, Karin M (1997) A cytokine-responsive IkappaB kinase that activates the transcription factor NF-kappaB. Nature 388: 548-54

Dikic I, Wakatsuki S, Walters KJ (2009) Ubiquitin-binding domains - from structures to functions. Nature reviews Molecular cell biology 10: 659-71

Dillon CP, Weinlich R, Rodriguez DA, Cripps JG, Quarato G, Gurung P, Verbist KC, Brewer TL, Llambi F, Gong YN, Janke LJ, Kelliher MA, Kanneganti TD, Green DR (2014) RIPK1 blocks early postnatal lethality mediated by caspase-8 and RIPK3. Cell 157: 1189-202

Dondelinger Y, Declercq W, Montessuit S, Roelandt R, Goncalves A, Bruggeman I, Hulpiau P, Weber K, Sehon CA, Marquis RW, Bertin J, Gough PJ, Savvides S, Martinou JC, Bertrand MJ, Vandenabeele P (2014) MLKL compromises plasma membrane integrity by binding to phosphatidylinositol phosphates. Cell Rep 7: 971-81

Dondelinger Y, Jouan-Lanhouet S, Divert T, Theatre E, Bertin J, Gough PJ, Giansanti P, Heck AJ, Dejardin E, Vandenabeele P, Bertrand MJ (2015) NF-kappaB-Independent Role of IKKalpha/IKKbeta in Preventing RIPK1 Kinase-Dependent Apoptotic and Necroptotic Cell Death during TNF Signaling. Mol Cell 60: 63-76

Douanne T, Gavard J, Bidere N (2016) The paracaspase MALT1 cleaves the LUBAC subunit HOIL1 during antigen receptor signaling. Journal of cell science 129: 1775-80

Douglas T, Champagne C, Morizot A, Lapointe JM, Saleh M (2015) The Inflammatory Caspases-1 and -11 Mediate the Pathogenesis of Dermatitis in Sharpin-Deficient Mice. J Immunol 195: 2365-73

Draber P, Kupka S, Reichert M, Draberova H, Lafont E, de Miguel D, Spilgies L, Surinova S, Taraborrelli L, Hartwig T, Rieser E, Martino L, Rittinger K, Walczak H (2015) LUBAC-Recruited CYLD and A20 Regulate Gene Activation and Cell Death by Exerting Opposing Effects on Linear Ubiquitin in Signaling Complexes. Cell Rep

Dynek JN, Goncharov T, Dueber EC, Fedorova AV, Izrael-Tomasevic A, Phu L, Helgason E, Fairbrother WJ, Deshayes K, Kirkpatrick DS, Vucic D (2010) c-IAP1 and UbcH5 promote K11-linked polyubiquitination of RIP1 in TNF signalling. EMBO J 29: 4198-209

Ea C-K, Deng L, Xia Z-P, Pineda G, Chen ZJ (2006) Activation of IKK by TNFα Requires Site-Specific Ubiquitination of RIP1 and Polyubiquitin Binding by NEMO. Mol Cell 22: 245-257

Eddins MJ, Varadan R, Fushman D, Pickart CM, Wolberger C (2007) Crystal structure and solution NMR studies of Lys48-linked tetraubiquitin at neutral pH. J Mol Biol 367: 204-11

Edelmann MJ, Kessler BM (2008) Ubiquitin and ubiquitin-like specific proteases targeted by infectious pathogens: Emerging patterns and molecular principles. Biochim Biophys Acta 1782: 809-16

Elliott PR, Leske D, Hrdinka M, Bagola K, Fiil BK, McLaughlin SH, Wagstaff J, Volkmar N, Christianson JC, Kessler BM, Freund SM, Komander D, Gyrd-Hansen M (2016) SPATA2 Links CYLD to LUBAC, Activates CYLD, and Controls LUBAC Signaling. Mol Cell 63: 990-1005

Elliott PR, Nielsen SV, Marco-Casanova P, Fiil BK, Keusekotten K, Mailand N, Freund SM, Gyrd-Hansen M, Komander D (2014) Molecular Basis and Regulation of OTULIN-LUBAC Interaction. Mol Cell

Ellis RE, Yuan JY, Horvitz HR (1991) Mechanisms and functions of cell death. Annu Rev Cell Biol 7: 663-98

Elmore S (2007) Apoptosis: a review of programmed cell death. Toxicol Pathol 35: 495-516

Elton L, Carpentier I, Staal J, Driege Y, Haegman M, Beyaert R (2016) MALT1 cleaves the E3 ubiquitin ligase HOIL-1 in activated T cells, generating a dominant negative inhibitor of LUBAC-induced NF-κB signaling. FEBS J 283: 403-12

Emmerich CH, Bakshi S, Kelsall IR, Ortiz-Guerrero J, Shpiro N, Cohen P (2016) Lys63/Met1-hybrid ubiquitin chains are commonly formed during the activation of innate immune signalling. Biochemical and biophysical research communications 474: 452-461

Emmerich CH, Ordureau A, Strickson S, Arthur JS, Pedrioli PG, Komander D, Cohen P (2013) Activation of the canonical IKK complex by K63/M1-linked hybrid ubiquitin chains. Proc Natl Acad Sci U S A

Enari M, Sakahira H, Yokoyama H, Okawa K, Iwamatsu A, Nagata S (1998) A caspase-activated DNase that degrades DNA during apoptosis, and its inhibitor ICAD. Nature 391: 43-50

Enesa K, Zakkar M, Chaudhury H, Luong le A, Rawlinson L, Mason JC, Haskard DO, Dean JL, Evans PC (2008) NF-kappaB suppression by the deubiquitinating enzyme Cezanne: a novel negative feedback loop in pro-inflammatory signaling. J Biol Chem 283: 7036-45

Enslen H, Davis RJ (2001) Regulation of MAP kinases by docking domains. Biol Cell 93: 5-14

Ermolaeva MA, Michallet MC, Papadopoulou N, Utermohlen O, Kranidioti K, Kollias G, Tschopp J, Pasparakis M (2008) Function of TRADD in tumor necrosis factor

receptor 1 signaling and in TRIF-dependent inflammatory responses. Nat Immunol 9: 1037-46

Eskes R, Desagher S, Antonsson B, Martinou JC (2000) Bid induces the oligomerization and insertion of Bax into the outer mitochondrial membrane. Mol Cell Biol 20: 929-35

Evans PC, Ovaa H, Hamon M, Kilshaw PJ, Hamm S, Bauer S, Ploegh HL, Smith TS (2004) Zinc-finger protein A20, a regulator of inflammation and cell survival, has de-ubiquitinating activity. Biochem J 378: 727-734

Fadok VA, Voelker DR, Campbell PA, Cohen JJ, Bratton DL, Henson PM (1992) Exposure of phosphatidylserine on the surface of apoptotic lymphocytes triggers specific recognition and removal by macrophages. J Immunol 148: 2207-16

Fan CM, Maniatis T (1991) Generation of p50 subunit of NF-kappa B by processing of p105 through an ATP-dependent pathway. Nature 354: 395-8

Feldman AM, Combes A, Wagner D, Kadakomi T, Kubota T, Li YY, McTiernan C (2000) The role of tumor necrosis factor in the pathophysiology of heart failure. J Am Coll Cardiol 35: 537-44

Feng S, Yang Y, Mei Y, Ma L, Zhu DE, Hoti N, Castanares M, Wu M (2007) Cleavage of RIP3 inactivates its caspase-independent apoptosis pathway by removal of kinase domain. Cell Signal 19: 2056-67

Feoktistova M, Geserick P, Kellert B, Dimitrova DP, Langlais C, Hupe M, Cain K, MacFarlane M, Hacker G, Leverkus M (2011) cIAPs block Ripoptosome formation, a RIP1/caspase-8 containing intracellular cell death complex differentially regulated by cFLIP isoforms. Mol Cell 43: 449-63

Fiil BK, Damgaard RB, Wagner SA, Keusekotten K, Fritsch M, Bekker-Jensen S, Mailand N, Choudhary C, Komander D, Gyrd-Hansen M (2013) OTULIN restricts Met1-linked ubiquitination to control innate immune signaling. Mol Cell 50: 818-30

Finley D (2009) Recognition and processing of ubiquitin-protein conjugates by the proteasome. Annu Rev Biochem 78: 477-513

Finley D, Sadis S, Monia BP, Boucher P, Ecker DJ, Crooke ST, Chau V (1994) Inhibition of proteolysis and cell cycle progression in a multiubiquitination-deficient yeast mutant. Mol Cell Biol 14: 5501-9

Fiskin E, Bionda T, Dikic I, Behrends C (2016) Global Analysis of Host and Bacterial Ubiquitinome in Response to Salmonella Typhimurium Infection. Mol Cell 62: 967-81

Fritsch J, Stephan M, Tchikov V, Winoto-Morbach S, Gubkina S, Kabelitz D, Schutze S (2014) Cell fate decisions regulated by k63 ubiquitination of tumor necrosis factor receptor 1. Mol Cell Biol 34: 3214-28

Fuentes-Prior P, Salvesen GS (2004) The protein structures that shape caspase activity, specificity, activation and inhibition. Biochem J 384: 201-32

Fujita N, Morita E, Itoh T, Tanaka A, Nakaoka M, Osada Y, Umemoto T, Saitoh T, Nakatogawa H, Kobayashi S, Haraguchi T, Guan JL, Iwai K, Tokunaga F, Saito K, Ishibashi K, Akira S, Fukuda M, Noda T, Yoshimori T (2013) Recruitment of the

autophagic machinery to endosomes during infection is mediated by ubiquitin. J Cell Biol 203: 115-28

Fujita T, Nolan GP, Liou HC, Scott ML, Baltimore D (1993) The candidate proto-oncogene bcl-3 encodes a transcriptional coactivator that activates through NF-kappa B p50 homodimers. Genes Dev 7: 1354-63

Fulda S (2013) Alternative cell death pathways and cell metabolism. Int J Cell Biol 2013: 463637

Fulda S (2014) Molecular pathways: targeting death receptors and smac mimetics. Clin Cancer Res 20: 3915-20

Fulda S, Debatin KM (2006) Extrinsic versus intrinsic apoptosis pathways in anticancer chemotherapy. Oncogene 25: 4798-811

Ganchi PA, Sun SC, Greene WC, Ballard DW (1992) I kappa B/MAD-3 masks the nuclear localization signal of NF-kappa B p65 and requires the transactivation domain to inhibit NF-kappa B p65 DNA binding. Mol Biol Cell 3: 1339-52

García-Mata R, Bebök Z, Sorscher EJ, Sztul ES (1999) Characterization and dynamics of aggresome formation by a cytosolic GFP-chimera. J Cell Biol 146: 1239-54

Genestier L, Bonnefoy-Berard N, Rouault JP, Flacher M, Revillard JP (1995) Tumor necrosis factor-alpha up-regulates Bcl-2 expression and decreases calcium-dependent apoptosis in human B cell lines. Int Immunol 7: 533-40

Gerlach B, Cordier SM, Schmukle AC, Emmerich CH, Rieser E, Haas TL, Webb AI, Rickard JA, Anderton H, Wong WW, Nachbur U, Gangoda L, Warnken U, Purcell AW, Silke J, Walczak H (2011) Linear ubiquitination prevents inflammation and regulates immune signalling. Nature 471: 591-6

Giard DJ, Aaronson SA, Todaro GJ, Arnstein P, Kersey JH, Dosik H, Parks WP (1973) In vitro cultivation of human tumors: establishment of cell lines derived from a series of solid tumors. J Natl Cancer Inst 51: 1417-23

Gijbels MJ, Zurcher C, Kraal G, Elliott GR, HogenEsch H, Schijff G, Savelkoul HF, Bruijnzeel PL (1996) Pathogenesis of skin lesions in mice with chronic proliferative dermatitis (cpdm/cpdm). Am J Pathol 148: 941-50

Girardin SE, Boneca IG, Viala J, Chamaillard M, Labigne A, Thomas G, Philpott DJ, Sansonetti PJ (2003) Nod2 is a general sensor of peptidoglycan through muramyl dipeptide (MDP) detection. J Biol Chem 278: 8869-72

Glickman MH, Ciechanover A (2002) The ubiquitin-proteasome proteolytic pathway: destruction for the sake of construction. Physiological reviews 82: 373-428

Goldberg AL, Cascio P, Saric T, Rock KL (2002) The importance of the proteasome and subsequent proteolytic steps in the generation of antigenic peptides. Mol Immunol 39: 147-64

Goldstein G, Scheid M, Hammerling U, Schlesinger DH, Niall HD, Boyse EA (1975) Isolation of a polypeptide that has lymphocyte-differentiating properties and is probably represented universally in living cells. Proc Natl Acad Sci U S A 72: 11-5

Graham FL, Smiley J, Russell WC, Nairn R (1977) Characteristics of a human cell line transformed by DNA from human adenovirus type 5. J Gen Virol 36: 59-74

Grell M, Wajant H, Zimmermann G, Scheurich P (1998) The type 1 receptor (CD120a) is the high-affinity receptor for soluble tumor necrosis factor. Proc Natl Acad Sci U S A 95: 570-5

Guo H, Omoto S, Harris PA, Finger JN, Bertin J, Gough PJ, Kaiser WJ, Mocarski ES (2015) Herpes simplex virus suppresses necroptosis in human cells. Cell Host Microbe 17: 243-51

Gupta S, Barrett T, Whitmarsh AJ, Cavanagh J, Sluss HK, Dérijard B, Davis RJ (1996) Selective interaction of JNK protein kinase isoforms with transcription factors. EMBO J 15: 2760-70

Haas TL, Emmerich CH, Gerlach B, Schmukle AC, Cordier SM, Rieser E, Feltham R, Vince J, Warnken U, Wenger T, Koschny R, Komander D, Silke J, Walczak H (2009) Recruitment of the linear ubiquitin chain assembly complex stabilizes the TNF-R1 signaling complex and is required for TNF-mediated gene induction. Mol Cell 36: 831-44

Hadian K, Griesbach RA, Dornauer S, Wanger TM, Nagel D, Metlitzky M, Beisker W, Schmidt-Supprian M, Krappmann D (2011) NF-kappaB essential modulator (NEMO) interaction with linear and lys-63 ubiquitin chains contributes to NF-kappaB activation. The Journal of biological chemistry 286: 26107-17

Haglund K, Di Fiore PP, Dikic I (2003) Distinct monoubiquitin signals in receptor endocytosis. Trends Biochem Sci 28: 598-603

Hartmann-Petersen R, Gordon C (2004) Integral UBL domain proteins: a family of proteasome interacting proteins. Semin Cell Dev Biol 15: 247-59

Hayden MS, Ghosh S (2008) Shared principles in NF-kappaB signaling. Cell 132: 344-62

He S, Liang Y, Shao F, Wang X (2011) Toll-like receptors activate programmed necrosis in macrophages through a receptor-interacting kinase-3-mediated pathway. Proc Natl Acad Sci U S A 108: 20054-9

He S, Wang L, Miao L, Wang T, Du F, Zhao L, Wang X (2009) Receptor interacting protein kinase-3 determines cellular necrotic response to TNF-alpha. Cell 137: 1100-11

Henson PM, Hume DA (2006) Apoptotic cell removal in development and tissue homeostasis. Trends Immunol 27: 244-50

Hershko A, Ciechanover A (1998) The ubiquitin system. Annu Rev Biochem 67: 425-79

Hershko A, Ciechanover A, Rose IA (1979) Resolution of the ATP-dependent proteolytic system from reticulocytes: a component that interacts with ATP. Proc Natl Acad Sci U S A 76: 3107-10

Hibi M, Lin A, Smeal T, Minden A, Karin M (1993) Identification of an oncoprotein- and UV-responsive protein kinase that binds and potentiates the c-Jun activation domain. Genes Dev 7: 2135-48

Hicke L, Schubert HL, Hill CP (2005) Ubiquitin-binding domains. Nat Rev Mol Cell Biol 6: 610-21

Hildebrand JM, Tanzer MC, Lucet IS, Young SN, Spall SK, Sharma P, Pierotti C, Garnier JM, Dobson RC, Webb AI, Tripaydonis A, Babon JJ, Mulcair MD, Scanlon MJ, Alexander WS, Wilks AF, Czabotar PE, Lessene G, Murphy JM, Silke J (2014) Activation of the pseudokinase MLKL unleashes the four-helix bundle domain to induce membrane localization and necroptotic cell death. Proc Natl Acad Sci U S A 111: 15072-7

Hirano S, Kawasaki M, Ura H, Kato R, Raiborg C, Stenmark H, Wakatsuki S (2006a) Double-sided ubiquitin binding of Hrs-UIM in endosomal protein sorting. Nat Struct Mol Biol 13: 272-7

Hirano S, Suzuki N, Slagsvold T, Kawasaki M, Trambaiolo D, Kato R, Stenmark H, Wakatsuki S (2006b) Structural basis of ubiquitin recognition by mammalian Eap45 GLUE domain. Nat Struct Mol Biol 13: 1031-2

Hitomi J, Christofferson DE, Ng A, Yao J, Degterev A, Xavier RJ, Yuan J (2008) Identification of a molecular signaling network that regulates a cellular necrotic cell death pathway. Cell 135: 1311-23

Hitotsumatsu O, Ahmad RC, Tavares R, Wang M, Philpott D, Turer EE, Lee BL, Shiffin N, Advincula R, Malynn BA, Werts C, Ma A (2008) The ubiquitin-editing enzyme A20 restricts nucleotide-binding oligomerization domain containing 2-triggered signals. Immunity 28: 381-90

Hjerpe R, Aillet F, Lopitz-Otsoa F, Lang V, England P, Rodriguez MS (2009) Efficient protection and isolation of ubiquitylated proteins using tandem ubiquitin-binding entities. EMBO reports 10: 1250-8

Hoesel B, Schmid JA (2013) The complexity of NF-κB signaling in inflammation and cancer. Mol Cancer 12: 86

Hoffmann A, Baltimore D (2006) Circuitry of nuclear factor kappaB signaling. Immunol Rev 210: 171-86

HogenEsch H, Gijbels MJ, Offerman E, van Hooft J, van Bekkum DW, Zurcher C (1993) A spontaneous mutation characterized by chronic proliferative dermatitis in C57BL mice. Am J Pathol 143: 972-82

HogenEsch H, Janke S, Boggess D, Sundberg JP (1999) Absence of Peyer's patches and abnormal lymphoid architecture in chronic proliferative dermatitis (cpdm/cpdm) mice. J Immunol 162: 3890-6

HogenEsch H, Torregrosa SE, Boggess D, Sundberg BA, Carroll J, Sundberg JP (2001) Increased expression of type 2 cytokines in chronic proliferative dermatitis (cpdm) mutant mice and resolution of inflammation following treatment with IL-12. Eur J Immunol 31: 734-42

Hogquist KA, Baldwin TA, Jameson SC (2005) Central tolerance: learning self-control in the thymus. Nat Rev Immunol 5: 772-82

Holler E, Rogler G, Herfarth H, Brenmoehl J, Wild PJ, Hahn J, Eissner G, Schölmerich J, Andreesen R (2004) Both donor and recipient NOD2/CARD15 mutations associate with transplant-related mortality and GvHD following allogeneic stem cell transplantation. Blood 104: 889-94

Holler N, Zaru R, Micheau O, Thome M, Attinger A, Valitutti S, Bodmer JL, Schneider P, Seed B, Tschopp J (2000) Fas triggers an alternative, caspase-8-independent cell death pathway using the kinase RIP as effector molecule. Nat Immunol 1: 489-95

Hrdinka M, Fiil BK, Zucca M, Leske D, Bagola K, Yabal M, Elliott PR, Damgaard RB, Komander D, Jost PJ, Gyrd-Hansen M (2016) CYLD Limits Lys63- and Met1-Linked Ubiquitin at Receptor Complexes to Regulate Innate Immune Signaling. Cell Rep 14: 2846-58

Hsu H, Xiong J, Goeddel DV (1995) The TNF receptor 1-associated protein TRADD signals cell death and NF-κB activation. Cell 81: 495-504

Hu M, Li P, Song L, Jeffrey PD, Chenova TA, Wilkinson KD, Cohen RE, Shi Y (2005) Structure and mechanisms of the proteasome-associated deubiquitinating enzyme USP14. EMBO J 24: 3747-56

Huang L, Kinnucan E, Wang G, Beaudenon S, Howley PM, Huibregtse JM, Pavletich NP (1999) Structure of an E6AP-UbcH7 complex: insights into ubiquitination by the E2-E3 enzyme cascade. Science 286: 1321-6

Huen MS, Grant R, Manke I, Minn K, Yu X, Yaffe MB, Chen J (2007) RNF8 transduces the DNA-damage signal via histone ubiquitylation and checkpoint protein assembly. Cell 131: 901-14

Hugot JP, Chamaillard M, Zouali H, Lesage S, Cézard JP, Belaiche J, Almer S, Tysk C, O'Morain CA, Gassull M, Binder V, Finkel Y, Cortot A, Modigliani R, Laurent-Puig P, Gower-Rousseau C, Macry J, Colombel JF, Sahbatou M, Thomas G (2001) Association of NOD2 leucine-rich repeat variants with susceptibility to Crohn's disease. Nature 411: 599-603

Huibregtse JM, Scheffner M, Beaudenon S, Howley PM (1995) A family of proteins structurally and functionally related to the E6-AP ubiquitin-protein ligase. Proc Natl Acad Sci U S A 92: 2563-7

Hurley JH, Lee S, Prag G (2006) Ubiquitin-binding domains. Biochem J 399: 361-72

Husnjak K, Dikic I (2012) Ubiquitin-binding proteins: decoders of ubiquitin-mediated cellular functions. Annual review of biochemistry 81: 291-322

Hutti JE, Shen RR, Abbott DW, Zhou AY, Sprott KM, Asara JM, Hahn WC, Cantley LC (2009) Phosphorylation of the tumor suppressor CYLD by the breast cancer oncogene IKKepsilon promotes cell transformation. Molecular cell 34: 461-72

Ikeda F, Deribe YL, Skanland SS, Stieglitz B, Grabbe C, Franz-Wachtel M, van Wijk SJ, Goswami P, Nagy V, Terzic J, Tokunaga F, Androulidaki A, Nakagawa T, Pasparakis M, Iwai K, Sundberg JP, Schaefer L, Rittinger K, Macek B, Dikic I (2011)

SHARPIN forms a linear ubiquitin ligase complex regulating NF-kappaB activity and apoptosis. Nature 471: 637-41

Inn KS, Gack MU, Tokunaga F, Shi M, Wong LY, Iwai K, Jung JU (2011) Linear ubiquitin assembly complex negatively regulates RIG-I- and TRIM25-mediated type I interferon induction. Mol Cell 41: 354-65

Israël A (2010) The IKK complex, a central regulator of NF-kappaB activation. Cold Spring Harb Perspect Biol 2: a000158

Jin W, Chang M, Paul EM, Babu G, Lee AJ, Reiley W, Wright A, Zhang M, You J, Sun SC (2008) Deubiquitinating enzyme CYLD negatively regulates RANK signaling and osteoclastogenesis in mice. J Clin Invest 118: 1858-66

Johnston JA, Ward CL, Kopito RR (1998) Aggresomes: a cellular response to misfolded proteins. J Cell Biol 143: 1883-98

Johnston SC, Riddle SM, Cohen RE, Hill CP (1999) Structural basis for the specificity of ubiquitin C-terminal hydrolases. EMBO J 18: 3877-87

Jones SJ, Ledgerwood EC, Prins JB, Galbraith J, Johnson DR, Pober JS, Bradley JR (1999) TNF recruits TRADD to the plasma membrane but not the trans-Golgi network, the principal subcellular location of TNF-R1. J Immunol 162: 1042-8

Jono H, Lim JH, Chen LF, Xu H, Trompouki E, Pan ZK, Mosialos G, Li JD (2004) NF-kappaB is essential for induction of CYLD, the negative regulator of NF-kappaB: evidence for a novel inducible autoregulatory feedback pathway. J Biol Chem 279: 36171-4

Jung D, Alt FW (2004) Unraveling V(D)J recombination; insights into gene regulation. Cell 116: 299-311

Kaiser WJ, Sridharan H, Huang C, Mandal P, Upton JW, Gough PJ, Sehon CA, Marquis RW, Bertin J, Mocarski ES (2013) Toll-like receptor 3-mediated necrosis via TRIF, RIP3, and MLKL. J Biol Chem 288: 31268-79

Kaiser WJ, Upton JW, Long AB, Livingston-Rosanoff D, Daley-Bauer LP, Hakem R, Caspary T, Mocarski ES (2011) RIP3 mediates the embryonic lethality of caspase-8-deficient mice. Nature 471: 368-72

Kaiser WJ, Upton JW, Mocarski ES (2013) Viral modulation of programmed necrosis. Curr Opin Virol 3: 296-306

Kanarek N, London N, Schueler-Furman O, Ben-Neriah Y (2010) Ubiquitination and degradation of the inhibitors of NF-kappaB. Cold Spring Harb Perspect Biol 2: a000166

Kanayama A, Seth RB, Sun L, Ea CK, Hong M, Shaito A, Chiu YH, Deng L, Chen ZJ (2004) TAB2 and TAB3 activate the NF-kappaB pathway through binding to polyubiquitin chains. Molecular cell 15: 535-48

Kang YJ, Chen J, Otsuka M, Mols J, Ren S, Wang Y, Han J (2008) Macrophage deletion of p38alpha partially impairs lipopolysaccharide-induced cellular activation. J Immunol 180: 5075-82

Katzmann DJ, Babst M, Emr SD (2001) Ubiquitin-dependent sorting into the multivesicular body pathway requires the function of a conserved endosomal protein sorting complex, ESCRT-I. Cell 106: 145-55

Kerr JF, Wyllie AH, Currie AR (1972) Apoptosis: a basic biological phenomenon with wide-ranging implications in tissue kinetics. Br J Cancer 26: 239-57

Keusekotten K, Elliott Paul R, Glockner L, Fiil Berthe K, Damgaard Rune B, Kulathu Y, Wauer T, Hospenthal Manuela K, Gyrd-Hansen M, Krappmann D, Hofmann K, Komander D (2013) OTULIN Antagonizes LUBAC Signaling by Specifically Hydrolyzing Met1-Linked Polyubiquitin. Cell 153: 1312-1326

Kiernan R, Brès V, Ng RW, Coudart MP, El Messaoudi S, Sardet C, Jin DY, Emiliani S, Benkirane M (2003) Post-activation turn-off of NF-kappa B-dependent transcription is regulated by acetylation of p65. J Biol Chem 278: 2758-66

Kim C, Sano Y, Todorova K, Carlson BA, Arpa L, Celada A, Lawrence T, Otsu K, Brissette JL, Arthur JS, Park JM (2008) The kinase p38 alpha serves cell type-specific inflammatory functions in skin injury and coordinates pro- and anti-inflammatory gene expression. Nat Immunol 9: 1019-27

Kim H, Chen J, Yu X (2007a) Ubiquitin-binding protein RAP80 mediates BRCA1-dependent DNA damage response. Science 316: 1202-5

Kim HC, Huibregtse JM (2009) Polyubiquitination by HECT E3s and the determinants of chain type specificity. Mol Cell Biol 29: 3307-18

Kim HT, Kim KP, Lledias F, Kisselev AF, Scaglione KM, Skowyra D, Gygi SP, Goldberg AL (2007b) Certain pairs of ubiquitin-conjugating enzymes (E2s) and ubiquitin-protein ligases (E3s) synthesize nondegradable forked ubiquitin chains containing all possible isopeptide linkages. J Biol Chem 282: 17375-86

Kirisako T, Kamei K, Murata S, Kato M, Fukumoto H, Kanie M, Sano S, Tokunaga F, Tanaka K, Iwai K (2006) A ubiquitin ligase complex assembles linear polyubiquitin chains. EMBO J 25: 4877-4887

Kishimoto H, Surh CD, Sprent J (1998) A role for Fas in negative selection of thymocytes in vivo. J Exp Med 187: 1427-38

Kisselev AF, Akopian TN, Woo KM, Goldberg AL (1999) The sizes of peptides generated from protein by mammalian 26 and 20 S proteasomes. Implications for understanding the degradative mechanism and antigen presentation. J Biol Chem 274: 3363-71

Kisselev AF, Goldberg AL (2001) Proteasome inhibitors: from research tools to drug candidates. Chem Biol 8: 739-58

Klein T, Fung SY, Renner F, Blank MA, Dufour A, Kang S, Bolger-Munro M, Scurll JM, Priatel JJ, Schweigler P, Melkko S, Gold MR, Viner RI, Regnier CH, Turvey SE, Overall CM (2015) The paracaspase MALT1 cleaves HOIL1 reducing linear ubiquitination by LUBAC to dampen lymphocyte NF-kappaB signalling. Nature communications 6: 8777

Kolas NK, Chapman JR, Nakada S, Ylanko J, Chahwan R, Sweeney FD, Panier S, Mendez M, Wildenhain J, Thomson TM, Pelletier L, Jackson SP, Durocher D (2007)

Orchestration of the DNA-damage response by the RNF8 ubiquitin ligase. Science 318: 1637-40

Komander D, Barford D (2008) Structure of the A20 OTU domain and mechanistic insights into deubiquitination. Biochem J 409: 77-85

Komander D, Clague MJ, Urbe S (2009a) Breaking the chains: structure and function of the deubiquitinases. Nature reviews Molecular cell biology 10: 550-63

Komander D, Lord CJ, Scheel H, Swift S, Hofmann K, Ashworth A, Barford D (2008) The structure of the CYLD USP domain explains its specificity for Lys63-linked polyubiquitin and reveals a B box module. Mol Cell 29: 451-64

Komander D, Rape M (2012) The ubiquitin code. Annual review of biochemistry 81: 203-29

Komander D, Reyes-Turcu F, Licchesi JD, Odenwaelder P, Wilkinson KD, Barford D (2009b) Molecular discrimination of structurally equivalent Lys 63-linked and linear polyubiquitin chains. EMBO Rep 10: 466-73

Korb A, Tohidast-Akrad M, Cetin E, Axmann R, Smolen J, Schett G (2006) Differential tissue expression and activation of p38 MAPK alpha, beta, gamma, and delta isoforms in rheumatoid arthritis. Arthritis Rheum 54: 2745-56

Kovalenko A, Chable-Bessia C, Cantarella G, Israel A, Wallach D, Courtois G (2003) The tumour suppressor CYLD negatively regulates NF-kappaB signalling by deubiquitination. Nature 424: 801-5

Krammer PH (2000) CD95's deadly mission in the immune system. Nature 407: 789-95

Kravtsova-Ivantsiv Y, Cohen S, Ciechanover A (2009) Modification by single ubiquitin moieties rather than polyubiquitination is sufficient for proteasomal processing of the p105 NF-kappaB precursor. Mol Cell 33: 496-504

Kulathu Y, Akutsu M, Bremm A, Hofmann K, Komander D (2009) Two-sided ubiquitin binding explains specificity of the TAB2 NZF domain. Nat Struct Mol Biol 16: 1328-30

Kumar S (2007) Caspase function in programmed cell death. Cell Death Differ 14: 32-43

Kumari S, Redouane Y, Lopez-Mosqueda J, Shiraishi R, Romanowska M, Lutzmayer S, Kuiper J, Martinez C, Dikic I, Pasparakis M, Ikeda F (2014) Sharpin prevents skin inflammation by inhibiting TNFR1-induced keratinocyte apoptosis. eLife 3: e03422

Kupka S, De Miguel D, Draber P, Martino L, Surinova S, Rittinger K, Walczak H (2016a) SPATA2-Mediated Binding of CYLD to HOIP Enables CYLD Recruitment to Signaling Complexes. Cell Rep 16: 2271-80

Kupka S, Reichert M, Draber P, Walczak H (2016b) Formation and removal of poly-ubiquitin chains in the regulation of tumor necrosis factor-induced gene activation and cell death. FEBS J 283: 2626-39

Kyriakis JM, Avruch J (1996) Sounding the alarm: protein kinase cascades activated by stress and inflammation. J Biol Chem 271: 24313-6

Kyriakis JM, Avruch J (2001) Mammalian mitogen-activated protein kinase signal transduction pathways activated by stress and inflammation. Physiol Rev 81: 807-69

Kyriakis JM, Woodgett JR, Avruch J (1995) The stress-activated protein kinases. A novel ERK subfamily responsive to cellular stress and inflammatory cytokines. Ann N Y Acad Sci 766: 303-19

Lamkanfi M, Dixit VM (2014) Mechanisms and functions of inflammasomes. Cell 157: 1013-22

Lange OF, Lakomek NA, Farès C, Schröder GF, Walter KF, Becker S, Meiler J, Grubmüller H, Griesinger C, de Groot BL (2008) Recognition dynamics up to microseconds revealed from an RDC-derived ubiquitin ensemble in solution. Science 320: 1471-5

LaRock DL, Chaudhary A, Miller SI (2015) Salmonellae interactions with host processes. Nat Rev Microbiol 13: 191-205

Laster SM, Wood JG, Gooding LR (1988) Tumor necrosis factor can induce both apoptic and necrotic forms of cell lysis. J Immunol 141: 2629-34

Lau CM, Broughton C, Tabor AS, Akira S, Flavell RA, Mamula MJ, Christensen SR, Shlomchik MJ, Viglianti GA, Rifkin IR, Marshak-Rothstein A (2005) RNA-associated autoantigens activate B cells by combined B cell antigen receptor/Toll-like receptor 7 engagement. J Exp Med 202: 1171-7

Lecis D, De Cesare M, Perego P, Conti A, Corna E, Drago C, Seneci P, Walczak H, Colombo MP, Delia D, Sangaletti S (2013) Smac mimetics induce inflammation and necrotic tumour cell death by modulating macrophage activity. Cell Death Dis 4: e920

Lee EG, Boone DL, Chai S, Libby SL, Chien M, Lodolce JP, Ma A (2000) Failure to regulate TNF-induced NF-kappaB and cell death responses in A20-deficient mice. Science 289: 2350-4

Lee S, Tsai YC, Mattera R, Smith WJ, Kostelansky MS, Weissman AM, Bonifacino JS, Hurley JH (2006) Structural basis for ubiquitin recognition and autoubiquitination by Rabex-5. Nat Struct Mol Biol 13: 264-71

Legler DF, Micheau O, Doucey MA, Tschopp J, Bron C (2003) Recruitment of TNF receptor 1 to lipid rafts is essential for TNFalpha-mediated NF-kappaB activation. Immunity 18: 655-64

Li B, Dou QP (2000) Bax degradation by the ubiquitin/proteasome-dependent pathway: involvement in tumor survival and progression. Proc Natl Acad Sci U S A 97: 3850-5

Li H, Kobayashi M, Blonska M, You Y, Lin X (2006) Ubiquitination of RIP is required for tumor necrosis factor alpha-induced NF-kappaB activation. J Biol Chem 281: 13636-43

Li H, Zhu H, Xu CJ, Yuan J (1998) Cleavage of BID by caspase 8 mediates the mitochondrial damage in the Fas pathway of apoptosis. Cell 94: 491-501

Li J, McQuade T, Siemer AB, Napetschnig J, Moriwaki K, Hsiao YS, Damko E, Moquin D, Walz T, McDermott A, Chan FK, Wu H (2012) The RIP1/RIP3 necrosome

forms a functional amyloid signaling complex required for programmed necrosis. Cell 150: 339-50

Li L, Hailey DW, Soetandyo N, Li W, Lippincott-Schwartz J, Shu HB, Ye Y (2008) Localization of A20 to a lysosome-associated compartment and its role in NFkappaB signaling. Biochim Biophys Acta 1783: 1140-9

Li P, Nijhawan D, Budihardjo I, Srinivasula SM, Ahmad M, Alnemri ES, Wang X (1997) Cytochrome c and dATP-dependent formation of Apaf-1/caspase-9 complex initiates an apoptotic protease cascade. Cell 91: 479-89

Li Q, Van Antwerp D, Mercurio F, Lee KF, Verma IM (1999) Severe liver degeneration in mice lacking the IkappaB kinase 2 gene. Science 284: 321-5

Li S, Finley J, Liu ZJ, Qiu SH, Chen H, Luan CH, Carson M, Tsao J, Johnson D, Lin G, Zhao J, Thomas W, Nagy LA, Sha B, DeLucas LJ, Wang BC, Luo M (2002) Crystal structure of the cytoskeleton-associated protein glycine-rich (CAP-Gly) domain. J Biol Chem 277: 48596-601

Li W, Bengtson MH, Ulbrich A, Matsuda A, Reddy VA, Orth A, Chanda SK, Batalov S, Joazeiro CA (2008) Genome-wide and functional annotation of human E3 ubiquitin ligases identifies MULAN, a mitochondrial E3 that regulates the organelle's dynamics and signaling. PLoS One 3: e1487

Liang C, Zhang M, Sun SC (2006) beta-TrCP binding and processing of NF-kappaB2/p100 involve its phosphorylation at serines 866 and 870. Cell Signal 18: 1309-17

Lim S, Sala C, Yoon J, Park S, Kuroda S, Sheng M, Kim E (2001) Sharpin, a novel postsynaptic density protein that directly interacts with the shank family of proteins. Mol Cell Neurosci 17: 385-97

Lin J, Kumari S, Kim C, Van TM, Wachsmuth L, Polykratis A, Pasparakis M (2016) RIPK1 counteracts ZBP1-mediated necroptosis to inhibit inflammation. Nature 540: 124-128

Lin Y, Devin A, Rodriguez Y, Liu ZG (1999) Cleavage of the death domain kinase RIP by caspase-8 prompts TNF-induced apoptosis. Genes Dev 13: 2514-26

Ling YH, Liebes L, Ng B, Buckley M, Elliott PJ, Adams J, Jiang JD, Muggia FM, Perez-Soler R (2002) PS-341, a novel proteasome inhibitor, induces Bcl-2 phosphorylation and cleavage in association with G2-M phase arrest and apoptosis. Mol Cancer Ther 1: 841-9

Linkermann A, Hackl MJ, Kunzendorf U, Walczak H, Krautwald S, Jevnikar AM (2013) Necroptosis in immunity and ischemia-reperfusion injury. Am J Transplant 13: 2797-804

Liu J, Lin A (2005) Role of JNK activation in apoptosis: a double-edged sword. Cell Res 15: 36-42

Lo YC, Lin SC, Rospigliosi CC, Conze DB, Wu CJ, Ashwell JD, Eliezer D, Wu H (2009) Structural basis for recognition of diubiquitins by NEMO. Molecular cell 33: 602-15

Lopes UG, Erhardt P, Yao R, Cooper GM (1997) p53-dependent induction of apoptosis by proteasome inhibitors. J Biol Chem 272: 12893-6

Lozzio CB, Lozzio BB (1975) Human chronic myelogenous leukemia cell-line with positive Philadelphia chromosome. Blood 45: 321-34

Lu KP (2004) Pinning down cell signaling, cancer and Alzheimer's disease. Trends Biochem Sci 29: 200-9

Lu TT, Onizawa M, Hammer GE, Turer EE, Yin Q, Damko E, Agelidis A, Shifrin N, Advincula R, Barrera J, Malynn BA, Wu H, Ma A (2013) Dimerization and Ubiquitin Mediated Recruitment of A20, a Complex Deubiquitinating Enzyme. Immunity

Luo X, Budihardjo I, Zou H, Slaughter C, Wang X (1998) Bid, a Bcl2 interacting protein, mediates cytochrome c release from mitochondria in response to activation of cell surface death receptors. Cell 94: 481-90

Macville M, Schröck E, Padilla-Nash H, Keck C, Ghadimi BM, Zimonjic D, Popescu N, Ried T (1999) Comprehensive and definitive molecular cytogenetic characterization of HeLa cells by spectral karyotyping. Cancer Res 59: 141-50

Mahoney DJ, Cheung HH, Mrad RL, Plenchette S, Simard C, Enwere E, Arora V, Mak TW, Lacasse EC, Waring J, Korneluk RG (2008) Both cIAP1 and cIAP2 regulate TNFalpha-mediated NF-kappaB activation. Proc Natl Acad Sci U S A 105: 11778-83

Marienfeld RB, Palkowitsch L, Ghosh S (2006) Dimerization of the I kappa B kinase-binding domain of NEMO is required for tumor necrosis factor alpha-induced NF-kappa B activity. Mol Cell Biol 26: 9209-19

Massoumi R, Chmielarska K, Hennecke K, Pfeifer A, Fassler R (2006) Cyld inhibits tumor cell proliferation by blocking Bcl-3-dependent NF-kappaB signaling. Cell 125: 665-77

Masuko-Hongo K, Berenbaum F, Humbert L, Salvat C, Goldring MB, Thirion S (2004) Up-regulation of microsomal prostaglandin E synthase 1 in osteoarthritic human cartilage: critical roles of the ERK-1/2 and p38 signaling pathways. Arthritis Rheum 50: 2829-38

Maxfield FR, McGraw TE (2004) Endocytic recycling. Nat Rev Mol Cell Biol 5: 121-32

Mazzone A, Tietz P, Jefferson J, Pagano R, LaRusso NF (2006) Isolation and characterization of lipid microdomains from apical and basolateral plasma membranes of rat hepatocytes. Hepatology 43: 287-96

McStay GP, Salvesen GS, Green DR (2008) Overlapping cleavage motif selectivity of caspases: implications for analysis of apoptotic pathways. Cell Death Differ 15: 322-31

Mevissen TE, Hospenthal MK, Geurink PP, Elliott PR, Akutsu M, Arnaudo N, Ekkebus R, Kulathu Y, Wauer T, El Oualid F, Freund SM, Ovaa H, Komander D (2013) OTU deubiquitinases reveal mechanisms of linkage specificity and enable ubiquitin chain restriction analysis. Cell 154: 169-84

Meyer HJ, Rape M (2014) Enhanced protein degradation by branched ubiquitin chains. Cell 157: 910-21

Miceli-Richard C, Lesage S, Rybojad M, Prieur AM, Manouvrier-Hanu S, Häfner R, Chamaillard M, Zouali H, Thomas G, Hugot JP (2001) CARD15 mutations in Blau syndrome. Nat Genet 29: 19-20

Micheau O, Lens S, Gaide O, Alevizopoulos K, Tschopp J (2001) NF-kappaB signals induce the expression of c-FLIP. Mol Cell Biol 21: 5299-305

Micheau O, Thome M, Schneider P, Holler N, Tschopp J, Nicholson DW, Briand C, Grütter MG (2002) The long form of FLIP is an activator of caspase-8 at the Fas death-inducing signaling complex. J Biol Chem 277: 45162-71

Micheau O, Tschopp J (2003) Induction of TNF Receptor I-Mediated Apoptosis via Two Sequential Signaling Complexes. Cell 114: 181-190

Min M, Mevissen TE, De Luca M, Komander D, Lindon C (2015) Efficient APC/C substrate degradation in cells undergoing mitotic exit depends on K11 ubiquitin linkages. Mol Biol Cell 26: 4325-32

Misaki T, Yamamoto T, Suzuki S, Fukasawa H, Togawa A, Ohashi N, Suzuki H, Fujigaki Y, Oda T, Uchida C, Kitagawa K, Hattori T, Kitagawa M, Hishida A (2009) Decrease in tumor necrosis factor-alpha receptor-associated death domain results from ubiquitin-dependent degradation in obstructive renal injury in rats. Am J Pathol 175: 74-83

Moffatt OD, Devitt A, Bell ED, Simmons DL, Gregory CD (1999) Macrophage recognition of ICAM-3 on apoptotic leukocytes. J Immunol 162: 6800-10

Moquin DM, McQuade T, Chan FK (2013) CYLD deubiquitinates RIP1 in the TNFalpha-induced necrosome to facilitate kinase activation and programmed necrosis. PLoS One 8: e76841

Moreau P, Richardson PG, Cavo M, Orlowski RZ, San Miguel JF, Palumbo A, Harousseau JL (2012) Proteasome inhibitors in multiple myeloma: 10 years later. Blood 120: 947-59

Moriwaki K, Chan FK (2013) RIP3: a molecular switch for necrosis and inflammation. Genes Dev 27: 1640-9

Murphy JM, Czabotar PE, Hildebrand JM, Lucet IS, Zhang JG, Alvarez-Diaz S, Lewis R, Lalaoui N, Metcalf D, Webb AI, Young SN, Varghese LN, Tannahill GM, Hatchell EC, Majewski IJ, Okamoto T, Dobson RC, Hilton DJ, Babon JJ, Nicola NA et al. (2013) The pseudokinase MLKL mediates necroptosis via a molecular switch mechanism. Immunity 39: 443-53

Müller-Sienerth N, Dietz L, Holtz P, Kapp M, Grigoleit GU, Schmuck C, Wajant H, Siegmund D (2011) SMAC mimetic BV6 induces cell death in monocytes and maturation of monocyte-derived dendritic cells. PLoS One 6: e21556

Nagabhushana A, Bansal M, Swarup G (2011) Optineurin is required for CYLD-dependent inhibition of TNFα-induced NF-κB activation. PLoS One 6: e17477

Nakamura N, Hirose S (2008) Regulation of mitochondrial morphology by USP30, a deubiquitinating enzyme present in the mitochondrial outer membrane. Mol Biol Cell 19: 1903-11

Nelson DE, Ihekwaba AE, Elliott M, Johnson JR, Gibney CA, Foreman BE, Nelson G, See V, Horton CA, Spiller DG, Edwards SW, McDowell HP, Unitt JF, Sullivan E, Grimley R, Benson N, Broomhead D, Kell DB, White MR (2004) Oscillations in NF-kappaB signaling control the dynamics of gene expression. Science 306: 704-8

Newton K, Wickliffe KE, Maltzman A, Dugger DL, Strasser A, Pham VC, Lill JR, Roose-Girma M, Warming S, Solon M, Ngu H, Webster JD, Dixit VM (2016) RIPK1 inhibits ZBP1-driven necroptosis during development. Nature 540: 129-133

Nicholson DW (1999) Caspase structure, proteolytic substrates, and function during apoptotic cell death. Cell Death Differ 6: 1028-42

Nijman SM, Luna-Vargas MP, Velds A, Brummelkamp TR, Dirac AM, Sixma TK, Bernards R (2005) A genomic and functional inventory of deubiquitinating enzymes. Cell 123: 773-86

Nikolaou K, Tsagaratou A, Eftychi C, Kollias G, Mosialos G, Talianidis I (2012) Inactivation of the deubiquitinase CYLD in hepatocytes causes apoptosis, inflammation, fibrosis, and cancer. Cancer Cell 21: 738-50

Novack DV, Yin L, Hagen-Stapleton A, Schreiber RD, Goeddel DV, Ross FP, Teitelbaum SL (2003) The IkappaB function of NF-kappaB2 p100 controls stimulated osteoclastogenesis. J Exp Med 198: 771-81

O'Donnell MA, Perez-Jimenez E, Oberst A, Ng A, Massoumi R, Xavier R, Green DR, Ting AT (2011) Caspase 8 inhibits programmed necrosis by processing CYLD. Nat Cell Biol 13: 1437-42

Oeckinghaus A, Hayden MS, Ghosh S (2011) Crosstalk in NF-kappaB signaling pathways. Nature immunology 12: 695-708

Onisto M, Slongo LM, Graziotto R, Zotti L, Negro A, Merico M, Moro E, Foresta C (2001) Evidence for FSH-dependent upregulation of SPATA2 (spermatogenesis-associated protein 2). Biochem Biophys Res Commun 283: 86-92

Ori D, Kato H, Sanjo H, Tartey S, Mino T, Akira S, Takeuchi O (2013) Essential roles of K63-linked polyubiquitin-binding proteins TAB2 and TAB3 in B cell activation via MAPKs. J Immunol 190: 4037-45

Orth K, Xu Z, Mudgett MB, Bao ZQ, Palmer LE, Bliska JB, Mangel WF, Staskawicz B, Dixon JE (2000) Disruption of signaling by Yersinia effector YopJ, a ubiquitin-like protein protease. Science 290: 1594-7

O'Donnell MA, Perez-Jimenez E, Oberst A, Ng A, Massoumi R, Xavier R, Green DR, Ting AT (2011) Caspase 8 inhibits programmed necrosis by processing CYLD. Nature cell biology 13: 1437-1442

Park YH, Jeong MS, Park HH, Jang SB (2013) Formation of the death domain complex between FADD and RIP1 proteins in vitro. Biochim Biophys Acta 1834: 292-300

Pasparakis M, Vandenabeele P (2015) Necroptosis and its role in inflammation. Nature 517: 311-20

Peltzer N, Rieser E, Taraborrelli L, Draber P, Darding M, Pernaute B, Shimizu Y, Sarr A, Draberova H, Montinaro A, Martinez-Barbera JP, Silke J, Rodriguez TA, Walczak H (2014) HOIP deficiency causes embryonic lethality by aberrant TNFR1-mediated endothelial cell death. Cell Rep 9: 153-65

Penack O, Smith OM, Cunningham-Bussel A, Liu X, Rao U, Yim N, Na IK, Holland AM, Ghosh A, Lu SX, Jenq RR, Liu C, Murphy GF, Brandl K, van den Brink MR (2009) NOD2 regulates hematopoietic cell function during graft-versus-host disease. J Exp Med 206: 2101-10

Peng J, Schwartz D, Elias JE, Thoreen CC, Cheng D, Marsischky G, Roelofs J, Finley D, Gygi SP (2003) A proteomics approach to understanding protein ubiquitination. Nat Biotechnol 21: 921-6

Peyrin-Biroulet L (2010) Anti-TNF therapy in inflammatory bowel diseases: a huge review. Minerva Gastroenterol Dietol 56: 233-43

Pfeffer K, Matsuyama T, Kündig TM, Wakeham A, Kishihara K, Shahinian A, Wiegmann K, Ohashi PS, Krönke M, Mak TW (1993) Mice deficient for the 55 kd tumor necrosis factor receptor are resistant to endotoxic shock, yet succumb to L. monocytogenes infection. Cell 73: 457-67

Pobezinskaya YL, Kim YS, Choksi S, Morgan MJ, Li T, Liu C, Liu Z (2008) The function of TRADD in signaling through tumor necrosis factor receptor 1 and TRIF-dependent Toll-like receptors. Nat Immunol 9: 1047-54

Poon IK, Lucas CD, Rossi AG, Ravichandran KS (2014) Apoptotic cell clearance: basic biology and therapeutic potential. Nat Rev Immunol 14: 166-80

Rahighi S, Dikic I (2012) Selectivity of the ubiquitin-binding modules. FEBS Lett 586: 2705-10

Rahighi S, Ikeda F, Kawasaki M, Akutsu M, Suzuki N, Kato R, Kensche T, Uejima T, Bloor S, Komander D, Randow F, Wakatsuki S, Dikic I (2009) Specific recognition of linear ubiquitin chains by NEMO is important for NF-kappaB activation. Cell 136: 1098-109

Raingeaud J, Gupta S, Rogers JS, Dickens M, Han J, Ulevitch RJ, Davis RJ (1995) Pro-inflammatory cytokines and environmental stress cause p38 mitogen-activated protein kinase activation by dual phosphorylation on tyrosine and threonine. J Biol Chem 270: 7420-6

Rao VK, Straus SE (2006) Causes and consequences of the autoimmune lymphoproliferative syndrome. Hematology 11: 15-23

Ravichandran KS (2011) Beginnings of a good apoptotic meal: the find-me and eat-me signaling pathways. Immunity 35: 445-55

Razani B, Zarnegar B, Ytterberg AJ, Shiba T, Dempsey PW, Ware CF, Loo JA, Cheng G (2010) Negative feedback in noncanonical NF-kappaB signaling modulates NIK stability through IKKalpha-mediated phosphorylation. Sci Signal 3: ra41

Redman KL, Rechsteiner M (1989) Identification of the long ubiquitin extension as ribosomal protein S27a. Nature 338: 438-40

Reiley W, Zhang M, Wu X, Granger E, Sun SC (2005) Regulation of the deubiquitinating enzyme CYLD by IkappaB kinase gamma-dependent phosphorylation. Mol Cell Biol 25: 3886-95

Reiley WW, Zhang M, Jin W, Losiewicz M, Donohue KB, Norbury CC, Sun SC (2006) Regulation of T cell development by the deubiquitinating enzyme CYLD. Nature immunology 7: 411-7

Reyes-Turcu FE, Shanks JR, Komander D, Wilkinson KD (2008) Recognition of polyubiquitin isoforms by the multiple ubiquitin binding modules of isopeptidase T. The Journal of biological chemistry 283: 19581-92

Rickard JA, Anderton H, Etemadi N, Nachbur U, Darding M, Peltzer N, Lalaoui N, Lawlor KE, Vanyai H, Hall C, Bankovacki A, Gangoda L, Wong WW-L, Corbin J, Huang C, Mocarski ES, Murphy JM, Alexander WS, Voss AK, Vaux DL et al. (2014a) TNFR1-dependent cell death drives inflammation in Sharpin-deficient mice. eLife 3: e03464

Rickard JA, O'Donnell JA, Evans JM, Lalaoui N, Poh AR, Rogers T, Vince JE, Lawlor KE, Ninnis RL, Anderton H, Hall C, Spall SK, Phesse TJ, Abud HE, Cengia LH, Corbin J, Mifsud S, Di Rago L, Metcalf D, Ernst M et al. (2014b) RIPK1 regulates RIPK3-MLKL-driven systemic inflammation and emergency hematopoiesis. Cell 157: 1175-88

Rieux-Laucat F, Le Deist F, Fischer A (2003) Autoimmune lymphoproliferative syndromes: genetic defects of apoptosis pathways. Cell Death Differ 10: 124-33

Ritorto MS, Ewan R, Perez-Oliva AB, Knebel A, Buhrlage SJ, Wightman M, Kelly SM, Wood NT, Virdee S, Gray NS, Morrice NA, Alessi DR, Trost M (2014) Screening of DUB activity and specificity by MALDI-TOF mass spectrometry. Nature communications 5: 4763

Rivkin E, Almeida SM, Ceccarelli DF, Juang YC, Maclean TA, Srikumar T, Huang H, Dunham WH, Fukumura R, Xie G, Gondo Y, Raught B, Gingras AC, Sicheri F, Cordes SP (2013) The linear ubiquitin-specific deubiquitinase gumby regulates angiogenesis. Nature

Rothe J, Mackay F, Bluethmann H, Zinkernagel R, Lesslauer W (1994) Phenotypic analysis of TNFR1-deficient mice and characterization of TNFR1-deficient fibroblasts in vitro. Circ Shock 44: 51-6

Rotin D, Kumar S (2009) Physiological functions of the HECT family of ubiquitin ligases. Nat Rev Mol Cell Biol 10: 398-409

Roux PP, Blenis J (2004) ERK and p38 MAPK-activated protein kinases: a family of protein kinases with diverse biological functions. Microbiol Mol Biol Rev 68: 320-44

Rubinfeld H, Hanoch T, Seger R (1999) Identification of a cytoplasmic-retention sequence in ERK2. J Biol Chem 274: 30349-52

Rudolph D, Yeh WC, Wakeham A, Rudolph B, Nallainathan D, Potter J, Elia AJ, Mak TW (2000) Severe liver degeneration and lack of NF-kappaB activation in NEMO/IKKgamma-deficient mice. Genes Dev 14: 854-62

Rutz S, Kayagaki N, Phung QT, Eidenschenk C, Noubade R, Wang X, Lesch J, Lu R, Newton K, Huang OW, Cochran AG, Vasser M, Fauber BP, DeVoss J, Webster J, Diehl L, Modrusan Z, Kirkpatrick DS, Lill JR, Ouyang W et al. (2015) Deubiquitinase DUBA is a post-translational brake on interleukin-17 production in T cells. Nature 518: 417-21

Ryo A, Suizu F, Yoshida Y, Perrem K, Liou YC, Wulf G, Rottapel R, Yamaoka S, Lu KP (2003) Regulation of NF-kappaB signaling by Pin1-dependent prolyl isomerization and ubiquitin-mediated proteolysis of p65/RelA. Mol Cell 12: 1413-26

Saccani S, Pantano S, Natoli G (2002) p38-Dependent marking of inflammatory genes for increased NF-kappa B recruitment. Nat Immunol 3: 69-75

Sahai E, Olson MF, Marshall CJ (2001) Cross-talk between Ras and Rho signalling pathways in transformation favours proliferation and increased motility. EMBO J 20: 755-66

Saito K, Kigawa T, Koshiba S, Sato K, Matsuo Y, Sakamoto A, Takagi T, Shirouzu M, Yabuki T, Nunokawa E, Seki E, Matsuda T, Aoki M, Miyata Y, Hirakawa N, Inoue M, Terada T, Nagase T, Kikuno R, Nakayama M et al. (2004) The CAP-Gly domain of CYLD associates with the proline-rich sequence in NEMO/IKKgamma. Structure 12: 1719-28

Saitoh T, Nakayama M, Nakano H, Yagita H, Yamamoto N, Yamaoka S (2003) TWEAK induces NF-kappaB2 p100 processing and long lasting NF-kappaB activation. J Biol Chem 278: 36005-12

Sasaki Y, Sano S, Nakahara M, Murata S, Kometani K, Aiba Y, Sakamoto S, Watanabe Y, Tanaka K, Kurosaki T, Iwai K (2013) Defective immune responses in mice lacking LUBAC-mediated linear ubiquitination in B cells. The EMBO journal

Sato Y, Fujita H, Yoshikawa A, Yamashita M, Yamagata A, Kaiser SE, Iwai K, Fukai S (2011) Specific recognition of linear ubiquitin chains by the Npl4 zinc finger (NZF) domain of the HOIL-1L subunit of the linear ubiquitin chain assembly complex. Proc Natl Acad Sci U S A 108: 20520-5

Sato Y, Yoshikawa A, Mimura H, Yamashita M, Yamagata A, Fukai S (2009) Structural basis for specific recognition of Lys 63-linked polyubiquitin chains by tandem UIMs of RAP80. EMBO J 28: 2461-8

Sato Y, Yoshikawa A, Yamagata A, Mimura H, Yamashita M, Ookata K, Nureki O, Iwai K, Komada M, Fukai S (2008) Structural basis for specific cleavage of Lys 63-linked polyubiquitin chains. Nature 455: 358-62

Scaffidi P, Misteli T, Bianchi ME (2002) Release of chromatin protein HMGB1 by necrotic cells triggers inflammation. Nature 418: 191-5

Schaeffer V, Akutsu M, Olma MH, Gomes LC, Kawasaki M, Dikic I (2014) Binding of OTULIN to the PUB domain of HOIP controls NF-kappaB signaling. Mol Cell 54: 349-61

Schauber C, Chen L, Tongaonkar P, Vega I, Lambertson D, Potts W, Madura K (1998) Rad23 links DNA repair to the ubiquitin/proteasome pathway. Nature 391: 715-8

Scheffner M, Nuber U, Huibregtse JM (1995) Protein ubiquitination involving an E1-E2-E3 enzyme ubiquitin thioester cascade. Nature 373: 81-3

Scherer DC, Brockman JA, Chen Z, Maniatis T, Ballard DW (1995) Signal-induced degradation of I kappa B alpha requires site-specific ubiquitination. Proc Natl Acad Sci U S A 92: 11259-63

SCHERER WF, SYVERTON JT, GEY GO (1953) Studies on the propagation in vitro of poliomyelitis viruses. IV. Viral multiplication in a stable strain of human malignant epithelial cells (strain HeLa) derived from an epidermoid carcinoma of the cervix. J Exp Med 97: 695-710

Schilling R, Geserick P, Leverkus M (2014) Characterization of the ripoptosome and its components: implications for anti-inflammatory and cancer therapy. Methods Enzymol 545: 83-102

Schlicher L, Wissler M, Preiss F, Brauns-Schubert P, Jakob C, Dumit V, Borner C, Dengjel J, Maurer U (2016) SPATA2 promotes CYLD activity and regulates TNF-induced NF-κB signaling and cell death. EMBO Rep 17: 1485-1497

Schmidt-Supprian M, Bloch W, Courtois G, Addicks K, Israël A, Rajewsky K, Pasparakis M (2000) NEMO/IKKγ-Deficient Mice Model Incontinentia Pigmenti. Mol Cell 5: 981-992

Schneider-Brachert W, Tchikov V, Neumeyer J, Jakob M, Winoto-Morbach S, Held-Feindt J, Heinrich M, Merkel O, Ehrenschwender M, Adam D, Mentlein R, Kabelitz D, Schutze S (2004) Compartmentalization of TNF receptor 1 signaling: internalized TNF receptosomes as death signaling vesicles. Immunity 21: 415-28

Scott FL, Stec B, Pop C, Dobaczewska MK, Lee JJ, Monosov E, Robinson H, Salvesen GS, Schwarzenbacher R, Riedl SJ (2009) The Fas-FADD death domain complex structure unravels signalling by receptor clustering. Nature 457: 1019-22

Sebbagh M, Renvoizé C, Hamelin J, Riché N, Bertoglio J, Bréard J (2001) Caspase-3-mediated cleavage of ROCK I induces MLC phosphorylation and apoptotic membrane blebbing. Nat Cell Biol 3: 346-52

Seeman P, Cheng D, Iles GH (1973) Structure of membrane holes in osmotic and saponin hemolysis. J Cell Biol 56: 519-27

Segawa K, Kurata S, Nagata S (2016) Human Type IV P-type ATPases That Work as Plasma Membrane Phospholipid Flippases and Their Regulation by Caspase and Calcium. J Biol Chem 291: 762-72

Segawa K, Kurata S, Yanagihashi Y, Brummelkamp TR, Matsuda F, Nagata S (2014) Caspase-mediated cleavage of phospholipid flippase for apoptotic phosphatidylserine exposure. Science 344: 1164-8

Sen R, Baltimore D (1986a) Inducibility of kappa immunoglobulin enhancer-binding protein Nf-kappa B by a posttranslational mechanism. Cell 47: 921-8

Sen R, Baltimore D (1986b) Multiple nuclear factors interact with the immunoglobulin enhancer sequences. Cell 46: 705-16

Shaul YD, Seger R (2007) The MEK/ERK cascade: from signaling specificity to diverse functions. Biochim Biophys Acta 1773: 1213-26

Shin D, Lee SY, Han S, Ren S, Kim S, Aikawa Y, Lee S (2012) Differential polyubiquitin recognition by tandem ubiquitin binding domains of Rabex-5. Biochem Biophys Res Commun 423: 757-62

Silke J, Vucic D (2014) IAP family of cell death and signaling regulators. Methods Enzymol 545: 35-65

Silva MT (2010) Secondary necrosis: the natural outcome of the complete apoptotic program. FEBS Lett 584: 4491-9

Simon A, Park H, Maddipati R, Lobito AA, Bulua AC, Jackson AJ, Chae JJ, Ettinger R, de Koning HD, Cruz AC, Kastner DL, Komarow H, Siegel RM (2010) Concerted action of wild-type and mutant TNF receptors enhances inflammation in TNF receptor 1-associated periodic fever syndrome. Proc Natl Acad Sci U S A 107: 9801-6

Sims JJ, Scavone F, Cooper EM, Kane LA, Youle RJ, Boeke JD, Cohen RE (2012) Polyubiquitin-sensor proteins reveal localization and linkage-type dependence of cellular ubiquitin signaling. Nat Methods 9: 303-9

Solan NJ, Miyoshi H, Carmona EM, Bren GD, Paya CV (2002) RelB cellular regulation and transcriptional activity are regulated by p100. J Biol Chem 277: 1405-18

Solt LA, Madge LA, Orange JS, May MJ (2007) Interleukin-1-induced NF-kappaB activation is NEMO-dependent but does not require IKKbeta. J Biol Chem 282: 8724-33

Song AX, Zhou CJ, Peng Y, Gao XC, Zhou ZR, Fu QS, Hong J, Lin DH, Hu HY (2010) Structural transformation of the tandem ubiquitin-interacting motifs in ataxin-3 and their cooperative interactions with ubiquitin chains. PLoS One 5: e13202

Sowa ME, Bennett EJ, Gygi SP, Harper JW (2009) Defining the human deubiquitinating enzyme interaction landscape. Cell 138: 389-403

Spence J, Sadis S, Haas AL, Finley D (1995) A ubiquitin mutant with specific defects in DNA repair and multiubiquitination. Mol Cell Biol 15: 1265-73

Spencer E, Jiang J, Chen ZJ (1999) Signal-induced ubiquitination of IkappaBalpha by the F-box protein Slimb/beta-TrCP. Genes Dev 13: 284-94

Srinivasula SM, Ahmad M, Fernandes-Alnemri T, Alnemri ES (1998) Autoactivation of procaspase-9 by Apaf-1-mediated oligomerization. Mol Cell 1: 949-57

Stewart GS, Panier S, Townsend K, Al-Hakim AK, Kolas NK, Miller ES, Nakada S, Ylanko J, Olivarius S, Mendez M, Oldreive C, Wildenhain J, Tagliaferro A, Pelletier L, Taubenheim N, Durandy A, Byrd PJ, Stankovic T, Taylor AM, Durocher D (2009) The RIDDLE syndrome protein mediates a ubiquitin-dependent signaling cascade at sites of DNA damage. Cell 136: 420-34

Stieglitz B, Morris-Davies AC, Koliopoulos MG, Christodoulou E, Rittinger K (2012) LUBAC synthesizes linear ubiquitin chains via a thioester intermediate. EMBO reports 13: 840-6

Stieglitz B, Rana RR, Koliopoulos MG, Morris-Davies AC, Schaeffer V, Christodoulou E, Howell S, Brown NR, Dikic I, Rittinger K (2013) Structural basis for ligase-specific conjugation of linear ubiquitin chains by HOIP. Nature

Straus SE, Jaffe ES, Puck JM, Dale JK, Elkon KB, Rösen-Wolff A, Peters AM, Sneller MC, Hallahan CW, Wang J, Fischer RE, Jackson CM, Lin AY, Bäumler C, Siegert E, Marx A, Vaishnaw AK, Grodzicky T, Fleisher TA, Lenardo MJ (2001) The development of lymphomas in families with autoimmune lymphoproliferative syndrome with germline Fas mutations and defective lymphocyte apoptosis. Blood 98: 194-200

Sulston JE, Horvitz HR (1977) Post-embryonic cell lineages of the nematode, Caenorhabditis elegans. Dev Biol 56: 110-56

Sun L, Wang H, Wang Z, He S, Chen S, Liao D, Wang L, Yan J, Liu W, Lei X, Wang X (2012) Mixed lineage kinase domain-like protein mediates necrosis signaling downstream of RIP3 kinase. Cell 148: 213-27

Sun SC (2011) Non-canonical NF-κB signaling pathway. Cell Res 21: 71-85

Sun SC, Ganchi PA, Ballard DW, Greene WC (1993) NF-kappa B controls expression of inhibitor I kappa B alpha: evidence for an inducible autoregulatory pathway. Science 259: 1912-5

Sundström C, Nilsson K (1976) Establishment and characterization of a human histiocytic lymphoma cell line (U-937). Int J Cancer 17: 565-77

Sweet CR, Conlon J, Golenbock DT, Goguen J, Silverman N (2007) YopJ targets TRAF proteins to inhibit TLR-mediated NF-kappaB, MAPK and IRF3 signal transduction. Cell Microbiol 9: 2700-15

Takeda K, Akira S (2015) Toll-like receptors. Curr Protoc Immunol 109: 14.12.1-10

Takeuchi O, Akira S (2010) Pattern recognition receptors and inflammation. Cell 140: 805-20

Takiuchi T, Nakagawa T, Tamiya H, Fujita H, Sasaki Y, Saeki Y, Takeda H, Sawasaki T, Buchberger A, Kimura T, Iwai K (2014) Suppression of LUBAC-mediated linear ubiquitination by a specific interaction between LUBAC and the deubiquitinases CYLD and OTULIN. Genes Cells 19: 254-72

Tang F, Tang G, Xiang J, Dai Q, Rosner MR, Lin A (2002) The absence of NF-kappaB-mediated inhibition of c-Jun N-terminal kinase activation contributes to tumor necrosis factor alpha-induced apoptosis. Mol Cell Biol 22: 8571-9

Tang G, Minemoto Y, Dibling B, Purcell NH, Li Z, Karin M, Lin A (2001) Inhibition of JNK activation through NF-kappaB target genes. Nature 414: 313-7

Tanoue T, Adachi M, Moriguchi T, Nishida E (2000) A conserved docking motif in MAP kinases common to substrates, activators and regulators. Nat Cell Biol 2: 110-6

Tanoue T, Nishida E (2003) Molecular recognitions in the MAP kinase cascades. Cell Signal 15: 455-62

Tao M, Scacheri PC, Marinis JM, Harhaj EW, Matesic LE, Abbott DW (2009) ITCH K63-ubiquitinates the NOD2 binding protein, RIP2, to influence inflammatory signaling pathways. Curr Biol 19: 1255-63

Tian B, Nowak DE, Brasier AR (2005) A TNF-induced gene expression program under oscillatory NF-kappaB control. BMC Genomics 6: 137

Tokunaga F, Nakagawa T, Nakahara M, Saeki Y, Taniguchi M, Sakata S, Tanaka K, Nakano H, Iwai K (2011) SHARPIN is a component of the NF-kappaB-activating linear ubiquitin chain assembly complex. Nature 471: 633-6

Tokunaga F, Nishimasu H, Ishitani R, Goto E, Noguchi T, Mio K, Kamei K, Ma A, Iwai K, Nureki O (2012) Specific recognition of linear polyubiquitin by A20 zinc finger 7 is involved in NF-kappaB regulation. The EMBO journal 31: 3856-70

Tokunaga F, Sakata S, Saeki Y, Satomi Y, Kirisako T, Kamei K, Nakagawa T, Kato M, Murata S, Yamaoka S, Yamamoto M, Akira S, Takao T, Tanaka K, Iwai K (2009) Involvement of linear polyubiquitylation of NEMO in NF-kappaB activation. Nature cell biology 11: 123-32

Tournier C, Hess P, Yang DD, Xu J, Turner TK, Nimnual A, Bar-Sagi D, Jones SN, Flavell RA, Davis RJ (2000) Requirement of JNK for stress-induced activation of the cytochrome c-mediated death pathway. Science 288: 870-4

Tracey KJ, Fong Y, Hesse DG, Manogue KR, Lee AT, Kuo GC, Lowry SF, Cerami A (1987) Anti-cachectin/TNF monoclonal antibodies prevent septic shock during lethal bacteraemia. Nature 330: 662-4

Tracy LE, Minasian RA, Caterson EJ (2016) Extracellular Matrix and Dermal Fibroblast Function in the Healing Wound. Adv Wound Care (New Rochelle) 5: 119-136

Trautmann A (2009) Extracellular ATP in the immune system: more than just a "danger signal". Sci Signal 2: pe6

Trompouki E, Hatzivassiliou E, Tsichritzis T, Farmer H, Ashworth A, Mosialos G (2003) CYLD is a deubiquitinating enzyme that negatively regulates NF-[kappa]B activation by TNFR family members. Nature 424: 793-796

Trompouki E, Tsagaratou A, Kosmidis SK, Dollé P, Qian J, Kontoyiannis DL, Cardoso WV, Mosialos G (2009) Truncation of the catalytic domain of the cylindromatosis tumor suppressor impairs lung maturation. Neoplasia 11: 469-76

Truman LA, Ford CA, Pasikowska M, Pound JD, Wilkinson SJ, Dumitriu IE, Melville L, Melrose LA, Ogden CA, Nibbs R, Graham G, Combadiere C, Gregory CD (2008) CX3CL1/fractalkine is released from apoptotic lymphocytes to stimulate macrophage chemotaxis. Blood 112: 5026-36

Turer EE, Tavares RM, Mortier E, Hitotsumatsu O, Advincula R, Lee B, Shifrin N, Malynn BA, Ma A (2008) Homeostatic MyD88-dependent signals cause lethal inflamMation in the absence of A20. J Exp Med 205: 451-64

Upton JW, Kaiser WJ, Mocarski ES (2012) DAI/ZBP1/DLM-1 complexes with RIP3 to mediate virus-induced programmed necrosis that is targeted by murine cytomegalovirus vIRA. Cell Host Microbe 11: 290-7

Vallabhapurapu S, Matsuzawa A, Zhang W, Tseng PH, Keats JJ, Wang H, Vignali DA, Bergsagel PL, Karin M (2008) Nonredundant and complementary functions of TRAF2 and TRAF3 in a ubiquitination cascade that activates NIK-dependent alternative NF-kappaB signaling. Nat Immunol 9: 1364-70

van Dam EM, Stoorvogel W (2002) Dynamin-dependent transferrin receptor recycling by endosome-derived clathrin-coated vesicles. Mol Biol Cell 13: 169-82

van Wijk SJ, Fiskin E, Putyrski M, Pampaloni F, Hou J, Wild P, Kensche T, Grecco HE, Bastiaens P, Dikic I (2012) Fluorescence-based sensors to monitor localization and functions of linear and K63-linked ubiquitin chains in cells. Mol Cell 47: 797-809

Vanlangenakker N, Bertrand MJM, Bogaert P, Vandenabeele P, Vanden Berghe T (2011) TNF-induced necroptosis in L929 cells is tightly regulated by multiple TNFR1 complex I and II members. Cell Death and Disease 2: e230

Varadan R, Walker O, Pickart C, Fushman D (2002) Structural properties of polyubiquitin chains in solution. J Mol Biol 324: 637-47

Varfolomeev E, Goncharov T, Fedorova AV, Dynek JN, Zobel K, Deshayes K, Fairbrother WJ, Vucic D (2008) c-IAP1 and c-IAP2 are critical mediators of tumor necrosis factor alpha (TNFalpha)-induced NF-kappaB activation. J Biol Chem 283: 24295-9

Varfolomeev EE, Schuchmann M, Luria V, Chiannilkulchai N, Beckmann JS, Mett IL, Rebrikov D, Brodianski VM, Kemper OC, Kollet O, Lapidot T, Soffer D, Sobe T, Avraham KB, Goncharov T, Holtmann H, Lonai P, Wallach D (1998) Targeted disruption of the mouse Caspase 8 gene ablates cell death induction by the TNF receptors, Fas/Apo1, and DR3 and is lethal prenatally. Immunity 9: 267-76

Verdecia MA, Joazeiro CA, Wells NJ, Ferrer JL, Bowman ME, Hunter T, Noel JP (2003) Conformational flexibility underlies ubiquitin ligation mediated by the WWP1 HECT domain E3 ligase. Mol Cell 11: 249-59

Verhelst K, Carpentier I, Kreike M, Meloni L, Verstrepen L, Kensche T, Dikic I, Beyaert R (2012) A20 inhibits LUBAC-mediated NF-kappaB activation by binding linear polyubiquitin chains via its zinc finger 7. The EMBO journal 31: 3845-55

Vince JE, Pantaki D, Feltham R, Mace PD, Cordier SM, Schmukle AC, Davidson AJ, Callus BA, Wong WWL, Gentle IE, Carter H, Lee EF, Walczak H, Day CL, Vaux DL, Silke J (2009) TRAF2 Must Bind to Cellular Inhibitors of Apoptosis for Tumor Necrosis Factor (TNF) to Efficiently Activate NF- B and to Prevent TNF-induced Apoptosis. Journal of Biological Chemistry 284: 35906-35915

Vince JE, Wong WW, Khan N, Feltham R, Chau D, Ahmed AU, Benetatos CA, Chunduru SK, Condon SM, McKinlay M, Brink R, Leverkus M, Tergaonkar V, Schneider P, Callus BA, Koentgen F, Vaux DL, Silke J (2007) IAP antagonists target cIAP1 to induce TNFalpha-dependent apoptosis. Cell 131: 682-93

Wada T, Penninger JM (2004) Mitogen-activated protein kinases in apoptosis regulation. Oncogene 23: 2838-49

Wagner S, Carpentier I, Rogov V, Kreike M, Ikeda F, Lohr F, Wu CJ, Ashwell JD, Dotsch V, Dikic I, Beyaert R (2008) Ubiquitin binding mediates the NF-kappaB inhibitory potential of ABIN proteins. Oncogene 27: 3739-45

Wagner SA, Satpathy S, Beli P, Choudhary C (2016) SPATA2 links CYLD to the TNF-α receptor signaling complex and modulates the receptor signaling outcomes. EMBO J: n/a-n/a

Wajant H, Henkler F, Scheurich P (2001) The TNF-receptor-associated factor family: scaffold molecules for cytokine receptors, kinases and their regulators. Cell Signal 13: 389-400

Wajant H, Pfizenmaier K, Scheurich P (2003) Tumor necrosis factor signaling. Cell Death Differ 10: 45-65

Walczak H, Iwai K, Dikic I (2012) Generation and physiological roles of linear ubiquitin chains. BMC biology 10: 23

Wang C, Deng L, Hong M, Akkaraju GR, Inoue J, Chen ZJ (2001) TAK1 is a ubiquitin-dependent kinase of MKK and IKK. Nature 412: 346-51

Wang CY, Mayo MW, Korneluk RG, Goeddel DV, Baldwin AS (1998) NF-kappaB antiapoptosis: induction of TRAF1 and TRAF2 and c-IAP1 and c-IAP2 to suppress caspase-8 activation. Science 281: 1680-3

Wang H, Sun L, Su L, Rizo J, Liu L, Wang LF, Wang FS, Wang X (2014) Mixed Lineage Kinase Domain-like Protein MLKL Causes Necrotic Membrane Disruption upon Phosphorylation by RIP3. Mol Cell 54: 133-46

Wang Y, Gu X (2001) Functional divergence in the caspase gene family and altered functional constraints: statistical analysis and prediction. Genetics 158: 1311-20

Welz PS, Wullaert A, Vlantis K, Kondylis V, Fernandez-Majada V, Ermolaeva M, Kirsch P, Sterner-Kock A, van Loo G, Pasparakis M (2011) FADD prevents RIP3-mediated epithelial cell necrosis and chronic intestinal inflammation. Nature 477: 330-4

Wen R, Wang S, Xiang D, Venglat P, Shi X, Zang Y, Datla R, Xiao W, Wang H (2014) UBC13, an E2 enzyme for Lys63-linked ubiquitination, functions in root development by affecting auxin signaling and Aux/IAA protein stability. Plant J 80: 424-36

Wenzel DM, Klevit RE (2012) Following Ariadne's thread: a new perspective on RBR ubiquitin ligases. BMC Biol 10: 24

Wenzel DM, Lissounov A, Brzovic PS, Klevit RE (2011) UBCH7 reactivity profile reveals parkin and HHARI to be RING/HECT hybrids. Nature 474: 105-8

Wertz IE (2014) TNFR1-activated NF-kappaB signal transduction: regulation by the ubiquitin/proteasome system. Curr Opin Chem Biol 23C: 71-77

Wertz IE, Newton K, Seshasayee D, Kusam S, Lam C, Zhang J, Popovych N, Helgason E, Schoeffler A, Jeet S, Ramamoorthi N, Kategaya L, Newman RJ, Horikawa K, Dugger D, Sandoval W, Mukund S, Zindal A, Martin F, Quan C et al. (2015) Phosphorylation and linear ubiquitin direct A20 inhibition of inflammation. Nature 528: 370-5

Wertz IE, O'Rourke KM, Zhou H, Eby M, Aravind L, Seshagiri S, Wu P, Wiesmann C, Baker R, Boone DL, Ma A, Koonin EV, Dixit VM (2004) De-ubiquitination and ubiquitin ligase domains of A20 downregulate NF-[kappa]B signalling. Nature 430: 694-699

Wiborg O, Pedersen MS, Wind A, Berglund LE, Marcker KA, Vuust J (1985) The human ubiquitin multigene family: some genes contain multiple directly repeated ubiquitin coding sequences. EMBO J 4: 755-9

Widmann C, Gibson S, Jarpe MB, Johnson GL (1999) Mitogen-activated protein kinase: conservation of a three-kinase module from yeast to human. Physiol Rev 79: 143-80

Wilkinson KD (1997) Regulation of ubiquitin-dependent processes by deubiquitinating enzymes. FASEB J 11: 1245-56

Williams JR, Little JB, Shipley WU (1974) Association of mammalian cell death with a specific endonucleolytic degradation of DNA. Nature 252: 754-5

Winston JT, Strack P, Beer-Romero P, Chu CY, Elledge SJ, Harper JW (1999) The SCFbeta-TRCP-ubiquitin ligase complex associates specifically with phosphorylated destruction motifs in IkappaBalpha and beta-catenin and stimulates IkappaBalpha ubiquitination in vitro. Genes Dev 13: 270-83

Wright A, Reiley WW, Chang M, Jin W, Lee AJ, Zhang M, Sun SC (2007) Regulation of early wave of germ cell apoptosis and spermatogenesis by deubiquitinating enzyme CYLD. Dev Cell 13: 705-16

Wu W, Koike A, Takeshita T, Ohta T (2008) The ubiquitin E3 ligase activity of BRCA1 and its biological functions. Cell Div 3: 1

Xiao G, Fong A, Sun SC (2004) Induction of p100 processing by NF-kappaB-inducing kinase involves docking IkappaB kinase alpha (IKKalpha) to p100 and IKKalpha-mediated phosphorylation. J Biol Chem 279: 30099-105

Xiao G, Harhaj EW, Sun SC (2001) NF-kappaB-inducing kinase regulates the processing of NF-kappaB2 p100. Mol Cell 7: 401-9

Xu D, Shan B, Lee BH, Zhu K, Zhang T, Sun H, Liu M, Shi L, Liang W, Qian L, Xiao J, Wang L, Pan L, Finley D, Yuan J (2015) Phosphorylation and activation of ubiquitin-specific protease-14 by Akt regulates the ubiquitin-proteasome system. Elife 4: e10510

Xu M, Skaug B, Zeng W, Chen ZJ (2009a) A ubiquitin replacement strategy in human cells reveals distinct mechanisms of IKK activation by TNFalpha and IL-1beta. Molecular cell 36: 302-14

Xu P, Duong DM, Seyfried NT, Cheng D, Xie Y, Robert J, Rush J, Hochstrasser M, Finley D, Peng J (2009b) Quantitative proteomics reveals the function of unconventional ubiquitin chains in proteasomal degradation. Cell 137: 133-45

Yamaguchi N (2015) The seventh zinc finger motif of A20 is required for the suppression of TNF-alpha-induced apoptosis. FEBS Lett 589: 1369-75

Yamanaka K, Ishikawa H, Megumi Y, Tokunaga F, Kanie M, Rouault TA, Morishima I, Minato N, Ishimori K, Iwai K (2003) Identification of the ubiquitin-protein ligase that recognizes oxidized IRP2. Nature cell biology 5: 336-40

Yamaoka S, Courtois G, Bessia C, Whiteside ST, Weil R, Agou F, Kirk HE, Kay RJ, Israël A (1998) Complementation cloning of NEMO, a component of the IkappaB kinase complex essential for NF-kappaB activation. Cell 93: 1231-40

Yang S, Wang B, Humphries F, Jackson R, Healy ME, Bergin R, Aviello G, Hall B, McNamara D, Darby T, Quinlan A, Shanahan F, Melgar S, Fallon PG, Moynagh PN (2013) Pellino3 ubiquitinates RIP2 and mediates Nod2-induced signaling and protective effects in colitis. Nat Immunol 14: 927-36

Yao T, Cohen RE (2002) A cryptic protease couples deubiquitination and degradation by the proteasome. Nature 419: 403-7

Yaron A, Hatzubai A, Davis M, Lavon I, Amit S, Manning AM, Andersen JS, Mann M, Mercurio F, Ben-Neriah Y (1998) Identification of the receptor component of the IkappaBalpha-ubiquitin ligase. Nature 396: 590-4

Yau R, Rape M (2016) The increasing complexity of the ubiquitin code. Nature cell biology 18: 579-586

Yeh WC, Itie A, Elia AJ, Ng M, Shu HB, Wakeham A, Mirtsos C, Suzuki N, Bonnard M, Goeddel DV, Mak TW (2000) Requirement for Casper (c-FLIP) in regulation of death receptor-induced apoptosis and embryonic development. Immunity 12: 633-42

Yoon S, Seger R (2006) The extracellular signal-regulated kinase: multiple substrates regulate diverse cellular functions. Growth Factors 24: 21-44

Yuan J, Shaham S, Ledoux S, Ellis HM, Horvitz HR (1993) The C. elegans cell death gene ced-3 encodes a protein similar to mammalian interleukin-1 beta-converting enzyme. Cell 75: 641-52

Zarnegar BJ, Wang Y, Mahoney DJ, Dempsey PW, Cheung HH, He J, Shiba T, Yang X, Yeh WC, Mak TW, Korneluk RG, Cheng G (2008) Noncanonical NF-kappaB activation requires coordinated assembly of a regulatory complex of the adaptors cIAP1, cIAP2, TRAF2 and TRAF3 and the kinase NIK. Nat Immunol 9: 1371-8

Zarubin T, Han J (2005) Activation and signaling of the p38 MAP kinase pathway. Cell Res 15: 11-8

Zhang J, Stirling B, Temmerman ST, Ma CA, Fuss IJ, Derry JM, Jain A (2006) Impaired regulation of NF-kappaB and increased susceptibility to colitis-associated tumorigenesis in CYLD-deficient mice. The Journal of clinical investigation 116: 3042-9

Zhang SQ, Kovalenko A, Cantarella G, Wallach D (2000) Recruitment of the IKK signalosome to the p55 TNF receptor: RIP and A20 bind to NEMO (IKKγ) upon receptor stimulation. Immunity 12: 301-311

Zhang W, Liu HT (2002) MAPK signal pathways in the regulation of cell proliferation in mammalian cells. Cell Res 12: 9-18

Zheng N, Wang P, Jeffrey PD, Pavletich NP (2000) Structure of a c-Cbl-UbcH7 complex: RING domain function in ubiquitin-protein ligases. Cell 102: 533-9

Zhong H, SuYang H, Erdjument-Bromage H, Tempst P, Ghosh S (1997) The transcriptional activity of NF-kappaB is regulated by the IkappaB-associated PKAc subunit through a cyclic AMP-independent mechanism. Cell 89: 413-24

Zhou A, Scoggin S, Gaynor RB, Williams NS (2003) Identification of NF-kappa B-regulated genes induced by TNFalpha utilizing expression profiling and RNA interference. Oncogene 22: 2054-64

Zhou H, Monack DM, Kayagaki N, Wertz I, Yin J, Wolf B, Dixit VM (2005) Yersinia virulence factor YopJ acts as a deubiquitinase to inhibit NF-kappa B activation. J Exp Med 202: 1327-32

Zhou H, Wertz I, O'Rourke K, Ultsch M, Seshagiri S, Eby M, Xiao W, Dixit VM (2004) Bcl10 activates the NF-kappaB pathway through ubiquitination of NEMO. Nature 427: 167-71

Zhou Q, Wang H, Schwartz DM, Stoffels M, Park YH, Zhang Y, Yang D, Demirkaya E, Takeuchi M, Tsai WL, Lyons JJ, Yu X, Ouyang C, Chen C, Chin DT, Zaal K, Chandrasekharappa SC, P Hanson E, Yu Z, Mullikin JC et al. (2016) Loss-of-function mutations in TNFAIP3 leading to A20 haploinsufficiency cause an early-onset autoinflammatory disease. Nat Genet 48: 67-73

Zhu L, Wang L, Wang X, Zhou L, Liao Z, Xu L, Wu H, Ren J, Li Z, Yang L, Chen S, Li B, Wu X, Zhou Y, Li Y (2015) Characteristics of A20 gene polymorphisms and clinical significance in patients with rheumatoid arthritis. J Transl Med 13: 215

Zinngrebe J, Montinaro A, Peltzer N, Walczak H (2014) Ubiquitin in the immune system. EMBO Rep 15: 28-45

Zong WX, Thompson CB (2006) Necrotic death as a cell fate. Genes Dev 20: 1-15

Zou H, Henzel WJ, Liu X, Lutschg A, Wang X (1997) Apaf-1, a human protein homologous to C. elegans CED-4, participates in cytochrome c-dependent activation of caspase-3. Cell 90: 405-13